Master's thesis

NTNU
Norwegian University of Science and Technology
Faculty of Natural Sciences
Department of Biotechnology and Food Science

Helga Munkeby Tingstad

Use of Homologous Recombination to Study Alginate Biosynthesis in *Azotobacter vinelandii*.

Master's thesis in MBIOT5
Supervisor: Helga Ertesvåg
May 2021

NTNU
Kunnskap for en bedre verden

Helga Munkeby Tingstad

Use of Homologous Recombination to Study Alginate Biosynthesis in *Azotobacter vinelandii*.

Master's thesis in MBIOT5
Supervisor: Helga Ertesvåg
May 2021

Norwegian University of Science and Technology
Faculty of Natural Sciences
Department of Biotechnology and Food Science

NTNU
Norwegian University of
Science and Technology

Preface

The following thesis is the final report of the course BIOTBT3900 Master Thesis in Biotechnology at the Department of Biotechnology and Food Science, Norwegian University of Science and Technology, and concludes the five year Master's Degree Programme in Biotechnology. The thesis is written in collaboration with the supervisor Helga Ertesvåg and her molecular genetics group.

The experimental and theoretical work involved was of enormous educational value, and I grew to enjoy both work in the laboratory and the scientific writing. I would like to thank my supervisor for her guidance and support throughout the project. Additionally, I would like to thank the other members of the molecular genetics group for their help, as well as my friends and family for the support I received during the course of this year.

Trondheim, May 2021
Helga Munkeby Tingstad

Summary

Alginate is a linear, anionic biopolymer made up of mannuronate (M) and guluronate (G). It is of great industrial interest, particularly because of its gel-forming properties which stem from interactions of divalent cations with consecutive G-blocks. The properties of alginate vary depending on the source, and alginate synthesizing bacteria such as *Azotobacter vinelandii* could be utilized to produce alginates with sought after properties, such as a higher G-content. Genetic engineering could further be used to alter and improve the properties of the alginate. This study aimed to construct, verify and test *A. vinelandii* strains with mutations to several genes believed to be involved in alginate biosynthesis, to gain insight into its biosynthesis and potential ways of manipulating it.

Inactivated *algB* and *algW* mutants were constructed by homologous recombination. AlgB and AlgW are positive regulators of biosynthetic genes in *Pseudomonas aeruginosa*, and AlgB is essential for alginate production. This study investigated if the *algB* and *algW* genes of *A. vinelandii* had similar roles by inactivating the genes and evaluating the alginate production of mutants. The results were consistent with previous findings and suggest that the role of *A. vinelandii algB* differs from that of *P. aeruginosa* in that it is not required for alginate biosynthesis. Results also indicated that *algW* is required for alginate biosynthesis, just like its *P. aeruginosa* homolog. The alginate production of an *algF*, *mucA* double mutant was also evaluated. AlgF is not essential for alginate production but is involved in acetylation of M-residues, which prevents epimerization and lyase activity. An *algF* mutation alone could therefore result in a higher G-content alginate with lowered molecular weight. MucA is an anti-σ factor that impacts alginate biosynthesis negatively, and its disruption could result in increased alginate production. The double mutant was found to produce very low amounts of alginate, which is inconsistent with previous studies and suggests that a secondary mutation detrimental to alginate production occurred.

A CRISPR-Cas9 assisted system that disrupts *algL* was constructed and tested. Obtaining pure *A. vinelandii* mutants by homologous recombination alone is often challenging as the organism may contain up to 80 chromosome copies. A CRISPR-Cas9 vector was therefore used along with homologous recombination in an attempt to obtain a pure *algL* mutant where *algL* or the less efficient mutant *algLH199R* associated with a weaker promoter was incorporated into the genome by transposition. *algL* is an essential gene that encodes an alginate lyase, and the gene cannot be removed entirely. A mutant with lowered AlgL activity could however result in a higher molecular weight alginate. Homologous recombination was used to disrupt the acetylation genes *algI*, *algV* and *algF* in addition to wild type *algL*, which could increase the G-content of the alginate. Homologous recombination yielded mutants that most likely contained both wild type and mutated chromosomes, but conjugation with the CRISPR-Cas9 vector was not successful.

Sammendrag

Alginat er en lineær, anionisk biopolymer bestående av mannuronsyre (M) og guluronsyre (G). Polymeren har mange bruksområder innen industri og er særlig interessant på grunn av dens evne til å danne geler, en egenskap som stammer fra interaksjoner mellom divalente kationer og G-blokker i alginaten. Egenskapene varierer avhengig av kilden, og det er økende interesse rundt alginatsyntetiserende bakterier som *Azotobacter vinelandii* som potensielt kan brukes til å produsere alginat med ønskede egenskaper slik som et høyere innhold av guluronsyre. Genmodifisering kan også brukes for å videre forbedre egenskapene. Denne studien ønsket å lage, verifisere og teste *A. vinelandii*-mutanter der flere av genene involvert i biosyntese av alginat muteres, noe som kan bidra til innsikt i alginatbiosyntesen i *A. vinelandii* og potensielle muligheter for å modifisere biosyntesen.

Effekten av inaktivering av *algB* og *algW* ble undersøkt ved hjelp av homolog rekombinering etterfulgt av måling av alginatproduksjon. AlgB og AlgW regulerer biosyntesegener i *Pseudomonas aeruginosa* positivt, hvor AlgB også er nødvendig for alginatproduksjon. Denne studien undersøkte om genene har en lignende rolle i *A. vinelandii*. Resultatene sammenfalt med tidligere resultater og indikerer at *algB* har en annen rolle i *A. vinelandii* da inaktivering av genet ikke så ut til å være ødeleggende for alginatbiosyntesen. Resultatene indikerte også at *algW* er nødvendig for alginatproduksjon i *A. vinelandii*, som *P. aeruginosa algW*. Alginatproduksjonen til en *algF*, *mucA* mutant ble også undersøkt. AlgF er ikke nødvendig for alginatproduksjon men er involvert i acetylering av mannuronsyre, som forhindrer epimerisering og lyaseaktivitet. *algF*-mutasjonen kunne derfor føre til et høyere innhold av guluronsyre samt en lavere molekylvekt. MucA er en anti-σ faktor som har negativ innvirkning på alginatbiosyntesen, og *mucA*-mutasjonen kunne derfor medføre økt alginatproduksjon. Alginatproduksjonen til mutanten økte ikke slik som forventet, noe som indikerer at en skadelig sekundærmutasjon oppsto.

Et CRISPR-Cas9-assistert system som angriper *algL* ble også utviklet og testet. Homolog rekombinering er ofte ikke tilstrekkelig for å oppnå rene mutanter, siden *A. vinelandii* kan innholde opptil 80 kromosomkopier. En CRISPR-Cas9-vektor ble derfor brukt sammen med homolog rekombinering for å oppnå en ren *algL*-mutant der *algL* eller den mindre aktive mutanten *algLH199R* ble kombinert med en svakere promoter og satt inn ved hjelp av transposjon. *algL* er et essensielt gen som koder for en alginatlyase, og genet kan derfor ikke fjernes. Ved å introdusere en versjon av *algL* med lavere aktivitet var målet likevel å oppnå en mutant som produserte alginat med høyere molekylvekt. Homolog rekombinering ble også brukt til å ødelegge acetyleringsgenene *algI*, *algV* og *algF*, noe som kunne gi produksjon av alginat med et økt innhold av guluronsyre. Homolog rekombinering resulterte sannsynligvis i mutanter som inneholdt både villtype- og muterte kromosomer, men konjugering med CRISPR-Cas9-vektoren gav ingen transkonjuganter.

Abbreviations

Am^r	Ampicillin resistant
Ap^r	Apramycin resistant
BA	Burks medium with agar
BM	Burks medium
bp	Base pair(s)
Cas	CRISPR associated protein
CRISPR	Clustered regularly interspaced short palindromic repeats
crRNA	CRISPR RNA
DMSO	Dimethyl sulfoxide
DNA	Deoxyribonucleic acid
DSB	Double strand break
dsDNA	Double stranded DNA
HDR	Homology-directed repair
indel	Insertion or deletion mutation
kb	Kilobase(s)
Km^r	Kanamycin resistant
LA	Luria-Bertani medium with agar
LB	Luria-Bertani medium
NHEJ	Non-homologus end joining
PAM	Protospacer adjacent motif
PCR	Polymerase chain reaction
PHB	Poly-β-hydroxybutyrate
RNA	Ribonucleic acid
SDS	Sodium dodecyl sulphate
Sp^r	Spectinomycin resistant
sgRNA	Single-guide RNA
ssDNA	Single stranded DNA
TALENs	Transcription activator–like effector nucleases
Tc^r	Tetracyline resistant
tracrRNA	Trans-activating crRNA
ZFNs	Zinc-finger nucleases

TABLE OF CONTENTS

CHAPTER 1

INTRODUCTION

This chapter presents the relevant background information for the experimental work of this master's thesis. This includes the bacterium which is the focus of this work, *Azotobacter vinelandii*, as well as genes involved in regulation and biosynthesis of alginate. In addition, this chapter presents the relevant genetic engineering technologies used to obtain *A. vinelandii* mutants. In addition to using transposition and homologous recombination to obtain mutant strains, a CRISPR-Cas9 vector was also used in an attempt to remove remaining wild type chromosome copies. The plasmid systems used as well as the host organism for cloning procedures, *Escherichia coli*, are also presented.

1.1 Alginate structure and properties

Alginates are linear anionic polysaccharides that are of particular interest because of their gelling properties [1], and as a result they have a wide variety of applications in medicine and various other industries. Alginates for commercial use are typically extracted from brown algae, where they act as a structural part of the cell wall [2], but they are also produced by some genera of bacteria such as *Azotobacter* [3] and *Pseudomonas* [4].

Alginates are block copolymers made up of the (1,4)-linked monomers β-D-mannuronate (M) and α-L-guluronate (G) [1]. The monomers are found in both alternating patterns and as blocks of consecutive M- and G-residues [1]. As depicted in figure 1.1, M- and G-residues are C5 epimers with different chair conformations, resulting in four possible glycosidic linkages [5] that may affect the structure and properties of the alginate. The ability of G-residues to form cavities in the chain is especially important for the alginat's properties, as G- and MG-blocks can bind divalent cations [1] such as Ca^{2+}. This in turn results in intermolecular cross-linking and water binding [2], yielding alginate solutions with increased viscosity and enabling alginate to form hydrogels [1, 2].

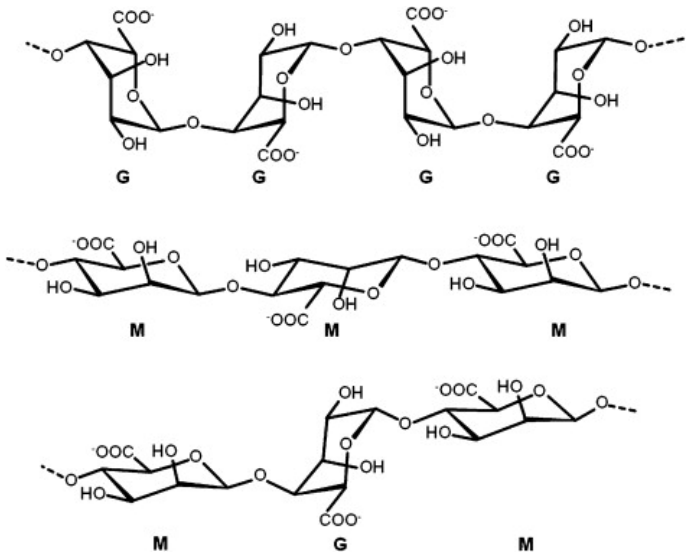

Figure 1.1: The chemical structures of the (1,4)-linked β-D-mannuronate (M) and α-L-guluronate (G) monomers of alginate and their glycosidic linkages. Figure copied from from Lee and Mooney [1].

The M- to G-ratio, the length of blocks, the acetyl content and the molecular weight of the alginate varies depending on the source it is extracted from, and affect its physical properties [1, 2]. Important physical properties of alginates include water-binding capacity, viscosity [2], gel strength and stability, the permeability or rate at which a gel can release

a substance such as a drug [1] and biocompatibility [2].

For many applications, the optimal alginate is one that has long G-blocks and a high molecular weight [1]. These alginates are able to bind more cations, resulting in increased mechanical rigidity and thus a higher strength gel [5]. The highest viscosity of alginate is found around pH 3-3.5, which is the pH at which the carboxylate groups are protonated and able to form hydrogen bonds [1]. Acetyl groups also increase the capacity to bind water, affecting the viscosity and flexibility of the alginate [6]. In addition, viscosity and gel strength depends on polymer length [2], and a high molecular weight alginate results in both higher viscosity and increases the elasticity of the hydrogel [1]. Too high viscosity however, may be undesirable for some uses. For example, when used to encapsulate living cells, the resulting high shear forces of high viscosity alginate can damage proteins and cells [1]. The increased elasticity that a high molecular weight alginate provides may still be advantageous, and a gel with both low viscosity and high elasticity may be achieved by using a mixture of both high and low molecular weight alginates [1].

The alginate extracted from brown algae tends to have varied chemical structure and thus also variable physical properties [1]. Bacterial alginates often have a more defined chemical structure, which has led to increased interest in bacterial biosynthesis of alginate [1]. Bacterial alginate production involves first synthesizing a precursor substrate, before the polymer is assembled in the periplasm, modified and transported out of the cell [1]. Modifications to and regulation of the bacterial biosynthesis apparatus could therefore enable production of alginates with specific properties. For example, the alginate may be modified *in vitro* using recombinant enzymes such as mannuronan C-5 epimerases, which are able to alter the amount and distribution of G residues [5]. Other enzymes involved in bacterial alginate production are useful in and of themselves. Since their discovery, alginate lyases have for example become useful tools for characterization of alginates [2].

1.1.1 Applications of alginate

Alginates are relatively low cost polymers [1] used in solutions to increase their viscosity, as an emulsifier and as a gelling agent [2]. In addition, when divalent cations like Ca^{2+} are allowed to diffuse into an alginate solution, beads, fibers and films may be created [5] that have many applications within industry. This internal gelation also has potential to replace more expensive agar and agarose gels [5]. Depending on purity and composition [7], alginates may be biocompatible, and the low immunogenic response [1] means that alginate may be used for medical purposes.

Alginates are used as a thickener in the pastes used to dye textiles, and its thickening properties are also exploited by food manufacturers [8]. For instance, McHugh [8] details the use of alginates in food to thicken sauces and syrups, as a stabilizer in ice cream, as both a thickener and a moisture barrier in pie fillings and as a gelling agent in jellies and animal foods. Some restructured meat and fish products also use alginate as a binder. Alginic acid is used in many diet foods, as it swells upon contact with water and thus can

provide a filling sensation without contributing calories. Alginates are also used in surface sizing by the paper industry, resulting in a smoother and more oil resistant surface [8].

The alginate hydrogel matrix is structurally similar to the extracellular matrices of living tissues [1]. This has led to the use of sodium calcium alginate fibres to stop bleeding in wound dressing [8]. In addition, alginate gels are used to encapsulate and deliver drugs and cells for cell transplantation [1]. The pharmaceutical industry also utilizes alginic acid in tablets, where it provides strength and acts as a disintegrating agent once it comes into contact with water [8]. Sodium alginate is used to suspend solids and provide viscosity to liquid form medicines [8]. Lastly, since alginates form cold-setting gels, they are also used to make dental impressions [8].

Encapsulation in alginate gel beads enables the controlled release of chemicals, and high G-content alginates that form strong gels are used to encapsulate biocatalysts such as enzymes or living cells [8]. For example, alginate has been used in treatment of type I diabetes to encapsulate pancreatic islets [5]. These types of medical applications depend on the use of biocompatible materials, and alginates with high G-content are useful here as they appear not to be immunogenic [7]. Immobilization of biocatalysts make their recovery and reuse easier, and alginate has therefore also been used in processes such as ethanol production from starch [9], in beer brewing with yeast [10] and in yoghurt production [11].

Alginates may additionally be modified to gain specific useful properties. Chemical modification of alginates to alcohol containing alginate esters has for example been used to create drug carriers, and esterified alginates using propyleneoxide is used to form propylene glycol alginate (PGA), which is used in beer and salad dressings [5]. With the advent of genetic engineering of alginate-producing organisms and possibilities for further alginate modifications, this biopolymer could potentially find many new uses in the future.

1.2 Biology of *A. vinelandii*

A. vinelandii is a Gram-negative aerobic free-living soil bacterium [12] of the gammaproteobacteria [13]. The bacterium is found in soils worldwide [13] but gets its name from Vineland, New Jersey, where it was first isolated in 1903 [14]. Since its discovery, *A. vinelandii* has been used as a model organism to study various biological processes including respiration [15], aerobic nitrogen fixation [13] and enzyme kinetics [15]. Important discoveries such as the Lineweaver–Burk kinetic models [16] were made using enzymes isolated from *A. vinelandii*, and use of *A. vinelandii* polynucleotide phosphorylase aided the discovery of the genetic code [17].

The bacterium's ability to fix N_2 from the atmosphere at atmospheric O_2 concentrations has also made *A. vinelandii* itself a target of extensive research [12], and this makes it a useful organism within agriculture [18]. *A. vinelandii* has a very high respiration rate [19] and can adjust its respiration rate in a process called respiratory protection, allowing it to keep its cytoplasmic O_2 concentration low to protect oxygen-sensitive enzymes such

as nitrogenase [13]. In addition, *A. vinelandii* is an alginate producer, and will produce alginate constitutively in the lab [2]. The alginate is exported out of the cell where it forms a layer that does not seem to impair growth or fitness [2]. The alginate layer is however thought to aid diazotroph activity by protecting nitrogenase from O_2 inactivation [12]. Alginate production, along with sequence similarities, indicate that *A. vinelandii* is closely related to another alginate producer, *Pseudomonas* [15].

Vegetative *A. vinelandii* cells are large prolate spheroids with peritrichous flagella that provide motility, and they have a volume and DNA content ten times that of of *E. coli* [20, 21]. In Burk's medium, the generation time of *A. vinelandii* is approximately 2.5-3 hours [20]. An interesting characteristic of the *A. vinelandii* life cycle is its ability to form a metabolically dormant cyst [20] upon carbon depletion that leaves the cells resistant to desiccation [13]. Encystment involves loss of motility and cell volume as the cell differentiates into an oblate spheroid resting inside two layers of coating [20]. This structure enables the cells to survive until conditions improve and they can germinate [20]. Alginate production is integral to cyst formation, as mutants that lack alginate production are unable to form desiccation-resistant cells [22]. Alginate is part of the formed cyst coat, and might also explain why *A. vinelandii* alginates contain a high amount of G-blocks, as the gel network of the coat must provide the necessary strength for survival [2]. Encystment can be induced or triggered by exponential growth [20]. Exponential growth results in accumulation of poly-β-hydroxybutyrate (PHB) [13], which can later serve as a carbon and energy reserve. *A. vinelandii* also produces the copolymers hydroxybutyrate and hydroxyvalerate, which are useful in bioplastics [13].

Various *A. vinelandii* traits have enabled researchers to study it so extensively. Firstly, *A. vinelandii* can readily adapt its metabolism to various nutrient sources [13] such as carbohydrates, alcohols and organic acids [12]. Although somewhat dependent on the strain, the bacterium is also naturally competent during the late exponential phase if cultured under iron limitation using a sugar or glycerol as the carbon source [21, 23]. Competency enables *A. vinelandii* to take up linear and certain plasmid DNA, which in turn allows for genome modification using the bacterium's ability to incorporate DNA with regions of homology to the host genome by double recombination [15]. Plasmids carrying transposons may also be used to modify the genome of *A. vinelandii* [24].

Alginate production is often the target of studies into *A. vinelandii*, but the alginate coating is also potentially an issue during transformation, as it acts as a barrier that may prevent exogenous DNA from being taken up [15]. In addition, alginate production has been reported to affect cell yield in *Pseudomonas fluorescens* [25]. Another problem of working with *A. vinelandii* stems from its polyploidy. The bacterium can contain up to 80 chromosome copies per cell [26], which may make obtaining homozygous transformants difficult [15]. The number of chromosome copies does vary depending on the medium used and the growth phase of the bacterium, and the highest number of chromosome copies is typically found in the late-exponential and stationary phases of growth [26].

1.2.1 Alginate biosynthesis and modification

Most of the research into bacterial biosynthesis of alginate has been focused on the alginate production of *Pseudomonas aeruginosa*, as the alginate it produces is involved in the pathogenesis of cystic fibrosis [27]. However, the biosynthesis pathway of *A. vinelandii* is thought to be similar to that of *P. aeruginosa* [27].

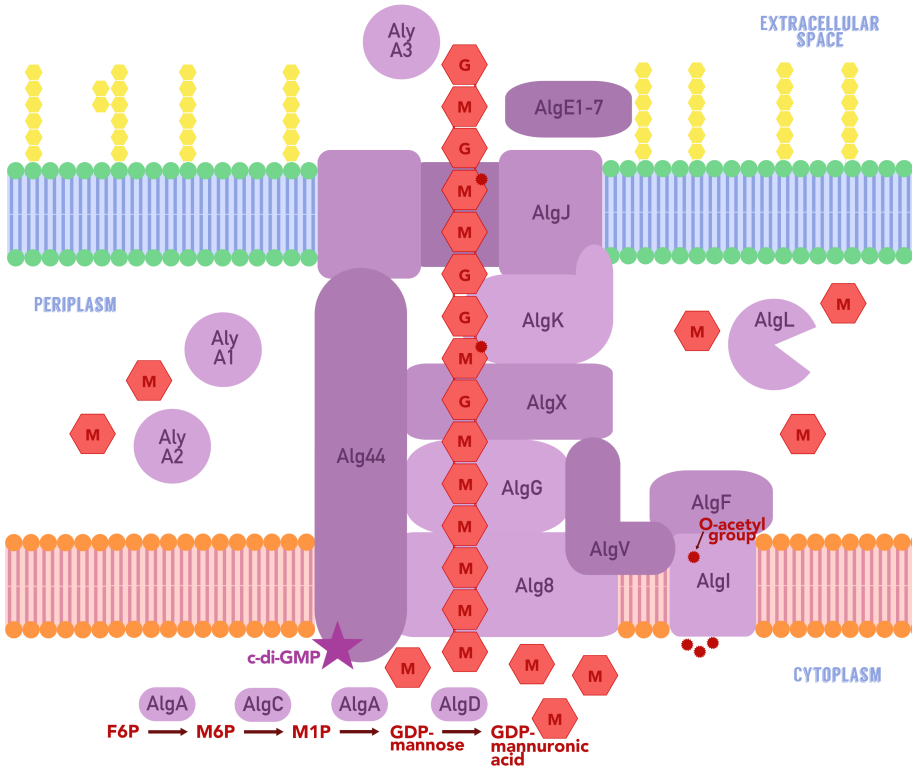

Figure 1.2: The enzymes involved in synthesis of the alginate precursor GDP-mannuronic acid, alginate biosynthesis and modification by epimerization and O-acetylation as well as removal of displaced alginate. Precursor synthesis occurs in the cytoplasm, and polymerization and modification occurs in the periplasm. The alginate is transported out of the cell, where further modification may be catalyzed. Figure adapted from Urtuvia et al. [28].

Bacterial alginate biosynthesis begins with conversion of the substrate fructose 6-phosphate (F6P), as depicted in figure 1.2. Biosynthesis also requires GTP [29]. F6P is converted to GDP-mannuronic acid in the cystoplasm in a series of enzymatic steps [29]. AlgA has both phosphomannose isomerase and GDP-mannose pyrophosphorylase activity [30], and catalyzes conversion of F6P to mannose-6-phosphate (M6P). M6P is next converted to mannose-1-phosphate (M1P) by AlgC, before AlgA converts M1P to to GDP-mannose [28]. The GDP-mannose dehydrogenase AlgD then catalyzes the rate-limiting and irre-

versible oxidation that converts GDP-mannose to GDP-mannuronic acid [31, 15]. GDP-mannuronic acid is then polymerized to polymannuronic acid through the action of a polymerase complex that contains the glycosyltransferase and polymerase Alg8 and the copolymerase Alg44 [28], which requires binding to dimeric cyclic di-GMP (c-di-GMP) [29]. The protein complex also contains AlgG, AlgX, AlgK and AlgJ, and is responsible for transport of the alginate through the periplasm and export out of the cell [29] via the AlgJ porin [28]. The mechanism involved in terminating the synthesis of an alginate molecule is unknown [2].

The functional properties of the produced alginate are mainly determined by modifications made to the polymannuronic acid post polymerization [2]. While still in the periplasm, polymannuronic acid is modified by epimerization and O-acetylation. Epimerization of β-D-mannuronic acid to α-L-guluronic acid is performed by mannuronan C-5 epimerases, and *A. vinelandii* encodes eight epimerases [2]. AlgG is a periplasmic mannuronan C-5-epimerase that converts some of the M-residues to G-residues [32], and it is thought to introduce equatorial-axial bonds to give the polymannuronate increased flexibility [33]. AlgG is only able to epimerize M-residues adjacent to other M-residues, and therefore cannot introduce G-blocks [34]. The calcium dependent epimerases AlgE1-E7 are secreted extracellularly [35, 2], and may also alter the G-content of the alginate once it has been transported out of the cells. Expression of these epimerases changes during the life cycle of *A. vinelandii*, such that different epimerases may introduce different G-distribution patterns at different times depending on the needs of the cell [36].

Several enzymes are involved in acetylation of some of the remaining M-residues at C-2 and/or C-3 hydroxyls [29, 37]. An AlgF, AlgI, AlgX and AlgV complex is involved in the acetylation, but these proteins are not required for alginate biosynthesis itself [2]. Acetylation begins with acetyl-CoA group transport from the cytoplasm to the periplasm by AlgI and then AlgV [28], before AlgX then acetylates mannuronan [37]. The exact function of AlgF in acetylation is not known, but it has been shown to be essential for acetylation in *P. aeruginosa* [38]. Acetylation of M-residues prevents epimerases and many lyases from modifying the residues further [2].

Some alginate molecules are not exported out of the cell and instead end up in the periplasm. Alginate is a polyanionic polymer that attracts cations, and accumulation of alginate in the periplasm causes an increase in osmotic pressure which could eventually lead to cell lysis [39, 40]. The alginate lyase AlgL catalyzes β-elimination of both M-M and M-G glycosidic bonds, but not G-G and G-M bonds [41]. It appears to favor cleavage of deacetylated monomers, but will also cleave acetylated ones [41]. The enzyme is found in the periplasm, where it controls the molecular weigth of the alginate chain [28] and prevents increased osmotic pressure by degrading rogue alginate molecules [29]. AlgL has endolytic activity, meaning that it cleaves the alginate molecules internally [42, 2]. No attempts to produce pure *algL* mutants have been successful [43], indicating that *algL* is an essential gene in *A. vinelandii*. It is however not known how much *algL* must be expressed for the cells to be viable, or how strong the promoter controlling its transcription is.

In addition to AlgL, the bifunctional lyase and mannuronan C-5 epimerase AlgE7 and the

lyases AlyA1-3 and AlyB may cleave alginate molecules [28]. AlyA1-3 can cleave any bond in the alginate chain, although at different rates [34]. AlyB is an exolyase whose exact function is not known [2]. The previously mentioned AlgE7 also possesses lyase activity. It is thought to catalyze formation of its own substrate for cleavage by first epimerizing an M-residue [42, 34]. The bifunctionality speaks to the fact that lyase and epimerase activity have similar catalytic mechanisms, as they both involve abstraction of a C-5 proton and neutralization of the negative charge of the carboxyl group [2].

1.2.2 Regulation of alginate biosynthesis

With the exception of *algC*, the *alg* gene cluster depicted in figure 1.3 contains all twelve of the thirteen genes involved in alginate biosynthesis [29], and the genes in this cluster are all transcribed together [27]. Alginate biosynthesis is very energy demanding, and therefore requires tight control by an intricate regulatory network that is also connected to other cellular processes [28]. This is achieved by regulation of the *alg* gene cluster [15]. In addition to the *alg* gene cluster, there is also a gene cluster containing algE1-4 and algE6-7 as well as regulatory enzymes.

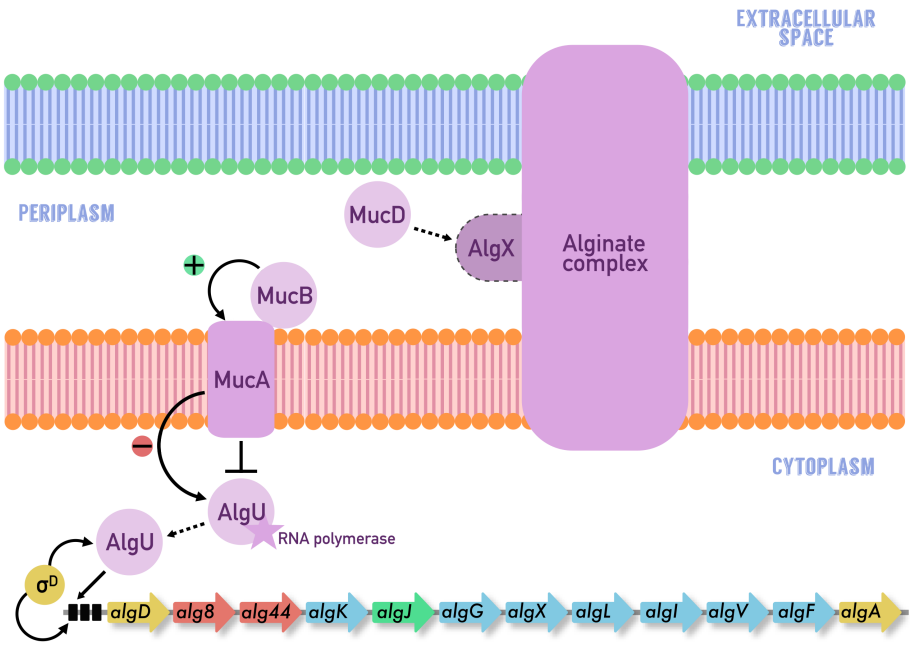

Figure 1.3: Some of the enzymes known to be involved in alginate regulation in *A. vinelandii* by regulation of *algD*. AlgU regulates alginate production positively by binding a promoter and thus inducing transcription of *algD*. MucA, MucB and MucD are involved in regulation of AlgU and algX. Figure adapted from Urtuvia et al. [28].

The proteins expressed from the gene cluster *algU-mucABCD* are regulators of alginate biosynthesis. AlgU is a cytoplasmic σ factor that acts as an essential positive regulator of alginate biosynthesis [44], as it is needed for expression of *algD* and potentially also other alginate biosynthesis genes [45]. It should be noted here that AlgL and AlgA are transcribed independently of the *algD* promoter [27]. AlgU acts as a positive regulator by inducing transcription from the strongest promoter associated with *algD*, thus stimulating alginate production [27, 46]. When associated with AlgU, RNA polymerase can transcribe the alginate biosynthesis genes [28].

The operon that encodes AlgU also contains the genes *mucABCD*, which are all transcribed together [28] and act as regulators of the *alg* gene cluster [27]. MucA is an anti-σ factor and is found in the inner membrane, where it represses AlgU by sequestration [46]. MucA is stabilized by the periplasmic MucB [28]. MucA and MucB together thus prevent AlgU from initiating transcription, which affects alginate biosynthesis negatively [47]. A *mucA* mutation would result in increased alginate production, as AlgU activity would no longer be repressed by MucA. This in turn would result in increased production of AlgD. Mærk et al. [46] confirmed the results of previous studies [27, 47], showing that an *A. vinelandii mucA* mutant displayed increased alginate production. It is not known what, if any, regulatory role MucC plays in the cell [28], but MucD is also a periplasmic negative regulator [47]. It has serine protease activity and also acts as a chaperone, and is involved both in activation of AlgU [47] and interaction with the biosynthesis complex via AlgX [44].

In *P. aeruginosa*, AlgU may be released from sequestration by a proteolytic cascade that results in degradation of MucA [44]. This cascade begins with the protease AlgW, which responds to envelope stress by cleaving MucA [44]. AlgW is activated by accumulation of the misfolded outer membrane protein MucE [44]. Once cleaved by AlgW, MucA may then be cleaved by other proteases, eventually resulting in AlgU release [44]. AlgW is thus a positive regulator of alginate biosynthesis in *P. aeruginosa*. Mærk et al. [46] identified an *A. vinelandii* AlgW mutant that did not produce alginate, suggesting that *A. vinelandii* and *P. aeruginosa* AlgW have similar functions. Still, *A. vinelandii* does not encode a MucE homolog [13], and complementation of the *A. vinelandii* mutant by Mærk et al. did not restore alginate production. It should be noted that Mærk et al. constructed a transposon library, and transposon inserts therefore might have affected their results.

Other regulators include the cytoplasmic positive auxiliary regulators AlgR, AlgB and AlgZ, which all belong to the two-component family of regulators [28]. AlgR controls *algD* by binding the *algD* promoter, and its transcription is promoted by AlgU [44]. AlgB and AlgZ also bind the *algD* promoter [44]. By binding to the *algD* promoter in *P. aeruginosa*, AlgB has been shown to act as a positive regulator of biosynthetic genes [48]. In fact, the *P. aeruginosa* AlgB protein is required for alginate production [49, 50, 51]. It is identical in length and shares 75% sequence identity with *A. vinelandii* AlgB [46]. A recent study by Mærk et al. [46] however, suggests that *A. vinelandii* AlgB is not required for alginate production. Their study analyzed a mutant with a transposon insert that split *algB* in half. An amino acid at the C-terminal end of the gene has previously been shown to be needed for P*algD* binding [52, 48]. If *A. vinelandii* AlgB has the same function as its

P. aeruginosa homolog, it is therefore unlikely that alginate production was not affected due to expression of a truncated AlgB protein that retained sufficient activity [46].

1.3 Genetic engineering technologies

This section presents the use of plasmids and the host organism *E. coli* in cloning procedures, as well as the use of homologous recombination, transposable elements and CRISPR-Cas9 to introduce mutations into the genome of *A. vinelandii*.

1.3.1 Construction of plasmids in *E. coli*

The bacterium *E. coli* is used in cloning procedures to generate and maintain copies of DNA fragments, even when the cloned DNA is eventually destined for a different host species. According to Reece [53], *E. coli* is a gram negative bacterium found in soil and water, as well as in the human digestive system. *E. coli* has been thoroughly studied, is easy and cheap to culture, divides rapidly in as little as 20 minutes, and most strains in use are safe to work with and have been altered such that the cells cannot survive outside the laboratory. Crucially, *E. coli* allows plasmid vectors to be used to carry foreign DNA. The use of closed-circular extra-chromosomal dsDNA fragments called plasmids [53] to serve as cloning vehicles is a central part of molecular biology [54]. Plasmids may facilitate DNA modification and transfer during cloning of a DNA construct, as they can be isolated and digested using restriction enzymes. Fragments may then be ligated to form new hybrid plasmids [54].

Prokaryotes often carry plasmids naturally, which may vary in size from approximately 1500 bp to over 300 kbp [53]. These DNA fragments are able to replicate [54] and are inherited from one generation to the next along with the chromosomal DNA, and typically carry genes that confer useful properties not found in the chromosomal DNA [53]. These may confer resistance to an antibiotic or a heavy metal, or encode DNA restriction and modification enzymes [53]. According to Reece [53], the number of plasmid copies the cell keeps varies. Hundreds of plasmid copies may be maintained for high copy number plasmids, whereas as little as 1-2 copies may be present of low copy number plasmids. The variation is in part due to differing replication mechanisms, as high copy number plasmids typically replicate with the help of host proteins and low copy number plasmids encode their own.

Several plasmid types exist that possess different qualities making them suitable for a variety of uses. A suicide or conditional suicide vector may be used to detect a transposition or homologous recombination event [55]. Vectors that for some reason cannot replicate in the host are called suicide vectors, and they may be useful as transposon vectors because they prevent repeated harmful transposition events from occurring. Suicide vectors include ColE1- and R6K-derived plasmids [56]. Plasmids that contain the *E. coli*-derived

[53] ColE1 origin of replication are unstable once conjugated to *A. vinelandii* [55]. The R6K origin of replication may be used as a suicide vector because it requires the π protein for replication, and these plasmids cannot replicate in species that do not encode the π protein, such as *A. vinelandii* [56]. *E. coli* S17.1-λpir on the other hand does. In R6K-derived plasmids, *ori* is the origin of replication, and *oriT* is the origin of conjugation transfer [57].

Conditional suicide vectors on the other hand, are able to replicate in the host, but only under certain conditions. For example, replication of R2K-derived plasmids using the P*m*-XylS expression system require the origin of vegetative replication, *oriV*. *oriV* in turn requires TrfA for initiation of replication [58]. If the P*m* promoter is made to control expression of *trfA*, R2K-derived plasmids may be used as conditional suicide vectors, as P*m* requires that the transcription factor XylS binds a benzoic acid derivative such as *m*-toluate. Transcription of *xylS* is controlled by the constitutive promoter from P*s1*. This results in plasmid replication only if *m*-toluate is added to the growth medium [58], otherwise the plasmid will be cured from the cells. It should be noted here that when such a plasmid is transformed to *E. coli* S17.1, which already encodes *trfA* because it has previously integrated the RP4 plasmid into its own genome, R2K-derived plasmids may replicate without addition of *m*-toluate [59]. The use of *m*-toluate as an inducer of plasmid replication could potentially have other unintended consequences however, as it is possible that *m*-toluate affects growth in *A. vinelandii* [29].

Plasmids tend to place a metabolic burden on the cell's biochemical capacities, as the cell has to replicate the plasmid and potentially also express plasmid-encoded proteins, and this tends to reduce the cell's growth rate [60]. If a plasmid is cured from cells without being integrated into the chromosome or another plasmid, the metabolic burden imposed by the plasmid will result in cured lineages being favored [61]. Over time, the plasmid might become extinct. If selective pressure is applied by using an antibiotic the plasmid confers resistance to however, plasmid-carrying cells will be favored [61].

1.3.2 Homologous recombination

To achieve insertion mutagenesis, plasmid DNA may be incorporated into the host genome through a process called homologous recombination. Bacteria naturally use homologous recombination in various ways, including during DNA repair at the replication fork [62]. Homologous recombination in genetic engineering is achieved using plasmids that contain regions of homology to target gene(s) [62]. The identical sequences then enable exchange of DNA between two DNA molecules, and mutations may in this way be inserted into or removed from the host chromosome [62].

To insert the desired DNA with flanking regions of homology into the host genome, a two-step process [63] described in figure 1.4 is used. Homologous recombination often involves the use of conditional suicide vectors which require an inducer for replication. When the medium contains a positive selection marker which the plasmid confers resistance to, and the inducer is absent, the cells are forced to implement the plasmid into the

chromosomes. By selecting for the presence of a positive selection marker such as an antibiotic resistance gene found in the plasmid, it is therefore possible to screen for cells where the first homologous recombination event, the single-crossover event, has taken place. Here, the entire plasmid is integrated into the host genome [63]. This is reversible, and the cells may revert back to the wild type [63]. A second homologous recombination event where the plasmid is excised from the genome is therefore necessary. This double-crossover event is rare and requires selection for the absence of a counter-selection marker [64]. Often, the gene *sacB* is placed on the plasmid backbone and used as the counter-selection marker [63]. The gene product of *sacB* converts sucrose into levan, which is toxic to the cells [64]. Growth on sucrose therefore enables screening for cells where a double-crossover event has taken place, as only cells that have lost *sacB* will survive. Counter-selection against *sacB* is not always successful, as mutations that confer sucrose resistance sometimes occur [62]. Thus, a final screening for recombinants that have lost resistance to the antibiotic previously used for positive selection is needed [62].

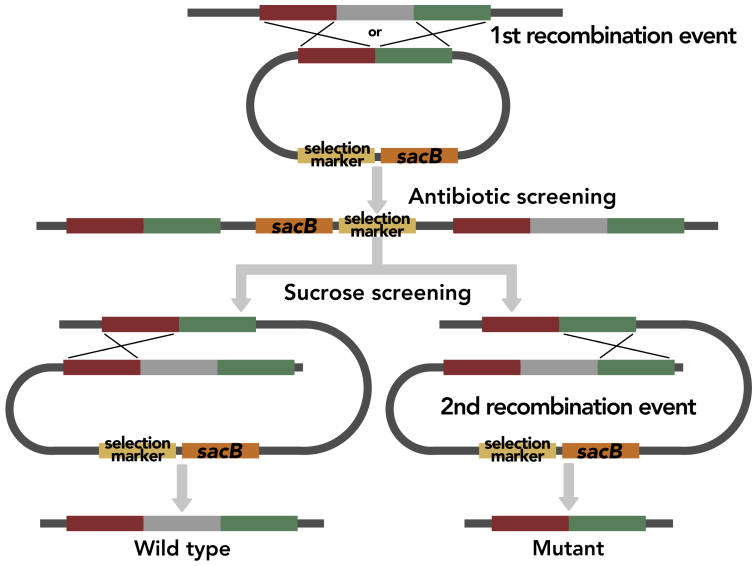

Figure 1.4: The two-step homologous recombination that results in a double-crossover event where, in this case, a region of DNA is permanently removed from the host genome. A region of homology (red and green segments) results in plasmid integration into the host genome in a single-crossover event. This is screened for with a positive selection marker such as an antibiotic resistance gene. Next, a region of homology results in a double-crossover event where the plasmid is excised and either the wild type is restored or the desired mutant is produced. This is screened for with a counter-selection marker such as *sacB*. Figure adapted from Nakashima and Miyazaki [65].

A. vinelandii is polyploid [26], and homologous recombination therefore requires several selection steps to ensure that as many chromosomes as possible are mutated. Several rounds of culturing using the appropriate antibiotic allows only cells that have incorpo-

rated the plasmid to grow, and the number of wild type chromosomes lost will therefore increase with each round of selection. Even after several selection steps however, the low homologous recombination frequency combined with the number of chromosome copies of *A. vinelandii* means that both wild type and mutated chromosome copies will often still be present. Mutations also tend to result in slowed growth, which may make obtaining pure mutants difficult.

1.3.3 Transposable elements

Transposable elements, or transposons, are DNA sequences capable of changing their own position in the genome by inserting themselves at new sites without using the previously discussed homologous recombination pathway [66]. Even though many of these sequences are no longer active transposons, transposons and transposon-derived sequences comprise over 40% of the genomes of humans, and around 1–5% of the genomes of bacteria [67]. Transposition may promote various genomic rearrangements such as insertions, deletions, inversions and even fusion of chromosomes [68]. Insertions or deletions may occur directly through transposition, or transposons may function as regions of homology in homologous recombination [67]. Insertion of a transposon upstream of a gene may result in gene activation, whereas insertion in the middle of a gene is likely to result in an inactivated gene [67]. Transposons may also rearrange and alter DNA by enabling transduction of flanking DNA [67]. Smaller transposons typically encode only genes needed to promote and regulate transposition, but larger bacterial transposons often encode antibiotic resistance and virulence genes which may be shared with other cells [66].

Different transposons use different pathways to insert themselves into new locations, and the pathway is determined by the type of transposase enzyme used [67]. Transposons may therefore be classified into five groups based on their use of a transposase from one of five protein families [67]. These include the DDE-transposases, the rolling-circle (RC)-transposases, tyrosine (Y)-transposases and the serine (S)-transposases [67]. Lastly, one group of transposons use a combination of a reverse transcriptase and an endonuclease [67]. The transposition pathways employed involve either 'cutting' or 'copying' the transposon out of the starting site, before the transposons either 'paste' or 'copy' themselves into the target site [67].

Barbara McClintock first discovered transposable elements [69] in 1947, and these transposons referred to as type II or DDE-transposons use the as of yet best characterized 'cut-and-paste' mechanism [67]. The encoded transposase of these transposons contains a DDE motif that enables it to both excise and integrate the transposon [67]. After excision, a circular DNA intermediate forms and the target sequence is captured, before the excised DNA is inserted [67]. Transposition using the 'copy' mechanism on the other hand, involves an additional replicative step that typically involves making a copy of the transposon with the help of the host's DNA replication machinery [67].

One of the first transposons identified was the bacterial composite transposon Tn5 [70, 68], which is a simple transposon that uses just one protein to perform most of the transposition steps [68], and it has therefore become a useful tool to better understand natural transposition mechanisms [71] as well as the role of transposons in evolution and genetic diseases [68]. Tn5 transposons have a low frequency of transposition, partly because of the relatively low activity of the encoded transposase [68]. The transposon also contains an inhibitor (Inh) that further down-regulates the transposase [72]. This has has made Tn5 transposons useful in genetic engineering, as they allow a sequence placed within the transposon to be used for stable insertion mutagenesis in gram-negative bacteria [56]. In addition, Tn5 transposons encode antibiotic resistance genes [73] which may be used as selectable markers to screen for transposon insertion. Maintenance of the cloning vector used to deliver the transposon can be avoided by using a suicide vector, and placement of the transposase gene outside the mobile element stops further transposition from occuring [56].

Tn5 encodes three genes conferring resistance to the antibiotics neomycin, streptomycin and bleomycin [73]. These are flanked by two IS50 elements, one of which (IS50R) is involved in transposition and encodes both the multifunctional cis-active transposase protein Tnp and a trans-dominant negative Inh [68]. The other IS50 element (IS50L) encodes an inactive version of Tnp [71]. The ends of Tn5 contain inverted 19-bp sequences called outside ends (OEs) which are recognized by Tnp and enable Tnp to catalyze transposition [68]. Tnp also recognizes a 19-bp inside end (IE) sequence, but this sequence is not involved in Tn5 transposition, which is an OE-OE event [68].

The Tn5 transposon uses the 'cut-and-paste' mechanism presented in figure 1.5 to insert itself into a target site [71], and Tnp is involved in almost all the steps [68]. It first recognizes and binds the OE sequences, and a synaptic complex is formed where one Tnp binds each OE [71]. Whether Tnp actually recognizes the OE sequences first, or Tnp oligomerization to form the Tnp:Tnp dimeric complex occurs prior to OE binding, is unknown [71]. Tnp then catalyzes DNA cleavage through a nucleolytic attack using water on phosphodiester bonds adjacent to the OEs [68]. The free 3'-OH group then attacks the opposite strand, resulting in the formation of a hairpin structure, and water mediated cleavage of the hairpin structure is catalyzed by Tnp [71]. The complex then binds the DNA target sequence and forms a target capture complex [68]. The sequence specificity required for target capture appears to be less specific than for the initial OE binding [71]. Both the transposon 3'-OH groups then carry out a concerted nucleophilic attack on the phosphodiester bonds of both target DNA strands [68]. This results in the strands being exchanged, as the transposon 3'-ends form covalent links to the 5'-ends of the target DNA [68]. Tnp is then released from the complex [74]. Insertion is most likely completed by host DNA repair mechanisms [71] that perform patch repair or a replicative resolution process [68] resulting in duplication of the 9-bp target sequence [71].

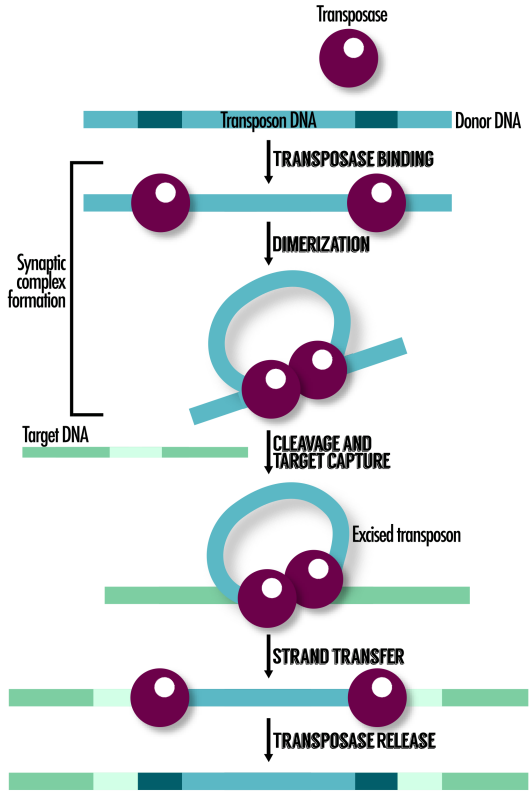

Figure 1.5: Transposition begins with transposase recognition and binding to the OE sequences of the transposon DNA, forming a synaptic complex. Transposase catalyzes cleavage, and the target DNA is captured. The transposase then catalyzes transfer of the transposon into the target DNA sequence, before the complex is disassembled. Figure adapted from Reznikoff [75].

1.3.4 The CRISPR microbial immunity system

CRISPRs, clustered regularly interspaced short palindromic repeats, were first discovered in the *E. coli* genome in 1987 by Ishino et al. [76]. The short protospacer sequences interspaced between the short direct repeats were later found to be exogenous sequences stemming from plasmids and viruses [77], forming the basis for the CRISPR-Cas microbial adaptive immune system [78]. Microbial immunity using CRISPR starts when a short DNA sequence from invading DNA is incorporated into the CRISPR array [77]. This is then transcribed to form precursor CRISPR RNA (pre-crRNA), which is eventually matured to crRNA [77]. crRNA contains the protospacer sequence and a repeat sequence [77], and the antisense RNA of the invading DNA thus serves as a memory of past invasions [79], enabling RNA guided endonucleases called Cas proteins to detect and cleave

foreign DNA complementary to the crRNA [78].

Three types (I-III) of CRISPR systems with different mechanisms are known [77], that all contain CRISPR-associated (Cas) genes, noncoding RNA and repetitive elements interspaced by short protospacer sequences [78]. Together, the repeats and protospacer sequences form the crRNA array [78]. A large complex of Cas proteins is involved in cleavage in both type I and III CRISPR systems, whereas type II systems only require a single Cas protein [77]. The simplicity of the type II CRISPR system has contributed to it becoming a powerful genome engineering tool [77]. In addition to the single Cas protein, type II CRISPR systems are characterized by having a protospacer adjacent motif (PAM) next to the crRNA target on the target DNA [78]. CRISPR type II also requires trans-activating crRNA (tracrRNA) that enables it to associate with Cas9 and for ribonuclease III to process the pre-crRNA [80].

The large multifunctional CRISPR-associated protein Cas9 of type II CRISPR sytems carries out the site-specific cleavage, and is presented in figure 1.6. Cas9 has two domains with nuclease ativity, the HNH and the RuvC-like domains [79]. The antirepeat-repeat RNA tracrRNA:crRNA duplex associates with Cas9 and guides DNA cleavage [81]. This is followed by processing by ribonuclease III and trimming [77]. Cas9 undergoes large conformational change upon binding the guiding RNA sequence, and again once the crRNA has identified the target sequence by base-pairing [77]. Both the target DNA and Cas9 also interact with the PAM, and PAM recognition seems to enable DNA separation and formation of an R-loop that enables RNA-DNA hybridization [82]. The HNH domain can then cleave the DNA strand complementary to the crRNA sequence, and the RuvC-like domain cleaves the other strand [81]. Cas9 has been shown to rarely cleave DNA off-target [77], and it seems that both near perfect base-pairing of the target and crRNA and PAM presence is necessary for cleavage to occur [81].

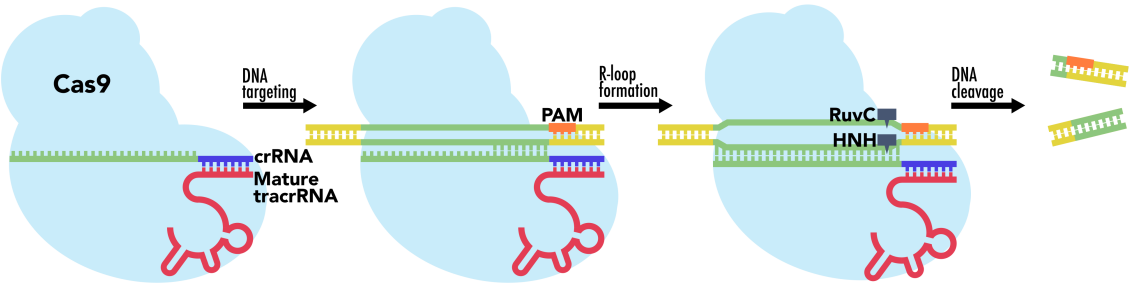

Figure 1.6: The natural CRISPR-Cas9 mechanism of the microbial immune system. A tracrRNA:crRNA duplex forms and associates with Cas9, thus guiding DNA cleavage. PAM interacts with Cas9 and the target DNA, and aids DNA separation and formation of an R-loop. RNA-DNA hybridization enables the HNH and RuvC domains of Cas9 to catalyze cleavage of the target DNA. Figure adapted from Doudna and Charpentier [77].

CRISPRS-Cas9 as a genetic engineering tool

Other genome editing technologies such as zinc-finger nucleases (ZFNs) and transcription activator–like effector nucleases (TALENs) can also cause double strand breaks (DSBs) at specific sites, but use DNA-binding proteins tethered to endonuclease catalytic domains [78]. The use of Cas9 and a guide RNA to target specific DNA loci by base-pairing however, has enabled highly specific and efficient genome modifications whilst also making the design process simpler [78]. Both ZFNs and TALENs call for protein engineering for every DNA target site [77], whereas CRISPR-Cas9 only requires that the target RNA sequence be modified to recognize the DNA target. With the use of CRISPR, it is also easy to target many loci at the same time.

Use of the natural CRISPR-Cas9 mechanism has been simplified further with the creation of a two-component system [77], constructed by fusing the tracrRNA:crRNA duplex of the natural microbial immune system into a chimeric single-guide RNA (sgRNA) [81]. The 5'-end of the sgRNA contains the 20-nucleotide target sequence, and the 3'-end the double-stranded structure that interacts with Cas9 [81]. The 20-nucleotide target sequence may be changed to target any DNA sequence adjacent to a PAM [81].

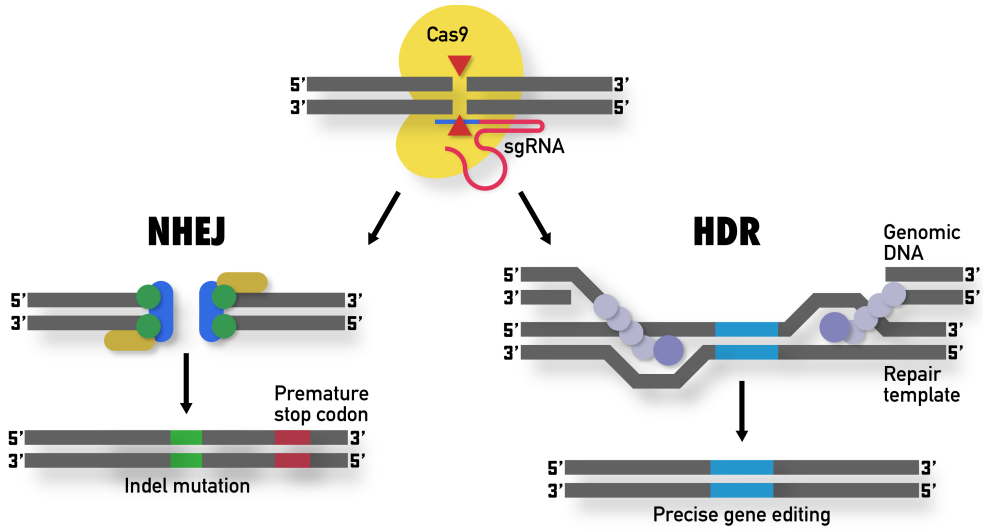

Figure 1.7: The DSB created by Cas9 can be repaired using one of two repair pathways. The error-prone NHEJ pathway uses the cell's DNA repair machinery to rejoin the cleaved ends. This may result in random insertion or deletion, and creation of a premature stop codon. If a repair template is present, the more precise HDR pathway may be used. Figure adapted from Ran et al. [78].

The mechanism that enables CRISPR-Cas9 to be used for genome modification is described by Ran et al. [78], and is presented in figure 1.7. Repair takes advantage of the

cell's already existing DNA damage repair pathways. If a DSB occurs and there is no repair template, the error-prone non-homologus end joining (NHEJ) pathway is used to repair the DNA. This results in an insertion or deletion (indel) mutation, which may in turn cause frameshifts and hence premature stop codons. If the goal is to create a gene knockout, the NHEJ pathway may be all that is required. Less frequently, and only if an exogenous repair template is present, is the high-fidelity homology-directed repair (HDR) pathway used to repair the DNA. This allows for precise modifications, and the template used may be dsDNA with homologous flanking regions to the insertion site, or an ssDNA oligonucleotide can be used if a minor edit is desirable.

Bacterial HDR involves one of three multi-subunit protein complexes RecBCD, AddAB or AdnAB [83]. These complexes have helicase and nuclease activity that enable them to bind to the DSB site and perform strand resection [83]. The result is processing of the DSB ends to create a 3'-overhang duplex [83]. The recombinase RecA is then loaded onto the duplex and forms a filament that is able to initiate strand invasion of the template strand [83]. DNA polymerase then uses the 3'-overhangs as primers to replicate the template strand [84]. Once complete, the protein complex resolves, before the ligase LigA seals the remaining ssDNA nicks [84].

Only a few bacteria, namely *Mycobacterium*, *Pseudomonas*, *Bacillus* and *Agrobacterium* [85], have the ability to use the NHEJ pathway. This means that if a template is not present, many species of bacteria are unable to repair the CRISPR-Cas9 DSB [85], and this may be lethal. The same goes for species that are not effective at using the HDR pathway. This may lower transformation efficiency and lead to negative pressure on non-edited cells. Toxicity due to Cas9 and off-target effects may prevent successful transformation [86]. DSBs may thus have a significant fitness cost, and in some cases may lead to cell death [87]. In the polyploid species *A. vinelandii* [26], repair without a template will result in disruption to the chromosome. CRISPR mutagenesis requires the use of a curable plasmid, such that once the mutation is complete, the risk of further off-target mutations is eliminated.

CHAPTER 2

METHODS

This chapter presents the methods used in this work, including general techniques, cloning procedures, methods for DNA transfer and incorporation into the genome, PCR, sequencing, enzymatic and luciferase assay procedures and bioinformatics tools used.

2.1 General techniques

E. coli DH5α was used for standard cloning purposes. The spectinomycin resistant [88] strain S17.1 was used for conjugation purposes. For transposons that require the π-protein to replicate, *E. coli* S17.1-λpir was used. The strain ATCC12518 was used as the wild type strain of *A. vinelandii*.

Bacterial strains were inoculated in liquid media or on plates with the appropriate antibiotics and the inducer *m*-toluate if necessary. *E. coli* was typically grown in liquid LB medium or on LA plates and was incubated ON at 37 °C. *A. vinelandii* was grown in liquid BM or RA1 medium or on BA plates and was incubated for 1-3 days at 30 °C.

For short-term storage of up to 3-4 weeks, *E. coli* plates were stored at 4 °C and *A. vinelandii* plates were stored at room temperature, wrapped up to avoid contamination and the plates drying out. For long-term storage of cells, glycerol stocks were prepared in which 300 µl 60% glycerol was mixed with 1 ml culture, for a final glycerol concentration of $\sim$15%. The stocks were then stored at -80 °C. To revive frozen cultures, the bacteria was streaked out on plates and inoculated until visible colonies were formed before being moved to liquid media.

A detailed description of the growth media, solutions and antibiotics used in this work is presented in appendix A.

2.2 DNA transfer

Section 2.2 presents the methods used in this work to transfer plasmid DNA to *E. coli* and *A. vinelandii*.

2.2.1 Preparation of competent *E. coli*

DNA molecules are highly negatively charged and are therefore unable to bind the negatively charged cell surface of most bacteria, pass through the wall-membrane complex and into the cytoplasm [89]. To promote transformation, the introduction of naked heterologous DNA into bacteria, the cells therefore first need to be made competent [89]. Competence may be achieved via electroporation, where an electrical voltage is discharged across the cell membrane, or with the use of chemicals [90]. In the early 1970s, Mandel and Higa [91] and Cohen et. al [92] were the first to show that subjecting bacteria to ice cold $CaCl_2$ followed by a heat shock made the cells capable of taking up bacteriophage and plasmid DNA [93].

E. coli is widely used as a host organism in DNA cloning, but the cells are not naturally competent [89]. To achieve the highest possible transformation efficiency, cells are first

harvested in their most fit state, during the log phase (OD_{600} ∼0.4) of growth. Once made competent, transformation is still highly inefficient [89]. More efficient transformation has been achieved with modifications to the original procedure, which includes a longer exposure time to $CaCl_2$, substitution of or addition to Ca^{2+} with Rb^{+}, Mg^{2+}, Mn^{2+} and K^{+}, as well as addition of compounds like dimethyl sulfoxide (DMSO), dithiothreitol and cobalt hexamine chloride [94, 89].

The mechanism through which these chemical treatments make the cells competent is not well understood, although $CaCl_2$ treatment is thought to help DNA interact with the cell surface [89]. Divalent cations are used to overcome the repulsion caused by the negative charges, as they bind both the negatively charged lipopolysaccharides on cell surfaces and the DNA itself, and thus neutralize the charges and coordinate interactions [95]. Ca^{2+} is also believed to help DNA adsorb to the cells [95]. Heat-shock treatment is then used to help the DNA pass into the cytosol [89]. DNA uptake is believed to occur via membrane channels [95]. It is also possible that Ca^{2+} alters membrane permeability by weakening and disrupting the membrane, enabling DNA to pass without the use of channels [95]. In addition, divalent cations may cause folding of DNA into a compact structure, which in turn may ease DNA uptake [95].

Procedure

A starter culture where *E. coli* was inoculated in 10 ml Psi medium was made and incubated ON at 37 °C. 1 ml of the ON culture was inoculated in 100 ml Psi medium and incubated at 37 °C. OD_{600} was measured periodically over a period of 1.5-2.5 hours until it reached 0.4. At this point, the culture was placed on ice for 15 minutes along with TFB1 and TFB2. Next, the culture was transferred to cold centrifuge bottles. Cells were harvested by centrifugation for 5 minutes (4 500 rpm, 4 °C), and the supernatnat was decanted. The cells were carefully resuspended in 40 ml cold TFB1, before they were incubated on ice for 5 minutes. Again the cells were harvested by centrifugation for 5 minutes (4 500 rpm, 4 °C), and the supernatnat was decanted. The cells were carefully resuspended in 3 ml cold TFB2. 100 µl was aliquoted into pre-chilled 1.5 ml tubes, which were next snap frozen in liquid N_2 for 5-10 seconds. The RbCl competent cells were stored at -80 °C.

The *E. coli* strains DH5α, S17.1 and S17.1-λpir were made competent in this work.

2.2.2 Transformation of DNA to competent *E. coli*

The process through which cells take up and express foreign DNA is called transformation [89]. This starts by using naturally competent cells or cells that have been electroporated or chemically manipulated with cations to become competent. Next, temperature manipulation facilitates uptake of the foreign DNA into the host cell [95].

In this work, heat-shock transformation was performed on RbCl-competent cells to facilitate transfer of plasmids into *E. coli*. Heat-shocking the cells produces increased brownian motions of molecules outside the cells, and this is thought to contribute to pushing the DNA into the cells [95]. The heat-shock also depolarizes the membrane, which may aid the negatively charged DNA in entering the cells [89].

Procedure

100 µl RbCl-competent cells was thawed on ice. 2 µl DNA was added to the tube and the contents were mixed gently, before the cells were incubated on ice for 1 hour. 900 µl SOC medium was pre-warmed to 37 °C. The cells were subjected to heat-shock at 37 °C for 2 minutes, before being incubated on ice for another 2 minutes. 900 µl SOC medium was then added to the cells, before the cells were incubated at 37 °C for 2 hours. Finally, 200 and 800 µl was plated on two LA plates.

2.2.3 Conjugation to *A. vinelandii*

Conjugation is a process by which DNA is transferred from a donor to a recipient cell by cell-to-cell contact [96]. The donor cell must be able to synthesize a conjugative pilus, which can identify and bring a recipient cell into close contact [96]. A mating bridge is formed between the cells that DNA is then transferred via [96]. The plasmid that is to be transferred must contain an origin of transfer (*oriT*) [97]. The DNA is nicked prior to tranfer and is then recircularized once transferred, before it is replicated and established in the recipient cell [96].

The *E. coli* strains S17.1 and S17.1-λpir were used as donor strains in this work. The strain S17.1 is a derivative of *E. coli* K-12 that has integrated the RK2 plasmid, which provides proteins that are necessary for conjugation [97]. For RK6 based transposons that require the π-protein to replicate, *E. coli* S17.1-λpir was used, which encodes the necessary π-protein (*pir*) in its genome [97]. *A. vinelandii* was used as the recipient of DNA.

Alginate producing strains of *A. vinelandii* contain an alginate coating that may acts as a barrier preventing exogenous DNA from being taken up [15]. Removal of alginate by washing the cells with glycerol could therefore increase the conjugation efficiency.

Procedure

A. vinelandii was incubated on BA for 2 days, before a colony was transferred to 10 ml BM which was incubated for 2 more days. Finally, 400 µl culture was inoculated in 10 ml BM and incubated for 18-20 hours, until reaching an OD_600 of 0.4.

E. coli containing the plasmid was incubated on LA ON, before a colony was transferred

to 10 ml LB which was incubated ON. Finally, 1 ml culture was inoculated in 10 ml LB without antibiotics for 2-3 hours, until reaching an OD_600 of 0.4.

5 ml *A. vinelandii* culture was transferred to a 50 ml tube and centrifuged for 7 minutes at 7350 rpm. The supernatant was discarded. The cell pellet was washed twice by resuspension in 5 ml 10% glycerol, before the tube was centrifuged and the supernatant removed. 5 ml *E. coli* culture was added. The tube was centrifuged for 5 minutes at 4000 rpm and the supernatant was removed. The pellet was resuspended in 100 µl BM. Next, the cells were plated as a drop on LA, and incubated ON.

The cells on the plate were collected, and BM was used to prepare a dilution series. 100 µl of the undiluted, 10^{-1} and 10^{-2} dilutions, as well as 250 µl of the 10^{-1} dilution, was plated on BA. 100 µl of the 10^{-5}, 10^{-6} and 10^{-7} dilutions was plated on BA without antibiotics. The plates were incubated for 3-5 days.

2.2.4 Homologous recombination in *A. vinelandii*

Because plasmids are inherently unstable, it is often desirable to incorporate DNA permanently into the host genome [63]. In addition, procedures that aim to inactivate genes or replace a promoter or gene also require that the DNA is incorporated into the chromosome. This can be achieved using homologous recombination, which uses plasmids with homologous regions to host target sequence(s) to transfer DNA into or out of the genome [62].

Homologous recombination is performed in two consecutive recombination steps. The plasmid used is typically made unable to replicate in the host, often with the use of an inducer needed for replication. A positive selection marker such as an antibiotic resistance gene is then used to screen for cells that underwent the first single-crossover event, where the entire plasmid is incorporated into the host genome [63]. In the next double-crossover event, the plasmid is excised, and selection for the absence of a counter-selection marker such as *sacB* is used to screen for cells that have undergone the double-crossover event [64]. Because mutations that confer sucrose resistance tend to occur, a third selection step is needed that screens surviving colonies for loss of resistance to the previously used antibiotic [62].

A. vinelandii is a polyploid organism, and may contain up to 80 chromosome copies [98]. Because of this, the process of homologous recombination in *A. vinelandii* requires many generations of selection for the insert, and even then it is often challenging to obtain pure mutants.

Procedure

Transconjugants were inoculated in BM. Half was inoculated with the inducer, and half was inoculated without. The cultures were incubated for 2-3 days. The cultivation was repeated 4 times (K1-K5) by transferring 1 ml from the previous culture to a new one containing the same medium. Glycerol stocks were prepared from each culture. A final culture (K6) was prepared without the addition of antibiotics.

K6 was used to prepare a dilution series. 100 µl of the undiluted, 10^{-1}, 10^{-2}, 10^{-3} and 10^{-4} dilutions was plated on BA with the counter-selection marker sucrose and the antibiotic. The plates were incubated for 2 days.

Fifty colonies from the counter-selection plates were plated on BA with and without addition of the antibiotic. The plates were incubated for 2 days. Next, screening for mutants from colonies displaying sensitivity to the antibiotic was achieved by colony PCR.

2.3 Isolation of DNA from culture

Section 2.3 presents the methods used to isolate genomic DNA from *A. vinelandii* and plasmid DNA from *E. coli*.

2.3.1 Isolation of genomic DNA from *A. vinelandii*

Isolation of total genomic DNA from a cell culture begins with cell wall lysis. Lysis is typically achieved with the use of detergents [53], but the process may also involve the use of lysozyme to break down peptidoglycan [99] and/or mechanical grinding [53]. The debris can then be removed using centrifugation, before proteins are removed [53]. Often, a concentrated salt is added that lowers the solubility of proteins and produces a protein-rich precipitate [100]. Finally, alcohol is typically used to precipitate the total nuclei acids [53]. If needed, RNA can be hydrolyzed by treatment with the nuclease RNase [101]. Conversely, DNA may be removed using DNase. For many applications however, this is not necessary [102].

In this work, genomic DNA from *A. vinelandii* ATCC12518 was isolated using the Epicentre MasterPure Complete DNA and RNA Purification Kit [102] from Lucigen. This kit uses a cell lysis reagent along with proteinase K for digestion of proteins. Debris are removed using a rapid desalting process, before the total nucleic acids are precipitated.

Procedure

For cell lysis, cells from an ON culture were pelleted down by centrifugation for 5 minutes at 13 000 rpm. The supernatant was removed before the pellet was resuspended in 300 µl Tissue and Cell Lysis Solution with 1 µl added Proteinase K. This was followed by incubation at 65 °C for 15 minutes, vortexing every 5 minutes. After cooling to 37 °C, 1 µl 5 µg/µl RNase A was added. The contents were mixed gently, before being incubated at 37 °C for 30 minutes followed by 3-5 minutes on ice.

Next, for precipitation of total nucleic acids, 150 µl MPC Protein Precipitation Reagent was added and the tube was vortexed for 10 seconds. Debris was pelleted by centrifugation for 10 minutes (15 000 rpm, 4 °C). The supernatant was transferred to a clean tube and 500 µl isopropanol was added and mixed by inverting the tube 30-40 times. The total nucleic acids were then pelleted by centrifugation for 10 minutes (15 000 rpm, 4 °C). Next, isopropanol was carefully removed. The pellet was rinsed twice by resuspension in 500 µl 70% ethanol followed by centrifugation for 10 minutes (15 000 rpm, 4 °C) and careful removal of the supernatant. To remove any remaining ethanol, the tube was left to air dry for 30 minutes. The total nucleic acids were then resuspended in 100 µl buffer EB, which was incubated at 30 °C for 1 hour. The isolate was stored at -20 °C.

2.3.2 Isolation of plasmid DNA from *E. coli*

During cloning work, plasmid have to be isolated from the chromosomal DNA present in the cells [53]. In 1979, Birnboim and Doly [103] first described the alkaline lysis procedure that is still commonly used today [53]. This procedure allows separation of plasmid and genomic DNA because of their differential denaturation [104]. In this work, the ZR Plasmid Miniprep-Classic from Zymo Research [105] was used to isolate plasmid DNA from *E. coli*. This kit uses a modified version of the original alkaline lysis procedure.

The alkaline lysis procedure begins with pelleting the cells and resuspending them in a resuspension buffer. Next, the cells are treated with a buffer containing sodium dodecyl sulphate (SDS) and NaOH. SDS is a detergent that damages the cell wall and denatures proteins, making their removal easier later on [53]. High pH also results in cell wall damage and protein denaturation, but more importantly in shearing of genomic DNA and disruption of the hydrogen bonds holding dsDNA together [53]. To avoid shearing the DNA into too small fragements, which could allow it to reanneal later and contaminate the plasmid DNA, the cells must be handled carefully [53].

A third buffer containing acidic potassium acetate is used to neutralize the solution [53]. This results in renaturing of the supercoiled plasmid DNA, enabling it to emerge unscathed from the previous step [53]. The longer genomic DNA molecules however are unable to correctly renature. Instead they aggregate and become insoluble [53]. The high salt concentration also cause high-molecular RNAs and protein-SDS complexes to precipitate [106]. In this way, the three major macromolecule contaminants can be removed in one

centrifugation step, leaving the plasmid DNA along with polysaccharides and low molecular weight RNA [103].

To remove remaining contaminants, the plasmid DNA is bound to a silica matrix with the help of hydrogen-disrupting ions called chaotropic agents [107, 108]. These denature the DNA by disturbing base-pairing, promoting adsorption of the DNA to the silica matrix [108]. Other contaminants do not bind and can instead be washed away [53] using ethanol-based buffers, before the DNA is finally renatured and eluted from the matrix using a buffer of low ionic strength [106].

Procedure

All centrifugation steps were performed at room temperature at 13 000 rpm. Cells from an ON culture were pelleted by centrifugation for 2 minutes. The supernatant was removed and the pellet was resuspended in 200 µl P1 Buffer. Next, 200 µl P2 Buffer was added. The contents were mixed by inverting the tube 2-4 times. Once the solution turned clear, purple and viscous (1-2 minutes), 400 µl P3 Buffer was added. The contents were mixed gently incubated (4-5 minutes) until turning yellow. This was followed by centrifugation for 5 minutes. The supernatant was carefully transferred to a Zymo-Spin IIN column. The flow-though was collected in a collection tube by centrifugation for 30 seconds, and subsequently discarded. The column was returned to the collection tube and 200 µl Endo-Wash Buffer was added, before being centrifuged for 1 minute. 400 µl Plasmid Wash Buffer was added, followed by another centrifugation for 2 minutes. The column was transferred to a clean tube, and 100 µl DNA Elution Buffer was added to the column. After incubation for 1 minute at room temperature, the DNA was eluted by centrifugation for 30 seconds. The isolate was stored at -20 °C.

For low copy number plasmids, the amount of cell culture used per Zymo-Spin IIN column was doubled by transferring the supernatant from one tube first, followed by centrifugation for 30 seconds. This was repeated with a second tube. In addition, the volume of DNA Elution Buffer was lowered to 30 µl.

2.4 Measurement of DNA concentration

Reactions and procedures that involve DNA, such as restriction endonuclease reactions or gel electrophoresis, often require that the amount of DNA present is known. To determine the average concentration of DNA in a sample of isolated plasmid DNA, the NanoDrop One Microvolume UV-Vis Spectrophotometer from Thermo Scientific was used.

Determination of DNA concentration by spectrophotometric analysis is based on the intrinsic absorptivity of DNA. Nucleic acids absorb light and produce a characteristic peak at 260 nm. When a DNA sample is exposed to UV light at a wavelength of 260 nm, the

light is passed through the sample and the attenuation in the light reaching the detector is measured and expressed as absorbance of the sample [109]. The absorbance can then be used to calculate concentration using the Beer-Lambert equation [109].

$$C = \frac{A}{\varepsilon L}$$

where C is the DNA concentration (M), A is the UV absorbance (AU), ε is the wavelength-dependent molar absorptivity coefficient ($M^{-1}cm^{-1}$) and L is the light path (cm). Nanodrop measures absorbance and calculates nucleic acid concentration automatically, and can also provide information on the purity of the sample [109].

Procedure

The NanoDrop One Spectrophotometer was set to measure concentration of dsDNA. The instrument was cleaned with 2 µl distilled water. 1 µl Zymo DNA Elution Buffer was used as a blank. 1 µl sample was loaded onto the pedestal, and a spectral measurement was initiated. Once measurements were completed, the instrument was again cleaned using distilled water.

2.5 Restriction cutting of DNA

Restriction endonucleases are enzymes that recognize and cleave DNA in a specific pattern at specific sequences within DNA [53]. Restriction enzymes, and in particular the class of restriction enzymes referred to as type II restriction endonucleases, are widely used in cloning work and for gene analysis [110]. They enable digestion of DNA at specific and predetermined sites so fragments can be separated and in turn cloned into new vectors. In addition, this site-specific cleavage is useful for verification of plasmids.

The first restriction enzyme was isolated from *E. coli* in 1968 [111], but its restriction site remained unclear. Two years later, Smith and Welcox [112] first isolated the restriction enzyme HindII and were able to demonstrate its recognition sequence [53]. Today, more than 3000 type II restriction enzymes are known [110]. The restriction enzymes are named after the source where they were first discovered, the first letter indicating the genus and the next two letters the species. The accompanying number indicates the order of discovery [53].

Most restriction enzymes in use are type II restriction enzymes, which may be divided further into subgroups depending on their features [110]. Type II restriction enzymes are typically homodimers [110] with a structural core consisting of a β-sheet and and two α-helices [53] that recognize a short 4-8 bp sequence [110]. The recognition sequence is usually palindromic, meaning that the 5' to 3' sequence of one strand is identical to

the 5' to 3' sequence of the other strand. This sequence may be continous, or it may be interrupted by one or more nucleotides [53]. Type II restriction enzymes tend to require Mg^{2+} as a cofactor, and they cleave DNA close to or within the recognition sequence [110].

Restriction endonucleases are used by their prokaryotic host organisms to protect against foreign DNA, in particular bacteriophage DNA [110]. The host DNA is protected against cleavage by methylases, enzymes that methylate the DNA recognition sequence to stop restriction enzymes from cleaving its own DNA [53]. In addition, restriction endonucleases may be involved in recombination and transposition [110]. They first bind non-specifically to DNA through interaction with the DNA backbone, and facilitated diffusion then aids in locating their target sequence [110]. Recognition of the target sequence occurs through direct interaction with the bases via hydrogen bonding and van der Waals interactions as well as hydrogen bonding with the backbone [110]. This triggers a large conformational change to both the DNA and the enzyme, activating the catalytic centers of each enzyme subunit [110]. Cleavage results in a DNA strand with a 3'-hydroxyl and a 5'-phosphate [110], and the cut can result in either blunt ends or ends with an overhang, called sticky ends [53]. The frequency at which a restriction enzyme cleaves DNA depends on the length and GC content of its recognition sequence [53].

All restriction enzymes used in this work are presented in appendix G.

Procedure

The appropriate endonuclease(s) were selected using Benchling. Depending on the enzyme(s) used, the 10X NEB Buffers 3.1 or CutSmart were used. 3-17 µl DNA, 2 µl buffer and 0.5-1.5 µl enzyme(s) was mixed and autoclaved deionized water was added to a total of 20 µl. The reaction mixture was incubated at 37 °C for 1 hour. The digested DNA was either stored at -20 °C or separated directly using gel electrophoresis.

The enzymes PstI and HindIII were used to digest λ-DNA for use as size markers during gel electrophoresis. The standards are presented in appendix B. They were prepared by mixing 10 µl λ-DNA, 10 µl NEB Buffer, 79 µl autoclaved deionized water and 1 µl enzyme. The reaction mixture was incubated at 37 °C for 1 hour, before inactivation at 65 °C for 10 minutes. The digested DNA was stored at -20 °C.

2.5.1 Blunting of DNA

To enable ligation of restriction digested fragments with incompatible sticky ends, the DNA can be blunted. Blunting involves single-stranded overhangs being removed or filled in by removal of nucleotides or addition of nucleotides to the complementary strand. The Klenow fragment of DNA Polymerase I and T4 DNA Polymerase may be used to fill in by using the sticky end as a template for DNA synthesis in the 5' to 3' direction, and they can also remove sticky ends in the 3' to 5' direction by using their exonuclease activity [113].

Procedure

When blunting with the Klenow fragment of DNA Polymerase I, 1 µl 10 mM dNTP and 0.5 µl of the Klenow fragment of DNA Polymerase I was added to a 20 µl completely digested restriction reaction. The contents were mixed and incubated at 37 °C for 15 minutes.

For blunting with T4 DNA polymerase, 2 µl 10 mM dNTP and 0.5 µl T4 DNA Polymerase was added to a 20 µl completely digested restriction reaction. The contents were mixed and incubated at 14 °C for 15 minutes.

2.6 Separation of DNA by gel electrophoresis

Gel electrophoresis is commonly used to visualize DNA from a PCR or restriction reaction. It takes advantage of the fact that DNA molecules, due to the phosphate groups in the sugar-phosphate backbone, are highly negatively charged [53]. The negative charge per unit of DNA is constant, enabling separation by size using a buffer that can carry a current and applying an electric field [53]. The voltage then forces DNA to move from the negative to the positive electrode [53]. In this work, TAE buffer composed of Tris, acetic acid and EDTA was used. Acetate and Tris provide anioinic and cationic ions that carry the current and buffer the pH, and EDTA inactivates any DNA nucleases present by chelating Mg^{2+} [114].

Agarose based gels were used in this study. Agarose is a linear polysaccharide isolated from seaweed made up of alternating galactose and 3,6-anhydrogalactose [53], and typically allows separation of DNA molecules ranging between 100 bp and 25 kb [115]. The polymers gelate to form a porous gel matrix that enable it to function like a molecular sieve [115]. The matrix imparts more friction on larger DNA molecules than smaller ones, and DNA of different sizes thus travel through the gel at different rates [115]. The size of separated DNA molecules can be determined as the distance migrated is proportional to the logarithm of molecular weight [115]. Alternatively, molecular markers of known size are often used as a comparison to determine fragment size. Standards used in this work are presented in appendix B.

The inverse relationship between distance migrated and the log of the molecular weight means that larger DNA molecules are harder to resolve from each other. Large DNA molecules tend to become entangled in the matrix beyond what is to be expected just based on their size [53]. Beyond molecular size, the conformation of the DNA also affects migration rate. For example, *E. coli* plasmid DNA is negatively supercoiled into compact structures that move through the gel relatively easily [53]. If such a plasmid is nicked and the supercoils are eliminated, migration rate will decrease. A linearized plasmid will have an intermediate migration rate [53]. In addition to these factors, migration rate depends on the agarose type and concentration used, most gels ranging between 0.5-2% [115]. Also, the voltage applied, the buffer used and stains such as ethidium bromide (EtBr) affect

migration rate [115].

Staining of DNA, either before or after gel electrophoresis, allows it to be visualized in the gel. The fluorescent compound EtBr is commonly used and works by binding to DNA, enabling it to be visualized under UV-light [53]. EtBr is toxic, and safer alternatives like GelRed and GelGreen were used in this work. GelRed is more sensitive [116], and was used for visualization of DNA fragments only. For excision of fragments from the gel, Gelgreen [117] was used along with a blue light conversion screen that prevents UV-induced damage to the DNA. Before DNA samples are loaded into the pre-cast wells of the gel, a loading dye is typically added. This dye adds density to the sample, making it sink into the wells. It also adds color so the sample can more easily be visualized during loading. The loading dye moves through the gel at a standard rate, and can therefore also be used to estimate how far the DNA has travelled [115].

Procedure

Samples were prepared by combining 100-150 ng DNA, autoclaved deionized water and 10X Loading Dye to a total of 15-20 µl. Standards were prepared by combining 3 µl DNA, 10 µl autoclaved deionized water and 1.5 µl Loading dye. 0.8% agarose with TAE buffer and GelRed or GelGreen was poured into a tray with a comb inserted. Once set, the comb was removed and the gel was placed in a buffer tank and TAE was added to soak the gel. Samples were loaded, the BioRad PowerPac Basic Power Supply was programmed to the desired voltage and current was applied for as long as needed. Typically, 100 V was applied for 40-90 minutes, depending on the size of the fragments to be separated. The BioRad ChemiDoc XRS+ was used with the ImageLab Software to visualize fragments. For gels containing GelGreen, a blue light conversion screen was used. DNA fragments were removed from the gel by visualization under UV-light using a scalpel or a cutting tool. Samples were either purified directly or stored at -20 °C.

2.6.1 Purification of DNA from gel

DNA fragments separated using gel electrophoresis were purified from the gel by the NEB Monarch DNA Gel Extraction Kit. This kit uses a buffer containing the chaotropic agents guanidine thiocyanate and sodium iodide combined with heating to dissolve the gel, before the DNA is transferred to a silica-based column and washed using an ethanol-based wash buffer. Chaotropic salts are known to disrupt the three-dimensional structure of macromolecules like DNA and facilitate binding to a silica matrix [118]. This enables the DNA to be separated from the dissolved gel, which can be removed by centrifugation. Remaining salt and other impurities can be removed using alcohol [118]. A low ionic strength elution buffer containing Tris and EDTA is finally used to elute the DNA from the column [118].

Procedure

All the centrifugation steps were carried out at 13 000 rpm at room temperature. The excised DNA fragment was diluted with four volumes of Gel Dissolving Buffer and incubated at 37-55 °C for 5-10 minutes. To ensure that the gel was dissolved, the sample was vortexed periodically. The solution was transferred to a Monarch DNA Cleanup Column, and the flow-through was collected in a collection tube by centrifugation for 1 minute, and subsequently discarded. The column was returned to the collection tube and 200 µl DNA Wash Buffer was added, before being centrifuged for 1 minute. The washing step was repeated a second time. The column was transferred to a clean tube, and 15 µl DNA Elution Buffer was added to the center of the matrix. After incubation at room temperature for 1 minute, the DNA was eluted by centrifugation for 30 seconds. The isolate was stored at -20 °C.

2.7 Ligation of DNA fragments

During cloning, the enzyme DNA ligase was used to join DNA molecules together. DNA ligases are capable of joining or repairing both single and double stranded breaks in DNA by catalyzing formation of phosphodiester bonds [119]. They are involved in replication, repair and recombination [119], and since its discovery in the 1960s ligases have also become useful as a tool for researchers [53].

The energy required for formation of a bond between the juxtaposed free 5'-phosphate and 3'-hydroxyl end of DNA fragments is supplied via NAD^+ in bacteria, and via ATP in animals and bacteriophages [53]. The ATP-dependent T4 DNA ligase originally discovered in the bacteriophage T4 was used in this work. Even though it ligates sticky ends more efficiently, T4 DNA ligase can be used to ligate both sticky and blunt ends [53]. The mechanism of action of ATP-dependent ligases begins with hydrolysis of pyrophosphate, which supplies the energy needed to drive the reaction [53]. ATP first reacts with and forms a bond to a lysine residue in the enzyme's active site, forming an enzyme-AMP intermediate [53]. AMP is transferred to and activates the 5'-phosphate end of a DNA fragment [53]. A 3'-hydroxyl end then acts as a nucleophile, AMP is released, and a phosphodiester bond is formed between the two ends [53].

Procedure

The molar ratio of insert to vector used for ligation was kept around 3:1, for a total of 17 µl DNA. 2 µl NEB 10X T4 DNA Ligase Buffer and 1 µl NEB T4 DNA Ligase was also added. The sample was incubated at 16 °C ON, and was subsequently transformed to competent *E. coli* cells or stored at -20 °C.

2.8 TOPO cloning

The Zero Blunt TOPO PCR Cloning Kit was used to insert blunt-end PCR products into a plasmid vector in one step, without the use of ligases. The one step process is made possible with the use of topoisomerase I from the *Vaccinia* virus [120]. DNA topoisomerases are enzymes that alter the supercoiling of DNA by introducing transient double or single strand breaks in the DNA. This is followed by strand rotation or passage, before the DNA is religated [121]. The topoisomerase I used for TOPO cloning recognizes and cleaves one strand of the DNA backbone after the sequence 5'-(C/T)CCTT-3' [122]. As depicted in figure 2.1, the energy from the cleavage reaction is conserved through formation of a covalent bond between a tyrosyl residue (Tyr-274) on the enzyme and the 3'-phosphate of the cleaved backbone. This energy may later be released when a 5'-hydroxyl from another cleaved strand attacks the bond, releasing the enzyme and joining the DNA [123].

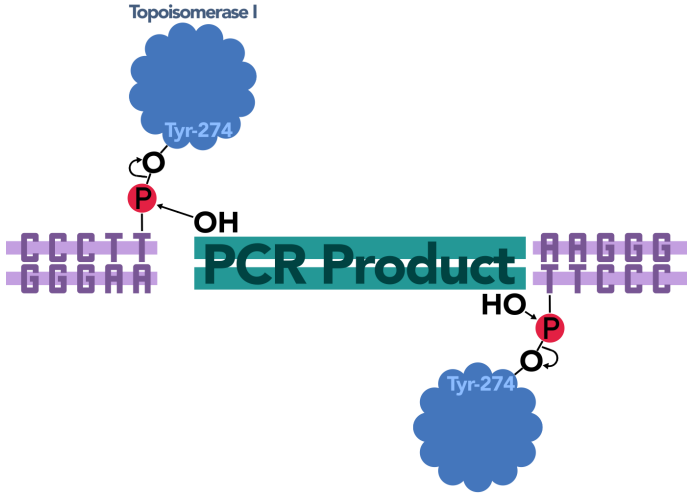

Figure 2.1: The pCRTM-Blunt II-TOPO vector contains topoisomerase I already bound to the 3'-end of each DNA strand. When a DNA fragment is inserted, energy conserved in the covalent bond between Tyr-274 of topoisomerase I and the 3'-phosphate of the DNA backbone is released as a 5'-hydroxyl attacks the bond, enabling release of the enzyme and joining of the two DNA fragments. Figure adapted from the Zero Blunt TOPO PCR Cloning Kit [120].

The plasmid used for TOPO cloning is a linearized version of pCRTM-Blunt II-TOPO, where topoisomerase I is already bound to the 3'-end of each strand [120]. The blunt-end insert may be inserted in either direction, and the plasmid can next be transformed into competent cells. The lethal *E. coli* gene *ccdB* is fused to the C-terminus of the LacZα fragment of pCRTM-Blunt II-TOPO [120]. This permits only colonies that are positive for the recombination to grow, as LacZα-ccdB will be disrupted in plasmids containing the inserted fragment [120]. Cells that contain the non-recombinant vector are killed,

and other screening techniques like blue/white screening are therefore not necessary. In addition, the vector contains EcoRI sites flanking the insertion site, making excision of the inserted fragment easy [120]. Selection in *E. coli* is made possible by the presence of both kanamycin and zeocin resistance genes, and the plasmid contains M13 forward and reverse primer sites that may be used for sequencing of the insert [120].

Procedure

For the reaction, 2 µl PCR product, 0.5 µl salt solution from the cloning kit and 0.5 µl vector was mixed gently and allowed to incubate at room temperature for 30 minutes. The tubes were placed on ice, before the plasmid was transformed to *E. coli*.

2.9 Polymerase chain reaction

The polymerase chain reaction (PCR) is used to amplify a DNA sequence in vitro. It was invented in the mid 1980s by Kary Mullis [124], and has since then become a widely used tool in molecular biology. PCR depends on the use of a heat stable DNA polymerase, an enzyme that catalyzes synthesis of DNA from mono-deoxyribonucleoside triphosphates (dNTPs) [125]. The reaction also requires an initiating oligo- or polynucleotide, called a primer, that has a 3-hydroxyl end that the polymerase can use a starting point for synthesis of a new DNA strand [125]. The PCR principle is thus based on the principles of DNA replication, but differs from replication in that copying of the DNA template is repeated over and over in cycles of repetitive heating and cooling [53]. This enables rapid synthesis of large amounts of the DNA sequence between two primers [53].

Reece [53] details how the reaction is based on the three stages denaturation, annealing and extension. During denaturation, heat makes the two DNA strands separate. Next, cooling during the annealing stage allows two primers flanking the target sequence to bind to the DNA. These primers are typically 17-30 nucleotides long, and are designed so that their free 3'-ends are facing each other. In the extension stage, a DNA polymerase can then attach to the free 3'-end of each primer and use dNTPs to synthesize a new strand in the 5'-to-3' direction. In this way, DNA is synthesized on both strands in the region between the two primers.

The DNA synthesis does not terminate at a specific point. As depicted in figure 2.2, it stops during the heat denaturation of the next cycle. Yet, at the end of the PCR program, almost all the DNA fragments produced will be of the same length. In the second cycle of PCR, both the original DNA and the products from cycle 1 serve as templates. New strands synthesized from the original DNA will again have undefined 3'-ends, but new strands synthesized from the strands produced in cycle 1 will have both a defined 5'- and 3'-end. In this case, replication terminates earlier simply because replication cannot continue past the template sequence. In the third cycle, the strands from the previous two cycles will

again be used as templates. After this round of replication, two DNA fragments where both strands are exact copies of the target sequence are produced. From here on out, the number of these fragments increases exponentially, and by the time the PCR amplification is complete, the vast majority of the fragments will be exact copies of the target sequence. A few PCR products with incorrect ends will remain, but the number will be so low as to be almost insignificant.

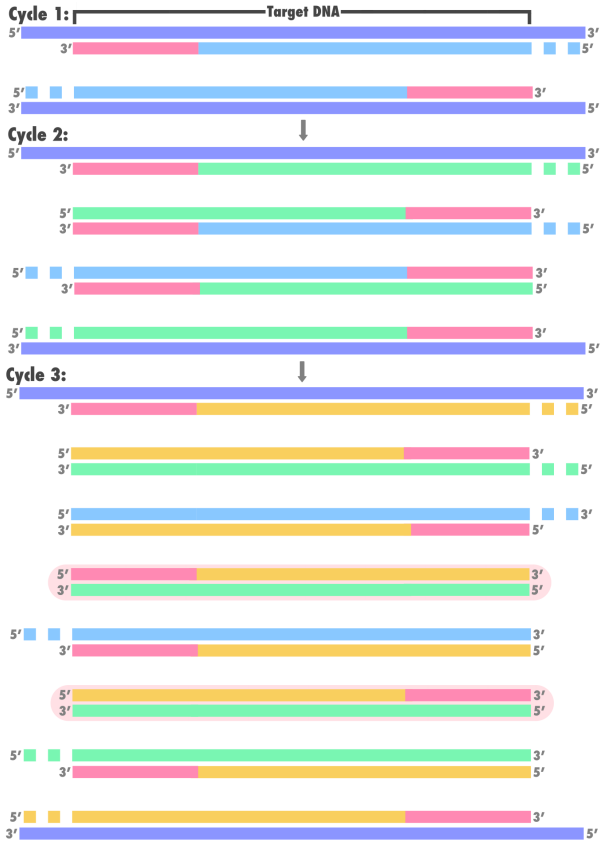

Figure 2.2: PCR products formed in the first three PCR cycles. Primers depicted in pink attach to the complementary sequence of the target DNA, and DNA polymerase synthesizes a new strand. The DNA polymerase continues extending the strand until the heat denaturation of the next cycle begins. The original and new strands then serve as templates for the next cycle. At the end of the third cycle two dsDNA molecules that match the template fragment exactly are formed, here marked in red. The number of DNA molecules of the same length as the template will increase exponentially from here on out. Figure adapted from Reece [53].

The breakthrough that enabled PCR to become such a success came when Taq polymerase from the thermophilic bacterium *Thermus aquaticus* was first used. Prior to this the poly-

merase used was inactivated during the heat denaturation, and new polymerase had to be added between each cycle. Taq polymerase however, tolerates the high temperature of the denaturation stage. It also has a high temperature optimum, allowing extension to occur at a high enough temperature for the primer annealing specificity not to be compromised [53]. In this work, Q5 DNA polymerase, which has a lower error rate than Taq polymerase, was used. This polymerase generates blunt ends [126], necessitating blunt-end cloning of PCR products.

Procedure

The reaction mixture described in table 2.1 was assembled in PCR tubes kept on ice and mixed gently. Water was added to a final volume of 25 µl. For high GC templates, 5 µl water was replaced by the Q5 High GC Enhancer. The tubes were quickly spun down to collect the liquid.

The Eppendorf thermocyclers Mastercycler gradient or the Mastercycler personal was pre-heated to the denaturation temperature (98 °C) and used to carry out the reaction using the PCR program described in table 2.1.

Table 2.1: The 25 µl reaction mixture and the program used for PCR.

5X Q5 Reaction Buffer	5 µl
10 mM dNTP	0.5 µl
10 µM Forward Primer	1.25 µl
10 µM Reverse Primer	1.25 µl
Template DNA	0.5 µl
5X Q5 High GC Enhancer	5 µl
Q5 DNA Polymerase	0.25 µl
MQ water	11.25 µl

1. Initial denaturation at 98 °C for 30 seconds.
2. 25-35 cycles of
   (a) 98 °C for 10 seconds.
   (b) Lowest T_m - 3 °C for 30 seconds.
   (c) 72 °C for 30 seconds/kb template.
3. Final extension at 72 °C for 2 minutes.
4. Hold at 4 °C.

The DNA used as the template was obtained by isolation of plasmid or genomic DNA, or by the boiling method used for colony PCR of *A. vinelandii* cells. The boiling method involved inoculation of colonies for 2 days. 1 ml bacterial culture was then centrifuged for 5 minutes at 13 000 rpm, and the supernatant was discharged. The cell pellet was resuspended in 100 µl MQ water and boiled for 15 minutes at 100 °C. For colony PCR, the initial denaturation time was increased to 3 minutes.

2.10 Sequencing of DNA

After cloning of PCR products into TOPO vectors, the LightRun Sequencing service from Eurofins Genomics was used to sequence the gene inserts. The sequencing was performed using an automated version of the Sanger sequencing technique.

Frederick Sanger and his colleagues [127] developed Sanger sequencing in 1977, and the technique has been in use ever since. The principle of Sanger sequencing is based on the use of a DNA polymerase that can synthesize new DNA strands with the help of a primer and a DNA template. The normal DNA precursors deoxynucleotide triphosphates (dNTPs) are added, but crucially, modified di-deoxynucleotide triphosphates (ddNTPs) are also used. ddNTPs lack the 3'-hydroxyl group necessary to form a new phosphodiester bond to another nucleotide, so whenever a ddNTP is incorporated into a strand, elongation by the polymerase terminates.

Originally, the sequencing was split into four reactions, one for each of the four di-deoxynucleotides ddATP, ddCTP, ddGTP and ddTTP [127]. The polymerase, primer, template, all the four deoxynucleotides and one of the four di-deoxynucleotides was then added to each reaction [127]. Today however, Sanger sequencing is often automated and extension is performed in a single reaction. Typically, different coloured fluorescent dyes are used to tag either the primer or the ddNTPs [128]. The ratio of dNTPs to ddNTPs is typically about 100, to ensure that the terminating ddNTP is only partially incorporated [127]. The polymerase is then allowed to synthesize fragments from the primer [127]. After extension by the polymerase, DNA fragments are separated by size using a capillary. The fluorescence signals of the fragments are detected by a laser, resulting in a chromatogram (figure 2.3) where the different coloured fluorescence peaks are translated into bases [128]. According to Eurofins Genomics [129], even though other next generation sequencing techniques are available, automated Sanger sequencing is still preferable for sequencing of single genes, for verification of cloned inserts or site-directed mutagenesis.

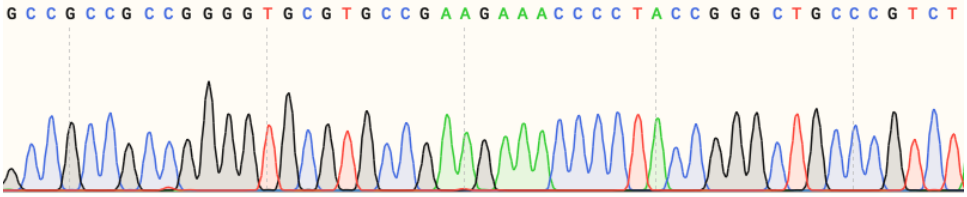

Figure 2.3: The Sanger sequencing principle is based on the use of fluorescently tagged ddNTPs that terminate extension by DNA polymerase. After extension, DNA fragments are separated by size and the fluorescence signals are detected by a laser. This results in a chromatogram where the different coloured fluorescence peaks are translated to bases. Here, an excerpt from a chromatogram result in this work is shown.

Procedure

Samples were prepared for sequencing by combining 5 µl 5 µM primer, 100 ng/µl plasmid DNA and MQ water to a total of 10 µl. Chromatograms were analyzed using SnapGene Viewer and Benchling.

2.11 Monitoring of cell cultures by spectrophotometry

To monitor the growth of bacterial cells in a liquid culture, the cell culture's turbidity, or optical density (OD), may be measured using a spectrophotometer [130]. The OD of a well dispersed culture sample is typically proportional to the bacterial density of the culture, and OD measurements thus provide a fast and non-destructive way of gaining insight into cell concentration [131] and the state of cells [130]. It is therefore widely used in laboratory work [130]. In this work, OD measurements were used to monitor cell growth when preparing competent cells, before conjugation and during measurement of alginate production and luciferase activity.

When bacterial cultures are incubated at optimal conditions in liquid media containing the required nutrients [132], several distinct growth phases characterized by variation in growth rate [131] can be observed. These growth phases are associated with certain physiological changes in the bacterial culture [132]. When first inoculated, cells remain in the lag phase for some time, as they are adapting to the culture conditions [132] and the growth rate is essentially zero [131]. Bacterial growth eventually accelerates until cells enter the exponential phase where growth rate is constant [131] and cell numbers are growing at the fastest possible rate given the conditions [132]. Inevitably, the carbon and energy source is fully exploited, an essential nutrient becomes limiting or a toxic build-up of waste causes the culture to enter the stationary phase [132]. Dead cells may still supply some needed nutrients, but the growth rate of the stationary phase goes back down to a net zero. Eventually, in the death phase, the growth rate becomes negative [131].

OD measurements are commonly taken at λ = 600 nm. For many procedures, such as for preparation of competent cells, the cells used should be as fit as possible. This is generally achieved by culturing cells until they are in the early stages of the exponential phase, which corresponds to an OD_{600} of approximately 0.4 [133].

Procedure

The Thermo Spectronic Helios Epsilon Spectrophotometer was used to measure OD_{600}. Cuvettes containing just the culture medium were used as blanks, before OD_{600} of the cell culture was measured. Samples were diluted with culture medium to obtain readings below 0.4.

2.12 Enzymatic alginate assay

To evaluate the alginate production of mutated *A. vinelandii* strains, an enzymatic alginate assay originally developed by Østgaard [134] was used. This assay is based on the action of alginate lyases, which cleave alginate by catalyzing a β-elimination reaction. Cleavage

results in a non-reducing end containing an unsaturated uronic acid, which has been shown to absorbs UV light at λ = 230 nm [135]. Alginate lyases cleave alginate molecules internally, initially resulting in formation of many slightly shorter polymers [2]. If the reaction is allowed to proceed for a few hours however, an excess of enzyme will have had time to break down the alginate, and only short oligomers will be left [2, 134]. The increase in A_{230} before and after addition of lyases will reflect the amount of substrate originally present [134]. By making a standard curve of increase in A_{230} for samples of known alginate concentrations, the amount of alginate in samples of unknown concentration can therefore be determined.

Both mannuronate (M-) lyase, which is unable to cleave G-blocks, and guluronate (G-) lyase, which is conversely unable to cleave M-blocks [136], are used. The composition of the alginate may vary, so the combination of M- and G-lyases ensures that potential effects of M- and G-blocks are eliminated [134]. In addition, acetylated M-residues might have an effect on A_{230} measurements. To avoid this, a mild alkali treatment is used to deacetylate the samples [137].

Procedure

Pre-cultures were prepared with 10 ml RA1, antibiotics and the inducer *m*-toluate if needed, and incubated at 30 °C for 2 days. Three biological replicates were used per strain. 100 µl cell culture was then transferred to fresh medium, and the cultures were incubated at 30 °C. OD_{600} was measured and 1 200 µl samples were collected at 24 and 48 hours of growth. If viscous, the sample was diluted (1:5 or 1:10) using 0.2 M NaCl. The samples were next centrifuged for 10 minutes at 13 000 rpm. 1 000 µl supernatant was transferred to a new tube before 33 µl 3 M NaOH was added. Samples were stored at -20 °C.

For the enzymatic alginate assay, samples were thawed and deacetylated by shaking for 1 hour. Samples were then centrifuged for 10 minutes at 13 000 rpm. 100 µl supernatant was then transferred to a new tube containing 300 µl 0.05 M Tris-HCl, 1.5% NaCl (pH 7.5).

Alginate standards were prepared by dissolving alginate (LF10/60) in distilled water to make concentrations of 0.0, 0.1, 0.2, 0.3, 0.4 and 0.5 g/l.

The assay was performed using Costar 96 well UV-plates. 150 µl 0.05 M Tris-HCl, 1.5% NaCl (pH 7.5) was added to each well. Three parallels of 75 µl blank, standard or sample was then added, and the contents of the well was mixed. A_{230} was measured using the SpectraMax Plus 384 Absorbance Plate Reader from Molecular Devices and the software SoftMax Pro. 8 µl 1 u/ml M-lyase and 8 µl 1 u/ml G-lyase was then added, and the contents of the well was mixed. The plates were subsequently incubated at room temperature. A_{230} was measured after 3 and 4 hours. If an increase in A_{230} was observed between the 3 and 4 hour measurements, a third A_{230} measurement was performed the next day. The final measurement was subsequently used to produce a standard curve and determine the alginate concentrations of the samples.

Measurements were corrected for blank, addition of lyase and dilution. Next, the increase in A_{230} was calculated by subtracting A_{230} before addition of lyases from A_{230} after addition of lyases. The average values of the alginate standards produced a standard curve which was subsequently used to determine the alginate concentration of the samples. Alginate concentration per OD_{600} was also calculated.

2.13 Luciferase assay

The Firefly luciferase enzyme is commonly used as to evaluate gene expression, and can also be used as a reporter gene to monitor promoter activity [138]. The *luc* gene of the firefly *Photinus pyralis* encodes luciferase, which catalyzes oxidation of its substrate luciferin using the cosubstrate ATP $\cdot$ Mg^{2+}. This produces an enzyme-bound luciferyl-adenylate [138]. The chemical energy of the luciferin oxidation then causes the luciferyl-adenylate to undergo oxidative decarboxylation, producing CO_2, oxyluciferin, AMP and light [138]. An excess supply of substrate leads the light flash produced to be proportional to the amount of luciferase added [138].

In this work, the Promega Luciferase Assay System [139] was used to measure the relative strengths of different promoters. This assay uses a Luciferase Assay Reagent to initiate enzyme activity, and light produced is measured using a luminometer.

Procedure

Pre-cultures were prepared with 10 ml BM and incubated at 30 °C for 2 days. Three biological replicates were used per strain. 100 µl cell culture was then transferred to fresh medium, and the cultures were incubated at 30 °C. OD_{600} was also measured at t = 0. OD_{600} was measured again at 24 and 48 hours of growth, and 90 µl cell culture was sampled and added to 10 µl 1 M K_2HPO_4 (pH 7.8), 20 mM EDTA. The samples were stored at -80 °C.

For the assay, samples and the 100 µl aliquots of Luciferase Assay Reagent were thawed in a room temperature water bath. The lysis mix was prepared, and 300 µl was added to each sample. The contents were mixed and incubated for 10 minutes at room temperature. The Turner BioSystems 20/20n Luminometer was programmed to perform a 10-second measurement read. 20 µl cell lysate was added to 100 µl of the Luciferase Assay Reagent and the contents were mixed, before the tube was placed in the luminometer and luciferase activity was measured.

2.14 Bioinformatics tools and data processing software

Section 2.14 presents the bioinformatics tools used in this work along with the software used to process experimental data.

2.14.1 Benchling

DNA sequences were uploaded to the cloud-based informatics platform Benchling [140], which was used to plan restriction digestion, ligation and PCR by linking primers to sequences. Benchling was also used to align sequencing results to a template. The alignment used the MAFFT (multiple alignment using fast Fourier transform) program, which is able to reverse sequences.

2.14.2 SnapGene Viewer

As a supplement to Benchling, SnapGene Viewer [141] was used to plan PCR, edit sequencing chromatograms and visualize sequence alignments obtained using Benchling. SnapGene Viewer is a free software that can be used to plan and document cloning procedures.

2.14.3 Microsoft Office Excel

Data from alginate and luciferase assays were processed using Microsoft Office Excel. Standard deviations (SD) of the samples were calculated using formula 2.1,

$$SD = \sqrt{\frac{\sum |x - \bar{x}|^2}{n - 1}} \tag{2.1}$$

where x is a value in the sample, $\bar{x}$ is the sample mean average and n is the sample size.

CHAPTER 3

AIM OF THE STUDY

Alginate is a biopolymer of great industrial interest because of its gel-forming properties, and alginate synthesizing bacteria such as *A. vinelandii* could potentially be utilized to produce alginates with sought after properties [1]. This study explores several genes believed to be involved in alginate biosynthesis in *A. vinelandii* in order to gain insight into its biosynthesis and potential ways of manipulating it, such that an increased amount of alginate with specific properties may be produced. This study is divided into three parts: 1) the construction, verification and testing of *algB* and *algW* mutants, 2) testing of an *algF*, *mucA* double mutant and 3) construction, verification and testing of a CRISPR-Cas9 assisted system that disrupts *algL*.

Construction, verification and testing of *algB* and *algW* mutants

This study aims to reevaluate findings by Mærk et al. [46] on the effect of disruption of the alginate biosynthesis regulatory genes *algB* and *algW* on alginate production. AlgB is a positive regulator of biosynthetic genes [48], and is known to be required for alginate production in *P. aeruginosa* [50, 49, 51], but the results of Mærk et al. suggest that disruption to its *A. vinelandii* analog does not affect alginate yield. AlgW is a protease involved in a proteolytic cascade [44] that acts as a positive regulator and is required for alginate production in *P. aeruginosa* [44], and the findings of Mærk et al. indicate that AlgW is also required for alginate production in *A. vinelandii*. To evaluate *algB* and *algW* mutants, the genes will be cloned into a vector and verified by sequencing. An antibiotic resistance gene will be used to disrupt the genes, before conjugation to *A. vinelandii*. Homologous recombination will be used to achieve insertion mutagenesis, before mutants will be verified by PCR. Finally, the amount of alginate produced by the mutants will be evaluated by

an enzymatic alginate assay.

Testing of an *algF*, *mucA* double mutant

The effect of mutations to the genes *algF* and *mucA* will also be evaluated. AlgF is required for acetylation of M-residues, which in turn prevents epimerization and protects against lyase activity but is not required for alginate biosynthesis itself [2]. An *algF* mutation alone could therefore be expected to result in a higher G-content alginate with lowered molecular weight due to increased lyase activity. MucA is an anti-σ factor that impacts alginate biosynthesis negatively [47] by acting as a regulator of the *alg* gene cluster [27]. MucA disruption has been shown to result in increased alginate production [27, 47, 46]. Because MucA regulates the entire *alg* gene cluster, its disruption affects *algL*, which encodes an alginate lyase [34]. *mucA* disruption could therefore also result in a lower molecular weight alginate. A previously constructed *algF*, *mucA* duble mutant will be verified and its alginate production evaluated by an enzymatic alginate assay.

Construction, verification and testing of a CRISPR-Cas9 assisted system that disrupts *algL*

Lastly, this study aims to construct a CRISPR-Cas9 assisted system that disrupts the gene encoding alginate lyase, *algL* [34]. This could result in a mutant that produces a higher molecular weight alginate. AlgL is essential and therefore cannot be removed entirely [43], but the aim is to reduce the amount of lyase produced in order to increase the molecular weight of the alginate. The amount of AlgL needed in *A. vinelandii* and the strength of the associated promoter is not known. To ultimately generate a less efficient version of *algL*, transposon vectors where *algL* is placed under control of three different promoters will therefore be constructed with to find a promoter that induces transcription of a low but sufficient amount of the gene. Transposon vectors will also be constructed where the less efficient mutant *algLH199R* is used, which could potentially further increase the molecular weight of the produced alginate.

The promoters used are P*m*, P*lac* and P*const*. P*m* has a low basal expression rate, but the use of the inducer *m*-toluate may result in a high-fold increase in transcription [58]. P*lac* originally controls transcription of the *E. coli lac* operon [142]. Transcription of this promoter is normally repressed and its expression rate is therefore low, but it exhibits basal expression [142]. Lactose or synthetic lactose analogs may be used to induce transcription from P*lac* [142]. P*const* is a strong synthetic constitutive promoter derived from the gram positive [143] bacterium *Streptomyces lividans* TK24 [144]. To evaluate the promoters in question, transposons will be constructed where the promoters control the expression of the luciferase encoding gene *luc*. All transposon vectors will be conjugated to *A. vinelandii*, and the expression levels of the promoters will then be evaluated by measuring the light produced by luciferase.

A homologous recombination vector that will disrupt wild type *algL* along with the non-essential acetylation genes *algI*, *algV* and *algF* [2] will also be constructed. Acetylation prevents epimerase and lyase modification [2], and as the acetylation genes are not required for alginate synthesis, their removal could thus be advantageous. The vector will be constructed by cloning parts of *algI* and *algF* into a plasmid containing parts of *algL* and *algX*, and the fragment will be integrated into the *A. vinelandii* genome by homologous recombination. Verification by PCR will be performed, and as ploidy has been shown to make obtaining pure mutants by homologous recombination alone difficult [26], a previously constructed CRISPR-Cas9 vector that targets *algI* will be used in an attempt to remove all remaining wild type copies of *algL* whilst avoiding affecting the transposon insert.

CHAPTER 4

RESULTS AND DISCUSSION

This chapter presents and discusses the results obtained in this work. Section 4.1 covers the construction and verification of *A. vinelandii algB* and *algW* mutants, as well as their complementation and subsequent measurement of alginate production. Section 4.2 covers the conjugation and verification of an *A. vinelandii algF*, *mucA* double mutant, along with measurements of alginate production. Lastly, section 4.3 covers the construction, verification and testing of an *A. vinelandii* CRISPR-Cas9 assisted system that targets *algL*, as well as testing of the relative strengths of different promoters used.

DNA standards, restriction enzymes, primers, bacterial strains, plasmids and plasmid maps used are presented in appendices B-G.

4.1 Construction, verification and testing of *algB* and *algW* mutants

Section 4.1 presents and discusses the inactivation of the *A. vinelandii* genes *algB* and *algW*, their integration into the *A. vinelandii* genome by homologous recombination and the following verification, complementation and testing of *algB* and *algW* mutants. As mentioned in section 1.2.2, findings by Mærk et al. [46] indicate that although the *P. aeruginosa* homolog of *algB* encodes a positive response regulator required for alginate biosynthesis, *A. vinelandii algB* appears not to be required for alginate production. Their results also suggest that *A. vinelandii algW* has a similar role to its *P. aeruginosa* homolog, which encodes a protease required for alginate biosynthesis. It should be noted that Mærk et al. constructed a transposon library, and that the placement of transposons could therefore have affected the results. The aim of this experiment therefore, was to use homologous recombination to inactivate the genes in question. The alginate production of mutants could then be used to verify or contradict previous findings by Mærk et al.

The experiment involved amplification of *algB* and *algW* by PCR, followed by TOPO cloning and transformation to *E. coli*. The mutants were verified by sequencing. Next, the spectinomycin resistance conferring gene *aadA* was used to inactivate *algB* and *algW*. The inactivated genes were transferred to a conjugation vector and conjugated to *A. vinelandii*. An overview of the cloning strategy for the *algB* and *algW* mutants is presented in figure 4.1 and 4.2. After integration by homologous recombination, colony PCR was used to verify mutants, and the mutants were complemented. Finally, an enzymatic alginate assay was performed to measure the alginate production of the *algB* and *algW* mutants and compare to that of complemented strains.

Figure 4.1: *algB* was amplified from *A. vinelandii* by PCR and TOPO cloned into pCR-Blunt II-TOPO. The PstI-SacI digested *aadA* fragment from pHE265 was then ligated into PshAI digested pHMT1. Lastly, the NotI-SpeI digested inactivated gene was transferred to the AvrII-NotI digested conjugation vector pHE326.

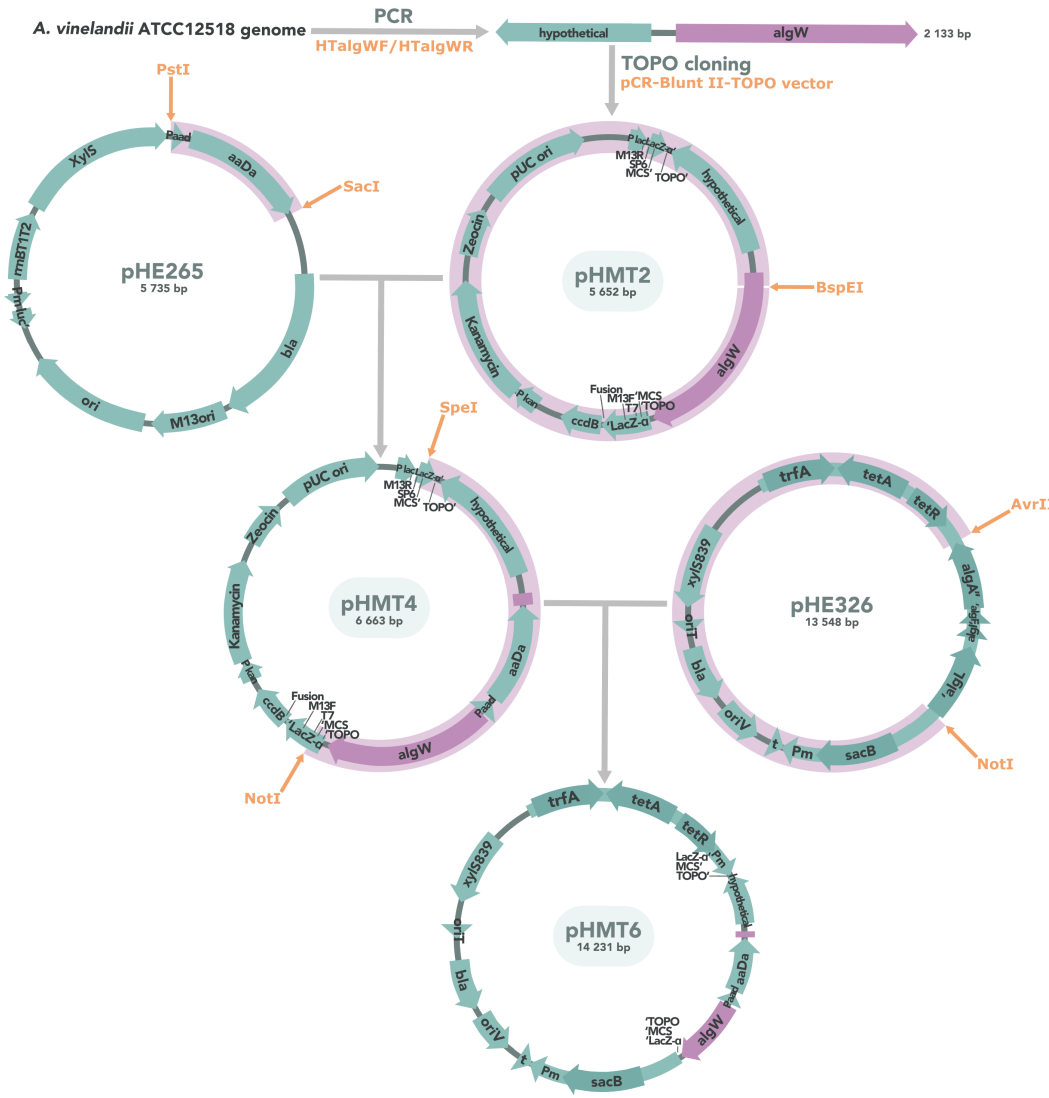

Figure 4.2: *algW* was amplified from *A. vinelandii* by PCR and TOPO cloned into pCR-Blunt II-TOPO. The PstI-SacI digested *aadA* fragment from pHE265 was then ligated into BspEI digested pHMT1. Lastly, the NotI-SpeI digested inactivated gene was transferred to the AvrII-NotI digested conjugation vector pHE326.

4.1.1 Construction of inactivated *algB* and *algW* homologous recombination vectors

To ultimately be able to evaluate the alginate production of *algB* and *algW* mutants, genomic DNA from *A. vinelandii* was first isolated. PCR was next used to amplify the genes. The primer pairs HTalgBF/HTalgBR and HTalgWF/HTalgWR were used for amplification of *algB* and *algW*, respectively. PCR products were analyzed using gel electrophoresis as shown in figure 4.3, which confirmed that the desired 2.6 kb *algB* and 2.1 kb *algW* fragments had been obtained.

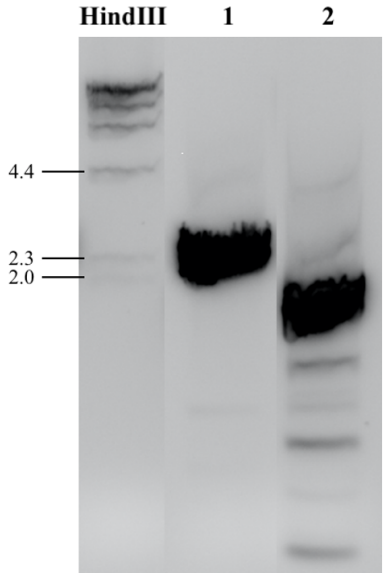

Figure 4.3: Separated PCR products. Lane 1 shows the expected 2.6 kb *algB* fragment and lane 2 shows the expected 2.1 kb *algW* fragment.

PCR amplified *algB* and *algW* fragments were cloned into pCR-Blunt II-TOPO, which was transformed into *E. coli* DH5α. Plasmid DNA from four transformants was isolated and digested with EcoRI for verification. Blunt end cloning could result in insertion of the fragment in either direction, and this was accounted for. The *algB* vector would give 3.5 and 2.6 kb fragments, and the *algW* vector would give 3.5 and 2.2 kb fragments. Figure 4.4 shows that several colonies contained bands of the correct size.

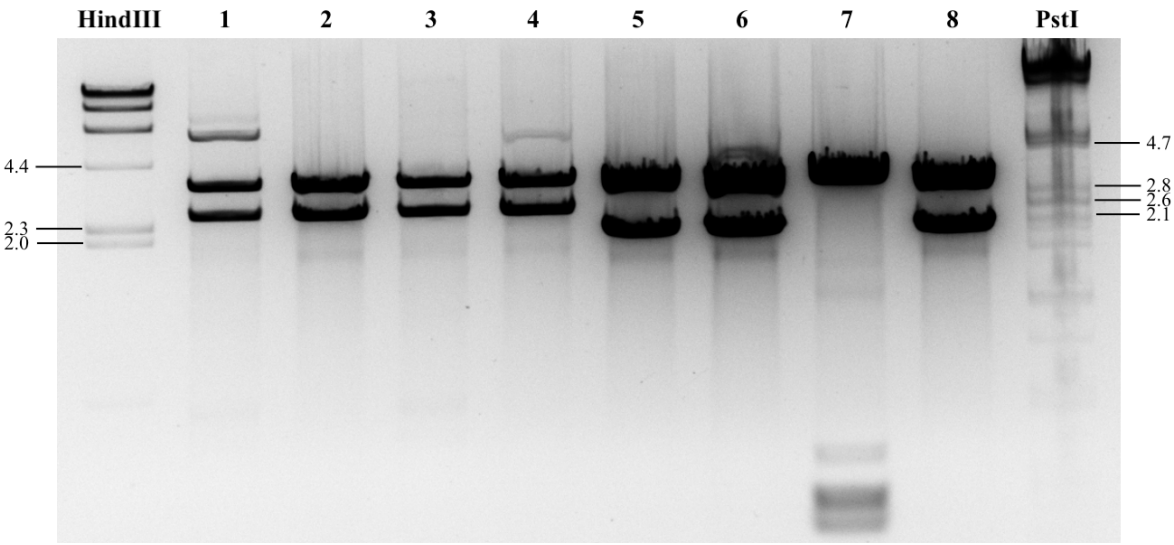

Figure 4.4: The pCR-Blunt II-TOPO vectors with *algB* or *algW* inserted, digested with EcoRI. Lane 1-4 shows the TOPO vector with *algB* inserted, with expected fragments of 2.6 and 3.5 kb. Lane 5-8 shows the TOPO vector with *algW* inserted, with expected fragments of 2.1 and 3.5 kb. With the exception of lane 7, which appears to contain only the TOPO vector, all lanes showed the correct fragments. The larger fragments of lanes 1 and 4 indicate partial digestion of the plasmid.

PCR amplification sometimes results in mutations, and plasmids were therefore sequenced to verify that PCR had yielded the correct fragments. The primers algBF, algBR, M13F and M13R were used for sequencing of *algB*, and algWseq, M13F and M13R were used for *algW*. The sequencing results were aligned with *algB* and *algW*. The alignment, presented in appendices H and I, showed no mismatches. The sequenced plasmid containing *algB* was designated pHMT1, and the sequenced plasmid containing *algW* was designated pHMT2.

To clone the spectinomycin resistance gene *aadA* into and thereby inactivate *algB* and *algW*, pHE265 was digested with PstI-SacI. pHMT1 and pHMT2 were simultaneously digested with PshAI and BspEI, respectively. pHMT2 and the *aadA* fragments were then blunted, before being separated. The 1.0 kb *aadA* band seen in figure 4.5 was excised, along with the 6.1 kb band of pHMT1 and the 5.7 kb band of pHMT2.

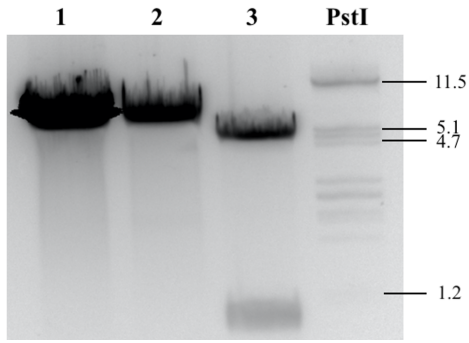

Figure 4.5: pHMT1 and pHMT2 digested with PshAI and BspEI, respectively, along with PstI-SacI digested pHE265. Lane 1 contains pHMT2 with the expected 5.7 kb fragment, and lane 2 contains pHMT1 with the expected 6.1 kb fragment. Lane 3 contains pHE265 with the expected 4.7 and 1.0 kb fragments. The pHMT1 and pHMT2 bands, along with the 1.0 kb *aadA* band, were excised.

The fragments were purified and *aadA* was ligated into the two vectors, which were then transformed into *E. coli* DH5α. Plasmids were isolated from three transformants from each ligation and then verified by digestion with DraIII. Insertion of the fragment in either direction was accounted for. The parental plasmids pHMT1 and pHMT2 would give a 6.1 and 5.7 kb fragment, respectively, while pHE265 would give 3.5, 1.6 and 0.6 kb fragments. The new inactivated *algB* vector would give 3.5, 3.0 and 0.6 kb fragments, and the inactivated *algW* vector would give 3.7, 2.4 and 0.6 kb fragments. Figure 4.6 shows that several colonies produced bands of the correct size.

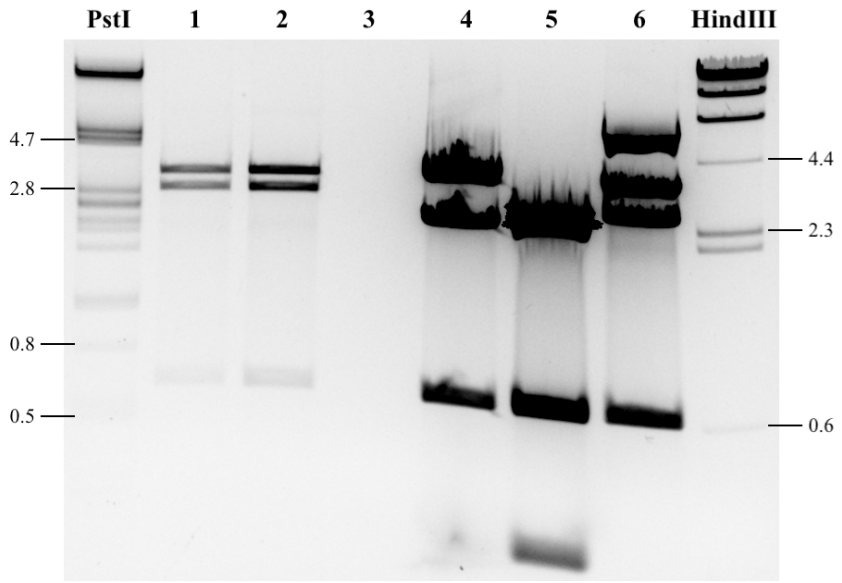

Figure 4.6: Plasmids formed when *aadA* was cloned into pHMT1 and pHMT2, digested with DraIII. Lane 1-3 shows the pHMT1 derivatives with expected fragments of 3.5, 3.0 and 0.6 kb. Lane 4-6 shows the pHMT2 derivatives with expected fragments of 3.7, 2.4 and 0.6 kb. Lanes 1, 2, 4 and 6 showed the correct fragments, even though the plasmid of lane 6 was only partially digested. Lane 5 lacks the larger band.

The *algB* vector was designated pHMT3, and the *algW* vector was designated pHMT4. Next, the inactivated genes were cloned into the conjugation vector pHE326. This was achieved by NotI-SpeI digestion of pHMT3 and pHMT4 to obtain the 3.7 kb inactivated *algB* and the 3.2 kb *algW* fragments, as shown in figure 4.7. To avoid bands in too close proximity, pHMT3 was also digested with RsrII, producing two smaller fragments of 1.9 and 1.5 kb. Similarly, pHMT4 was digested with HincII to produce smaller fragments of 1.9 and 1.6 kb. pHE326 was digested with AvrII-NotI to obtain the 11.0 kb fragment. After excision, the fragments were ligated and transformed into *E. coli* S17.1, which allows for conjugal transfer.

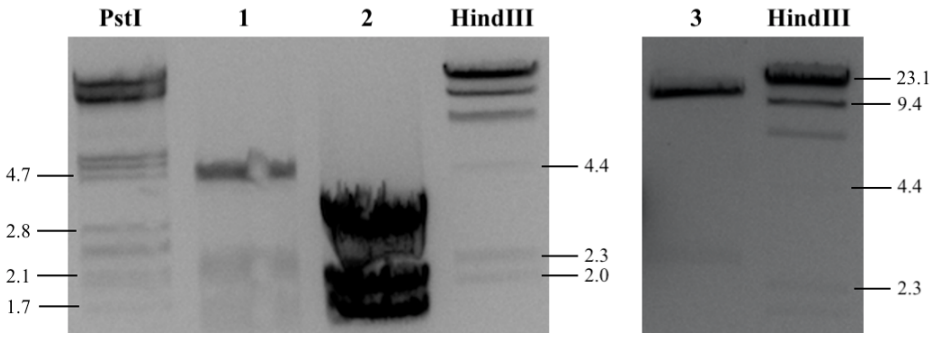

Figure 4.7: pHMT3 digested with NotI, RsrII and SpeI, pHMT4 digested with HincII, NotI and SpeI and pHE326 digested with AvrII and NotI. Lane 1 contains pHMT3 with the expected 3.7, 1.9 and 1.5 kb fragments, and lane 2 contains pHMT4 with the expected 3.2, 1.9 and 1.6 kb fragments. Lane 3 contains pHE326 with the expected 11.0 and 2.5 kb fragments. The 3.7 kb inactivated *algB* fragment of pHMT3, the 3.2 kb inactivated *algW* fragment of pHMT4 and the 11.0 kb fragment of pHE326 were excised.

Plasmids were isolated from one transformant and then verified by digestion of the pHMT3 derivative with BamHI and the pHMT4 derivative with BglII. The parental plasmid pHMT3 would give a 7.1 kb fragment and pHMT4 would give a 6.7 kb fragment. pHE326 digested with BamHI would give 8.7, 2.6 and 2.3 kb fragments, whereas pHE326 digested with BglII would give 11.3 and 2.3 kb fragments. The new conjugation vectors containing inactivated *algB* would give 8.7, 3.8 and 2.3 kb fragments, and those containing inactivated *algW* would give 8.9, 3.1 and 2.3 kb fragments. Figure 4.8 shows that both colonies contained plasmids with the correct bands. The pHMT3 derivative was designated pHMT5, and the pHMT4 derivative pHMT6.

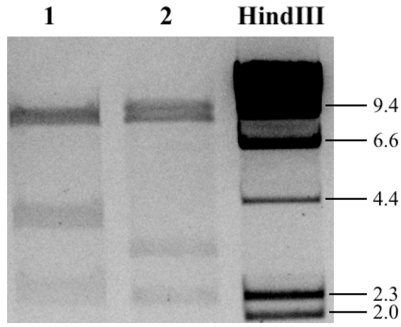

Figure 4.8: Plasmids formed when *algB* and *algW* inactivated by *aadA* was cloned into the conjugation vector pHE326, digested with BamHI and BglII, respectively. Lane 1 shows the pHMT3 derivative with expected fragments of 8.7, 3.8 and 2.3 kb. Lane 2 shows the pHMT4 derivative with expected fragments of 8.9, 3.1 and 2.3 kb. Both lanes showed the correct fragments.

4.1.2 Transfer of constructs to *A. vinelandii*, integration by homologous recombination, verification and complementation

To investigate if inactivation of *algB* and *algW* would impact alginate production in *A. vinelandii*, pHMT5 and pHMT6 were transferred from *E. coli* S17.1 to *A. vinelandii* ATCC12518 by conjugation. The spectinomycin resistance conferring gene *aadA*, used to inactivate *algB* and *algW*, was used to select for transconjugants. To remove the alginate-capsule that surrounds *A. vinelandii* and increase the chance of DNA uptake, the cells were washed with glycerol prior to conjugation.

Conjugation resulted in only one colony of transconjugants per plasmid. The inactivated *algB* and *algW* fragments from these two colonies were next integrated into the *A. vinelandii* chromosome by homologous recombination, as described in section 2.2.4. Spectineomycin was used for selection of cells that had undergone the first crossover-event. Cells that had undergone a second crossover-event were screened for using counter-selection by growth on plates containing BA with sucrose. Lastly, growth on and off tetracycline was used to screen for tetracycline sensitive colonies, which were then tested for the recombination.

Five tetracycline sensitive colonies from each conjugation were verified by PCR, using the boiling method to obtain DNA. Wild type *A. vinelandii* was included for comparison to the mutants. The primer pair HTalgBF/ HTalgBR was used for amplification of *algB*, and HTalgWF/HTalgWR was used for *algW*. Figure 4.9 shows the resulting PCR products. Wild type *algB* would give a 2.6 kb fragment, and wild type *algW* would give a 2.1 kb fragment. *algB* and *algW* inactivated by *aadA* would give 3.6 and 3.2 kb fragments, respectively. All colonies appeared to contain the mutated genes and no copies of the wild type genes.

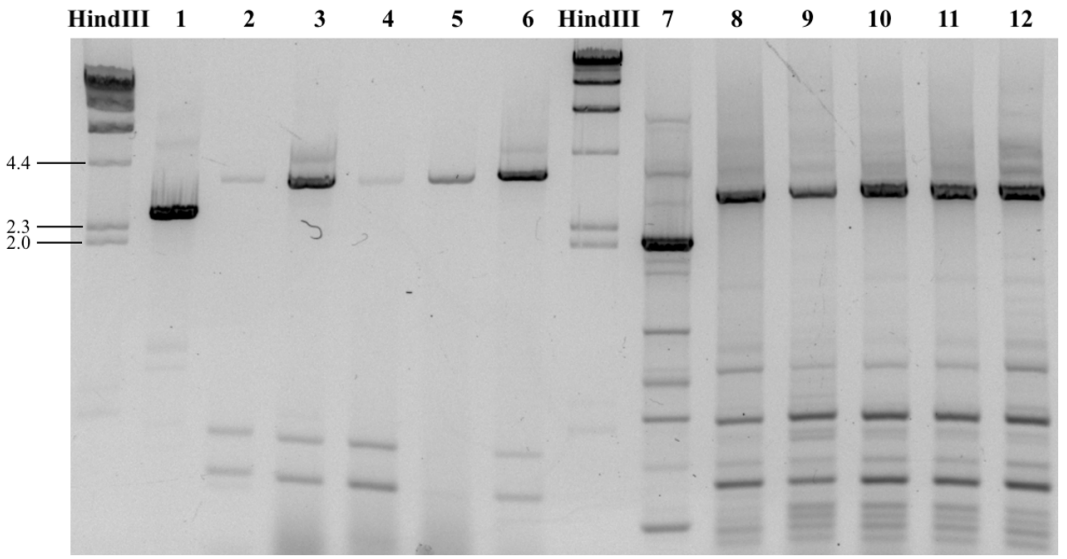

Figure 4.9: Separated PCR products for verification of *algB* and *algW* mutants. Wild type was included for comparison, with *algB* in lane 1 and *algW* in lane 7. Lanes 2-6 contain *algB* mutants, and lanes 8-12 contain *algW* mutants. *algB* mutants would give a 3.6 kb band, as opposed to the 2.6 kb wild type band. *algW* mutants would give a 3.1 kb band, while the wild type gene would give a 2.1 kb band. All mutants appeared to contain only copies of the longer mutated genes.

Prior to measurement of alginate production, *algB* and *algW* mutants were complemented with plasmids encoding the wild type genes. pHE539, encoding wild type *algB*, and pHE536, encoding wild type *algW*, were also conjugated to wild type *A. vinelandii*. The plasmid pIB11 was used as a control and was conjugated to both mutants and the wild type. pIB11 and its derivatives pHE539 and pHE536 are kanamycin resistant RK2 based vectors that contain the inducible P*m*-XylS promoter system. *m*-toluate was therefore used as an inducer, and kanamycin was used to select for transconjugants. Next, the alginate production of mutant strains was measured and compared to that of complemented strains and the wild type.

4.1.3 Measurement of alginate production by an enzymatic alginate assay

A. vinelandii mutants where the spectinomycin resistance encoding gene *aadA* had been used to inactivate *algB* and *algW* were constructed to investigate the effect of mutations to said genes on alginate production. Both mutant and wild type strains were complemented so their alginate production could be measured and compared to that of the mutant strains.

Three biological replicates were prepared from one colony of both the two mutant strains, the complemented strains and the wild type strains. RA1 medium was used to avoid *A. vinelandii* expending energy on nitrogen fixation. The antibiotics spectinomycin and kanamycin, along with *m*-toluate where necessary, was used for selection and induction. Samples were extracted after 24 and 48 hours, OD_{600} was measured, and an enzymatic alginate assay using M- and G-lyase, presented in section 2.12, was used to measure alginate production. The standard curve used to calculate alginate concentration is presented in appendix K, and the data from the alginate assay is presented in appendix L.

The measured alginate production (g/l) after 24 and 48 hours of the *algB* mutant compared to *algB* and wild type conjugated with pHE539 and pIB11 is presented in figure 4.10. The OD_{600} measurements presented in appendix L varied significantly. To account for this, alginate production (g/l) per OD_{600} is presented in figure 4.11.

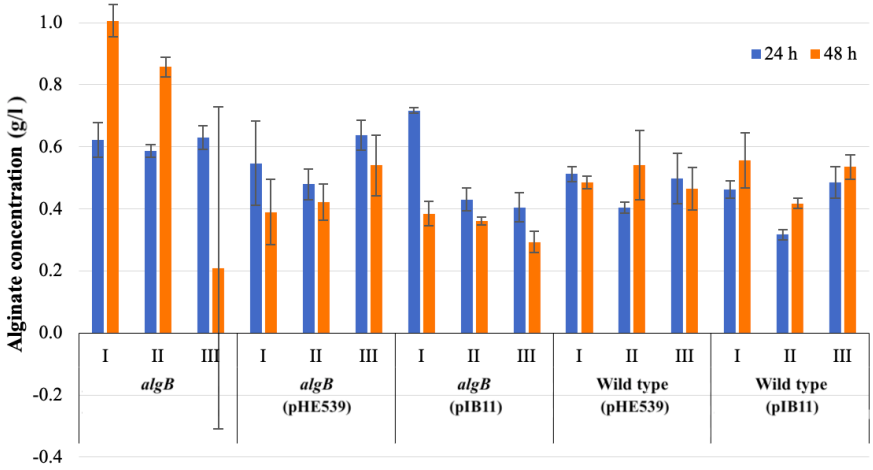

Figure 4.10: The alginate production (g/l) after 24 and 48 hours for three biological replicates of an *algB* mutant, *algB* conjugated with pHE539 and pIB11 and wild type conjugated with pHE539 and pIB11, measured using an enzymatic alginate assay. *algB* was found to produce some alginate, and so did all complemented strains.

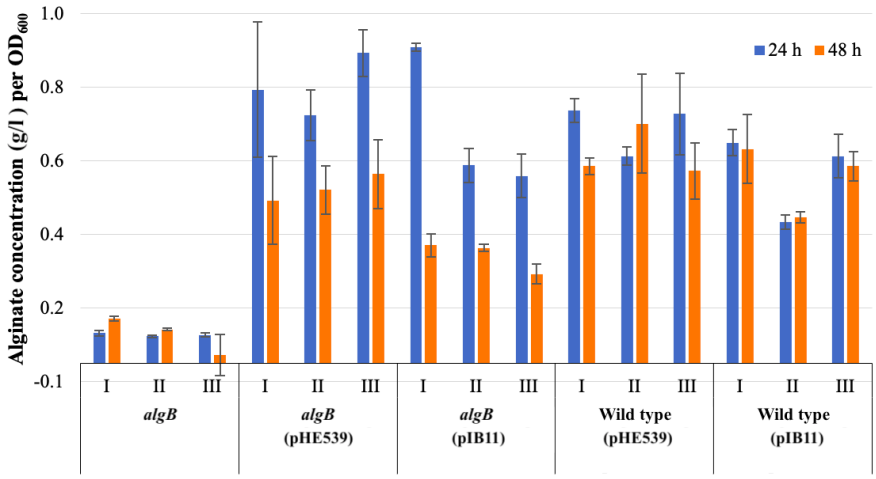

Figure 4.11: The alginate production (g/l), measured using an enzymatic alginate assay, per OD_{600} after 24 and 48 hours for three biological replicates of an *algB* mutant, *algB* conjugated with pHE539 and pIB11 and wild type conjugated with pHE539 and pIB11. *algB* was found to produce some alginate, and so did all complemented strains.

The measured alginate production (g/l) after 24 and 48 hours of the *algW* mutant compared to *algW* and wild type complemented with pHE536 and pIB11 is presented in figure 4.12. The OD_{600} measurements presented in appendix L varied somewhat. To account for this, alginate production (g/l) per OD_{600} is presented in figure 4.13.

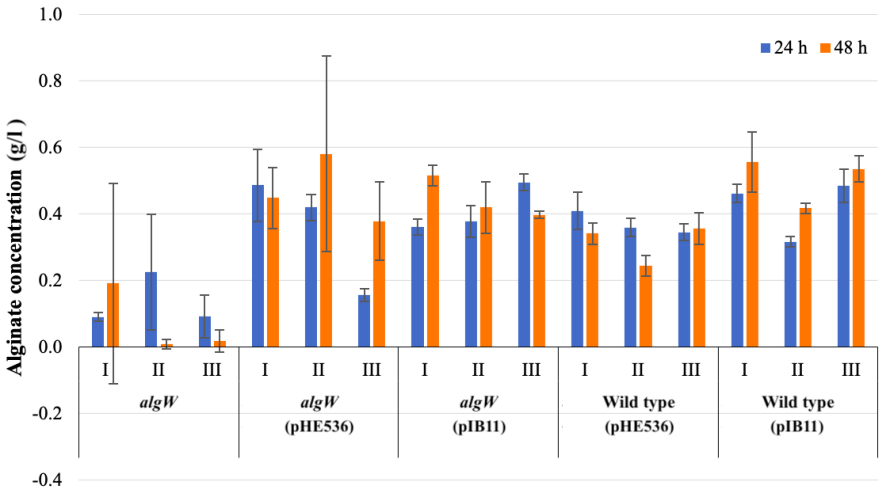

Figure 4.12: The alginate production (g/l) after 24 and 48 hours for three biological replicates of an *algW* mutant, *algW* complemented with pHE536 and pIB11 and wild type complemented with pHE536 and pIB11, measured using an enzymatic alginate assay. Although measurements varied widely, the *algW* mutant did not seem to produce much, if any, alginate. All complemented strains were found to produce some alginate.

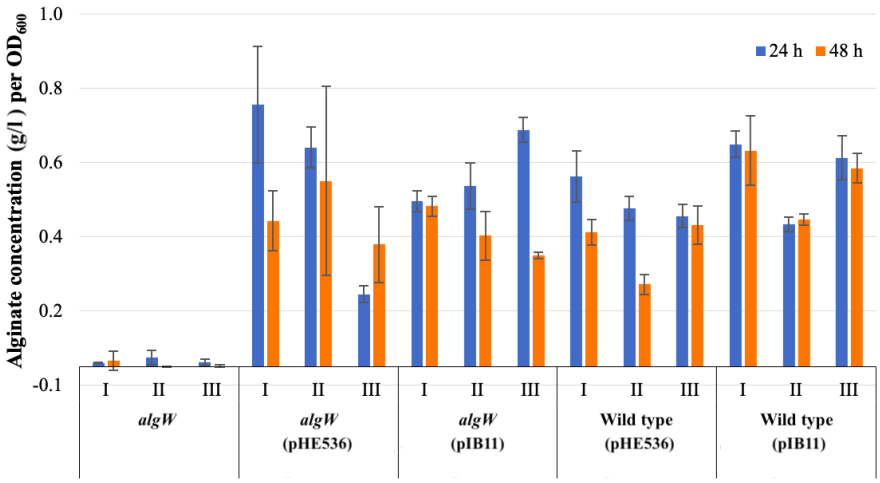

Figure 4.13: The alginate production (g/l), measured using an ezymatic alginate assay, per OD_{600} after 24 and 48 hours of growth for three biological replicates of an *algW* mutant, *algW* complemented with pHE536 and pIB11 and wild type complemented with pHE536 and pIB11. Although measurements varied, the *algW* mutant did not seem to produce much, if any, alginate. All complemented strains were found to produce alginate.

Table 4.1 shows the average alginate production (g/l) per OD_{600} for the three biological replicates after 24 and 48 hours for *algB* and *algW* mutants, complemented strains and wild type strains.

Table 4.1: The average alginate production (g/l) per OD_{600} for the three biological replicates after 24 and 48 hours for *algB* and *algW* mutants, complemented strains and wild type strains.

	Alginate (g/l) per OD600 ± SD	
	24 h	**48 h**
algB	0.0777 ± 0.00449	0.0787 ± 0.0506
algB (pHE539)	0.754 ± 0.0847	0.476 ± 0.0362
algB (pIB11)	0.636 ± 0.194	0.292 ± 0.0433
algW	0.0161 ± 0.00804	0.00626 ± 0.00865
algW (pHE536)	0.498 ± 0.268	0.408 ± 0.0867
algW (pIB11)	0.524 ± 0.102	0.362 ± 0.0674
Wild type (pHE539)	0.643 ± 0.0688	0.570 ± 0.0706
Wild type (pHE536)	0.449 ± 0.0562	0.322 ± 0.0872
Wild type (pIB11)	0.516 ± 0.115	0.505 ± 0.0961

algB is known to be required for alginate biosynthesis in *P. aeruginosa*, but Mærk et al. [46] found that loss of function of its *A. vinelandii* homolog did not affect alginate production. Their study constructed a transposon library however, so results may have been affected by the placement of transposon inserts. If the homologous recombination approach used in this study produced similar results however, this could further support the previous finding that the role of *A. vinelandii algB* is in fact different from *P. aeruginosa algB*. As is evident from both figures, the *algB* mutant created in this work was also found to produce alginate. The growth of the *algB* mutant was much higher than for the other strains however, so when factoring in OD_{600}, the alginate production of the *algB* mutant was significantly lower than for the complemented strains.

This could be due to the use of kanamycin and *m*-toluate to culture the other strains, which might have inhibited their growth. By comparing the complemented *algB* mutant and the *algB* mutant with the control plasmid however, which were cultured using the same medium and have the same plasmid burden, it is possible to see that the *algB* mutation alone did not affect alginate production much. Restoration of the wild type gene by complementation did increase alginate production somewhat, but not much. This is also confirmed by comparison of alginate production of these strains to that of wild type strains. In any case, the *algB* mutant was found to produce alginate. This is consistent with the findings of Mærk et al., and further supports the theory that *A. vinelandii algB* has a function that differs from that of *P. aeruginosa algB*.

The results of Mærk et al. indicated that *algW* is required for alginate biosynthesis in *A. vinelandii*, just like its *P. aeruginosa* homolog. The mutant encoding an inactivated *algW* gene constructed in this work was therefore not expected to produce alginate. The alginate

assay showed that the *algW* mutant did not produce much, if any, alginate. Measurements did however vary widely, so the data is somewhat uncertain. Again, the growth of the *algW* mutant was much higher than for the other strains. Growth of the other strains could have been inhibited by the use of kanamycin and *m*-toluate. Alginate production has been reported to affect cell yield in *P. fluorescens* [25], and it is also possible that m-toluate has an effect on growth. [29].

Complementation with pHE536 did restore alginate production. However, alginate production also increased in the mutant that was conjugated with the control plasmid pIB11. Assuming there were no mix-ups during conjugation, this could suggest that the addition of *m*-toluate somehow triggers alginate production. If that is the case, it calls into question whether or not complementation with pHE536 was actually successful. A simple experiment where the alginate production was measured after culturing the *algW* mutant with and without addition of *m*-toluate could be performed to gain insight into the effect of *m*-toluate on alginate production. Unfortunately, there was not enough time left to perform this experiment. Still, the alginate production of the *algW* mutant was very low, which is consistent with the findings of Mærk et al. and suggests that *algW* is required for alginate biosynthesis in *A. vinelandii*.

For both mutants, complemented strains and wild type strains, alginate production decreased with time, as the measurements after 48 hours are generally lower than the 24 hour measurements.

4.2 Conjugation, verification and testing of a CRISPR-Cas9 assisted mutation system that targets *mucA*

Section 4.2 presents and discusses the conjugation of a CRISPR-Cas9 vector constructed by Maråk [145] to an *A. vinelandii algF*, *mucA* double mutant constructed by Dalland [unpublished]. This was followed by verification of the *mucA* mutation by PCR, before alginate production was measured using an enzymatic alginate assay.

As mentioned in sections 1.2.1 and 1.2.2, AlgF is involved in acetylation of M-residues, which in turn prevents epimerization and lyase activity but is not required for alginate biosynthesis [2]. A loss-of-function mutation to *algF* could therefore potentially lead to production of lower molecular weight alginate with a higher G-content. The *mucA* gene encodes an anti-σ factor involved in regulation of alginate biosynthesis. It negatively affects alginate production [47], and disruption of *mucA* could therefore increase alginate production. MucA regulates the *alg* gene cluster [27], which includes the alginate lyase encoding gene *algL*, and disruption to *mucA* could therefore also result in a lower molecular weight alginate.

4.2.1 CRISPR-Cas9 modification of an *A. vinelandii algF*, *mucA* double mutant

The *algF*, *mucA* double mutant constructed by homologous recombination by Dalland [unpublished] was first shown to contain both wild type and mutated copies of *mucA*. Maråk [145] however, showed that the the strain contained only mutated *mucA*. Originally therefore, the intention was to go ahead with the strain verified by Maråk. However, the *algF*, *mucA* double mutant did not seem to produce any alginate when it was revived from -80 °C and streaked on BA. It was therefore decided to go back to the strain constructed by Dalland. This strain had been shown to contain wild type copies of *mucA*, so it was decided to conjugate the CRISPR-Cas9 vector pMM106 to the strain.

pMM106 was constructed and tested by Maråk [145], and encodes Cas9 along with a gRNA sequence that targets *mucA*. Conjugal transfer of pMM106 to the *algF*, *mucA* double mutant would therefore disrupt any remaining wild type chromosomes. Mutated *mucA* however does not contain the target sequence of the gRNA, and would therefore be unaffected. *A. vinelandii* cells were washed using glycerol to remove the alginate capsule surrounding the cells, easing the conjugation of DNA. The *algF*, *mucA* double mutant was inoculated with spectinomycin. pMM106 is an RK2 based vector that contains the inducible P*m*-XylS promoter system. *m*-toluate was therefore used to induce replication of pMM106, and selection for transconjugants was performed using apramycin.

No transconjugants were observed. This could be because 50 µg/ml apramycin was used instead of the recommended 25 µg/ml for *A. vinelandii*. However, the conjugation was repeated one more time with the correct antibiotic concentration, and still no colonies were

observed. As previous attempts to verify the mutant had contradicted each other, it was decided to repeat the verification performed by Maråk [145] on the strain constructed by Dalland. If this mutant did not contain wild type *mucA* after all, conjugation of pMM106 to the strain would not be necessary.

4.2.2 Verification of a *mucA* mutation

The *algF* mutation of the *algF*, *mucA* double mutant had previously been verified. The boiling method was used to obtain DNA, and colony PCR was performed to investigate whether the double mutant contained a mixture of wild type and mutated *mucA* or mutated *mucA* only. The primer pairs MD125sjekkF/MD125sjekkR and MD124A/mucAsjekkwtR were used.

MD125sjekkF and MD125sjekkR would result in a 1.1 kb PCR product for mutated *mucA* and a 0.4 kb product for wild type *mucA*. A second primer pair was also used, because PCR usually favors the more abundant template. This could result in wild type chromosomes being overlooked if there are only a few copies present. MD124A and mucAsjekkwtR would result in a 0.4 kb fragment for the wild type and no fragment for the mutant gene, ensuring that any wild type *mucA* copies would be visible on the gel. The PCR products were visualized using gel electrophoresis and are presented in figure 4.14. The strain appeared to have lost the wild type *mucA* chromosome copies as there is no PCR product in lane 2 and only a 1.1 kb product in lane 4. The wild type and mutant bands are also clearly distinguishable. Thus, the *algF*, *mucA* double mutant was a pure *mucA* mutant. An enzymatic alginate assay was next performed to measure the alginate production of the *algF*, *mucA* double mutant.

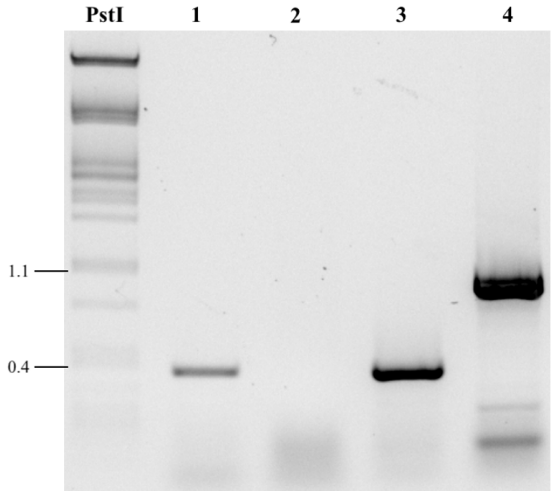

Figure 4.14: Separated PCR products for verification of a *mucA* mutation. Wild type was included as a comparison. Lanes 1-2 contain the PCR products when MD124A and mucAsjekkwtR were used, with the wild type in lane 1 and the *mucA* mutant in lane 2. Wild type would result in a 0.4 kb band, and *mucA* in no band. Lanes 3-4 contain the PCR products when MD125sjekkF and MD125sjekkR were used, with the wild type in lane 3 and the *mucA* mutant in lane 4. Wild type would result in a 0.4 kb band, and *mucA* in a 1.1 kb band. The lack of a PCR product in lane 2 and the 1.1 kb band in lane 4 appear to confirm that the strain is a pure *mucA* mutant.

4.2.3 Measurement of alginate production by an enzymatic alginate assay

The *A. vinelandii algF*, *mucA* double mutant was constructed to investigate the effects of mutations to the genes on alginate production. An enzymatic alginate assay was therefore performed. Both wild type *A. vinelandii* and an *algF* mutant constructed by Dalland [unpublished] were also included for comparison.

Three biological replicates were prepared from one colony per strain. RA1 medium was used to avoid *A. vinelandii* expending energy on nitrogen fixation. Samples were extracted after 24 and 48 hours, OD_{600} was measured, and an enzymatic alginate assay using M- and G-lyase, presented in section 2.12, was used to measure alginate production. The standard curve used to calculate alginate concentration and the data from the alginate assay is presented in appendix K.

The measured alginate production (g/l) after 24 and 48 hours of the *algF*, *mucA* double mutant compared to *algF* and wild type is presented in figure 4.15. The OD_{600} measurements presented in appendix K varied significantly. To account for this, alginate production (g/l) per OD_{600} is presented in figure 4.16. Because of a very high OD_{600} measurement paired

with very low alginate production of one of the *algF* biological replicates, this parallel was suspected to have been contaminated. It was therefore omitted from the figures.

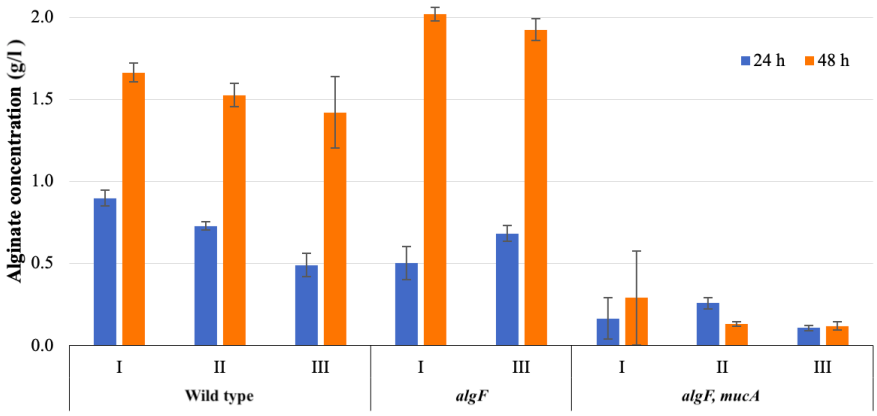

Figure 4.15: The alginate production (g/l) after 24 and 48 hours for three biological replicates of an *algF*, *mucA* double mutant, an *algF* mutant and wild type, measured using an enzymatic alginate assay. The measured alginate production of the *algF*, *mucA* double mutant was significantly lower than that of the other strains.

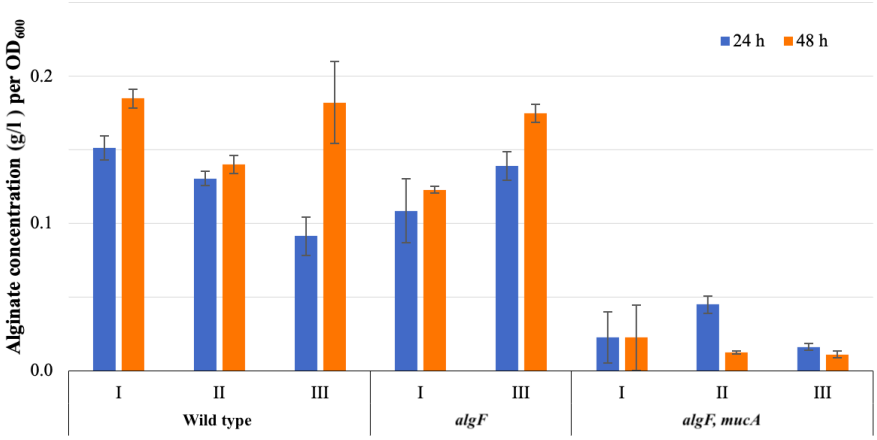

Figure 4.16: The alginate production (g/l), measured using an enzymatic alginate assay, per OD_{600} after 24 and 48 hours for three biological replicates of an *algF*, *mucA* double mutant, an *algF* mutant and wild type. The measured alginate production per OD_{600} of the *algF*, *mucA* double mutant was much lower than that of the other strains.

Several studies have previously showed that an *A. vinelandii mucA* mutant displayed in-

creased alginate production [46, 27, 47], which is in line with the role of *mucA* as a negative regulator of alginate production [47]. A *mucA* mutation should result in less repression of AlgU, which in turn would result in increased production of AlgD [45] and stimulation of alginate production. The *algF*, *mucA* double mutant was therefore expected to have a higher alginate production than both the wild type and *algF* mutant.

The results however, showed that both the wild type and the *algF* mutant produced significantly more alginate than the *algF*, *mucA* double mutant, which produced low amounts of alginate. This indicated that a secondary mutation had occured that was responsible for the low alginate production, as neither the *algF* or *mucA* mutations could explain the low alginate measurements. The nature of this secondary mutation was not known, but it clearly had a detrimental effect on alginate production.

4.3 Construction, verification and testing of a CRISPR-Cas9 assisted system that targets *algL*

Section 4.3 presents and discusses the construction of a CRISPR-Cas9 assisted system that disrupts the *A. vinelandii* gene *algL*. As described in section 1.2.1, *algL* encodes an alginate lyase that cleaves glycosidic bonds between alginate monomers [34]. *algL* is an essential gene [43], so removing it entirely would be lethal. However, mutants with a less efficient *algL* or a version of *algL* that is transcribed less could result in a higher molecular weight alginate. The aim of this work was to construct transposons where the P*m*, P*lac* and P*const* promoters control expression of *algL*, and integrate the transposons into the *A. vinelandii* genome by transposition. In addition, transposons were constructed where the promoters controlled expression of the *algL* mutant *algLH199R*, which has a lower activity than the wild type gene. By simultaneously constructing transposons where the promoters control expression of *luc*, which encodes a luciferase that produces bioluminescense, a luciferase assay could be used to measure the relative strengths of the promoters. The aim was to find a promoter that negatively impacts expression of AlgL such that a higher molecular weight alginate could be produced, without the mutation being lethal.

A homologous recombination vector that disrupts the wild type *algL* along with the acetylation genes *algI*, *algV* and *algF* was also constructed. After transposition, homologous recombination was used in an attempt to remove wild type copies of *algL*. In addition, disruption of *algI*, *algV* and *algF* could increase the G-content of the produced alginate, as the acetylation genes prevent epimerization of mannuronate [2]. Acetylation also prevents lyase activity [2] however, which could contribute to lowering the molecular weight of the produced alginate somewhat. After integration by homologous recombination, verification by PCR was performed. Because *A. vinelandii* contains many chromosome copies [26], pure mutants are often difficult to obtain. The CRISPR-Cas9 vector pMM114, constructed by Maråk [145], was therefore used to remove remaining wild type *algL* chromosomes that persisted after homologous recombination. This vector was constructed to target *algI*, and would therefore not affect transposon inserts. Because the conjugation was not successful,

and PCR verification produced some unexpected fragments, the homologous recombination vector was sequenced.

4.3.1 Construction of *algL* transposons

To investigate if *algL* expression controlled by different promoters would result in a higher molecular weight alginate, transposons containing *algL* controlled by the P*m*, P*lac* and P*const* promoters were constructed. An overview of the cloning strategy for the *algL* transposons is presented in figure 4.17.

Figure 4.17: The P*m* promoter of pCM1 was replaced by the P*lac* promoter from pMM107 by NdeI-SacI digestion of both plasmids. P*lac* along with the spectinomycin resistance gene *aaDa* was subsequently ligated with pCM1, containing *algL*. The P*lac* promoter of the resulting plasmid, pHMT7, was replaced by P*const* by NdeI-SbfI digestion of pHMT7 and pHE513. Ligation of P*const* into pHMT7 yielded the transposon vector pHMT8.

R6K-derived plasmids, which require the π protein for replication [56], were used to construct the transposon vectors. *E. coli* S17.1-λpir, which encodes the π protein, was therefore used to carry the vectors. *A. vinelandii* does not encode the π protein [56], and the vectors would therefore function as suicide vectors once conjugated to *A. vinelandii* such that harmful repeated transposon insertions were avoided.

pCM1, containing *algL* controlled by P*m*, was used to construct the remaining transposons. P*lac* had already been obtained by PCR by Maråk and cloned to form pMM107. To exchange P*m* with P*lac*, pCM1 and pMM107 were digested using NdeI-SacI. The digested plasmids were separated as shown in figure 4.18, and the 6.4 kb fragment of pCM1 along with the 1.2 kb fragment from pMM107 were excised, purified, ligated and transformed into *E. coli* S17.1-λpir.

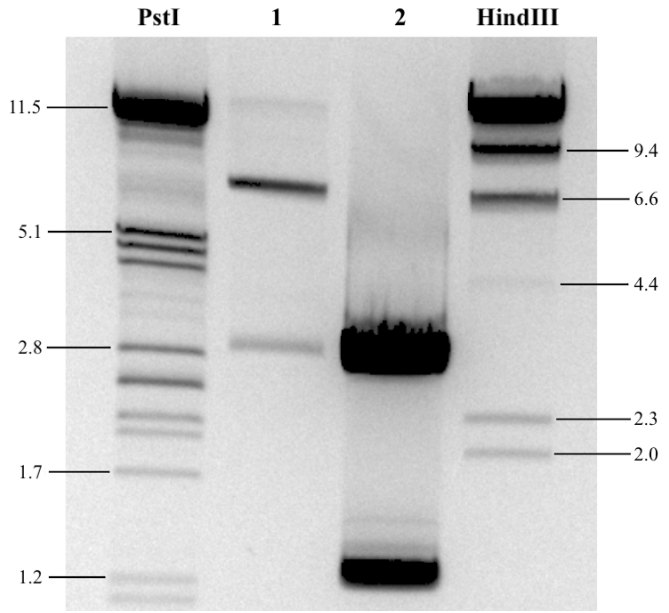

Figure 4.18: pCM1 and pMM107 digested with NdeI-SacI. Lane 1 contains pCM1 with expected fragments of 6.4 and 3.0 kb, and lane 2 contains pMM107 with the expected fragments of 2.9 and 1.2 kb. The 6.4 kb fragment of pCM1 containing *algL* and the 1.2 kb fragment of pMM107 containing P*lac* were excised.

Plasmids were isolated from four transformants and verified by digestion with EcoRI. Figure 4.19 shows the resulting fragments. The parental plasmid pCM1 would give 5.1 and 4.3 kb fragments, and pMM107 a 4.1 kb fragment. The new plasmid containing *algL* controlled by P*lac* would give 5.1, 1.3 and 1.2 kb fragments. Several colonies contained the correct bands, and the new plasmid was designated pHMT7.

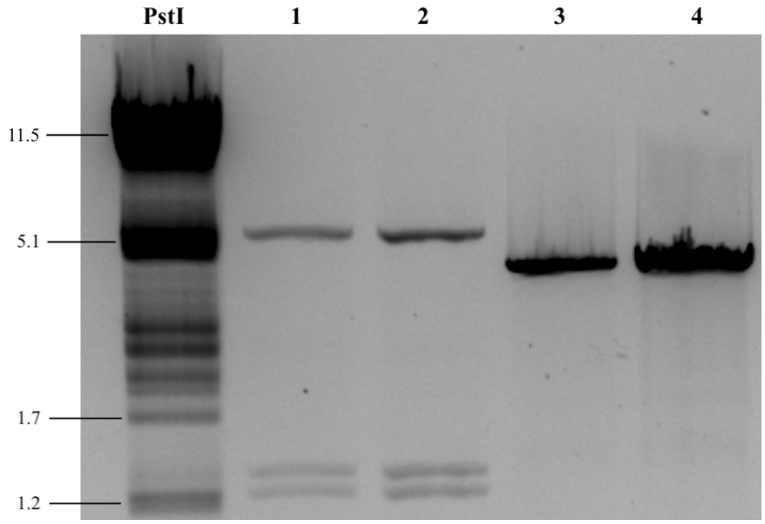

Figure 4.19: Plasmids formed when the P*m* promoter of pCM1 was exchanged with P*lac*, digested with EcoRI. Lanes 1-2 contain the expected 5.1, 1.3 and 1.2 kb bands. Lanes 3-4 contain a single band that is consistent with religation of pMM107, which would result in a 4.1 kb band.

The remaining transposon was constructed by exchanging P*lac* of pHMT7 with P*const* from pHE513. Both plasmids were digested using NdeI and SbfI. The digested plasmids were separated as shown in figure 4.20, and the 7.4 kb pHMT7 fragment along with the 0.2 kb pHE513 fragment were excised. The 0.2 kb fragment was difficult to visualize on the gel, but was obtained by increasing the amount of DNA and running it on a separate 1.5% agarose gel. The excised fragments were purified, ligated and transformed into *E. coli* S17.1-λpir.

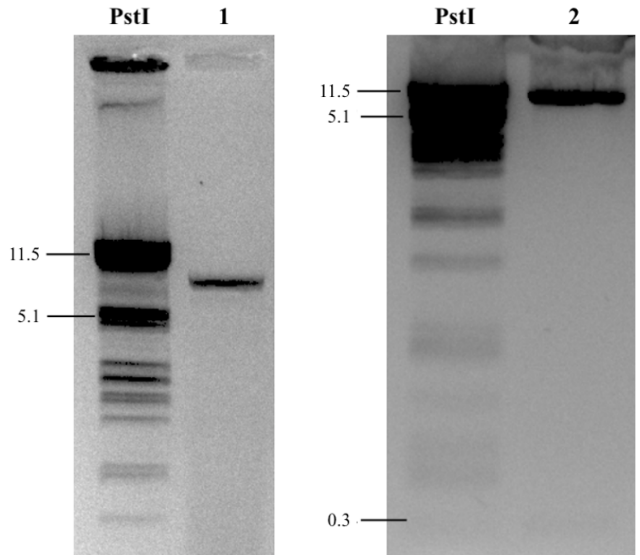

Figure 4.20: pHMT7 and pHE513 digested with NdeI-SbfI. Lane 1 contains pHMT7 with the expected 7.4 and 0.2 kb fragments, and lane 2 contains pHE513 with the expected 7.2 and 0.2 kb fragments. The 7.4 kb pHMT7 band and the 0.2 kb pHE513 P*const* band were excised.

Plasmids were isolated from five transformants and verified by digestion with SacI. Figure 4.21 shows the resulting fragments. The parental plasmid pHMT7 would give a 7.6 kb fragment, and pHE513 a 7.4 kb fragment. The new plasmid containing *algL* controlled by *Pconst* would give 6.6 and 1.0 kb fragments. A colony was verified to contain the correct bands, and the new plasmid was designated pHMT8.

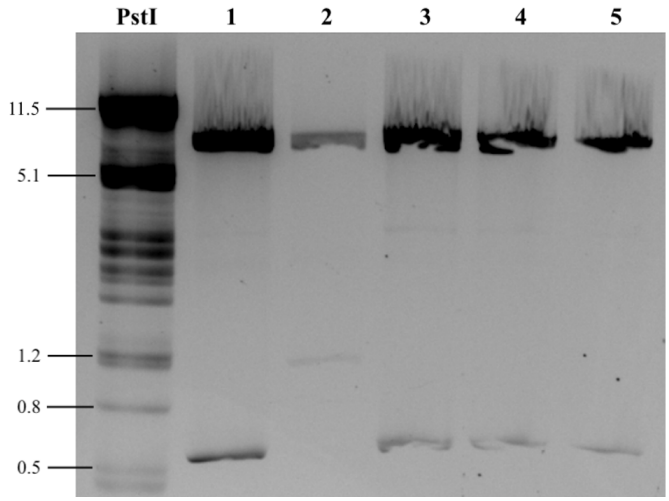

Figure 4.21: Plasmids formed when P*lac* of pHMT7 was exchanged with P*const*, digested with SacI. Lane 2 contains the expected 6.6 and 1.0 kb fragments. The fragments of the other lanes do not correspond with the parental plasmids.

4.3.2 Construction of *luc* transposons

To measure the relative strengths of promoters, transposons were constructed where P*m*, P*lac* and P*const* controlled expression of the reporter gene *luc*. As mentioned in section 2.13, *luc* encodes the enzyme luciferase, which uses luciferin as a substrate to produce bioluminescence [138]. By transferring the *luc* transposons to *A. vinelandii* and performing a luciferase assay, the relative strengths of the promoters could be evaluated. An overview of the cloning strategy for the *luc* transposons is presented in figure 4.22.

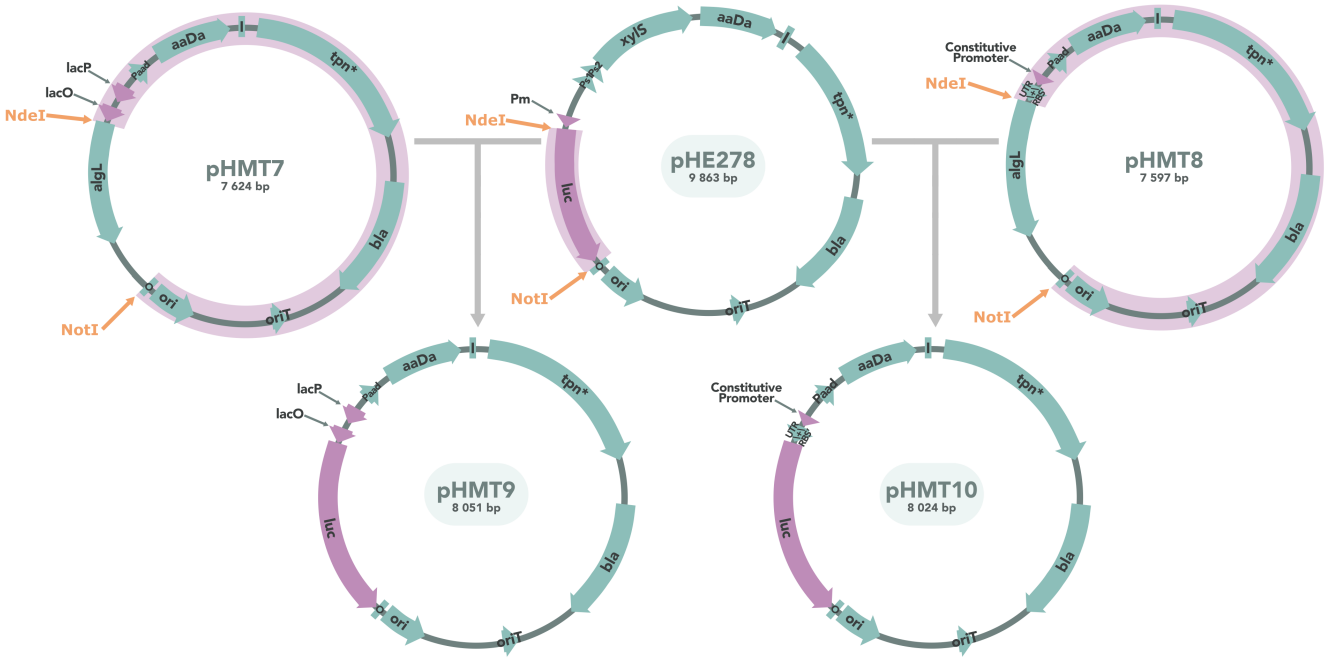

Figure 4.22: pHMT7, pHMT8 along with pHE278, which already contain *luc* controlled by the P*m* promoter, was used to construct two more transposon vectors containing P*lac* and P*const*. pHMT7, pHMT8 and pHE278 were digested using NdeI-NotI. The *luc* gene from pHE278 was then exchanged with *algL* in pHMT7 and pHMT8, producing pHMT9 and pHMT10.

pHE278 already contained *luc* controlled by P*m*. *luc* from pHE278 was exchanged with *algL* in pHMT7 and pHMT8 by digestion of all three plasmids with NdeI and NotI. The digested plasmids were separated as shown in figure 4.23. The 6.3 kb pHMT7 fragment, the 6.3 kb pHMT8 fragment and the 1.7 kb pHE278 fragment were excised, purified, ligated and transformed into *E. coli* S17.1-λpir.

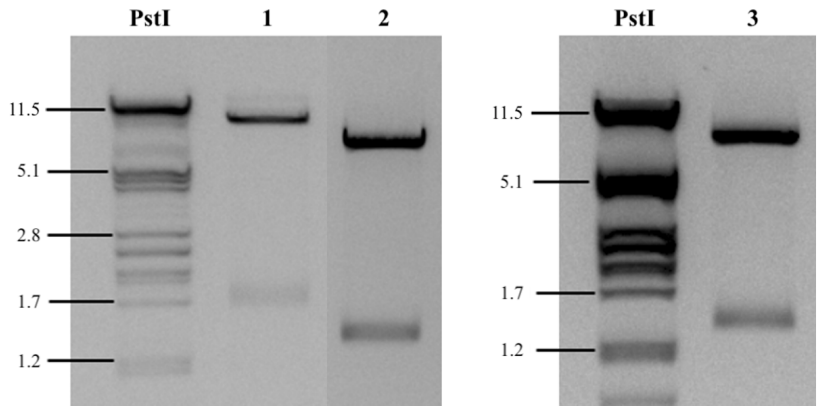

Figure 4.23: pHE278, pHMT7 and pHMT8 digested with NdeI-NotI. Lane 1 contains pHE278 with the expected 8.2 and 1.7 kb fragments, lane 2 contains pHMT8 with the expected 6.3 and 1.3 kb fragments and lane 3 contains pHMT7 with the expected 6.3 and 1.3 kb fragments. The 1.7 kb pHE278 band containing *luc*, along with the 6.3 kb pHMT8 and the 6.3 bp pHMT7 bands were excised.

Plasmids were isolated from four transformants and verified by digestion with BamHI. Figure 4.24 shows the resulting fragments. The parental plasmid pHE278 would in this case give 5.3, 2.9 and 1.7 kb bands, and pHMT7 and pHMT8 would give 2.9, 2.5, 1.7 and 0.5 kb bands. The new plasmid containing *luc* controlled by P*lac* would give 3.5, 2.9 and 1.7 kb bands, and the plasmid with P*const* would give 3.4, 2.9 and 1.7 kb bands. All lanes contained the correct fragments. The pHMT7 derivative was designated pHMT9 and the pHMT8 derivative was designated pHMT10.

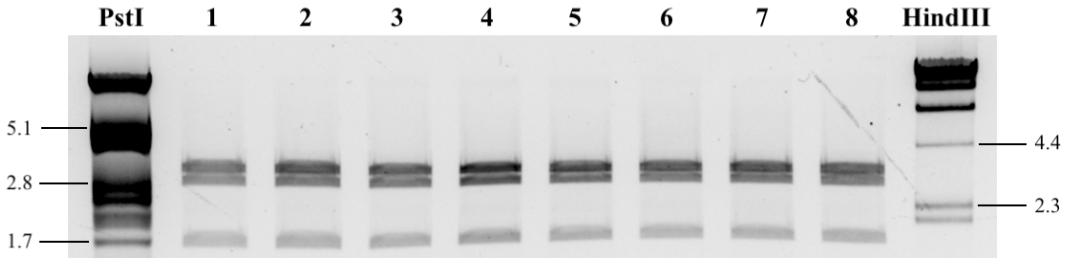

Figure 4.24: Plasmids formed when *luc* of pHE278 was exchanged with *algL* in pHMT7 and pHMT8, digested with BamHI. Lanes 1-4 contain the pHMT7 derivative with the expected 3.5, 2.9 and 1.7 kb fragments. Lanes 5-8 contain the pHMT8 derivative with the expected 3.4, 2.9 and 1.7 kb fragments. All lanes contained the correct fragments.

4.3.3 Construction of *algLH199R* transposons

Vectors containing the less efficient *algL* mutant *algLH199R* were constructed with the aim of ultimately producing a mutant strain that produced higher molecular weight alginate. Transposons were constructed where P*m*, P*lac* and P*const* controlled expression of *algLH199R*. As mentioned in section 1.2.1, *algLH199R* encodes a less active alginate lyase, and combining it with a suitable promoter could therefore result in an alginate with increased molecular weight. An overview of the cloning strategy for the *algLH199R* transposons is presented in figure 4.25.

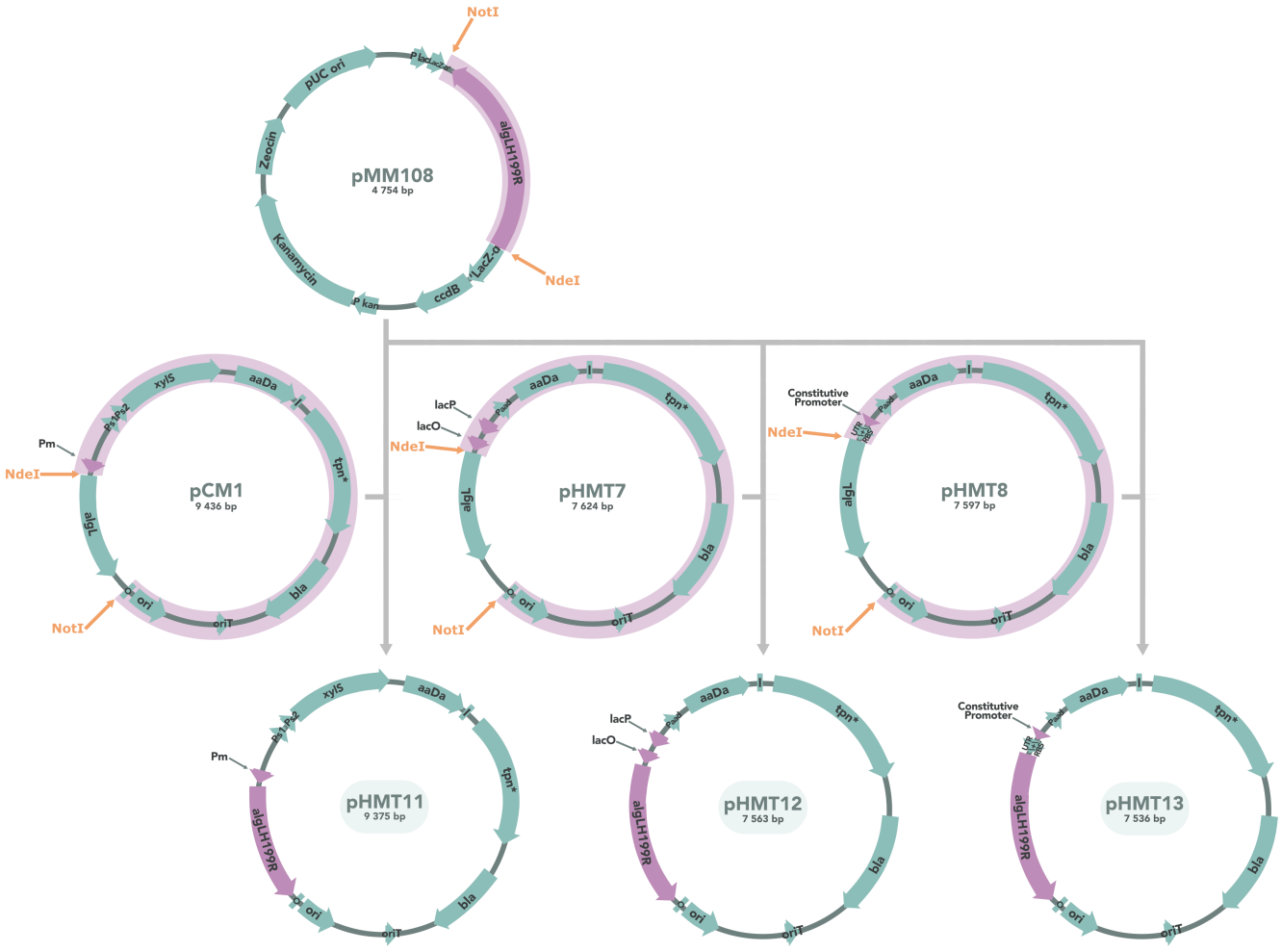

Figure 4.25: *algLH199R* was excised from pMM108 using NdeI-NotI digestion, and subsequently ligated into the NdeI-NotI digested backbones of pCM1, pHMT7 and pHMT8. This exchanged *algL* for *algLH199R*, producing the three new transposons pHMT11, pHMT12 and pHMT13, with *algLH199R* controlled by P*m*, P*lac* and P*const*, respectively.

algLH199R had already been obtained by PCR, cloned to form pMM108 and verified by sequencing by Maråk [145]. The *algL* vectors were used as backbones for the new transposons. To remove *algL* and replace it with *algLH199R*, pMM108, pCM1, pHMT7 and pHMT8 were digested with NdeI and NotI. The digested plasmids were separated as shown in figure 4.26. The 1.2 kb *algLH199R* fragments of pMM108, along with the 6.3 kb pHMT8, 8.2 kb pCM1 and 6.3 kb pHMT7 backbones were excised. The pMM108 restriction reaction contained a lot of DNA, which could explain why the bands moved somewhat fast through the gel. After excision, the fragments were purified, ligated and transformed into *E. coli* S17.1-λpir.

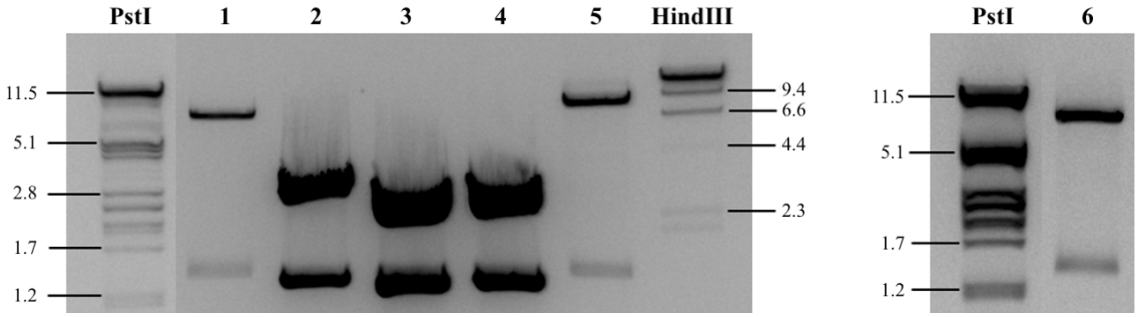

Figure 4.26: pMM108, pCM1, pHMT7 and pHMT8 digested with NdeI-NotI. Lane 1 contains pHMT8 with the expected 6.3 and 1.3 kb fragments, lane 2-4 contains pMM108 with the expected 3.5 kb, 1.2 kb and 44 bp fragments, lane 5 contains pCM1 with the expected 8.2 and 1.3 kb fragments and lane 6 contains pHMT7 with the expected 6.3 and 1.3 kb fragments. The 1.2 kb *algLH199R* fragments of pMM108, along with the 6.3 kb pHMT8, 8.2 kb pCM1 and 6.3 kb pHMT7 fragments were excised.

Plasmids were isolated from four transformants from each ligation and verified by digestion with BamHI. Figure 4.27 shows the resulting fragments. The parental plasmid pMM108 would give a 4.8 kb fragment, pCM1 would give 4.3, 2.9, 1.7 and 0.5 kb fragments and pHMT7 and pHMT8 would both give 2.9, 2.5, 1.7 and 0.5 kb fragments. The new pCM1 derivative would give 4.8, 2.9 and 1.7 kb fragments, the pHMT7 derivative would give 3.0, 2.9 and 1.7 kb fragments and the pHMT8 derivative would give 2.9, 2.9 and 1.7 kb fragments. All lanes appeared to contain the correct fragments, although the 3.0 and 2.9 bands were difficult to distinguish. The new pCM1 derivative was designated pHMT11, the pHMT7 derivative was designated pHMT12 and the pHMT8 derivative was designated pHMT13.

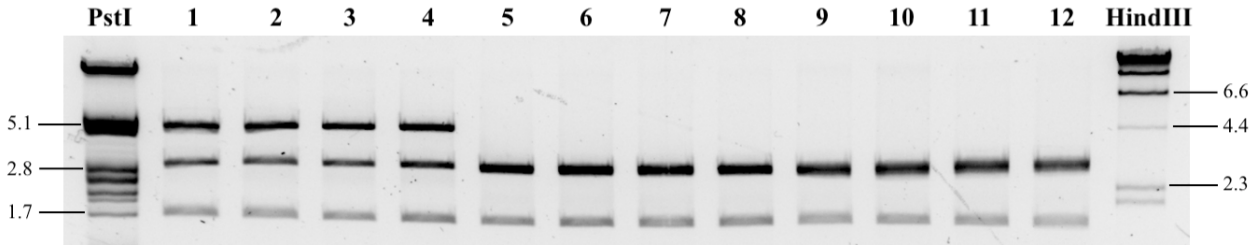

Figure 4.27: Plasmid formed when *algL* of pCM1, pHMT7 and pHMT8 was exchanged with *algLH199R* from pMM108, digested with BamHI. Lanes 1-4 contain the pCM1 derivative with the expected 4.8, 2.9 and 1.7 kb fragments. Lanes 5-8 contain the pHMT7 derivative with the expected 3.0, 2.9 and 1.7 kb fragments. Lanes 9-12 contain the pHMT8 derivative with the expected 2.9, 2.9 and 1.7 kb fragments. Although the 3.0 and 2.9 kb bands were difficult to distinguish, all lanes appeared to contain the correct fragments.

4.3.4 Construction of a homologous recombination vector that disrupts *algL*, *algI*, *algV* and *algF*

After insertion of transposons into the *A. vinelandii* genome, wild type *algL* would be disrupted using a homologous recombination vector. This vector would also disrupt the acetylation genes *algI*, *algV* and *algF*, which could increase the G-content of the alginate.

An overview of the cloning strategy used to construct the homologous recombination vector is presented in figure 4.28. An R2K-derived plasmid that requires the inducer *m*-toluate for replication in *A. vinelandii* was used as a conditional suicide vector. Construction involved removing most of the *algL* gene in pHE103 and replacing it with a fragment from pMM109 containing *algA* and parts of *algF*. pMM109 was previously constructed by Maråk [145] by first isolating the fragment containing *algA* and *algF* followed by cloning and sequencing. The resulting plasmid would contain regions of homology to *algX* and parts of *algL* as well as to *algA* and parts of *algF*, enabling homologous recombination and thus removal of or disruption to the wild type genes found between *algA* and *algX*. The gene cluster is depicted in figure 1.3 of section 1.2.2. Tetracycline resistance conferring genes were inserted into the vector, which was followed by transfer to a conjugation vector.

Figure 4.28: The backbone of pHE103, containing *algX* and parts of *algL*, was obtained by EcoRV-SacI digestion. Similarly, the fragment containing *algA* and parts of *algF* from pMM109 was obtained by EcoRV-SacI digestion. The fragments were subsequently ligated to form pHMT14. SacI-SbfI digestion of pHMT14 and PstI-SacI digested pHE573 enabled removal and insertion of tetracycline resistance conferring genes into pHMT14 to form pHMT15. SacI-SpeI digestion was next used to transfer the genes into the conjugation vector pHE216, forming pHMT16.

pHE103 and pMM109 were digested using EcoRV and SacI to remove parts of *algL* and replace it with *algA* and parts of *algF*. The digested plasmids were separated as shown in figure 4.29. The 4.4 kb fragment from pHE103 and the 1.3 kb fragment from pMM109 were excised, purified, ligated and transformed into *E. coli* S17.1-λpir.

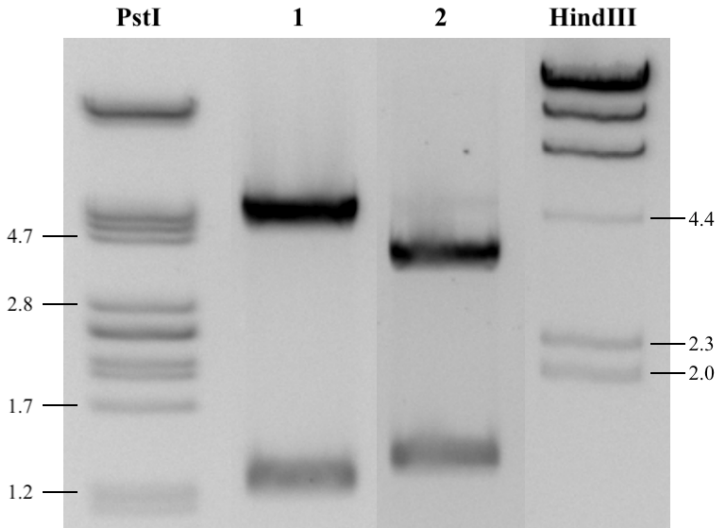

Figure 4.29: pHE103 and pMM109 digested with EcoRV-SacI. Lane 1 contains pHE103 with the expected 4.4 and 1.2 kb fragments and lane 2 contains pMM109 with the expected 3.5 and 1.3 kb fragments, although the PstI marker appeared to have moved a bit too fast through the gel. The 4.4 kb pHE103 band, along with the 1.3 kb pMM109 band, were excised.

Plasmids were isolated from five transformants from each ligation and verified by digestion with XhoI. Figure 4.30 shows the resulting fragments. The parental plasmid pHE103 would give a 5.6 kb band, and pMM109 would give 3.7, 0.6 and 0.4 kb bands. The new plasmid would give 3.0, 2.3 and 0.4 kb bands. All lanes appeared to contain the correct plasmid, which was designated pHMT14.

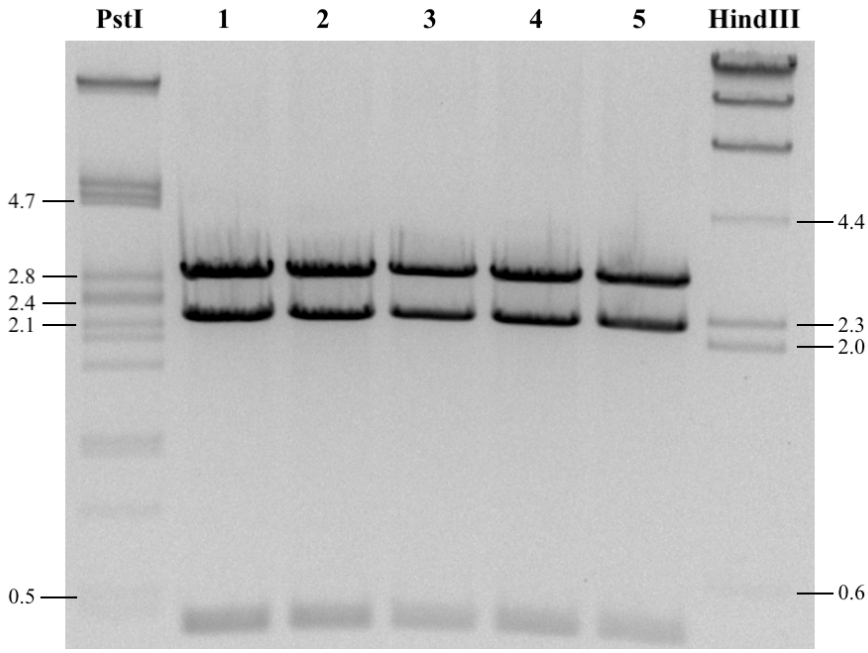

Figure 4.30: Plasmids formed when *algA* and parts of *algF* from pMM109 replaced parts of *algL* of pHE103, digested with XhoI. Lanes 1-5 contain the new plasmid with the expected 3.0, 2.3 and 0.4 kb fragments.

Tetracycline resistance conferring genes were next inserted into pHMT14 by digestion of pHMT14 with SacI and SbfI and pHE573 with DraI, PstI and SacI. The digested plasmids were separated as shown in figure 4.31. The 2.3 kb fragment from pHE573 and the 5.7 kb fragment from pMM109 were excised, purified, ligated and transformed into *E. coli* S17.1-λpir.

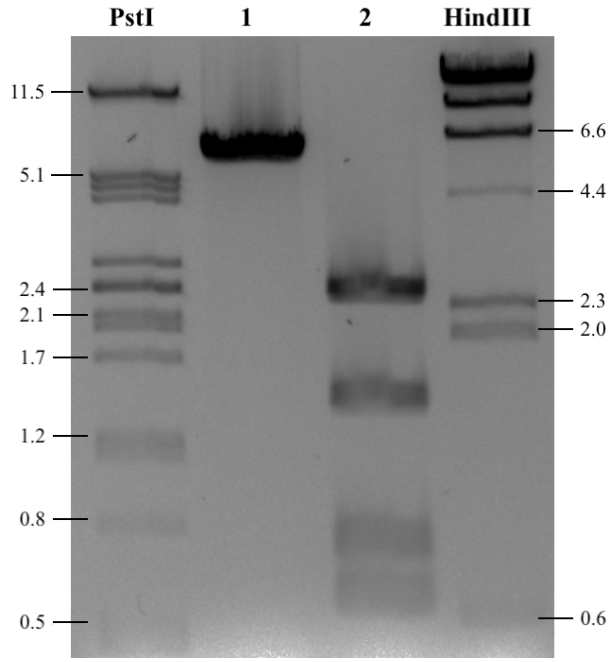

Figure 4.31: SacI-SbfI digested pHMT14 and DraI, PstI and SacI digested pHE573. DraI was used to avoid close bands. Lane 1 contains pHMT14 with the expected 5.7 kb and 53 bp fragments. Lane 2 contains pHE573 with the expected 2.3, 1.4, 0.8 and 0.6 kb fragments. The 5.7 kb pHMT14 band and the 2.3 kb pHE573 fragments were excised.

Plasmids were isolated from five transformants and verified by digestion with BamHI. Figure 4.32 shows the resulting fragments. The parental plasmid pHMT14 would give a 5.7 kb band, and pHE573 would give 2.8 and 2.3 kb bands. The new plasmid would give 5.7 and 2.3 kb bands. All lanes contained the correct plasmid, designated pHMT15.

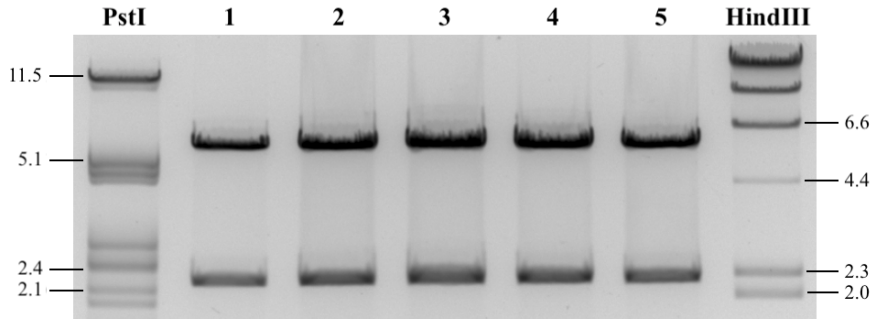

Figure 4.32: Plasmids formed when *tetA* and *tetR* were inserted into pHMT14, digested with BamHI. Lanes 1-5 contain the expected 5.7 and 2.3 kb fragments.

Finally, the fragment constructed for homologous recombination was transferred to the conjugation vector pHE216. Both plasmids were digested using SacI and SpeI. pHMT15 was also digested with DraIII to avoid bands in close proximity. The digested plasmids were separated as shown in figure 4.33. The 5.3 kb fragment from pHMT15 and the 9.3 kb fragment from pHE216 were excised, purified, ligated and transformed into *E. coli* S17.1-λpir.

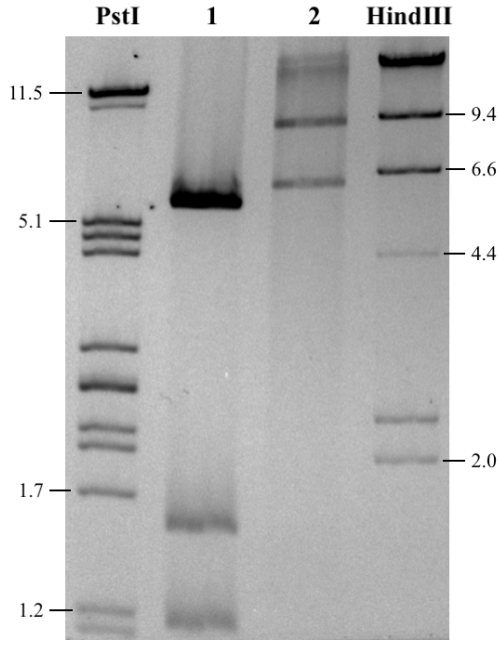

Figure 4.33: SacI-SpeI digested pHMT15 and pHE216. pHMT15 was also digested using DraIII to avoid close bands. Lane 1 contains pHMT15 with the expected 5.3, 1.6 and 1.1 kb fragments. Lane 2 contains pHE216 with the expected 9.3 and 6.2 kb fragments. An additional larger band was visible in lane 2 that was consistent with partial digestion. However, the desired 9.3 kb fragment was clearly visible and was excised along with the 5.3 kb fragment of pHMT15.

Plasmids were isolated from seven transformants and verified by digestion with EcoRV. Figure 4.34 shows the resulting fragments. The parental plasmid pHMT15 would give 5.9, 1.2 and 0.9 kb fragments, and pHE216 would give 11.1 and 4.4 kb fragments. The new plasmid would give 8.8, 3.6, 1.2 and 0.9 kb fragments. All lanes appeared to contain the correct plasmid, which was designated pHMT16.

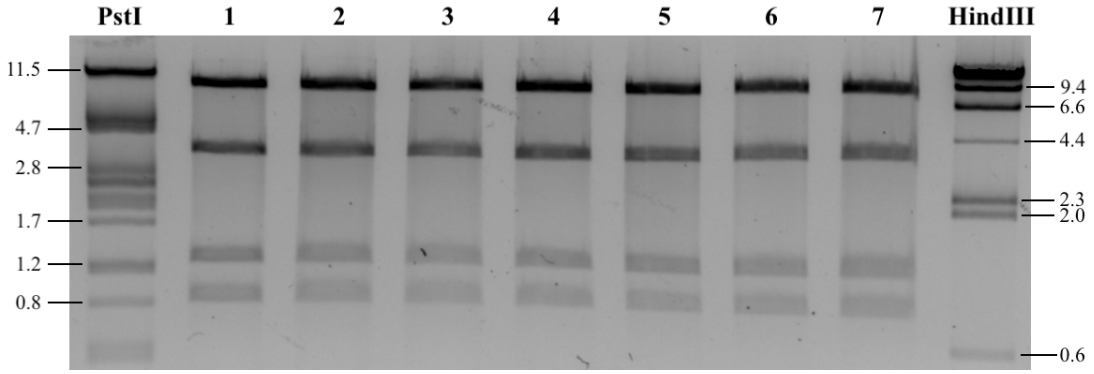

Figure 4.34: Plasmids formed when the fragment constructed for homologous recombination was inserted into the conjugation vector pHE216. Lanes 1-7 contain the new plasmid with the expected 8.8, 3.6, 1.2 and 0.9 kb fragments.

4.3.5 Transfer of transposons to *A. vinelandii*, measurement of promoter strength and verification of alginate production

To save time, all nine transposons containing *algL*, *luc* and *algLH199R* controlled by P*m*, P*lac* or P*const* were transferred from *E. coli* S17.1-λpir to *A. vinelandii* ATCC12518 by conjugation. The transposons were transferred to *A. vinelandii* prior to disruption of wild type *algL*, even though homologous recombination would likely not have disrupted all wild type copies. The conjugation was performed using ampicillin and spectinomycin for selection of transconjugants. To remove the alginate-capsule that surrounds *A. vinelandii* and increase the chance of DNA uptake, the cells were washed with glycerol prior to conjugation. The conjugation was successful, resulting in several transconjugants per conjugation.

Next, a luciferase assay was performed to measure the relative strength of the promoters P*m*, P*lac* and P*const*. BM was used to prepare three biological replicates from one transconjugant colony per strain. For P*m*, which is inducible, six biological replicates were prepared, and three had the inducer *m*-toluate added after 8 hours. Samples were extracted after 24 and 48 hours, OD_{600} was measured, and the luciferase assay presented in section 2.13 was performed. The data from the luciferase assay are presented in appendix N.

The measured relative light units (RLU) after 24 and 48 hours of the different promoters is presented in figure 4.35. The OD_{600} measurements varied slightly, and to account for this, RLU per OD_{600} is presented in figure 4.36.

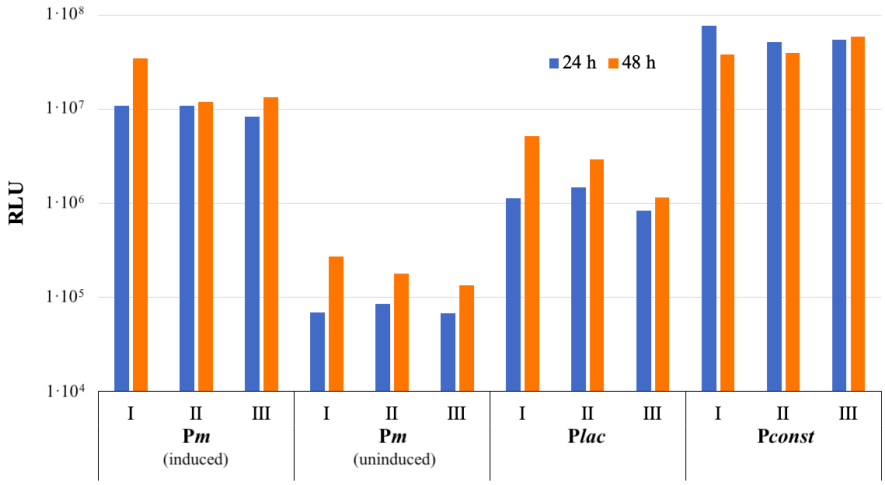

Figure 4.35: The RLU measurements obtained from a luciferase assay after 24 and 48 hours for *A. vinelandii* transposon mutants containing *luc* controlled by the promoters P*m*, P*lac* and P*const*. Half of the biological replicates of P*m* were induced after 8 hours, while half were left uninduced.

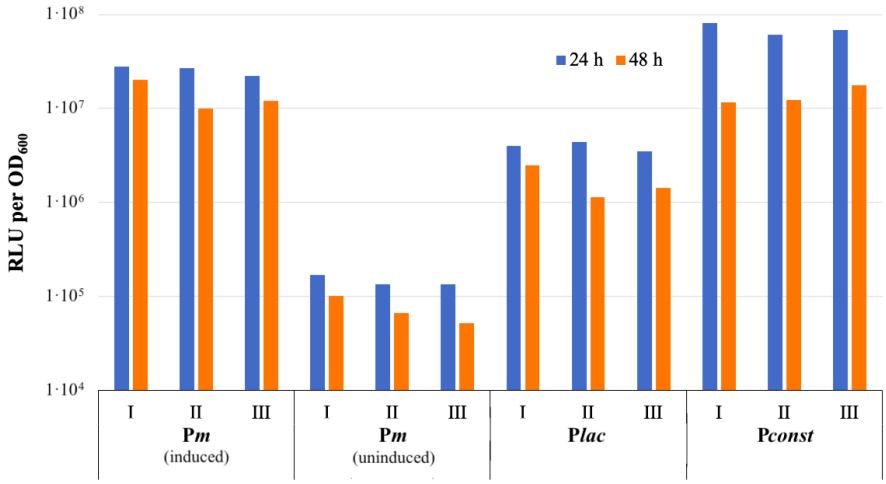

Figure 4.36: The RLU measurements obtained from a luciferase assay per OD_{600} after 24 and 48 hours for *A. vinelandii* transposon mutants containing *luc* controlled by the promoters P*m*, P*lac* and P*const*. Half of the biological replicates of P*m* were induced after 8 hours, while half were left uninduced.

When accounting for growth, the strength of all promoters weakened somewhat with time. P*lac* produced relatively low levels of light overall, indicating a relatively low expression

of luciferase as compared to the other strains. This suggests that it is a relatively weak promoter compared to P*const* and the induced P*m* promoter. The relative strength of P*const* in *A. vinelandii* on the other hand, was found to be very strong. P*const* is originally a strong synthetic promoter from a gram positive species of bacteria [143, 144], and it was therefore uncertain if it would perform similarly in the gram negative species *A. vinelandii*. These measurements indicate however, that P*const* may be used as a strong promoter in *A. vinelandii*.

As expected, the uninduced P*m* promoter produced low levels of light compared to induced P*m* as well as the other strains. The ability to regulate the expression from this promoter up or down with the use of an inducer would be useful, especially when working with an essential gene such as *algL*. The strength of the promoter originally controlling expression of *algL*, and the lowest expression level needed for the cells to be viable, is uncertain. Using a promoter that allows its expression level to be adjusted would therefore be preferable. It was therefore decided to proceed with the transposon mutants containing *algL* and *algLH199R* controlled by the P*m* promoter.

Before proceeding to removal of wild type *algL* in the *A. vinelandii* transposon mutants, their alginate production was measured. Although unlikely, transposon insertion could potentially disrupt genes involved in alginate production, thus resulting in mutants with low or no alginate production. To make sure that this was not the case, a small enzymatic alginate assay was performed. Wild type *A. vinelandii* was included for comparison.

One biological replicate was prepared per strain. RA1 medium was used to avoid *A. vinelandii* expending energy on nitrogen fixation. Samples were extracted after 24 hours, OD_{600} was measured, and an enzymatic alginate assay using M- and G-lyase, presented in section 2.12, was used to measure alginate production. The standard curve used to calculate alginate concentration and the data from the alginate assay is presented in appendix M. The measured alginate production (g/l) after 24 hours of the *algL* and *algLH199R* mutants compared to that of wild type *A. vinelandii* is presented in table 4.2. The table also includes alginate production (g/l) per OD_{600} values.

Table 4.2: The measured alginate production (g/l) and alginate production (g/l) per OD_{600} after 24 hours of the *algL* and *algLH199R* mutants compared to that of wild type *A. vinelandii*.

	Alginate concentration (g/l) ± SD	**Alginate concentration (g/l) per OD_{600} ± SD**
Wild type	0.225 ± 0.115	0.223 ± 0.114
***algL* with *Pm* promoter**	0.389 ± 0.274	0.731 ± 0.211
***algLH199R* with *Pm* promoter**	0.302 ± 0.0470	0.468 ± 0.0727

The mutants were found to produce alginate, indicating that transposon inserts did not affect the alginate biosynthesis machinery of *A. vinelandii*. Next, wild type *algL* chromosome copies were removed by homologous recombination and CRISPR-Cas9.

4.3.6 Removal of wild type *algL* by homologous recombination, verification and removal of remaining wild type *algL* using CRISPR-Cas9

The homologous recombination vector pHMT16 made to disrupt *algL*, *algI*, *algV* and *algF* was constructed in section 4.3.4. pHMT16 was conjugated to the transposon mutants containing *algL* and *algLH199R* controlled by the *Pm* promoter in an attempt to remove wild type chromosome copies of *algL*. In addition, disruption of the acetylation genes could increase the G-content of the produced alginate. pHMT16 was also conjugated to wild type *A. vinelandii* as a comparison, which was not expected to survive removal of all wild type *algL*. Homologous recombination would however likely not disrupt all copies of *algL*.

pHMT16 was transferred from *E. coli* S17.1-λpir to *A. vinelandii* mutants and wild type by conjugation. pHMT16 contains tetracycline resistance conferring genes, and tetracycline was therefore used to select for colonies that had taken up the plasmid. To remove the alginate-capsule that surrounds *A. vinelandii* and increase the chance of DNA uptake, the cells were washed with glycerol prior to conjugation.

The conjugation was successful and resulted in several transconjugants per mutant strain. The fragment containing regions of homology to *algA* and *algX* was next integrated into the *A. vinelandii* chromosome by homologous recombination, as described in section 2.2.4. Tetracycline was used for selection of cells that had undergone the first crossover-

event. Cells that had undergone a second crossover-event were screened for using counter-selection by growth on plates containing BA with sucrose. Lastly, growth on and off tetracycline was used to screen for tetracycline sensitive colonies, which were then tested for the recombination.

Four tetracycline sensitive colonies from each conjugation were verified by PCR, using the boiling method to obtain DNA. For *algLH199R* (pHMT16) however, 250 colonies were tested for tetracycline sensitivity with no success. *sacB* was placed on the plasmid backbone to select for a double-crossover event as described in section 1.3.2, yet tetracycline resistance suggested that the plasmid remained integrated in the genome even though the cells were able to grow on sucrose. This suggests that a mutation that conferred sucrose resistance had occured, which is known to occasionally happen [62]. Four colonies from *algLH199R* (pHMT16) were still verified by PCR.

Three different primer pairs were used in the PCR reactions. Unfortunately, wild type *A. vinelandii* and pHMT16 was not included as a comparison. First, the primer pair pHMT16F/pHMT16R was used to determine if the mutants had lost pHMT16. If pHMT16 had been lost during homologous recombination, the PCR reaction would result in no product. If pHMT16 was present, it would result in a 1.6 kb PCR product. Figure 4.37 shows the resulting PCR products. No bands were visible, indicating that none of the colonies appeared to contain pHMT16. The tetracycline resistance of the *algLH199R* (pHMT16) mutant indicated that at least some portion of the plasmid remained in this strain, but PCR did not result in any fragments. This may indicate that only parts of pHMT16 remained integrated in this mutant. Because pHMT16 was not used to control that the primers were functional however, the results were slightly uncertain.

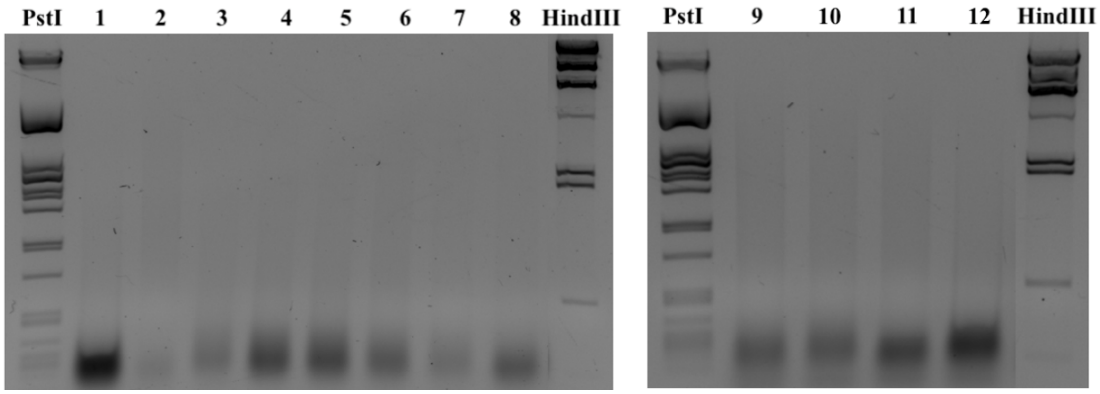

Figure 4.37: Separated PCR products for verification of pHMT16 loss after homologous recombination. Lanes 1-4 show wild type + pHMT16, lanes 5-8 show *algL* (pHMT16) and lanes 9-12 show *algLH199R* (pHMT16). Loss of pHMT16 would result in no PCR product, whereas presence of pHMT16 would give a 1.6 kb PCR product. None of the lanes contain a PCR product, indicating that all strains had lost pHMT16.

Next, the primer pair HalgVF/HalgVR was used to determine if the strains still contained wild type chromosomes. That is, if the cells still contained chromosome copies where the region between *algA* and *algX* had not been disrupted. The *algV* gene is located in this segment and should have been removed entirely if homologous recombination had been successful in all chromosomes, thus resulting in no PCR product. If wild type copies were present, PCR would give a 1.1 kb fragment. Figure 4.38 shows the PCR products. All PCR products were of approximately the size corresponding to presence of *algV*, indicating that wild type chromosomes were still present after homologous recombination. PCR produced a lot of DNA, which could explain why some fragments moved somewhat fast through the gel.

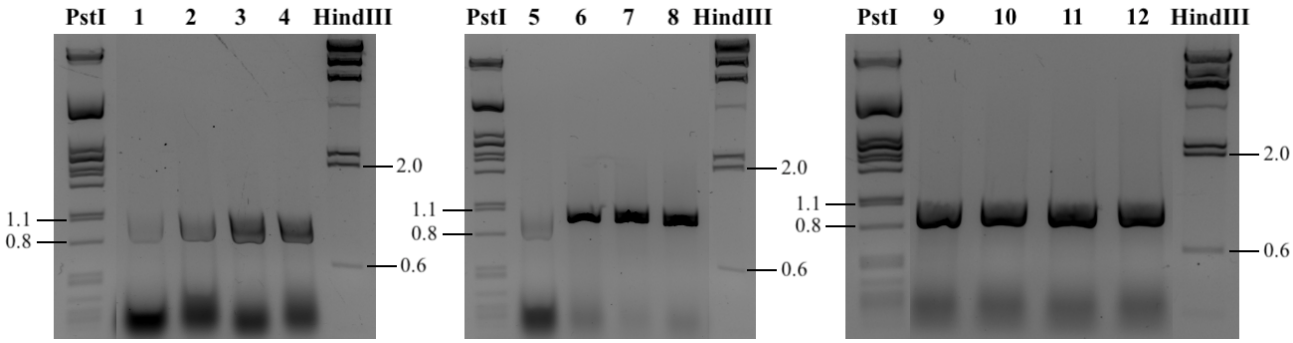

Figure 4.38: Separated PCR products for verification of presence of wild type chromosomes after homologous recombination. Lanes 1-4 show wild type + pHMT16, lanes 5-8 show *algL* (pHMT16) and lanes 9-12 show *algLH199R* (pHMT16). No remaining wild type chromosomes and thus no remaining copies of *algV* would result in no PCR product. Presence of *algV* would give a 1.1 kb PCR product. All lanes contain bands that suggest wild type chromosome copies were still present.

Lastly, the primer pair algF-XF/algF-XR was used. The primers were used to determine if the region between *algA* and *algX* had been disrupted. If homologous recombination had been successful, this primer pair would result in a 0.9 kb fragment, as opposed to a 1.2 kb fragment of wild type chromosomes. Figure 4.39 shows the visualized PCR products. At least one lane per strain contained a band of approximately 0.9 kb, indicating that homologous recombination had successfully disrupted some chromosomes.

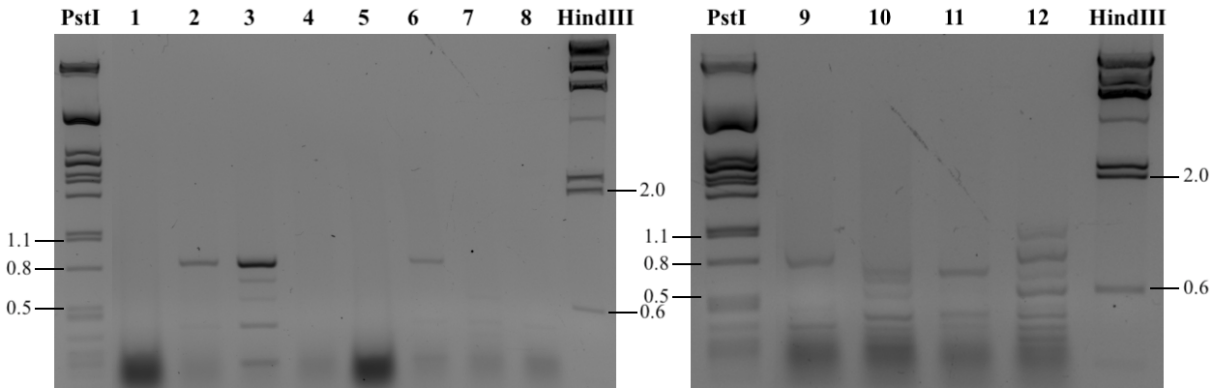

Figure 4.39: Separated PCR products for verification of removal of *algL* and acetylation genes using homologous recombination. Lanes 1-4 show wild type (pHMT16), lanes 5-8 show *algL* (pHMT16) and lanes 9-12 show *algLH199R* (pHMT16). If homologous recombination was successful, mutant chromosome copies would result in a 0.9 kb fragment, as opposed to a 1.2 kb fragment of wild type chromosomes. Lanes 2, 3, 6, 9 and possibly 12 contain bands that correspond to presence of mutated chromosomes. The bands of lanes 10 and 11 are slightly too short, and lane 12 additionally contains several other bands.

PCR suggested that several mutant strains were found that had lost pHMT16 and contained a mixture of wild type and mutated chromosomes. Because wild type *A. vinelandii* and pHMT16 was not included for comparison, it was not possible to be completely sure that the primers were functional. However, because of time constraints it was decided to proceed with trying to remove remaining wild type *algL* chromosomes with the use of CRISPR-Cas9. The PCR was redone simultaneously.

It was decided to proceed with 1-2 of the colonies of wild type (pHMT16), *algL* (pHMT16) and *algLH199R* (pHMT16) that PCR suggested contained both wild type and mutated chromosomes. The CRISPR-Cas9 vector pMM114, targeting *algI*, was transferred from *E. coli* S17.1 to the *A. vinelandii* strains by conjugation. Targeting of *algI* ensured that the *algL* and *algLH199R* transposon inserts would not be targeted by Cas9. pMM114 was constructed by Maråk [145] to be apramycin resistant. It is also an RK2 based vector that contains the inducible P*m*-XylS promoter system. *m*-toluate was therefore used as an inducer, and apramycin was used to select for transconjugants. To remove the alginate-capsule that surrounds *A. vinelandii* and increase the chance of DNA uptake, the cells were washed with glycerol prior to conjugation.

pMM114 had not previously been tested by conjugation to *A. vinelandii* to verify that its CRISPR-Cas9 system was functional. It is however a derivative of pMM106, also constructed by Maråk, which was shown to be functional. Because the functionality of the CRISPR-Cas9 vector pMM114 had not been tested before, it was also conjugated to wild type *A. vinelandii*. Since *algL* is an essential gene, the wild type strain was not expected to survive if the CRISPR-Cas9 system was functional and able to disrupt all *algL* copies.

The conjugation experiment was not successful, as transconjugants were not observed in any plates for any of the strains pMM114 was tested on. This was as expected for wild type *A. vinelandii*. The control plates showed a lot of growth, suggesting that the *A. vinelandii* strains were able to grow and that the problem was the conjugation itself. The conjugation efficiency of *A. vinelandii* is not very high, and it is of course possible that remaining alginate in the capsule surrounding *A. vinelandii* cells made the cells unable to take up DNA. It is also possible however, that that the CRISPR-Cas9 vector should have been designed such that the plasmid could be established in the cell prior to beginning to express Cas9. Toxicity due to Cas9 as well as off-target effects are known to prevent successful transformation [86]. In addition, the effect of DSBs and thus disruption to entire chromosomes in *A. vinelandii* is not well understood, and it may be that disruption of a number of chromosomes has a negative effect on fitness.

Disruption of *algL* using homologous recombination in combination with CRISPR-Cas9 required that *algL* was present in some form, which should have been accomplished by conjugation of transposon vectors to *A. vinelandii*. *m*-toluate was used for the conjugation experiment, and should have induced the P*m* promoter associated with *algL*/*algLH199R* of the transposon mutants, thus resulting in increased gene expression. However, it is possible that after removal of wild type *algL* the cells still did not produce enough AlgL to be viable. It is not known how much of the essential enzyme AlgL is necessary for survival, and the strength of the promoter associated with wild type *algL* is also unknown.

The PCR verification was also repeated using the same primer pairs, and wild type *A. vinelandii* and pHMT16 was included for comparison. This time, only colonies that were used in the conjugation experiment using pMM114 were investigated, and these are presented in figure 4.40. Again, pHMT16F/pHMT16R would result in a 1.6 kb PCR product if pHMT16 was present, and no product otherwise. HalgVF/HalgVR would similarly result in a 1.1 kb fragment if *algV* copies remained, and no product if not. algF-XF/algF-XR would result in a 0.9 kb fragment for mutants and a 1.2 kb fragment for wild type.

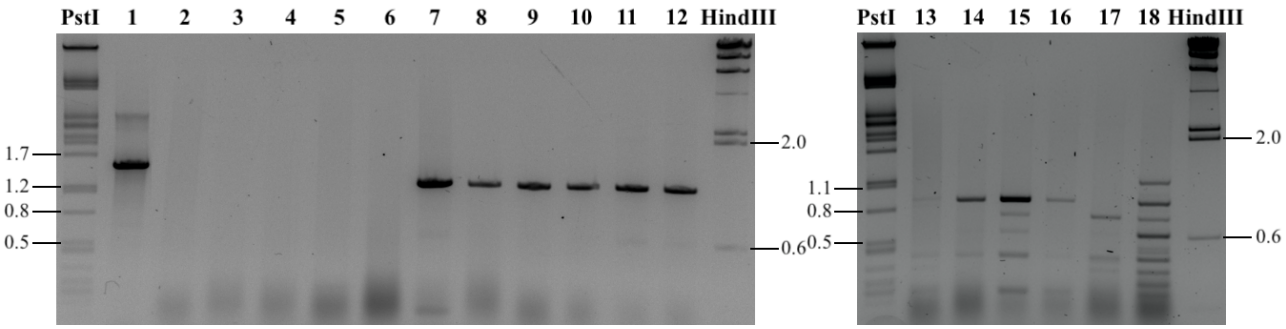

Figure 4.40: Separated PCR products for determination of loss of pHMT16 as well as presence of wild type and/or disrupted *algL*. PCR products of lanes 1-6 were obtained using pHMT16F/pHMT16R, which would result in a 1.6 kb fragment if pHMT16 was present. Lane 1 contains pHMT16, lanes 2-3 contain wild type (pHMT16), lane 4 contains *algL* (pHMT16) and lanes 5-6 contain *algLH199R* (pHMT16). PCR products of lanes 7-12 were obtained using HalgVF/HalgVR, which would result in a 1.1 kb fragment if *algV* was present. Lane 7 contains wild type *A. vinelandii*, lanes 8-9 contain wild type (pHMT16), lane 10 contains *algL* (pHMT16) and lanes 11-12 contain *algLH199R* (pHMT16). PCR products of lanes 13-18 were obtained using algF-XF/algF-XR, which would result in a 0.9 kb fragment for mutants and a 1.2 kb fragment for wild type. Lane 13 contains wild type *A. vinelandii*, lanes 14-15 contain wild type (pHMT16), lane 16 contains *algL* (pHMT16) and lanes 17-18 contain *algLH199R* (pHMT16).

pHMT16F/pHMT16R was found to be functional, as PCR of pHMT16 produced a band of the correct size. This also indicated that the mutant strains had in fact lost pHMT16. HalgVF/HalgVR was also found to be functional, as both wild type and mutants contained the expected wild type band. When algF-XF/algF-XR was used however, the wild type did not result in a clear band of the correct size that could be compared to that of the mutants. There was also a faint band that corresponded to the mutant band found in the wild type comparison. This was unexpected, and suggested that something was wrong with this primer pair. PCR with this primer pair was attempted two more times with the same result. It is possible that the primer pair resulted in some imprecise binding, which would mean that the PCR results could not be used to determine if mutated chromosome copies were present or not. A second primer pair that was also designed to determine if mutated chromosome copies were present, algF-LF/algF-LR, was also tried. This yielded similar results, and the wild type comparison did not result in a band of the correct size.

In a final attempt to verify mutants by PCR, three new primer pairs were used that had previously been tested and found to be functional. First, algXBF/algXBR was used. This primer pair would verify whether wild type chromosome copies were present or not. Wild type *A. vinelandii* was therefore included as a comparison. This primer pair would result in no PCR products if only mutated chromosomes were present, and a 1.1 kb wild type fragment. Figure 4.41 shows the resulting PCR products. All strains appeared to contain a band consistent with the wild type fragments.

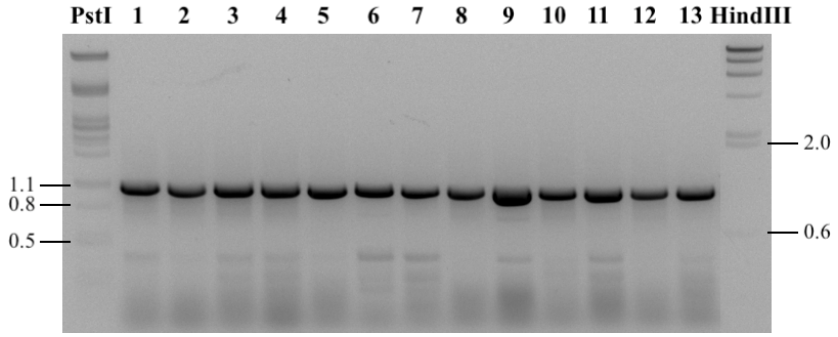

Figure 4.41: Separated PCR products for verification of wild type chromosomes, obtained using the primer pair algXBF/algXBR. Lanes 1-4 contain wild type (pHMT16), lanes 5-8 contain *algL* (pHMT16), lanes 9-12 contain *algLH199R* (pHMT16) and lane 13 contains wild type *A. vinelandii*. Mutated chromosome copies would give no PCR product, and wild type would give a 1.1 kb band. All lanes appear to contain wild type bands.

Next, algLsjekkF/algFR was used to verify mutated chromosome copies. Wild type and pHMT16 was included for comparison. pHMT16 was linearized by digestion with SacI, separated using gel electrophoresis, excised and purified prior to PCR. This primer pair would give a 0.5 kb PCR product for mutant chromosomes, and a 4.8 kb PCR product for wild type. Figure 4.42 shows the resulting PCR products. Several lanes appeared to contain a band consistent with mutated chromosome copies. However, pHMT16 used for comparison did not result in the expected 0.5 kb band. Instead, one slightly longer and one slightly shorter band was observed. In addition, wild type *A. vinelandii* did not produce the expected 4.8 kb band. Instead, it appeared to also produce a 0.5 kb band.

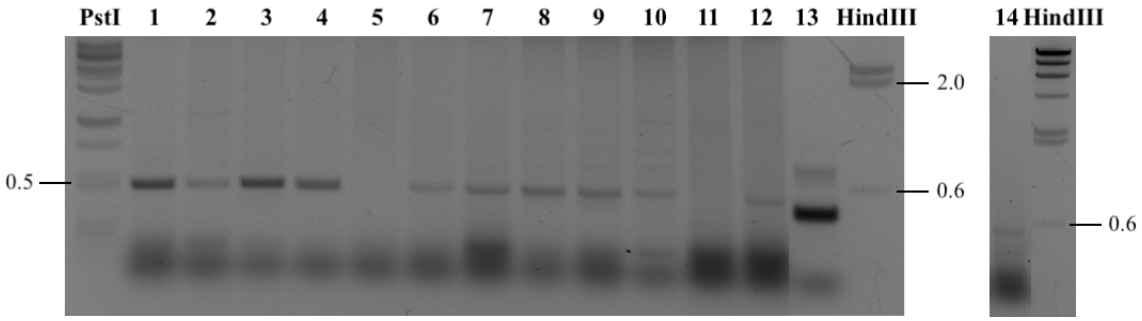

Figure 4.42: Separated PCR products for verification of mutated chromosomes, obtained using the primer pair algLsjekkF/algFR. Lanes 1-4 contain wild type (pHMT16), lanes 5-8 contain *algL* (pHMT16), lanes 9-12 contain *algLH199R* (pHMT16), lane 13 contains pHMT16 and lane 14 contains wild type *A. vinelandii*. Mutated chromosome copies would give a 0.5 kb PCR product, and wild type would give a 4.8 kb band. Most lanes appeared to contain the mutant fragments. pHMT16 and wild type *A. vinelandii*, used for comparison, did however not give the expected fragments.

Lastly, algXBF/algFR was also used to verify mutated chromosome copies. Wild type and pHMT16 was included for comparison. pHMT16 was linearized by digestion with SacI, separated using gel electrophoresis, excised and purified prior to PCR. This primer pair would give a 1.4 kb PCR product for mutant chromosomes, and a 5.6 kb PCR product for wild type. Figure 4.43 shows the resulting PCR products. Several lanes appeared to contain a band consistent with mutated chromosome copies. In addition, many lanes contained additional shorter fragments. Again, pHMT16 used for comparison did not result in the expected 1.4 kb band. Instead, a shorter band was observed. In addition, wild type *A. vinelandii* did not produce the expected 5.6 kb band. Instead, it appeared to also produce a short band.

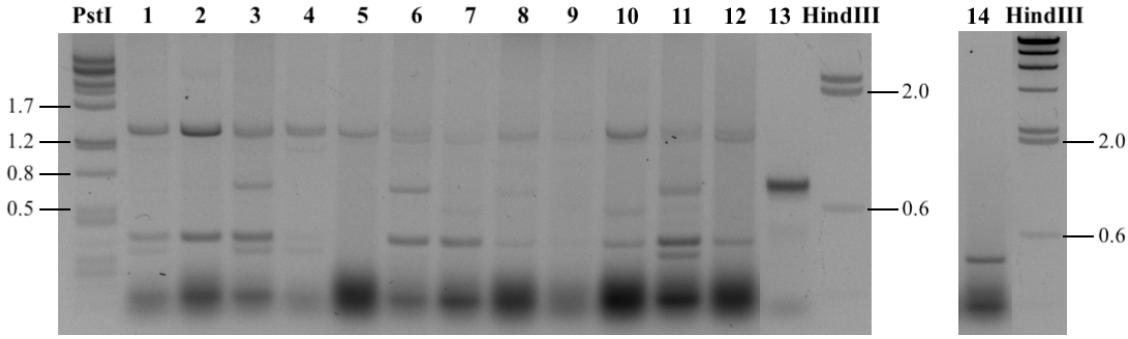

Figure 4.43: Separated PCR products for verification of mutated chromosomes, obtained using the primer pair algXBF/algFR. Lanes 1-4 contain wild type (pHMT16), lanes 5-8 contain *algL* (pHMT16), lanes 9-12 contain *algLH199R* (pHMT16), lane 13 contains pHMT16 and lane 14 contains wild type *A. vinelandii*. Mutated chromosome copies would give a 1.4 kb PCR product, and wild type would give a 5.6 kb band. Most lanes appeared to contain the mutant fragments, in addition to one or more shorter bands. pHMT16 and wild type *A. vinelandii*, used for comparison, did however not give the expected fragments.

PCR using algLsjekkF/algFR and algXBF/algFR was repeated one more time, and the results are presented in figures 4.44 and 4.45. Due to a new supplier of dNTPs for PCR however, the wrong concentration of dNTPs was used. This resulted in faint bands for many of the mutant strains. However, pHMT16 used for comparison this time produced a PCR product that corresponded to the bands of mutants. One of the the primer pairs also produced a wild type fragment for comparison.

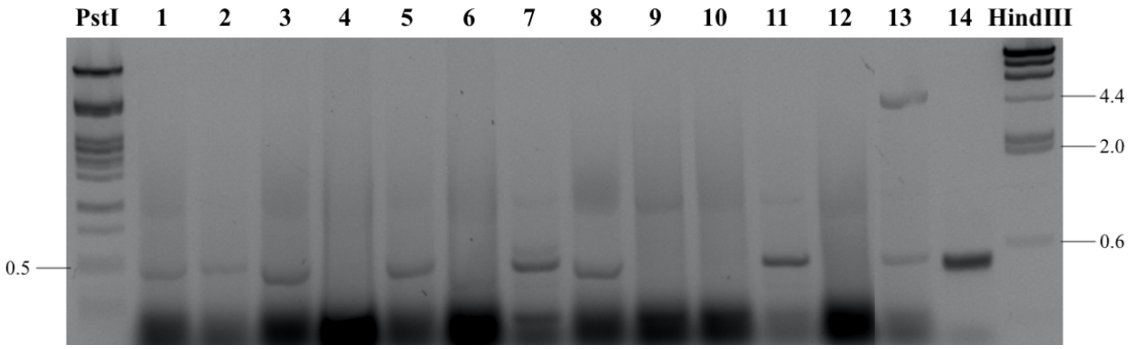

Figure 4.44: Separated PCR products for verification of mutated chromosomes, obtained using the primer pair algLsjekkF/algFR. Lanes 1-4 contain wild type (pHMT16), lanes 5-8 contain *algL* (pHMT16), lanes 9-12 contain *algLH199R* (pHMT16), lane 13 contains wild type *A. vinelandii* and lane 14 contains pHMT16. Mutated chromosome copies would give a 0.5 kb PCR product, and wild type would give a 4.8 kb band. Most lanes appeared to contain the mutant fragments.

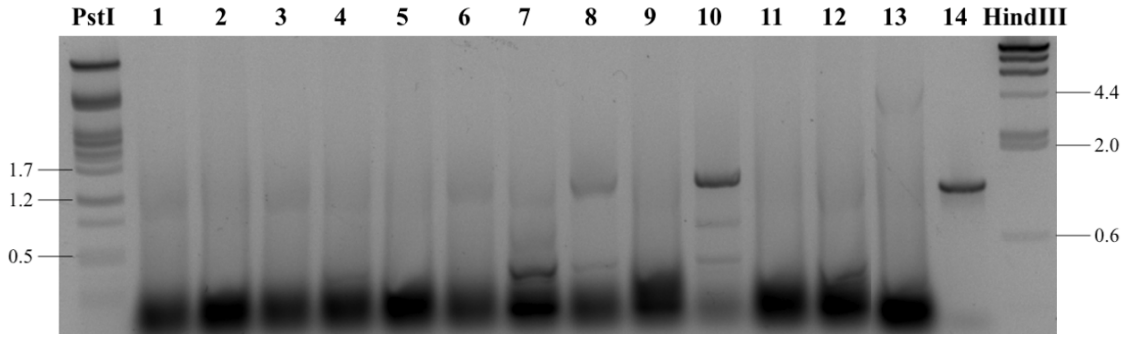

Figure 4.45: Separated PCR products for verification of mutated chromosomes, obtained using the primer pair algXBF/algFR. Lanes 1-4 contain wild type (pHMT16), lanes 5-8 contain *algL* (pHMT16), lanes 9-12 contain *algLH199R* (pHMT16), lane 13 contains wild type *A. vinelandii* and lane 14 contains pHMT16. Mutated chromosome copies would give a 1.4 kb PCR product, and wild type would give a 5.6 kb band. Most lanes appeared to contain the mutant fragments, in addition to one or more shorter bands. Wild type *A. vinelandii*, used for comparison, did however not give the expected fragments.

Because pHMT16 had produced several unexpected results, it was decided that the homologous recombination vector would be sequenced. pHMT14 was sequenced, as this plasmid would allow for use of the primer M13F. In addition, algLsjekkF, algXBF and 27IR were used. The sequencing results were aligned with the *algA-algG* fragment of pHMT14. The alignment is presented in appendix J, and showed a complete overlap with the entire fragment of interest, with no mismatches.

Because the sequencing of pHMT14 showed no mismatches, the results might be explained by the primers used. The primers could have been sub-optimal and therefore resulted in some unspecific binding, yielding unexpected fragments. It is also possible that something was wrong with the samples used as comparisons, although the wild type comparison sample was previously used for verification of *mucA* with no issues. Even though some lanes contained unexpected fragments, and the comparisons did not always result in expected fragments, pHMT16 was eventually shown to result in the correct mutant band. The wild type comparison also produced one wild type band. These results suggest that homologous recombination may in fact have resulted in mutants where at least some wild type chromosome copies were disrupted.

CHAPTER 5

CONCLUSION

The aim of the study was to construct, verify and test *A. vinelandii* strains with mutations to several genes believed to be involved in alginate biosynthesis, to gain insight into the alginate biosynthesis and shed light on potential ways of manipulating it. Inactivated *algB* and *algW* mutants were constructed by homologous recombination, before their alginate production was evaluated. The results suggest that the role of *A. vinelandii algB* differs from that of *P. aeruginosa* in that it is not required for alginate biosynthesis. Results also indicated that *algW* is required for alginate biosynthesis in *A. vinelandii*. The alginate production of an *algF*, *mucA* double mutant was also evaluated. It was found to produce very low amounts of alginate, which was unexpected and suggested that a secondary mutation detrimental to alginate production occurred. A CRISPR-Cas9 assisted system that disrupts *algL* was constructed and tested. A CRISPR-Cas9 vector was used along with homologous recombination in an attempt to obtain a pure *algL* mutant where *algL* or the less efficient mutant *algLH199R* associated with a weaker promoter was incorporated into the genome by transposition. During this work, a strong promoter from a gram positive species of bacteria was shown to work in *A. vinelandii*. Homologous recombination was also used to disrupt the acetylation genes *algI*, *algV* and *algF*, and resulted in mutants that most likely contained both wild type and mutated chromosomes. However, removal of remaining wild type chromosomes using CRISPR-Cas9 was not successful.

BIBLIOGRAPHY

[1] K. Y. Lee and D. J. Mooney. Alginate: properties and biomedical applications. *Progress in polymer science*, 37(1):106–126, 2012.

[2] H. Ertesvåg. Alginate-modifying enzymes: biological roles and biotechnological uses. *Frontiers in microbiology*, 6:523, 2015.

[3] P. A. J. Gorin and J. F. T. Spencer. Exocellular alginic acid from *Azotobacter vinelandii*. *Canadian journal of chemistry*, 44(9):993–998, 1966.

[4] A. Linker and R. S. Jones. A new polysaccharide resembling alginic acid isolated from pseudomonads. *Journal of Biological Chemistry*, 241(16):3845–3851, 1966.

[5] K. I. Draget, G. Skjåk-Bræk, and O. Smidsrød. Alginate based new materials. *International journal of biological macromolecules*, 21(1-2):47–55, 1997.

[6] G. Skjåk-Bræk, F. Zanetti, and S. Paoletti. Effect of acetylation on some solution and gelling properties of alginates. *Carbohydrate Research*, 185(1):131–138, 1989.

[7] T. Espevik, M. Otterlei, G. Skjåk-Braek, L. Ryan, S. D. Wright, and A. Sundan. The involvement of CD14 in stimulation of cytokine production by uronic acid polymers. *European journal of immunology*, 23(1):255–261, 1993.

[8] D. J. McHugh. Production, properties and uses of alginates. *Production and Utilization of Products from Commercial Seaweeds. FAO. Fish. Tech. Pap*, 288:58–115, 1987.

[9] J. E. McGhee, M. E. Carr, and G. St Julian. Continuous bioconversion of starch to ethanol by calcium-alginate immobilized enzymes and yeasts. 1984.

[10] T. Onaka, K. Nakanishi, T. Inoue, and S. Kubo. Beer brewing with immobilized yeast. *Bio/technology*, 3(5):467–470, 1985.

[11] H. Prevost, C. Divies, and E. Rousseau. Continuous yoghurt production with *Lactobacillus bulgaricus* and *Streptococcus thermophilus* entrapped in Ca-alginate. *Biotechnology letters*, 7(4):247–252, 1985.

[12] A. Van Dommelen and J. Vanderleyden. Associative nitrogen fixation. In *Biology of the nitrogen cycle*, pages 179–192. Elsevier, 2007.

[13] João C Setubal, Patricia Dos Santos, Barry S Goldman, H. Ertesvåg, G. Espin, L. M. Rubio, S. Valla, N. F. Almeida, D. Balasubramanian, L. Cromes, et al. Genome sequence of *Azotobacter vinelandii*, an obligate aerobe specialized to support diverse anaerobic metabolic processes. *Journal of bacteriology*, 191(14):4534–4545, 2009.

[14] J. G. Lipman. Experiments on the transformation and fixation of nitrogen by bacteria. *Rep. NJ St. Agric. Exp. Stn*, 1903:217–285, 1903.

[15] J. D. Noar and J. M. Bruno-Bárcena. *Azotobacter vinelandii*: the source of 100 years of discoveries and many more to come. *Microbiology*, 164(4):421–436, 2018.

[16] H. Lineweaver and D. Burk. The determination of enzyme dissociation constants. *Journal of the American chemical society*, 56(3):658–666, 1934.

[17] P. J. Ortiz and S. Ochoa. Studies on Polynucleotides Synthesized by Polynucleotide Phosphorylase: IV. P32-Labeled Ribonucleic Acid. *Journal of Biological Chemistry*, 234(5):1208–1212, 1959.

[18] R. W. F. Hardy and U. D. Havelka. Nitrogen fixation research: a key to world food? *Science*, 188(4188):633–643, 1975.

[19] D. Burk. The influence of oxygen gas upon the organic catalysis of nitrogen fixation by *Azotobacter*. *The Journal of Physical Chemistry*, 34(6):1195–1209, 2002.

[20] H. L. Sadoff. Encystment and germination in *Azotobacter vinelandii*. *Bacteriological reviews*, 39(4):516, 1975.

[21] W. J. Page and H. L. Sadoff. Physiological factors affecting transformation of *Azotobacter vinelandii*. *Journal of bacteriology*, 125(3):1080–1087, 1976.

[22] M. Campos, J. M. Martinez-Salazar, L. Lloret, S. Moreno, C. Núñez, G. Espín, and G. Soberon-Chavez. Characterization of the gene coding for GDP-mannose dehydrogenase (*algD*) from *Azotobacter vinelandii*. *Journal of Bacteriology*, 178(7):1793–1799, 1996.

[23] W. J. Page and M. Tigerstrom. Induction of transformation competence in *Azotobacter vinelandii* iron-limited cultures. *Canadian journal of microbiology*, 24(12):1590–1594, 1978.

[24] A. Contreras, R. Maldonado, and J. Casadesus. Tn5 mutagenesis and insertion replacement in *Azotobacter vinelandii*. *Plasmid*, 25(1):76–80, 1991.

[25] S. Maleki, M. Mærk, S. Valla, and H. Ertesvåg. Mutational analyses of glucose dehydrogenase and glucose-6-phosphate dehydrogenase genes in *Pseudomonas fluorescens* reveal their effects on growth and alginate production. *Applied and environmental microbiology*, 81(10):3349–3356, 2015.

[26] R. Maldonado, J. Jiménez, and J. Casadesús. Changes of ploidy during the *Azotobacter vinelandii* growth cycle. *Journal of bacteriology*, 176(13):3911–3919, 1994.

[27] J. M. Martinez-Salazar, S. Moreno, R. Najera, J. C. Boucher, G. Espín, G. Soberon-Chavez, and V. Deretic. Characterization of the genes coding for the putative sigma factor AlgU and its regulators MucA, MucB, MucC, and MucD in *Azotobacter vinelandii* and evaluation of their roles in alginate biosynthesis. *Journal of bacteriology*, 178(7):1800–1808, 1996.

[28] V. Urtuvia, N. Maturana, F. Acevedo, C. Peña, and A. Díaz-Barrera. Bacterial alginate production: An overview of its biosynthesis and potential industrial production. *World Journal of Microbiology and Biotechnology*, 33(11):1–10, 2017.

[29] H. Ertesvåg, H. Sletta, M. Senneset, Y. Sun, G. Klinkenberg, T. A. Konradsen, T. E. Ellingsen, and S. Valla. Identification of genes affecting alginate biosynthesis in *Pseudomonas fluorescens* by screening a transposon insertion library. *BMC genomics*, 18(1):1–13, 2017.

[30] D. Shinabarger, A. Berry, T. B. May, R. Rothmel, A. Fialho, and A. M. Chakrabarty. Purification and characterization of phosphomannose isomerase-guanosine diphospho-D-mannose pyrophosphorylase. A bifunctional enzyme in the alginate biosynthetic pathway of *Pseudomonas aeruginosa*. *Journal of Biological Chemistry*, 266(4):2080–2088, 1991.

[31] E. Galindo, C. Peña, C. Núñez, D. Segura, and G. Espín. Molecular and bioengineering strategies to improve alginate and polydydroxyalkanoate production by *Azotobacter vinelandii*. *Microbial Cell Factories*, 6(1):1–16, 2007.

[32] S. Maleki, M. Mærk, R. Hrudikova, S. Valla, and H. Ertesvåg. New insights into *Pseudomonas fluorescens* alginate biosynthesis relevant for the establishment of an efficient production process for microbial alginates. *New biotechnology*, 37:2–8, 2017.

[33] O. Smidsrød, R. M. Glover, , and S. G. Whittington. The relative extension of alginates having different chemical composition. *Carbohydrate research*, 27(1):107–118, 1973.

[34] M. Gimmestad, H. Ertesvåg, T. M. B. Heggeset, O. Aarstad, B. I. G. Svanem, and S. Valla. Characterization of three new *Azotobacter vinelandii* alginate lyases, one of which is involved in cyst germination. *Journal of bacteriology*, 191(15):4845–4853, 2009.

[35] W. Sabra, A. P. Zeng, and W. D. Deckwer. Bacterial alginate: physiology, product quality and process aspects. *Applied microbiology and biotechnology*, 56(3):315–325, 2001.

[36] H. K. Høidal, B. I. G. Svanem, M. Gimmestad, and S. Valla. Mannuronan C-5 epimerases and cellular differentiation of *Azotobacter vinelandii*. *Environmental microbiology*, 2(1):27–38, 2000.

[37] P. Baker, T. Ricer, P. J. Moynihan, E. N. Kitova, M. T. C. Walvoort, D. J. Little, J. C. Whitney, K. Dawson, J. T. Weadge, H. Robinson, et al. *P. aeruginosa* SGNH hydrolase-like proteins AlgJ and AlgX have similar topology but separate and distinct roles in alginate acetylation. *PLoS Pathog*, 10(8):e1004334, 2014.

[38] M. J. Franklin and D. E. Ohman. Mutant analysis and cellular localization of the AlgI, AlgJ, and AlgF proteins required for O acetylation of alginate in *Pseudomonas aeruginosa*. *Journal of bacteriology*, 184(11):3000–3007, 2002.

[39] K. Bakkevig, H. Sletta, M. Gimmestad, R. Aune, H. Ertesvåg, K. Degnes, B. E. Christensen, T. E. Ellingsen, and S. Valla. Role of the *Pseudomonas fluorescens* alginate lyase (AlgL) in clearing the periplasm of alginates not exported to the extracellular environment. *Journal of bacteriology*, 187(24):8375–8384, 2005.

[40] S. Jain and D. E. Ohman. Role of an alginate lyase for alginate transport in mucoid *Pseudomonas aeruginosa*. *Infection and immunity*, 73(10):6429–6436, 2005.

[41] Helga Ertesvåg, Frode Erlien, Gudmund Skjåk-Bræk, Bernd HA Rehm, and Svein Valla. Biochemical Properties and Substrate Specificities of a Recombinantly Produced *Azotobacter vinelandii* Alginate Lyase. *Journal of bacteriology*, 180(15):3779–3784, 1998.

[42] T. Y. Wong, L. A. Preston, and N. L. Schiller. Alginate lyase: review of major sources and enzyme characteristics, structure-function analysis, biological roles, and applications. *Annual Reviews in Microbiology*, 54(1):289–340, 2000.

[43] M. Trujillo-Roldán, S. Moreno, D. Segura, E. Galindo, and G. Espin. Alginate production by an *Azotobacter vinelandii* mutant unable to produce alginate lyase. *Applied microbiology and biotechnology*, 60(6):733–737, 2003.

[44] I. D. Hay, Z. U. Rehman, M. F. Moradali, Y. Wang, and B. H. A. Rehm. Microbial alginate production, modification and its applications. *Microbial biotechnology*, 6(6):637–650, 2013.

[45] C. Delgado, L. Florez, I. Lollett, C. Lopez, S. Kangeyan, H. Kumari, M. Stylianou, R. J. Smiddy, L. Schneper, R. T. Sautter, et al. *Pseudomonas aeruginosa* regulated intramembrane proteolysis: protease MucP can overcome mutations in the AlgO periplasmic protease to restore alginate production in nonmucoid revertants. *Journal of bacteriology*, 200(16), 2018.

[46] M. Mærk, Ø. M. Jakobsen, H. Sletta, G. Klinkenberg, A. Tøndervik, T. E. Ellingsen, S. Valla, and H. Ertesvåg. Identification of regulatory genes and metabolic processes important for alginate biosynthesis in *Azotobacter vinelandii* by screening of a transposon insertion mutant library. *Frontiers in bioengineering and biotechnology*, 7:475, 2020.

[47] C. Núñez, R. León, J. Guzmán, Espın E., and G. Soberón-Chávez. Role of *Azotobacter vinelandii mucA* and *mucC* Gene Products in Alginate Production. *Journal of bacteriology*, 182(23):6550–6556, 2000.

[48] A. J. Leech, A. Sprinkle, L. Wood, D. J. Wozniak, and D. E. Ohman. The NtrC family regulator AlgB, which controls alginate biosynthesis in mucoid *Pseudomonas aeruginosa*, binds directly to the *algD* promoter. *Journal of bacteriology*, 190(2):581–589, 2008.

[49] J. B. Goldberg and D. E. Ohman. Construction and characterization of *Pseudomonas aeruginosa algB* mutants: role of *algB* in high-level production of alginate. *Journal of bacteriology*, 169(4):1593–1602, 1987.

[50] J. B. Goldberg and T. Dahnke. *Pseudomonas aeruginosa* AlgB, which modulates the expression of alginate, is a member of the NtrC subclass of prokaryotic regulators. *Molecular microbiology*, 6(1):59–66, 1992.

[51] D. J. Wozniak and D. E. Ohman. Transcriptional analysis of the *Pseudomonas aeruginosa* genes *algR*, *algB*, and *algD* reveals a hierarchy of alginate gene expression which is modulated by *algT*. *Journal of Bacteriology*, 176(19):6007–6014, 1994.

[52] S. Ma, U. Selvaraj, D. E. Ohman, R. Quarless, D. J. Hassett, and D. J. Wozniak. Phosphorylation-Independent Activity of the Response Regulators AlgB and AlgR in Promoting Alginate Biosynthesis in Mucoid *Pseudomonas aeruginosa*. *Journal of Bacteriology*, 180(4):956–968, 1998.

[53] R. J. Reece. *Analysis of genes and genomes*. John Wiley & Sons Hoboken, NJ, 2004.

[54] H. C. Birnboim. A rapid alkaline extraction method for the isolation of plasmid DNA. In *Recombinant DNA Methodology*, pages 175–187. Elsevier, 1989.

[55] S. H. Phadnis and H. K. Das. Use of the plasmid pRK 2013 as a vehicle for transposition in *Azotobacter vinelandii*. *Journal of Biosciences*, 12(2):131–135, 1987.

[56] V. DeLorenzo, M. Herrero, U. Jakubzik, and K. N. Timmis. Mini-Tn5 transposon derivatives for insertion mutagenesis, promoter probing, and chromosomal insertion of cloned DNA in gram-negative eubacteria. *Journal of bacteriology*, 172(11):6568–6572, 1990.

[57] M. Herrero, V. DeLorenzo, and K. N. Timmis. Transposon vectors containing non-antibiotic resistance selection markers for cloning and stable chromosomal insertion of foreign genes in gram-negative bacteria. *Journal of bacteriology*, 172(11):6557–6567, 1990.

[58] A. Gawin, S. Valla, and T. Brautaset. The XylS/P*m* regulator/promoter system and its use in fundamental studies of bacterial gene expression, recombinant protein production and metabolic engineering. *Microbial biotechnology*, 10(4):702–718, 2017.

[59] C. Matsumoto-Mashimo, A. M. Guerout, and D. Mazel. A new family of conditional replicating plasmids and their cognate *Escherichia coli* host strains. *Research in microbiology*, 155(6):455–461, 2004.

[60] S. Flores, R. de Anda-Herrera, G. Gosset, and F. G. Bolívar. Growth-rate recovery of *Escherichia coli* cultures carrying a multicopy plasmid, by engineering of the pentose-phosphate pathway. *Biotechnology and bioengineering*, 87(4):485–494, 2004.

[61] A. Norman, L. H. Hansen, and S. J. Sørensen. Conjugative plasmids: vessels of the communal gene pool. *Philosophical Transactions of the Royal Society B: Biological Sciences*, 364(1527):2275–2289, 2009.

[62] D. L. Court, J. A. Sawitzke, and L. C. Thomason. Genetic engineering using homologous recombination. *Annual review of genetics*, 36(1):361–388, 2002.

[63] J. T. Heap, M. Ehsaan, C. M. Cooksley, Y. Ng, S. T. Cartman, K. Winzer, and N. P. Minton. Integration of dna into bacterial chromosomes from plasmids without a counter-selection marker. *Nucleic acids research*, 40(8):e59–e59, 2012.

[64] X. Li, L. C. Thomason, J. A. Sawitzke, N. Costantino, and D. L. Court. Positive and negative selection using the *tetA-sacB* cassette: recombineering and P1 transduction in *Escherichia coli*. *Nucleic acids research*, 41(22):e204–e204, 2013.

[65] N. Nakashima and K. Miyazaki. Bacterial cellular engineering by genome editing and gene silencing. *International journal of molecular sciences*, 15(2):2773–2793, 2014.

[66] N. Kleckner. Transposable elements in prokaryotes. *Annual review of genetics*, 15(1):341–404, 1981.

[67] M. J. Curcio and K. M. Derbyshire. The outs and ins of transposition: from Mu to Kangaroo. *Nature Reviews Molecular Cell Biology*, 4(11):865–877, 2003.

[68] I. Y. Goryshin and W. S. Reznikoff. Tn5 *in vitro* transposition. *Journal of Biological Chemistry*, 273(13):7367–7374, 1998.

[69] B. McClintock et al. Mutable loci in maize. *Mutable loci in maize*, 1947.

[70] D. E. Berg, J. Davies, B. Allet, and J. D. Rochaix. Transposition of R factor genes to bacteriophage *lambda*. *Proceedings of the National Academy of Sciences*, 72(9):3628–3632, 1975.

[71] W. S. Reznikoff. Transposon Tn5. *Annual review of genetics*, 42:269–286, 2008.

[72] R. C. Johnson, J. C. P. Yin, and W. S. Reznikoff. Control of Tn5 transposition in *Escherichia coli* is mediated by protein from the right repeat. *Cell*, 30(3):873–882, 1982.

[73] J. C. Makris, P. L. Nordmann, and W. S. Reznikoff. Mutational analysis of insertion sequence 50 (IS50) and transposon 5 (Tn5) ends. *Proceedings of the National Academy of Sciences*, 85(7):2224–2228, 1988.

[74] I. Levchenko, L. Luo, and T. A. Baker. Disassembly of the Mu transposase tetramer by the Clpx chaperone. *Genes & development*, 9(19):2399–2408, 1995.

[75] W. S. Reznikoff. The Tn5 transposon. *Annual review of microbiology*, 47(1):945–963, 1993.

[76] Y. Ishino, H. Shinagawa, K. Makino, M. Amemura, and A. Nakata. Nucleotide sequence of the *iap* gene, responsible for alkaline phosphatase isozyme conversion in *Escherichia coli*, and identification of the gene product. *Journal of bacteriology*, 169(12):5429–5433, 1987.

[77] J. A. Doudna and E. Charpentier. The new frontier of genome engineering with CRISPR-Cas9. *Science*, 346(6213), 2014.

[78] F. A. Ran, P. D. Hsu, J. Wright, V. Agarwala, D. A. Scott, and F. Zhang. Genome engineering using the CRISPR-Cas9 system. *Nature protocols*, 8(11):2281–2308, 2013.

[79] K. S. Makarova, N. V. Grishin, S. A. Shabalina, Y. I. Wolf, and E. V. Koonin. A putative RNA-interference-based immune system in prokaryotes: computational analysis of the predicted enzymatic machinery, functional analogies with eukaryotic RNAi, and hypothetical mechanisms of action. *Biology direct*, 1(1):1–26, 2006.

[80] E. Deltcheva, K. Chylinski, C. M. Sharma, K. Gonzales, Y. Chao, Z. A. Pirzada, M. R. Eckert, J. Vogel, and E. Charpentier. CRISPR RNA maturation by trans-encoded small RNA and host factor RNase III. *Nature*, 471(7340):602–607, 2011.

[81] M. Jinek, K. Chylinski, I. Fonfara, M. Hauer, J. A. Doudna, and E. Charpentier. A programmable dual-RNA-guided DNA endonuclease in adaptive bacterial immunity. *science*, 337(6096):816–821, 2012.

[82] C. Anders, O. Niewoehner, A. Duerst, and M. Jinek. Structural basis of PAM-dependent target DNA recognition by the Cas9 endonuclease. *Nature*, 513(7519):569–573, 2014.

[83] D. B. Wigley. Bacterial DNA repair: recent insights into the mechanism of RecBCD, AddAB and AdnAB. *Nature Reviews Microbiology*, 11(1):9–13, 2013.

[84] J. T. P. Yeeles and M. S. Dillingham. The processing of double-stranded DNA breaks for recombinational repair by helicase-nuclease complexes. *DNA repair*, 9(3):276–285, 2010.

[85] C. Bertrand, A. Thibessard, C. Bruand, F. Lecointe, and P. Leblond. Bacterial NHEJ: a never ending story. *Molecular microbiology*, 111(5):1139–1151, 2019.

[86] K. Nishida and A. Kondo. CRISPR-derived genome editing technologies for metabolic engineering. *Metabolic Engineering*, 2020.

[87] C. Ronda, L. E. Pedersen, M. O. A. Sommer, and A. T. Nielsen. CRMAGE: CRISPR optimized mage recombineering. *Scientific reports*, 6(1):1–11, 2016.

[88] R. Simon, U. Priefer, and A. Pühler. A broad host range mobilization system for *in vivo* genetic engineering: transposon mutagenesis in gram negative bacteria. *Bio/technology*, 1(9):784–791, 1983.

[89] S. Panja, S. Saha, B. Jana, and T. Basu. Role of membrane potential on artificial transformation of *E. coli* with plasmid dna. *Journal of biotechnology*, 127(1):14–20, 2006.

[90] C. T. Chung and R. H. Miller. Preparation and storage of competent *Escherichia coli* cells. In *Methods in enzymology*, volume 218, pages 621–627. Elsevier, 1993.

[91] M. Mandel and A. Higa. Calcium-dependent bacteriophage DNA infection. *Journal of molecular biology*, 53(1):159–162, 1970.

[92] S. N. Cohen, A. C. Y. Chang, and L. Hsu. Nonchromosomal antibiotic resistance in bacteria: genetic transformation of *Escherichia coli* by R-factor DNA.

[93] X. Tang, Y. Nakata, H. Li, M. Zhang, H. Gao, A. Fujita, O. Sakatsume, T. Ohta, and K. Yokoyama. The optimization of preparations of competent cells for transformation of *E. coli*. *Nucleic acids research*, 22(14):2857, 1994.

[94] Y. Nakata, X. Tang, and K. Yokoyama. Preparation of competent cells for high-efficiency plasmid transformation of *Escherichia coli*. In *cDNA Library Protocols*, pages 129–137. Springer, 1997.

[95] A. Asif, H. Mohsin, R. Tanvir, and Y. Rehman. Revisiting the mechanisms involved in calcium chloride induced bacterial transformation. *Frontiers in microbiology*, 8:2169, 2017.

[96] D. Arutyunov and L. S. Frost. F conjugation: back to the beginning. *Plasmid*, 70(1):18–32, 2013.

[97] T. Aa. Strand, R. Lale, K. F. Degnes, M. Lando, and S. Valla. A new and improved host-independent plasmid system for RK2-based conjugal transfer. *PLoS One*, 9(3):e90372, 2014.

[98] P. Nagpal, S. Jafri, M. A. Reddy, and H. K. Das. Multiple chromosomes of *Azotobacter vinelandii*. *Journal of bacteriology*, 171(6):3133–3138, 1989.

[99] P. Jollès and J. Jollès. What's new in lysozyme research? *Molecular and cellular biochemistry*, 63(2):165–189, 1984.

[100] Y. Shih, J. M. Prausnitz, and H. W. Blanch. Some characteristics of protein precipitation by salts. *Biotechnology and bioengineering*, 40(10):1155–1164, 1992.

[101] B. L. Dhananjaya and C. J. M. D'souza. An overview on nucleases (DNase, RNase, and phosphodiesterase) in snake venoms. *Biochemistry (Moscow)*, 75(1):1–6, 2010.

[102] Lucigen. MasterPure Complete DNA and RNA Purification Kit. https://www.lucigen.com/docs/manuals/MA110E-MasterPure-Complete.pdf. [Online; accessed 25-April-2021].

[103] H. C. Bimboim and J. Doly. A rapid alkaline extraction procedure for screening recombinant plasmid DNA. *Nucleic acids research*, 7(6):1513–1523, 1979.

[104] S. Ehrt and D. Schnappinger. Isolation of plasmids from *E. coli* by alkaline lysis. In *E. coli Plasmid Vectors*, pages 75–78. Springer, 2003.

[105] Zymo Research. Instruction manual ZR Plasmid Miniprep-Classic. https://files.zymoresearch.com/protocols/d4015d4016d4054zrplasmidminiprep.pdf. [Online; accessed 25-April-2021].

[106] M. A. Marko, R. Chipperfield, and H. C. Birnboim. A procedure for the large-scale isolation of highly purified plasmid DNA using alkaline extraction and binding to glass powder. *Analytical biochemistry*, 121(2):382–387, 1982.

[107] R. C. J. A. Boom, C. J. Sol, M. M. Salimans, C. L. Jansen, P. M. Wertheim-van Dillen, and J. P. M. E. Van der Noordaa. Rapid and simple method for purification of nucleic acids. *Journal of clinical microbiology*, 28(3):495–503, 1990.

[108] C. Katevatis, A. Fan, and C. M. Klapperich. Low concentration DNA extraction and recovery using a silica solid phase. *PLoS One*, 12(5):e0176848, 2017.

[109] Thermo Fisher Scientific. Easy choices for RNA and DNA quantification. https://assets.thermofisher.com/TFS-Assets/BID/brochures/rna-and-dna-quantification-brochure.pdf. [Online; accessed 25-April-2021].

[110] A. Pingoud and A. Jeltsch. Structure and function of type II restriction endonucleases. *Nucleic acids research*, 29(18):3705–3727, 2001.

[111] M. Meselson and R. Yuan. DNA restriction enzyme from *E. coli*. *Nature*, 217(5134):1110–1114, 1968.

[112] H. O. Smith and K. W. Welcox. A restriction enzyme from *Hemophilus influenzae*: I. Purification and general properties. *Journal of molecular biology*, 51(2):379–391, 1970.

[113] New England BioLabs. Blunting. https://international.neb.com/applications/cloning-and-synthetic-biology/dna-end-modification/blunting, 2021. [Online; accessed 25-April-2021].

[114] B. A. Sanderson, N. Araki, J. L. Lilley, G. Guerrero, and L. K. Lewis. Modification of gel architecture and TBE/TAE buffer composition to minimize heating during agarose gel electrophoresis. *Analytical biochemistry*, 454:44–52, 2014.

[115] P. Y. Lee, J. Costumbrado, C. Y. Hsu, and Y. H. Kim. Agarose gel electrophoresis for the separation of DNA fragments. *JoVE (Journal of Visualized Experiments)*, (62):e3923, 2012.

[116] Biotium. Product Information GelRed Nucleic Acid Gel Stain. https://biotium.com/wp-content/uploads/2013/11/PI-41001.pdf. [Online; accessed 25-April-2021].

[117] Biotium. Product Information GelGreen Nucleic Acid Gel Stain. https://biotium.com/wp-content/uploads/2015/02/PI-41004-41005.pdf. [Online; accessed 25-April-2021].

[118] K. J. Shaw, L. Thain, P. T. Docker, C. E. Dyer, J. Greenman, G. M. Greenway, and S. J. Haswell. The use of carrier RNA to enhance DNA extraction from microfluidic-based silica monoliths. *Analytica chimica acta*, 652(1-2):231–233, 2009.

[119] R. Rossi, A. Montecucco, G. Ciarrocchi, and G. Biamonti. Functional characterization of the T4 DNA ligase: a new insight into the mechanism of action. *Nucleic acids research*, 25(11):2106–2113, 1997.

[120] ThermoFisher Scientific. Zero Blunt TOPO PCR Cloning Kit. https://assets.thermofisher.com/TFS-Assets/LSG/manuals/zeroblunttopo$_m an.pdf$, 2014.

[121] J. J. Champoux. DNA topoisomerases: structure, function, and mechanism. *Annual review of biochemistry*, 70(1):369–413, 2001.

[122] S. Shuman. Recombination mediated by *vaccinia* virus DNA topoisomerase I in *Escherichia coli* is sequence specific. *Proceedings of the National Academy of Sciences*, 88(22):10104–10108, 1991.

[123] S. Shuman. Novel approach to molecular cloning and polynucleotide synthesis using *vaccinia* DNA topoisomerase. *Journal of Biological Chemistry*, 269(51):32678–32684, 1994.

[124] R. K. Saiki, S. Scharf, F. Faloona, K. B. Mullis, G. T. Horn, H. A. Erlich, and N. Arnheim. Enzymatic amplification of beta-globin genomic sequences and restriction site analysis for diagnosis of sickle cell anemia. *Science*, 230(4732):1350–1354, 1985.

[125] H. Eun. *Enzymology primer for recombinant DNA technology*. Elsevier, 1996.

[126] New England Biolabs Inc. Q5 High-Fidelity DNA Polymerase. https://international.neb.com/products/m0491-q5-high-fidelity-dna-polymeraseProtocols,%20Manuals%20%20Usage. [Online; accessed 25-April-2021].

[127] F. Sanger, S. Nicklen, and A. R. Coulson. DNA sequencing with chain-terminating inhibitors. *Proceedings of the national academy of sciences*, 74(12):5463–5467, 1977.

[128] M. L. Metzker. Emerging technologies in DNA sequencing. *Genome research*, 15(12):1767–1776, 2005.

[129] Eurofins Genomics. Sanger Sequencing. https://eurofinsgenomics.eu/en/eurofins-genomics/material-and-methods/sanger-sequencing/, 2021. [Online; accessed 25-April-2021].

[130] M. R. G. Maia, S. Marques, A. R. J. Cabrita, R. J. Wallace, G. Thompson, A. J. M. Fonseca, and H. M. Oliveira. Simple and versatile turbidimetric monitoring of bacterial growth in liquid cultures using a customized 3D printed culture tube holder and a miniaturized spectrophotometer: application to facultative and strictly anaerobic bacteria. *Frontiers in microbiology*, 7:1381, 2016.

[131] J. Monod. The growth of bacterial cultures. *Annual review of microbiology*, 3(1):371–394, 1949.

[132] R. M. Maier and I. L. Pepper. Bacterial growth. In *Environmental microbiology*, pages 37–56. Elsevier, 2015.

[133] D. D. Sledjeski, A. Gupta, and S. Gottesman. The small RNA, DsrA, is essential for the low temperature expression of RpoS during exponential growth in *Escherichia coli*. *The EMBO Journal*, 15(15):3993–4000, 1996.

[134] K. Østgaard. Enzymatic microassay for the determination and characterization of alginates. *Carbohydrate polymers*, 19(1):51–59, 1992.

[135] H. I. Nakada and P. C. Sweeny. Alginic acid degradation by eliminases from abalone hepatopancreas. *Journal of Biological Chemistry*, 242(5):845–851, 1967.

[136] K. Østgaard. Determination of alginate composition by a simple enzymatic assay. In *Fourteenth International Seaweed Symposium*, pages 513–520. Springer, 1993.

[137] H. Ertesvåg and G. Skjåk-Bræk. Modification of alginate using mannuronan C-5-epimerases. In *Carbohydrate biotechnology protocols*, pages 71–78. Springer, 1999.

[138] J. R. De Wet, K. V. Wood, M. DeLuca, D. R. Helinski, and S. Subramani. Firefly luciferase gene: structure and expression in mammalian cells. *Molecular and cellular biology*, 7(2):725–737, 1987.

[139] Promega Corporation. Technical bulletin, luciferase assay system. https://no.promega.com/-/media/files/resources/protocols/technical-bulletins/0/luciferase-assay-system-protocol.pdf?la=en, 2009. [Online; accessed 25-April-2021].

[140] Benchling: Cloud-based informatics platform for life sciences. https://benchling.com, 2021.

[141] Snapgene viewer. https://www.snapgene.com/snapgene-viewer/, 2021.

[142] B. L. Nielsen, V. C. Willis, and C. Y. Lin. Western blot analysis to illustrate relative control levels of the *lac* and *ara* promoters in *Escherichia coli*. *Biochemistry and Molecular Biology Education*, 35(2):133–137, 2007.

[143] J. Anné, K. Vrancken, L. Van Mellaert, J. Van Impe, and K. Bernaerts. Protein secretion biotechnology in Gram-positive bacteria with special emphasis on *Streptomyces lividans*. *Biochimica et Biophysica Acta (BBA)-Molecular Cell Research*, 1843(8):1750–1761, 2014.

[144] D. M. DeLorenzo, A. G. Rottinghaus, W. R. Henson, and T. S. Moon. Molecular toolkit for gene expression control and genome modification in *Rhodococcus opacus* PD630. *ACS synthetic biology*, 7(2):727–738, 2018.

[145] M. Maråk. Construction of a CRISPR-Cas9 assisted system for mutagenesis of *Azotobacter vinelandii*. Master's thesis, Norwegian University of Science and Technology, 2020.

[146] V. DeLorenzo, I. Cases, M. Herrero, and K. N. Timmis. Early and late responses of TOL promoters to pathway inducers: identification of postexponential promoters in *Pseudomonas putida* with *lacZ-tet* bicistronic reporters. *Journal of Bacteriology*, 175(21):6902–6907, 1993.

[147] I. Bakke, L. Berg, T. E. V. Aune, T. Brautaset, H. Sletta, A. Tøndervik, and S. Valla. Random mutagenesis of the *Pm* promoter as a powerful strategy for improvement of recombinant-gene expression. *Applied and environmental microbiology*, 75(7):2002–2011, 2009.

Appendices

A Materials

The growth media, solutions and antibiotics used in this work are described below. If not otherwise specified, deionized water was used to prepare the solutions.

Antibiotics

Stock solutions (g/l) of the antibiotics used were made as described below. The working concentration in *E. coli* (µg/ml) is also shown. For *A. vinelandii*, the working concentration of apramycin and kanamycin was 25 and 2 µg/ml, respectively.

Ampicillin	200 g/l	100 µg/ml
Apramycin	50 g/l	50 µg/ml
Kanamycin	50 g/l	50 µg/ml
Spectinomycin	20 g/l	20 µg/ml
Tetracycline	5 g/l	10 µg/ml

Tetracycline was dissolved in 80 % ethanol.

The antibiotic stock solutions were sterilized by filtration and stored at -20 °C. The antibiotic was only added to liquid media once cooled to below 50 °C.

Minerals

Stock solutions (g/l) of $FeSO_4$, $CaCl_2$ and Na_2MoO_4 were prepared as described below. The working concentration (mg/ml) is also shown.

$FeSO_4 \cdot 7H_2O$	150 g/l	15 mg/ml
$CaCl_2 \cdot 2H_2O$	500 g/l	50 mg/ml
$Na_2MoO_4 \cdot 2H_2O$	21 g/l	2.1 mg/ml

The solutions were sterilized by filtration and stored at -20 °C.

***m*-toluate**

A 0.5 M stock solution (g/l) of *m*-toluate was made as described below. The working concentration was 0.5 mM.

m-toluate	68.07 g/l

The *m*-toluate was dissolved in ethanol. The solution was stored at -20 °C.

Luria-Bertani (LB) medium

LB medium was prepared as described below.

Tryptone	10 g/l
Yeast extract	5 g/l
NaCl	5 g/l

The medium was autoclaved at 120 °C and stored at room temperature.

To make plates, 15 g/l agar was added before autoclaving. Plates were left to cool and dry, before they were stored at 4 °C.

Burk's medium (BM)

A 5X solution containing the salts listed below was prepared.

$MgSO_4 \cdot 7H_2O$	1.0 g/l
NaCl	1.0 g/l
K_2HPO_4	3.2 g/l
KH_2PO_4	0.8 g/l

The solution was stored at room temperature.

For use, 5X medium was diluted to 1X and autoclaved at 120 °C.

A glucose solution of 20 g/l in the final 1X Burk's medium was prepared and autoclaved at 120 °C separately. The solution was added to the 1X Burk's medium once cooled. In addition, mineral stock solutions were added to a concentration of 15 mg/l medium for FeSO4, 50 mg/l for CaCl2 and 2.1 mg/l for Na2MoO4. The 1X medium was stored at room temperature.

When using sucrose for counter-selection, the glucose solution was replaced by a sucrose solution of 60 g/l in the final 1X Burk's medium.

To make plates, 15 g/l agar was added before autoclaving. Plates were left to cool and dry, before they were stored at 4 °C.

RA1 medium

A phosphate solution was prepared as described below.

K_2HPO_4	50 g/l

pH was adjusted to 7.0 using HCl, before the solution was autoclaved at 120 °C. The solution was stored at room temperature.

A calcium chloride solution was prepared as described below.

$CaCl \cdot 2H_2O$	147.02 g/l

The solution was autoclaved at 120 °C and stored at room temperature.

The RA1 basis was prepared as described below.

$MgSO_4 \cdot 7H_2O$	2.0 g/l
NH_4NO_3	1.5 g/l
Peptone	2.0 g/l
Mops	10.5 g/l

pH was adjusted to 7.0 using NaOH, before the medium was autoclaved at 120 °C. The solution was stored at room temperature.

A fructose solution of 20 g/l in the final RA1 medium was prepared and autoclaved at 120 °C separately.

For use, the fructose solution was added to the RA1 basis once cooled. 10 ml/l phosphate solution and 2 ml/l $CaCl_2$ was also added. Mineral stock solutions were also added to a concentration of 15 mg/l medium for $FeSO_4$, and 2.1 mg/l for Na_2MoO_4. The RA1 medium was stored at room temperature.

SOC medium

SOC medium was prepared as described below.

Tryptone	20 g/l
Yeast extract	5 g/l
NaCl	0.5 g/l
KCl	0.186 g/l
Glucose	3.6 g/l
$MgCl_2$	5.08 g/l

The medium was sterilized by filtration and stored at -20 °C.

Psi medium

Psi medium was prepared as described below.

Tryptone	20 g/l
Yeast extract	5 g/l
$MgSO_4 \cdot 7H_2O$	10.24 g/l

pH was adjusted to 7.6 using KOH, before the medium was sterilized by autoclaving at 120 °C. The solution was stored at room temperature.

TFB1

TFB1 was prepared as described below.

KAc	2.94 g/l
RbCl	12.1 g/l
$CaCl_2 \cdot 2H_2O$	1.47 g/l
$MnCl_2 \cdot 4H_2O$	10.0 g/l
Glycerol	150 ml/l

pH was adjusted to 5.8 using dilute acetic acid. The solution was sterilized by filtration and stored at 4 °C.

TFB2

TFB2 was prepared as described below.

MOPS	2.1 g/l
RbCl	1.21 g/l
$CaCl_2 \cdot 2H_2O$	11 g/l
Glycerol	150 ml/l

pH was adjusted to 6.5 using dilute NaOH. The solution was sterilized by filtration and stored at 4 °C.

Alginate assay

0.2 M NaCl was prepared by dissolving NaCl to a concentration of 11.69 g/l. 3 M NaOH was prepared from 10 M NaOH. 1.5% NaCl (pH 7.5) was prepared as described below.

NaCl	15 g/l
Tris-base	6.072 g/l

pH was adjusted to 7.5 using concentrated HCl, before the solution was sterilized by

autoclaving at 120 °C. The solutions were stored at room temperature.

Luciferase assay

1 M K_2HPO_4 (pH 7.8), 20 mM EDTA was prepared as described below.

K_2HPO_4	174.2 g/l
EDTA	7.44 g/l

pH was adjusted to 7.8, before the solution was sterilized by autoclaving at 120 °C. The solutions were stored at room temperature.

Lysozyme Mix was prepared as described below.

1 volume 1 M K_2HPO_4 (pH 7.8),
20 mM EDTA
9 volumes water
Lysozyme to 5 mg/ml

The Lysozyme Mix was next used to prepare the Lysis Mix.

CCLR to 1X
Lysozyme to 1.25 mg/ml
BSA to 2.5 mg/ml

The Luciferase Assay Reagent was prepared by combining Luciferase Assay Buffer with lyophilized Luciferase Assay Substrate. 100 µl was aliquoted into tubes which were stored at -80 °C.

B DNA standards

Standards with pre-determined fragment sizes are used as size markers when separating DNA by gel electrophoresis. Figure B.1 shows the PstI and HindIII digested λ-DNA ladders used in this work.

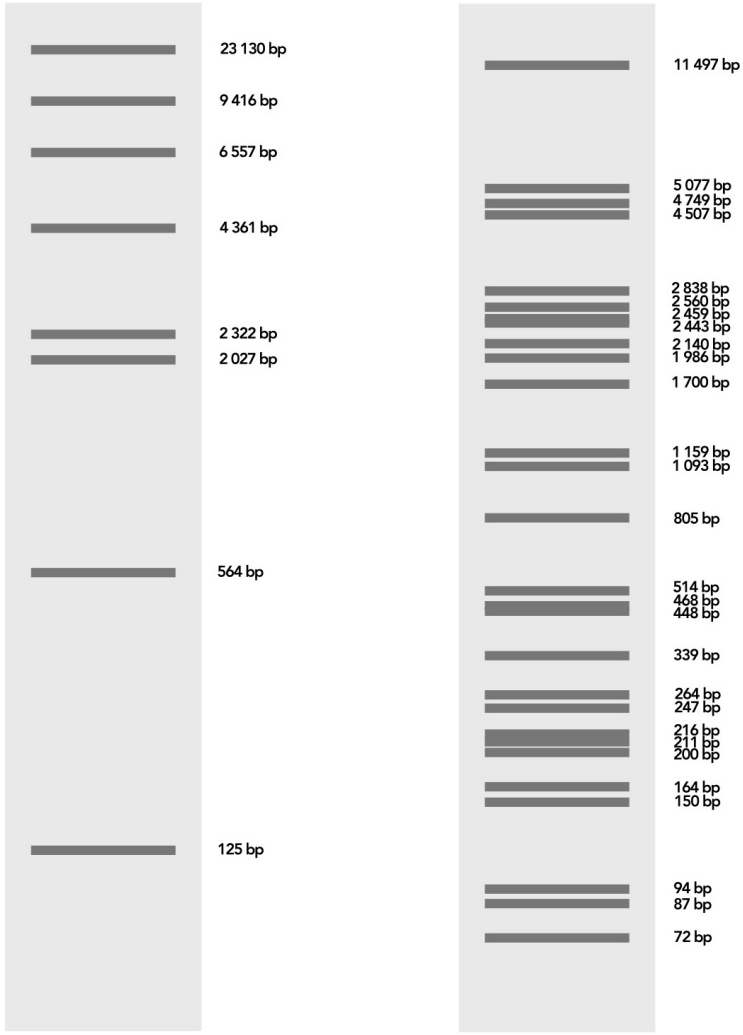

Figure B.1: DNA standards showing the fragments they contain on a gel. The left DNA ladder is the HindIII DNA standard, and the right DNA ladder is the PstI DNA standard. Both were prepared by digesting λ-DNA with the respective restriction enzymes.

C Bacterial strains

Table C.1 details the bacterial strains used in this work along with their source.

Table C.1: Description of the bacterial strains used in this work and their source.

Strains	Description	Source
Escherichia coli		
DH5α	Used in standard cloning work	Bethesda Research Laboratories
S17.1	Used in standard cloning work for plasmids with the inducible P*m*-XylS promoter system and for conjugation	[88]
S17.1-λpir	Used in standard cloning work for plasmids requiring the π protein and for conjugation	[146]
Azotobacter vinelandii		
ATCC12518	Alginate producing wild type strain	American Type Culture Collection
ATCC12518 *algF*	Pure *algF* mutant used as a comparison to the *algF*, *mucA* double mutant	[Ertesvåg, unpublished]
ATCC12518 *algF, mucA*	Pure *algF, mucA* mutant	[Dalland, unpublished]
ATCC12518 *algB*	Pure *algB* mutant, *algB* inactivated by *aaDa*. Sp^r	This work
ATCC12518 *algB* (pHE539)	Pure *algB* mutant, conjugated with pHE539 to restore wild type *algB*. Km^r, Sp^r	This work
ATCC12518 *algB* (pIB11)	Pure *algB* mutant, conjugated with the control plasmid pIB11. Km^r, Sp^r	This work
ATCC12518 *algW*	Pure *algW* mutant, *algW* inactivated by *aaDa*. Sp^r	This work
ATCC12518 *algW* (pHE536)	Pure *algW* mutant, conjugated with pHE536 to restore wild type *algW*. Km^r, Sp^r	This work
ATCC12518 *algW* (pIB11)	Pure *algW* mutant, conjugated with the control plasmid pIB11. Km^r, Sp^r	This work
ATCC12518 P*m:algL*	Transposon insertion mutant with *algL* controlled by P*m*. Wild type *algL* not disrupted	This work
ATCC12518 P*lac:algL*	Transposon insertion mutant with *algL* controlled by P*lac*. Wild type *algL* not disrupted	This work
ATCC12518 P*const:algL*	Transposon insertion mutant with *algL* controlled by P*const*. Wild type *algL* not disrupted	This work
ATCC12518 P*m:algLH199R*	Transposon insertion mutant with *algLH199R* controlled by P*m*. Wild type *algL* not disrupted	This work
ATCC12518 P*lac:algLH199R*	Transposon insertion mutant with *algLH199R* controlled by P*lac*. Wild type *algL* not disrupted	This work
ATCC12518 P*const:algLH199R*	Transposon insertion mutant with *algLH199R* controlled by P*const*. Wild type *algL* not disrupted	This work
ATCC12518 P*m:luc*	Transposon insertion mutant with *luc* controlled by P*m*	This work
ATCC12518 P*lac:luc*	Transposon insertion mutant with *luc* controlled by P*lac*	This work
ATCC12518 P*const:luc*	Transposon insertion mutant with *luc* controlled by P*const*	This work
ATCC12518 P*m:algL* (pHMT16)	Transposon insertion mutant with *algL* controlled by P*m*. Conjugated with pHMT16 to remove wild type *algL*. Most likely contains both mutated and wild type chromosomes	This work
ATCC12518 P*m:algLH199R* (pHMT16)	Transposon insertion mutant with *algLH199R* controlled by P*m*. Conjugated with pHMT16 to remove wild type *algL*. Most likely contains both mutated and wild type chromosomes	This work
ATCC12518 (pHMT16)	Wild type strain conjugated with pHMT16 to remove wild type *algL*. Contains both mutated and wild type chromosomes	This work

D Plasmids

Table D.1 details the plasmids used in this work along with their source. Table D.2 details the plasmids constructed in this work.

Table D.1: Plasmids used in this work and their source.

Plasmid	Description	Source
pCM1	R6K-derived transposon vector with a modified version of the composite transposon Tn5 transpoase (*tpn**). Contains *algL* associated with the inducible *Pm*-XylS promoter system. A*m*^{r}, *Sp*^{r}	[Moral, unpublished]
pCRTM-Blunt II-TOPO	TOPO vector, contains EcoRI sites and M13 forward and reverse primer sites. *Km*^{r}	[120]
pHE103	ColE1-derived plasmid with regions of homology to *algX* and *algG*. Contains *algL*. A*m*^{r}	[Ertesvåg, unpublished]
pHE216	RK2 based expression vector using the inducible *Pm*-XylS promoter system. Contains *oriT*, t*rfA* and *sacB*. A*m*^{r}, *Sp*^{r}, *Tc*^{r}	[Ertesvåg, unpublished]
pHE265	Vector containing *aaDa* and *bla* associated with the *Pm*-XylS promoter system. A*m*^{r}, *Sp*^{r}	[Ertesvåg, unpublished]
pHE278	R6K-derived transposon vector with a modified version of the composite transposon Tn5 transpoase (*tpn**). Contains *luc* associated with the inducible *Pm*-XylS promoter system. A*m*^{r}, *Sp*^{r}	[Ertesvåg, unpublished]
pHE326	RK2 based expression vector using the inducible *Pm*-XylS promoter system. contains *oriT*, t*rfA* and *sacB*. Fragments of *algL*, *algI*, *algF* and *algA*. A*m*^{r}, *Tc*^{r}	[Ertesvåg, unpublished]
pHE513	Vector containing *luc* associated with the constitutive promoter. *Km*^{r}	[Ertesvåg, unpublished]
pHE536	Derivative of pIB11 where a 1.2 kb PCR fragment encoding *algW* replaced *bla*. *Km*^{r}	[46]
pHE539	Derivative of pIB11 where a 1.3 kb PCR fragment encoding *algB* replaced *bla*. *Km*^{r}	[Ertesvåg, unpublished]
pHE573	Vector containing *bla* and *tetA*/*tetR*. A*m*^{r},*Tc*^{r}.	[Ertesvåg, unpublished]
pIB11	RK2 based expression vector using the inducible *Pm*-XylS promoter system. A*m*^{r}, *Km*^{r}	[147]
pMM106	RK2-derived replicon with the XylS/Pm expression cassette. Contains *cas9* and *gmucA*, targets *mucA*. Ap^{r}	[145]
pMM107	Derivative of pHE265, vector containing the *lac* promoter. A*m*^{r}, *Sp*^{r}	[145]
pMM108	TOPO cloned vector containing *algLH199R*. *Km*^{r}	[145]
pMM109	TOPO cloned vector containing *algA* and *algF*. *Km*^{r}	[145]
pMM114	RK2-derived replicon with the XylS/Pm expression cassette. Contains *cas9* and *gmucA*, targets *algI*. Ap^{r}	[145]

Table D.2: Plasmids constructed in this work.

Plasmid	Description
pHMT1	TOPO cloned vector where the 2.6 kb PCR product of genomic *A. vinelandii* DNA with the primer pair HTalgBF/HTalgBR is cloned into pCR-BluntII-TOPO. *Km*^{r}
pHMT2	TOPO cloned vector where the 2.1 kb PCR product of genomic *A. vinelandii* DNA with the primer pair HTalgWF/HTalgWR is cloned into pCR-BluntII-TOPO. *Km*^{r}
pHMT3	Derivative of pHMT1 where the PstI-SacI 1.0 kb fragment encoding *aaDa* from pHE265 is ligated into 6.1 kb PshAI digested pHMT1. *Km*^{r}, *Sp*^{r}
pHMT4	Derivative of pHMT2 where the PstI-SacI 1.0 kb fragment encoding *aaDa* from pHE265 is ligated into 5.7 kb BspEI digested pHMT2. *Km*^{r}, *Sp*^{r}
pHMT5	Derivative of pHE326 where the AvrII-NotI 11.0 kb fragment is ligated with the Noti-SpeI 3.7 kb fragment from pHMT3. Contains *sacB*. *Am*^{r}, *Sp*^{r}, *Tc*^{r}
pHMT6	Derivative of pHE326 where the AvrII-NotI 11.0 kb fragment is ligated with the Noti-SpeI 3.2 kb fragment from pHMT4. Contains *sacB*. *Am*^{r}, *Sp*^{r}, *Tc*^{r}
pHMT7	Tn5-based transposon vector. Derivative of pCM1 where the NdeI-SacI 6.4 kb fragment is ligated with the NdeI-SacI 1.2 kb fragment from pMM107. *Am*^{r}, *Sp*^{r}
pHMT8	Tn5-based transposon vector. Derivative of pHMT7 where the NdeI-SbfI 7.4 kb fragment is ligated with the NdeI-SbfI 156 bp fragment from pHE513. *Am*^{r}, *Sp*^{r}
pHMT9	Tn5-based transposon vector. Derivative of pHMT7 where the NdeI-NotI 6.3 kb fragment is ligated with the NdeI-NotI 1.7 kb fragment from pHE278. *Am*^{r}, *Sp*^{r}
pHMT10	Tn5-based transposon vector. Derivative of pHMT8 where the NdeI-NotI 6.3 kb fragment is ligated with the NdeI-NotI 1.7 kb fragment from pHE278. *Am*^{r}, *Sp*^{r}
pHMT11	Tn5-based transposon vector. Derivative of pCM1 where the NdeI-NotI 8.1 kb fragment is ligated with the NdeI-NotI 1.2 kb fragment from pMM108. *Am*^{r}, *Sp*^{r}
pHMT12	Tn5-based transposon vector. Derivative of pHMT7 where the NdeI-NotI 6.3 kb fragment is ligated with the NdeI-NotI 1.2 kb fragment from pMM108. *Am*^{r}, *Sp*^{r}
pHMT13	Tn5-based transposon vector. Derivative of pHMT8 where the NdeI-NotI 6.3 kb fragment is ligated with the NdeI-NotI 1.2 kb fragment from pMM108. *Am*^{r}, *Sp*^{r}
pHMT14	Derivative of pHE103 where the EcoRV-SacI 4.4 kb fragment is ligated with the EcoRV-SacI 1.3 kb fragment from pMM109. *Am*^{r}
pHMT15	Derivative of of pHMT14 where the SacI-SbfI 5.7 kb fragment is ligated with the PstI-SacI 2.3 kb fragment from pHE573. *Am*^{r}, *Tc*^{r}
pHMT16	Derivative of pHE216 where the SacI-SpeI 9.3 kb fragment is ligated with the SacI-SpeI 5.3 kb fragment from pHMT15. Contains *sacB*. *Am*^{r}, *Tc*^{r}

E Plasmid maps

This section presents plasmid maps for all plasmids in the order they were used or constructed, along with relevant restriction endonuclease recognition sites.

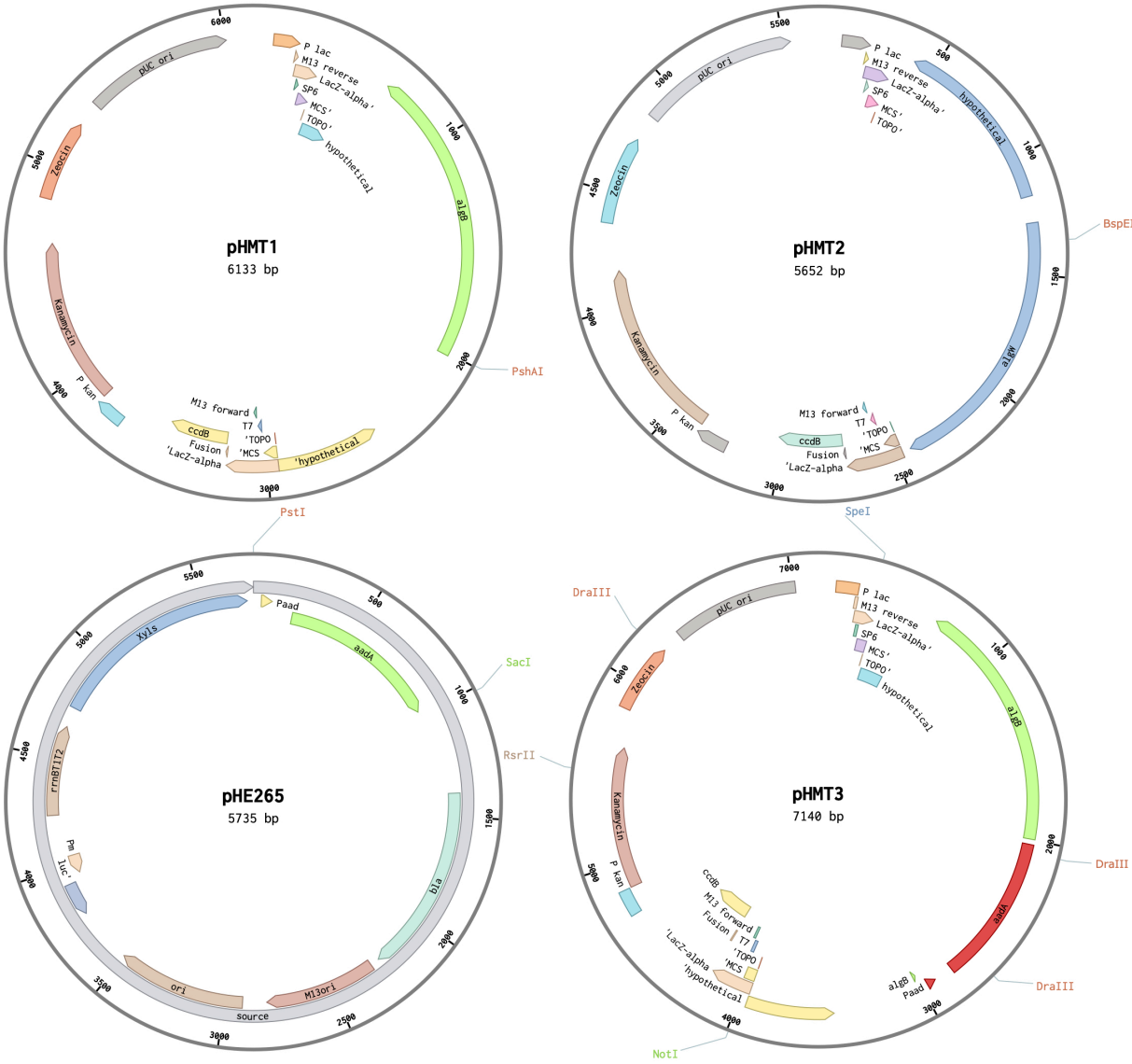

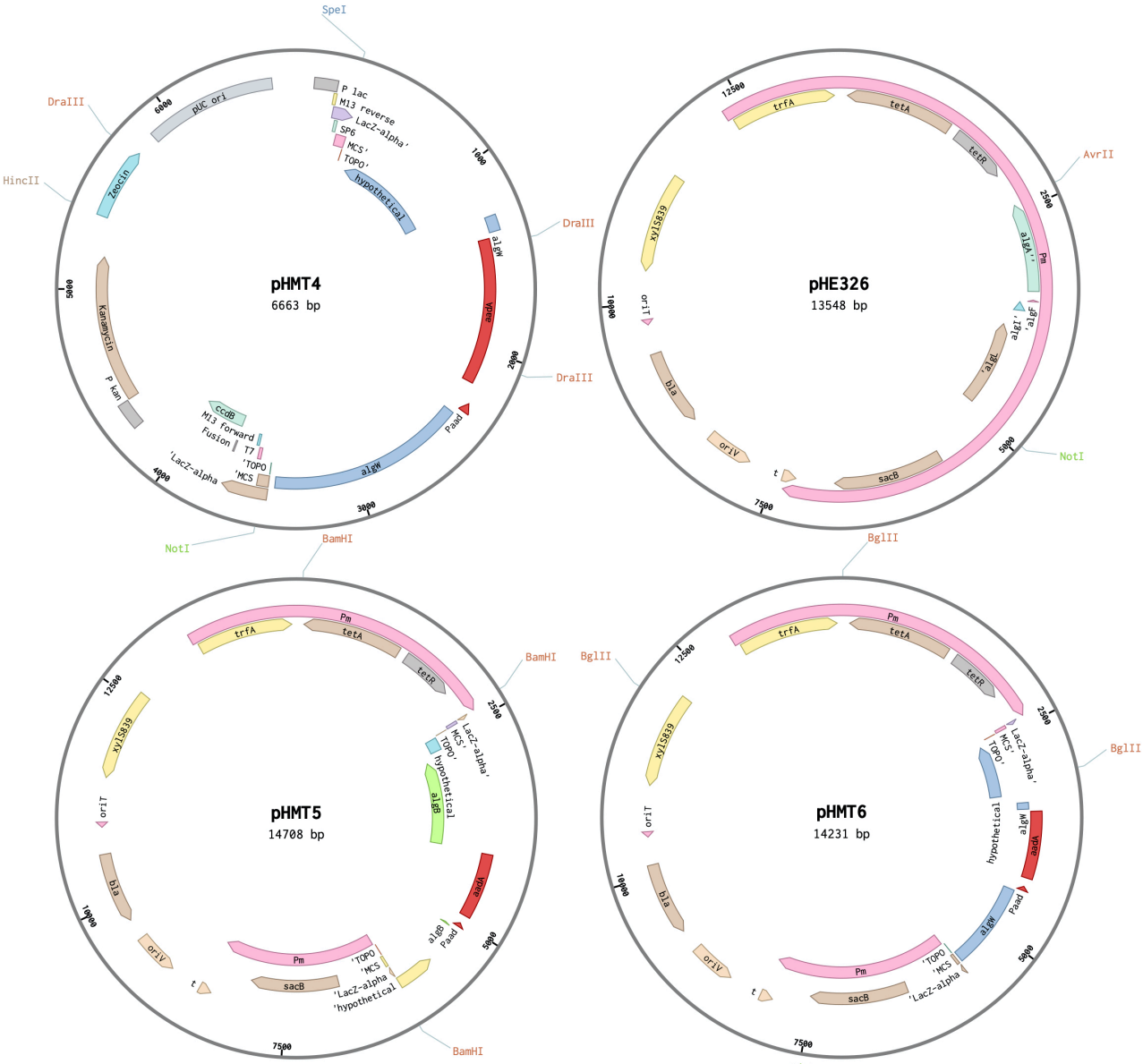
pHMT4
6663 bp
pHE326
13548 bp
pHMT5
14708 bp
pHMT6
14231 bp
SpeI
DraIII
HincII
AvrII
NotI
BamHI
BglII
P lac
M13 reverse
LacZ-alpha'
SP6
MCS'
TOPO'
hypothetical
algW
vgaa
kanamycin
P kan
ccdB
M13 forward
fusion
T7
'TOPO
'MCS
'LacZ-alpha
algW
PaadI
pUC ori
Zeocin
trfA
tetA
tetR
xylS839
oriT
bla
oriV
t
sacB
algA'
algF
algE
Pm
aadA
algB
'hypothetical

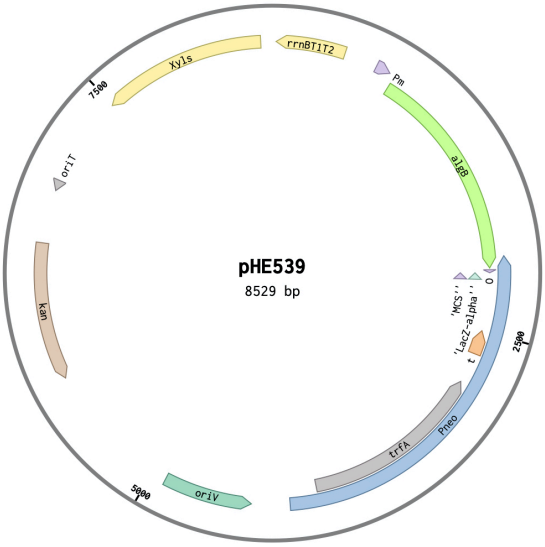
pHE539
8529 bp
rrnBT1T2
XylS
Pm
alkB
'MCS'
'LacZ-alpha'
t
Pneo
trfA
oriV
kan
oriT
7500
2500
5000


pHE536
8346 bp
rrnBT1T2
XylS
Pm
alkW
t
Pneo
trfA
oriV
kan
oriT
7500
2500
5000

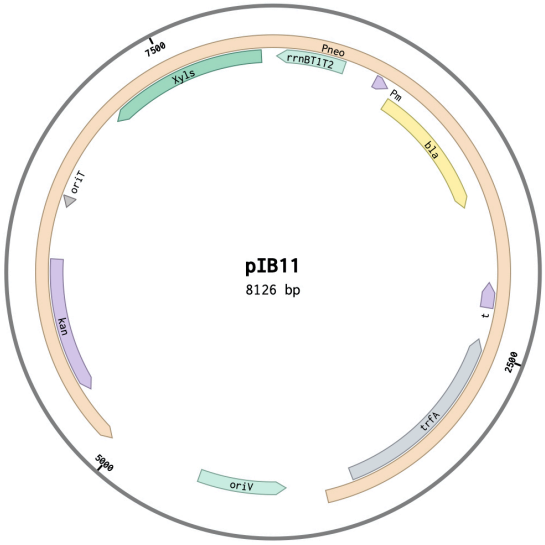
pIB11
8126 bp
Pneo
rrnBT1T2
XylS
Pm
bla
t
trfA
oriV
kan
oriT
7500
2500
5000

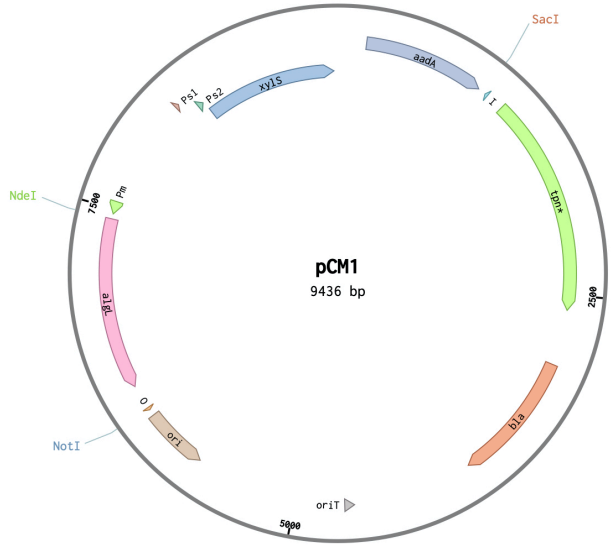
pCM1
9436 bp
SacI
aadA
r
Ps1
Ps2
xylS
tpm*
NdeI
Pm
alkL
O
ori
NotI
bla
oriT
7500
2500
5000

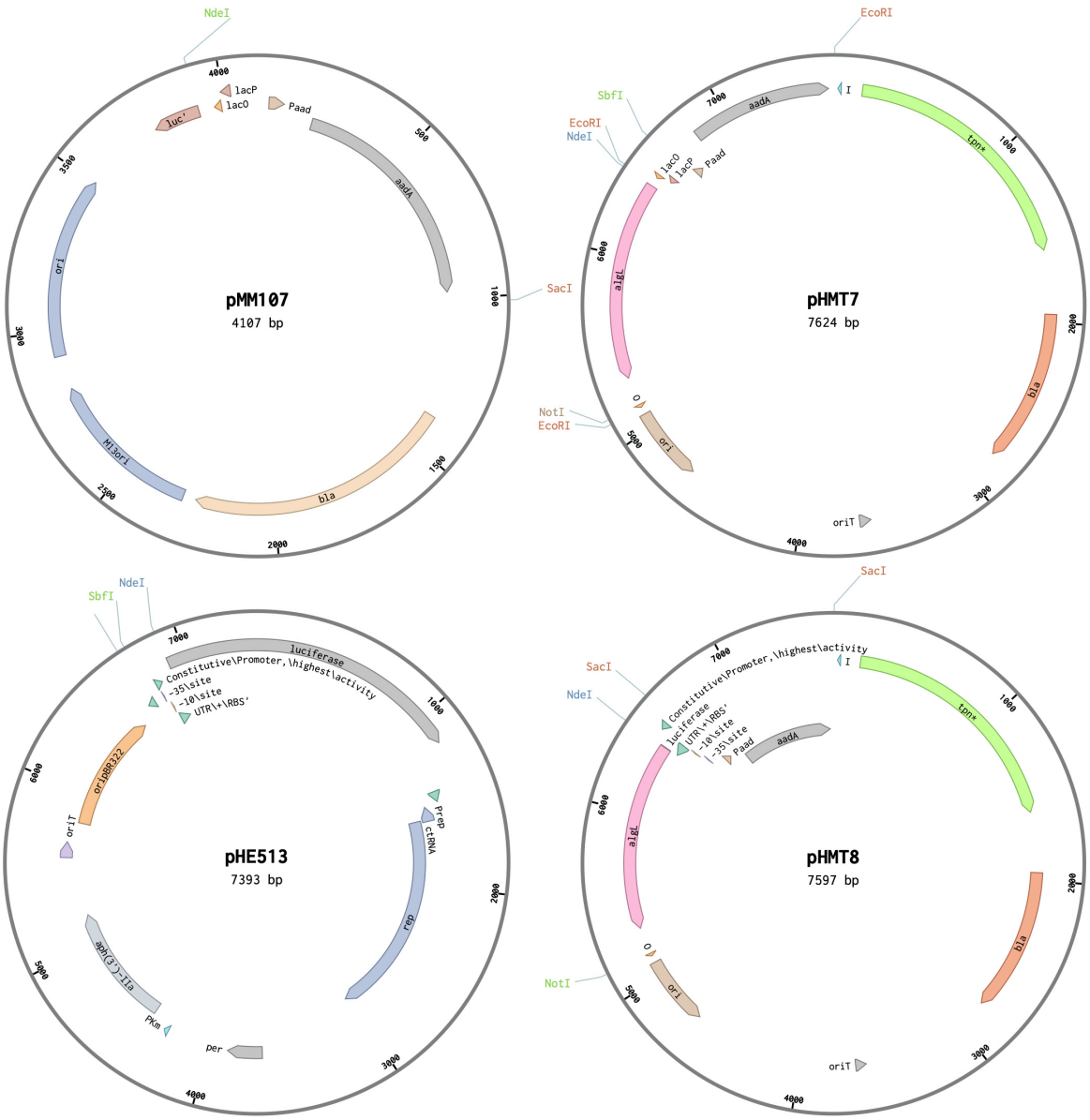
NdeI
lacP
lacO
Paad
luc'
aadA
ori
Mi3ori
bla
pMM107
4107 bp
SacI
EcoRI
SbfI
NdeI
aadA
I
tpnA
lacO
lacP
Paad
algL
bla
NotI
EcoRI
ori
oriT
pHMT7
7624 bp
SbfI
NdeI
luciferase
Constitutive\Promoter,\highest\activity
-35\site
-10\site
UTR1\+\RBS'
oriT
oriV8R322
prep
ctRNA
rep
aph(3')-IIa
Pkn
per
pHE513
7393 bp
SacI
SacI
NdeI
Constitutive\Promoter,\highest\activity
I
tpnA
luciferase
UTR1\+\RBS'
-10\site
-35\site
Paad
aadA
algL
bla
NotI
ori
oriT
pHMT8
7597 bp

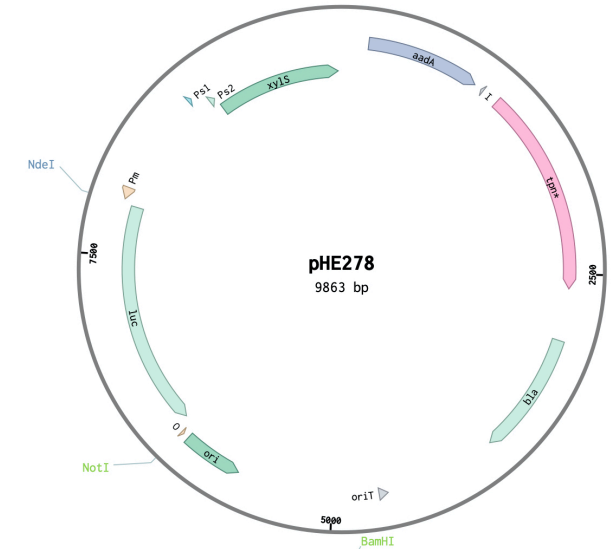
pHE278
9863 bp
aadA
I
tpn+
bla
oriT
ori
O
luc
Pm
Ps1
Ps2
xylS
NdeI
NotI
BamHI
2500
5000
7500

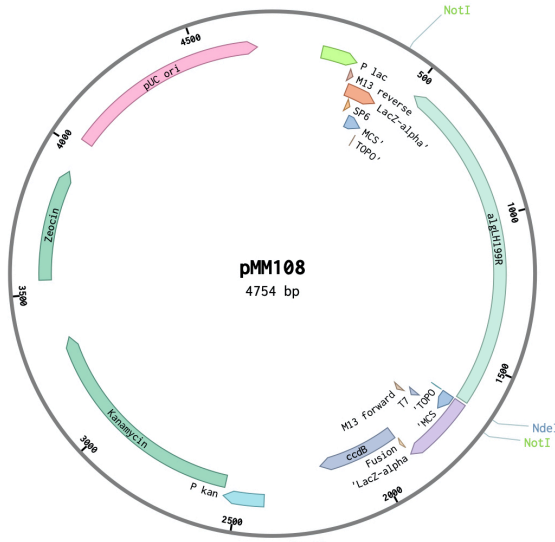
pMM108
4754 bp
pUC ori
P lac
M13 reverse
LacZ-alpha'
SP6
MCS'
TOPO'
algH199R
M13 forward
T1
'TOPO
'MCS
ccdB
Fusion
'LacZ-alpha
P kan
Kanamycin
Zeocin
NotI
NdeI
BamHI
1000
1500
2000
2500
3000
3500
4000
4500
5000

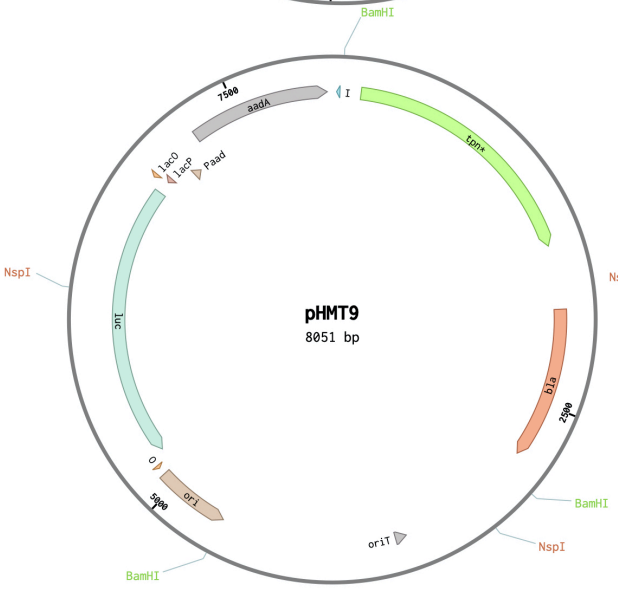
pHMT9
8051 bp
aadA
I
tpn+
bla
oriT
ori
O
luc
lacO
lacP
Paad
NspI
BamHI
2500
5000
7500

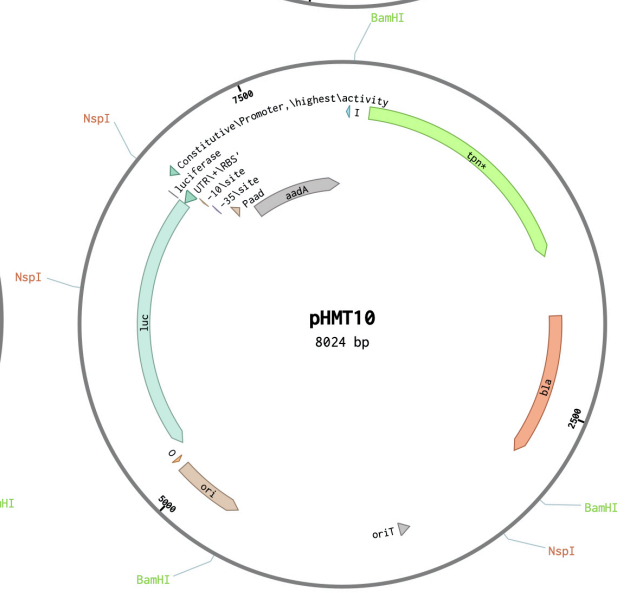
pHMT10
8024 bp
Constitutive\Promoter,\highest\activity
luciferase
UTR\+RBS'
-10\site
-35\site
Paad
aadA
I
tpn+
bla
oriT
ori
O
luc
NspI
BamHI
2500
5000
7500

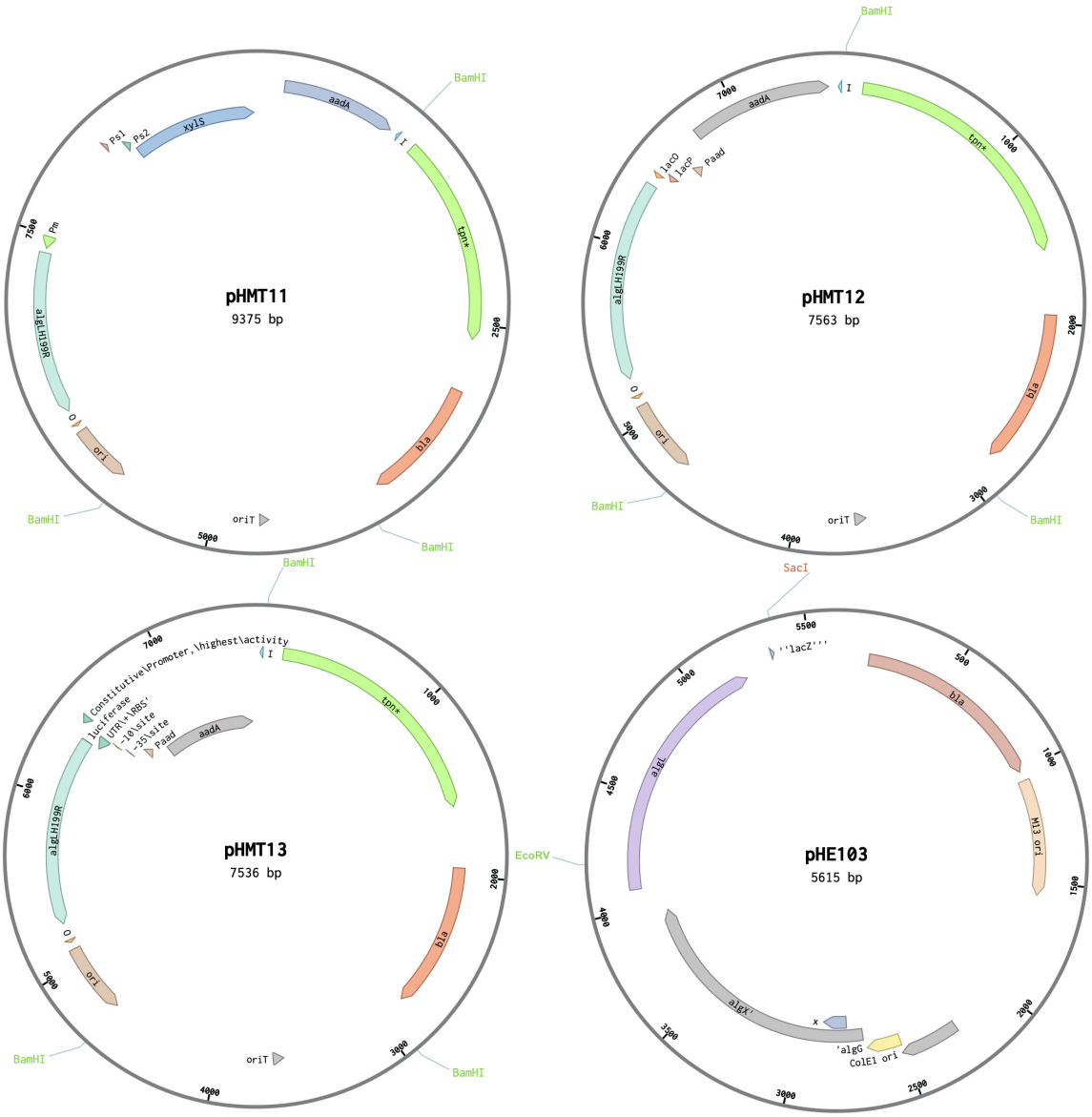
pHMT11
9375 bp
BamHI
aadA
I
tpnA
bla
ori
O
algLH199R
Pm
Ps1
Ps2
xylS
oriT
pHMT12
7563 bp
lacO
lacP
Paad
pHMT13
7536 bp
ConstitutivePromoter, highestactivity
luciferase
UTR+RBS'
-10site
-35site
Paad
EcoRV
pHE103
5615 bp
SacI
''lacZ'''
algL
algX'
x
'algG
ColE1 ori
M13 ori

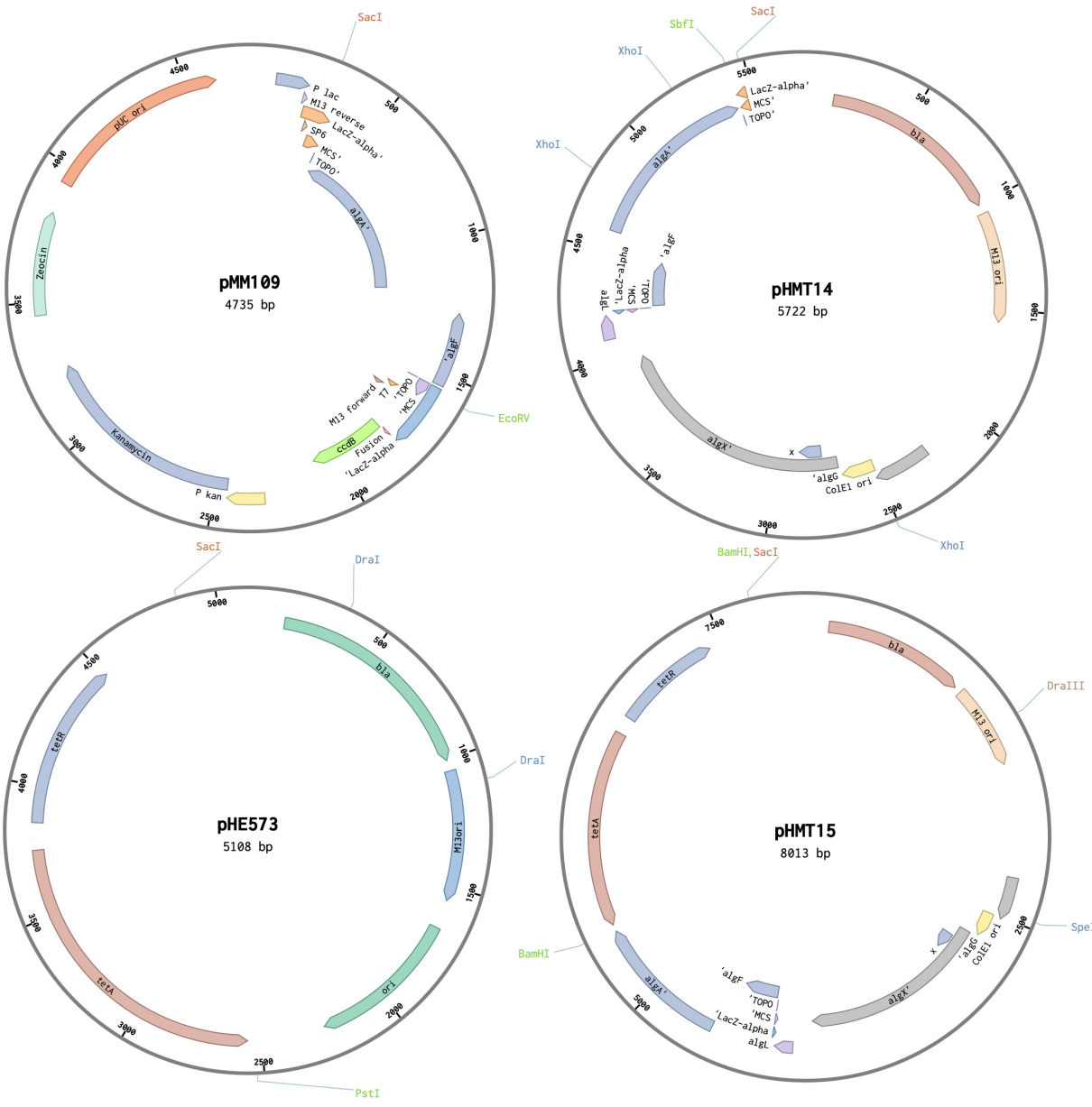
pMM109
4735 bp
SacI
P lac
M13 reverse
LacZ-alpha'
SP6
MCS'
TOPO'
algX'
algF
EcoRV
M13 forward
T7
'TOPO
'MCS
Fusion
'LacZ-alpha
ccdB
P kan
kanamycin
Zeocin
pUC ori
pHMT14
5722 bp
SbfI
XhoI
LacZ-alpha'
MCS'
TOPO'
bla
M13 ori
'algF
algX'
x
'algG
ColE1 ori
pHE573
5108 bp
DraI
bla
M13ori
ori
tetA
tetR
PstI
pHMT15
8013 bp
BamHI, SacI
DraIII
SpeI
'algF
'TOPO
'MCS
'LacZ-alpha
algL
algX'
'algG
ColE1 ori

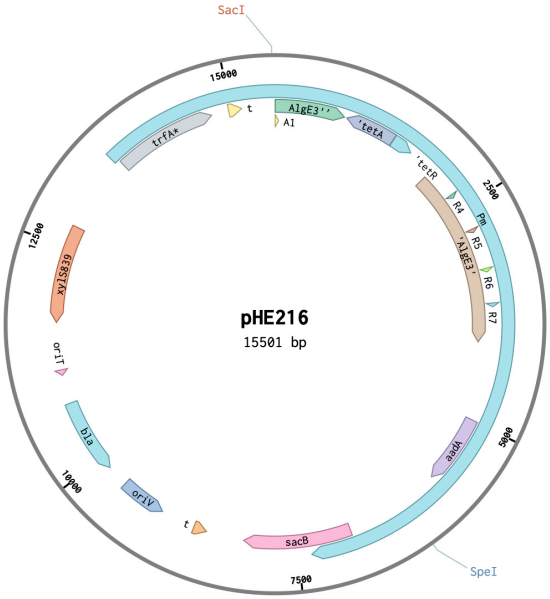
SacI
pHE216
15501 bp
SpeI

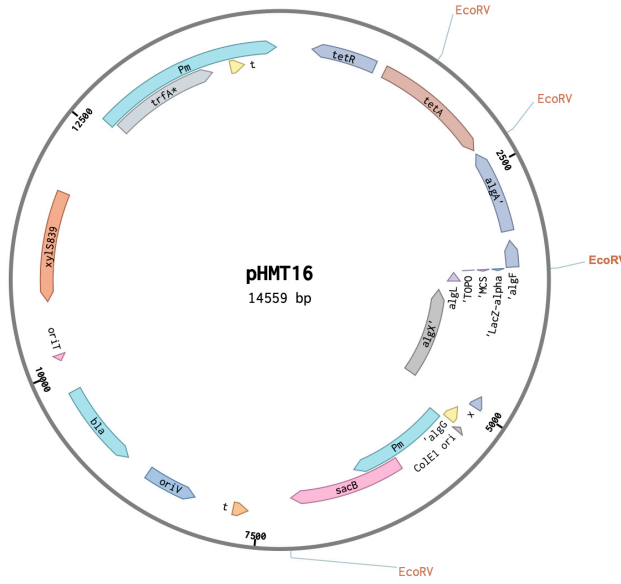
EcoRV
EcoRV
EcoRV
pHMT16
14559 bp
EcoRV

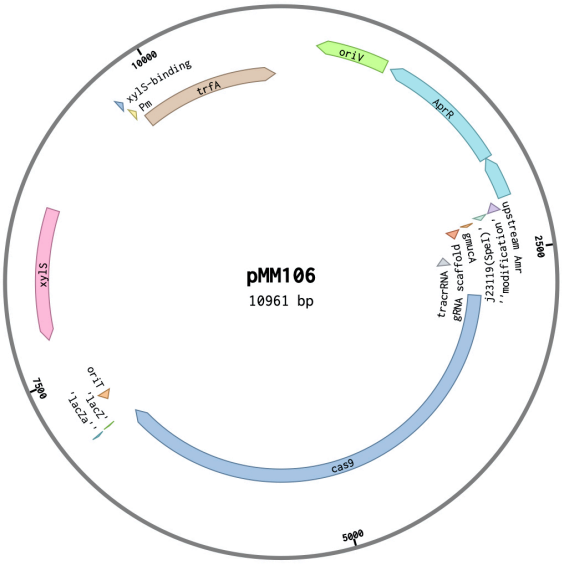
pMM106
10961 bp

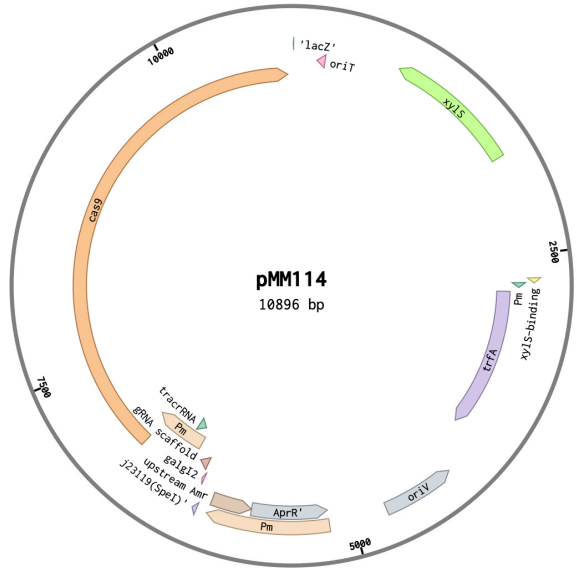
pMM114
10896 bp

F Primer sequences

The primers used for sequencing and PCR reactions in this work, their source and annealing temperature are presented in table F.1.

Table F.1: The primers used in PCR and for sequencing in this work, their source and the annealing temperature for primers used in PCR. F denotes the forward primer and R denotes the reverse primer.

Primer	Sequence	Source	T_m (°C)
27IR	**5'** AGTGGGCAGATCTTCGAATG **3'**	Sigma-Aldrich	seq.
algBF	**5'** TCCGCTCGTACTCCTTGTCC **3'**	Sigma-Aldrich	seq.
algBR	**5'** GGACAATCCGACGATGATGG **3'**	Sigma-Aldrich	seq.
algF-L F	**5'** CCTTCACCGGCGGTTTGAC **3'**	Invitrogen	70
algF-L R	**5'** GCGCCACGACTATCACGCTC **3'**	Invitrogen	71
algF-X F	**5'** GCGGCTTGTCGGAGAGGTTC **3'**	Invitrogen	71
algF-X R	**5'** CGAGCACAGCGACCAGTTC **3'**	Invitrogen	69
algFR	**5'** GACGAGCAACTCACTCCTTC **3'**	Sigma-Aldrich	65
algLsjekkF	**5'** CTGCAAGCGCCACGACTATC **3'**	MWG-Biotech AG	69
algXBF	**5'** CTTCCGCGGCGTGCACCACTGGACCTCCTAC **3'**	Sigma-Aldrich	83
algXBR	**5'** GTTCGGGCACCACCGGACAGGC **3'**	Sigma-Aldrich	79
algWseq	**5'** TTACGCCACTGACGACTCTG **3'**	Invitrogen	seq.
HalgVF	**5'** GGTTGGTAGCGGTGTTGTCG **3'**	Invitrogen	69
HalgVR	**5'** TGGTCTACGCCGGTACCTTC **3'**	Invitrogen	69
HTalgBF	**5'** GCTGTATTCGGCAGCTTGTATG **3'**	Invitrogen	66
HTalgBR	**5'** GCCTCAGATGGAGAAAGAAC **3'**	Invitrogen	63
HTalgWF	**5'** CGGCGCACTCTAGCACAGTC **3'**	Invitrogen	71
HTalgWR	**5'** CAAGTGGGCCCGTCTCGTTC **3'**	Invitrogen	71
M13F	**5'** GTAAAACGACGGCCAG **3'**	Thermo Fisher	seq.
M13R	**5'** CAGGAAACAGCTATGAC **3'**	Thermo Fisher	seq.
MD124A	**5'** CGTGAAGCCCTGTATGAATC **3'**	Sigma-Aldrich	63
MD125sjekkF	**5'** TTGGTCGCGTTATCAACTGG **3'**	Sigma-Aldrich	65
MD125sjekkR	**5'** CGCACGGGCATAAGGTAAAG **3'**	Sigma-Aldrich	66
mucAsjekkwtR	**5'** GAAGAAGGCTCCTGGGATTG **3'**	Sigma-Aldrich	65
pHMT16F	**5'** GGAAGAAGCAGACCGCTAAC **3'**	Invitrogen	66
pHMT16R	**5'** AAAGGGCGATCTTGCGACCG **3'**	Invitrogen	71

G Restriction endonucleases

The restriction endonucleases used in this work, their recognition and restriction sites, optimal temperatures and inactivation temperatures are presented in table G.1.

Table G.1: Restriction endonucleases used, their recognition and restriction sites, optimal temperature and inactivation temperature. N indicates any base, R indicates an A or a G, W indicates an A or a T and Y indicates a C or a T.

Restriction enzyme	Recognition and restriction site	Optimal temperature (°C)	Inactivation temperature (°C)
AvrII	**5'** C|C T A G|G **3'** **3'** G|G A T C|C **5'**	37	-
BamHI	**5'** G|G A T C C **3'** **3'** C C T A G|G **5'**	37	-
BglII	**5'** A|G A T C T **3'** **3'** T C T A G|A **5'**	37	-
BspEI	**5'** T|C C G G A **3'** **3'** A G G C C|T **5'**	37	80
DraI	**5'** T T T|A A A **3'** **3'** A A A|T T T **5'**	37	65
DraIII	**5'** C A C N N N|G T G **3'** **3'** G T G|N N N C A C **5'**	37	-
EcoRI	**5'** G|A A T T C **3'** **3'** C T T A A|G **5'**	37	65
EcoRV	**5'** G A T|A T C **3'** **3'** C T A|T A G **5'**	37	80
HincII	**5'** G T Y|R A C **3'** **3'** C A R|Y T G **5'**	37	65
NdeI	**5'** C A|T A T G **3'** **3'** G T A T|A C **5'**	37	65
NotI	**5'** G C|G G C C G C **3'** **3'** C G C C G G|C G **5'**	37	65
PshAI	**5'** G A C N N|N N G T C **3'** **3'** C T G N N|N N C A G **5'**	37	65
PstI	**5'** C T G C A|G **3'** **3'** G|A C G T C **5'**	37	80
RsrII	**5'** C G|G W C C G **3'** **3'** G C C W G|G C **5'**	37	65
SacI	**5'** G A G C T|C **3'** **3'** C|T C G A G **5'**	37	65
SbfI	**5'** C C T G C A|G G **3'** **3'** G G|A C G T C C **5'**	37	80
SpeI	**5'** A|C T A G T **3'** **3'** T G A T C|A **5'**	37	80
XhoI	**5'** C|T C G A G **3'** **3'** G A G C T|C **5'**	37	65

H Sequencing of pHMT1

The successful cloning of pHMT1 was confirmed by sequencing with the primers algBF, algBR, M13F and M13R, and aligned with *algB* using Benchling and SnapGene. The alignment is presented here, with any mismatches at each sequence end removed. The results show a complete overlap with the entire gene, with no mismatches.

1. *algB*
2. algBF
3. M13R
4. algBR
5. M13F

```
1   TCACAGGCCATACTGTTTGCGTTTGCGATACAGCGTCGAAGCATCGATGCCGAGCGTCCTGGCGGCCTGT  70
2   TCACAGGCCATACTGTTTGCGTTTGCGATACAGCGTCGAAGCATCGATGCCGAGCGTCCTGGCGGCCTGT  70
3   TCACAGGCCATACTGTTTGCGTTTGCGATACAGCGTCGAAGCATCGATGCCGAGCGTCCTGGCGGCCTGT  70
4   ------------------------------------------------------------------------
5   ------------------------------------------------------------------------

1   TCGAGGGTCTCGCTGCTCGCCAGCACCGCGGTGATATGGGCCTTCTCCAGTTCCTCGAGACGCAGCGGCA 140
2   TCGAGGGTCTCGCTGCTCGCCAGCACCGCGGTGATATGGGCCTTCTCCAGTTCCTCGAGACGCAGCGGCA 140
3   TCGAGGGTCTCGCTGCTCGCCAGCACCGCGGTGATATGGGCCTTCTCCAGTTCCTCGAGACGCAGCGGCA 140
4   ------------------------------------------------------------------------
5   ------------------------------------------------------------------------

1   TGCCCACCCGCGGCACGCTGCCACCCGGCTGCTCGCCCAGTCCCAGGTGACTCGTCCCGATTACCTCCTG 210
2   TGCCCACCCGCGGCACGCTGCCACCCGGCTGCTCGCCCAGTCCCAGGTGACTCGTCCCGATTACCTCCTG 210
3   TGCCCACCCGCGGCACGCTGCCACCCGGCTGCTCGCCCAGTCCCAGGTGACTCGTCCCGATTACCTCCTG 210
4   ------------------------------------------------------------------------
5   ------------------------------------------------------------------------

1   CGGACAGATGATGCTGGTCCGCTCCACCACGTTGCGCAGCTCGCGGATGTTGCCCGGCCAGTGGTAGCCC 280
2   CGGACAGATGATGCTGGTCCGCTCCACCACGTTGCGCAGCTCGCGGATGTTGCCCGGCCAGTGGTAGCCC 280
3   CGGACAGATGATGCTGGTCCGCTCCACCACGTTGCGCAGCTCGCGGATGTTGCCCGGCCAGTGGTAGCCC 280
4   ------------------------------------------------------------------------
5   ------------------------------------------------------------------------

1   AGCAGGGCCGCCTGCGCCGCCTCGCCGAAGCGGCGCGCCGGACGCCCGTAGTTCCTGACGAACATCCGCA 350
2   AGCAGGGCCGCCTGCGCCGCCTCGCCGAAGCGGCGCGCCGGACGCCCGTAGTTCCTGACGAACATCCGCA 350
3   AGCAGGGCCGCCTGCGCCGCCTCGCCGAAGCGGCGCGCCGGACGCCCGTAGTTCCTGACGAACATCCGCA 350
4   ------------------------------------------------------------------------
5   ------------------------------------------------------------------------

1   GGAAACGCTCGGCCAGGACGAGGATGTCCTCGGAACGCTCGCGCAGCGGCGGCAGATGCAGGGTGATCAC 420
2   GGAAACGCTCGGCCAGGACGAGGATGTCCTCGGAACGCTCGCGCAGCGGCGGCAGATGCAGGGTGATCAC 420
3   GGAAACGCTCGGCCAGGACGAGGATGTCCTCGGAACGCTCGCGCAGCGGCGGCAGATGCAGGGTGATCAC 420
4   ------------------------------------------------------------------------
5   ------------------------------------------------------------------------
```

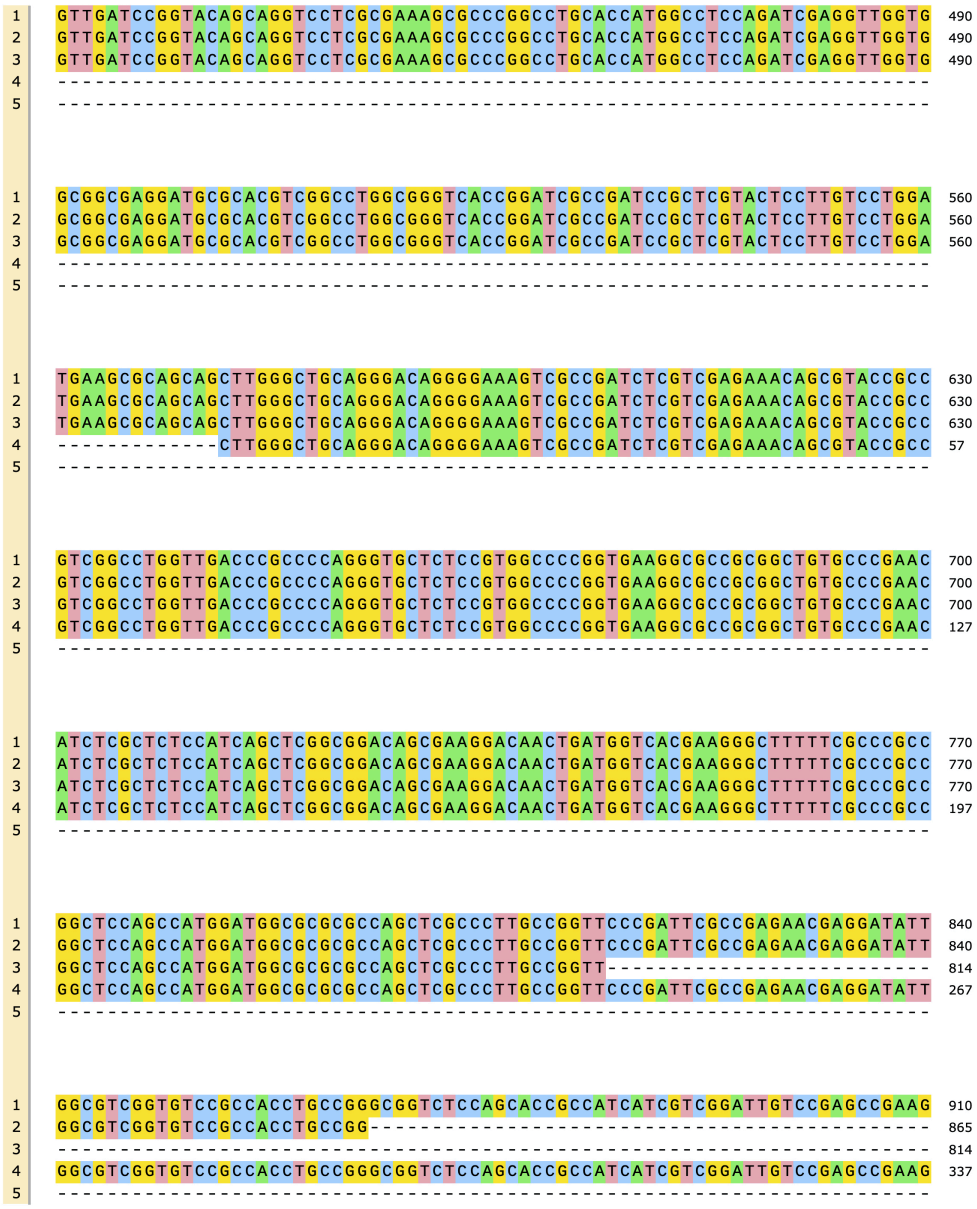
1 GTTGATCCGGTACAGCAGGTCCTCGCGAAAGCGCCCGGCCTGCACCATGGCCTCCAGATCGAGGTTGGTG 490
2 GTTGATCCGGTACAGCAGGTCCTCGCGAAAGCGCCCGGCCTGCACCATGGCCTCCAGATCGAGGTTGGTG 490
3 GTTGATCCGGTACAGCAGGTCCTCGCGAAAGCGCCCGGCCTGCACCATGGCCTCCAGATCGAGGTTGGTG 490
4 ----------
5 ----------
1 GCGGCGAGGATGCGCACGTCGGCCTGGCGGGTCACCGGATCGCCGATCCGCTCGTACTCCTTGTCCTGGA 560
2 GCGGCGAGGATGCGCACGTCGGCCTGGCGGGTCACCGGATCGCCGATCCGCTCGTACTCCTTGTCCTGGA 560
3 GCGGCGAGGATGCGCACGTCGGCCTGGCGGGTCACCGGATCGCCGATCCGCTCGTACTCCTTGTCCTGGA 560
4 ----------
5 ----------
1 TGAAGCGCAGCAGCTTGGGCTGCAGGGACAGGGGAAAGTCGCCGATCTCGTCGAGAAACAGCGTACCGCC 630
2 TGAAGCGCAGCAGCTTGGGCTGCAGGGACAGGGGAAAGTCGCCGATCTCGTCGAGAAACAGCGTACCGCC 630
3 TGAAGCGCAGCAGCTTGGGCTGCAGGGACAGGGGAAAGTCGCCGATCTCGTCGAGAAACAGCGTACCGCC 630
4 ----------CTTGGGCTGCAGGGACAGGGGAAAGTCGCCGATCTCGTCGAGAAACAGCGTACCGCC 57
5 ----------
1 GTCGGCCTGGTTGACCCGCCCCAGGGTGCTCTCCGTGGCCCCGGTGAAGGCGCCGCGGCTGTGCCCGAAC 700
2 GTCGGCCTGGTTGACCCGCCCCAGGGTGCTCTCCGTGGCCCCGGTGAAGGCGCCGCGGCTGTGCCCGAAC 700
3 GTCGGCCTGGTTGACCCGCCCCAGGGTGCTCTCCGTGGCCCCGGTGAAGGCGCCGCGGCTGTGCCCGAAC 700
4 GTCGGCCTGGTTGACCCGCCCCAGGGTGCTCTCCGTGGCCCCGGTGAAGGCGCCGCGGCTGTGCCCGAAC 127
5 ----------
1 ATCTCGCTCTCCATCAGCTCGGCGGACAGCGAAGGACAACTGATGGTCACGAAGGGCTTTTTCGCCCGCC 770
2 ATCTCGCTCTCCATCAGCTCGGCGGACAGCGAAGGACAACTGATGGTCACGAAGGGCTTTTTCGCCCGCC 770
3 ATCTCGCTCTCCATCAGCTCGGCGGACAGCGAAGGACAACTGATGGTCACGAAGGGCTTTTTCGCCCGCC 770
4 ATCTCGCTCTCCATCAGCTCGGCGGACAGCGAAGGACAACTGATGGTCACGAAGGGCTTTTTCGCCCGCC 197
5 ----------
1 GGCTCCAGCCATGGATGGCGCGCGCCAGCTCGCCCTTGCCGGTTCCCGATTCGCCGAGAACGAGGATATT 840
2 GGCTCCAGCCATGGATGGCGCGCGCCAGCTCGCCCTTGCCGGTTCCCGATTCGCCGAGAACGAGGATATT 840
3 GGCTCCAGCCATGGATGGCGCGCGCCAGCTCGCCCTTGCCGGTT---------- 814
4 GGCTCCAGCCATGGATGGCGCGCGCCAGCTCGCCCTTGCCGGTTCCCGATTCGCCGAGAACGAGGATATT 267
5 ----------
1 GGCGTCGGTGTCCGCCACCTGCCGGGCGGTCTCCAGCACCGCCATCATCGTCGGATTGTCCGAGCCGAAG 910
2 GGCGTCGGTGTCCGCCACCTGCCGG---------- 865
3 ---------- 814
4 GGCGTCGGTGTCCGCCACCTGCCGGGCGGTCTCCAGCACCGCCATCATCGTCGGATTGTCCGAGCCGAAG 337
5 ----------

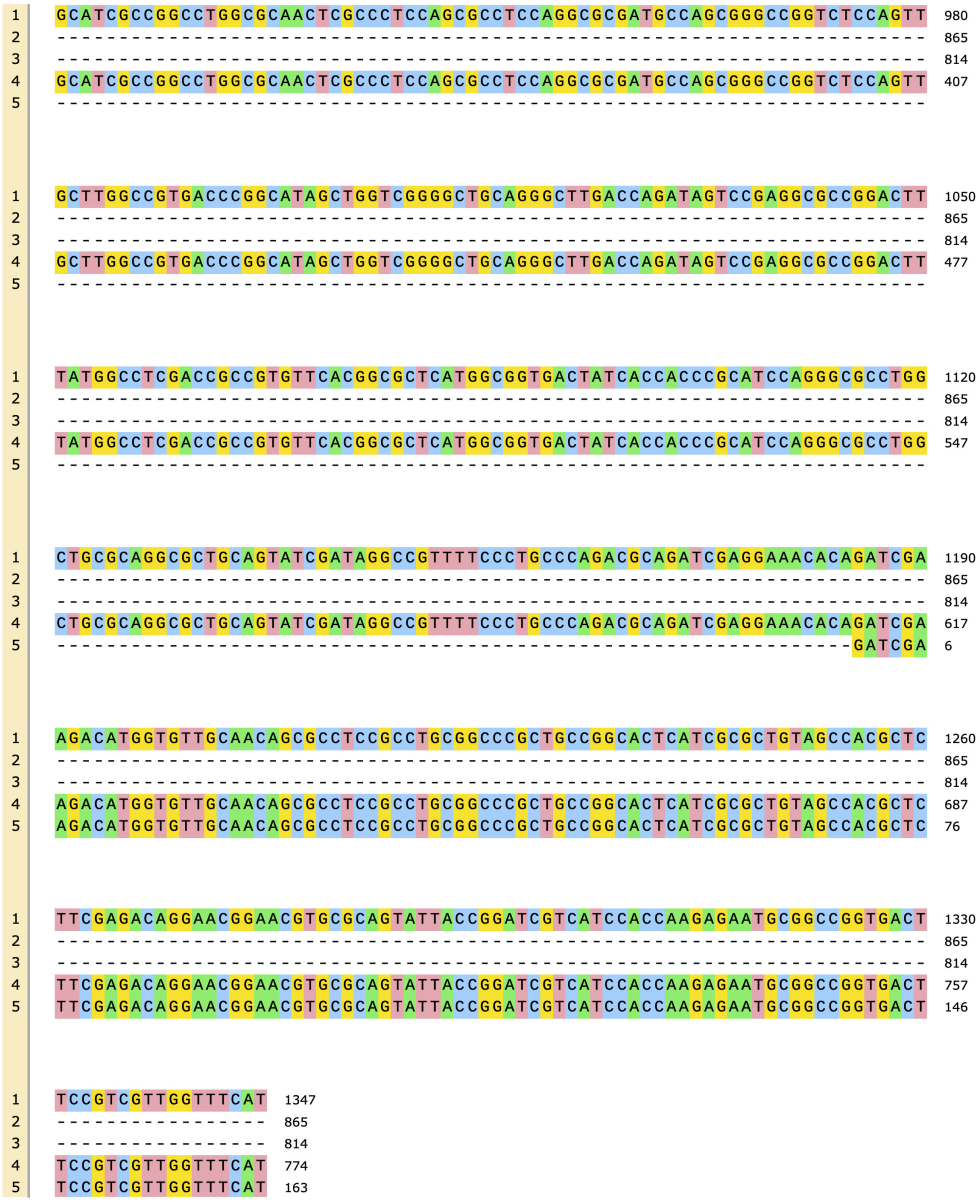
1 GCATCGCCGGCCTGGCGCAACTCGCCCTCCAGCGCCTCCAGGCGCGATGCCAGCGGGCCGGTCTCCAGTT 980
2 ---------- 865
3 ---------- 814
4 GCATCGCCGGCCTGGCGCAACTCGCCCTCCAGCGCCTCCAGGCGCGATGCCAGCGGGCCGGTCTCCAGTT 407
5 ----------
1 GCTTGGCCGTGACCCGGCATAGCTGGTCGGGGCTGCAGGGCTTGACCAGATAGTCCGAGGCGCCGGACTT 1050
2 ---------- 865
3 ---------- 814
4 GCTTGGCCGTGACCCGGCATAGCTGGTCGGGGCTGCAGGGCTTGACCAGATAGTCCGAGGCGCCGGACTT 477
5 ----------
1 TATGGCCTCGACCGCCGTGTTCACGGCGCTCATGGCGGTGACTATCACCACCCGCATCCAGGGCGCCTGG 1120
2 ---------- 865
3 ---------- 814
4 TATGGCCTCGACCGCCGTGTTCACGGCGCTCATGGCGGTGACTATCACCACCCGCATCCAGGGCGCCTGG 547
5 ----------
1 CTGCGCAGGCGCTGCAGTATCGATAGGCCGTTTTCCCTGCCCAGACGCAGATCGAGGAAACACAGATCGA 1190
2 ---------- 865
3 ---------- 814
4 CTGCGCAGGCGCTGCAGTATCGATAGGCCGTTTTCCCTGCCCAGACGCAGATCGAGGAAACACAGATCGA 617
5 ----------GATCGA 6
1 AGACATGGTGTTGCAACAGCGCCTCCGCCTGCGGCCCGCTGCCGGCACTCATCGCGCTGTAGCCACGCTC 1260
2 ---------- 865
3 ---------- 814
4 AGACATGGTGTTGCAACAGCGCCTCCGCCTGCGGCCCGCTGCCGGCACTCATCGCGCTGTAGCCACGCTC 687
5 AGACATGGTGTTGCAACAGCGCCTCCGCCTGCGGCCCGCTGCCGGCACTCATCGCGCTGTAGCCACGCTC 76
1 TTCGAGACAGGAACGGAACGTGCGCAGTATTACCGGATCGTCATCCACCAAGAGAATGCGGCCGGTGACT 1330
2 ---------- 865
3 ---------- 814
4 TTCGAGACAGGAACGGAACGTGCGCAGTATTACCGGATCGTCATCCACCAAGAGAATGCGGCCGGTGACT 757
5 TTCGAGACAGGAACGGAACGTGCGCAGTATTACCGGATCGTCATCCACCAAGAGAATGCGGCCGGTGACT 146
1 TCCGTCGTTGGTTTCAT 1347
2 ---------- 865
3 ---------- 814
4 TCCGTCGTTGGTTTCAT 774
5 TCCGTCGTTGGTTTCAT 163

I Sequencing of pHMT2

The successful cloning of pHMT2 was confirmed by sequencing with the primers algWseq, M13F and M13R, and aligned with *algW* using Benchling and SnapGene. The alignment is presented here, with any mismatches at each sequence end removed. The results show a complete overlap with the entire gene, with no mismatches.

1. *algW*
2. algWseq
3. M13R
4. M13F

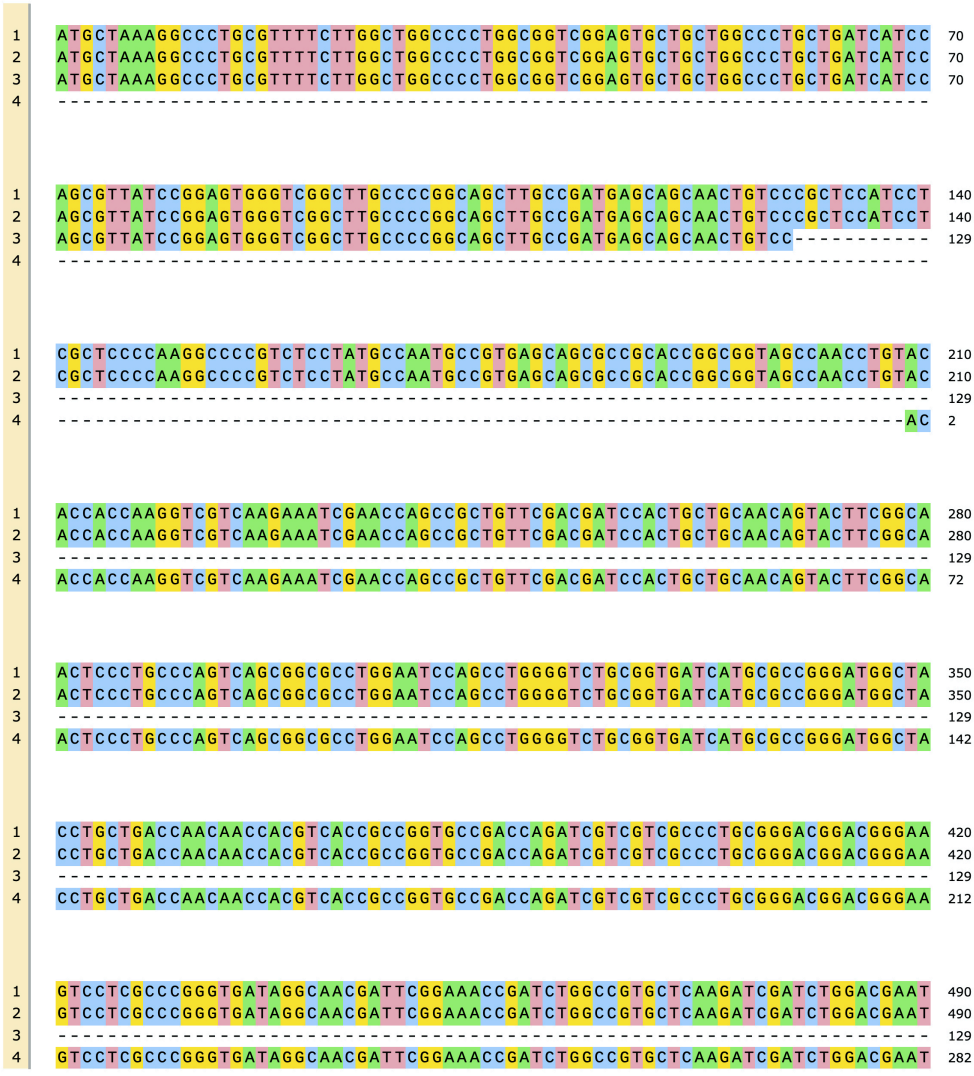

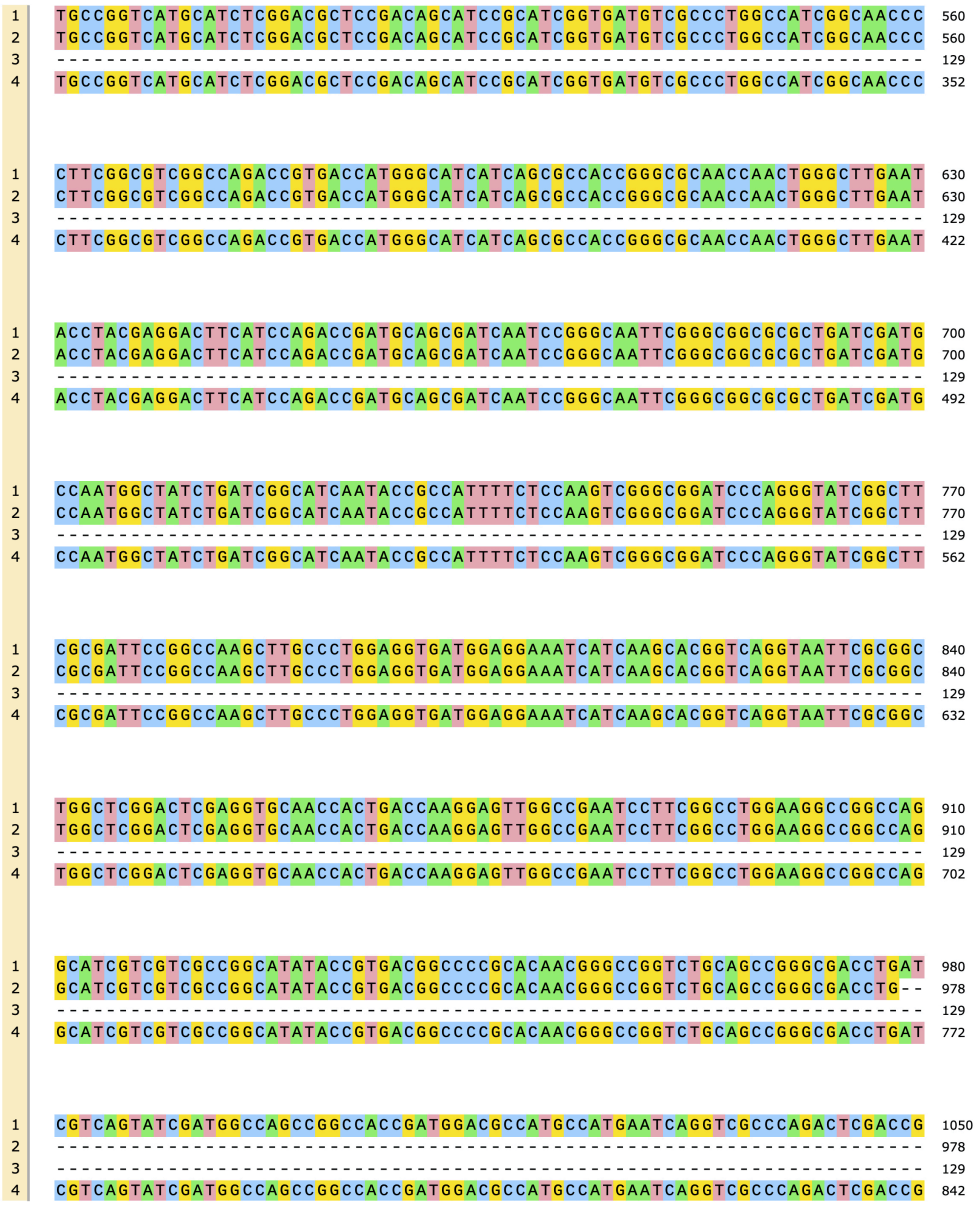
1 TGCCGGTCATGCATCTCGGACGCTCCGACAGCATCCGCATCGGTGATGTCGCCCTGGCCATCGGCAACCC 560
2 TGCCGGTCATGCATCTCGGACGCTCCGACAGCATCCGCATCGGTGATGTCGCCCTGGCCATCGGCAACCC 560
3 -- 129
4 TGCCGGTCATGCATCTCGGACGCTCCGACAGCATCCGCATCGGTGATGTCGCCCTGGCCATCGGCAACCC 352
1 CTTCGGCGTCGGCCAGACCGTGACCATGGGCATCATCAGCGCCACCGGGCGCAACCAACTGGGCTTGAAT 630
2 CTTCGGCGTCGGCCAGACCGTGACCATGGGCATCATCAGCGCCACCGGGCGCAACCAACTGGGCTTGAAT 630
3 -- 129
4 CTTCGGCGTCGGCCAGACCGTGACCATGGGCATCATCAGCGCCACCGGGCGCAACCAACTGGGCTTGAAT 422
1 ACCTACGAGGACTTCATCCAGACCGATGCAGCGATCAATCCGGGCAATTCGGGCGGCGCGCTGATCGATG 700
2 ACCTACGAGGACTTCATCCAGACCGATGCAGCGATCAATCCGGGCAATTCGGGCGGCGCGCTGATCGATG 700
3 -- 129
4 ACCTACGAGGACTTCATCCAGACCGATGCAGCGATCAATCCGGGCAATTCGGGCGGCGCGCTGATCGATG 492
1 CCAATGGCTATCTGATCGGCATCAATACCGCCATTTTCTCCAAGTCGGGCGGATCCCAGGGTATCGGCTT 770
2 CCAATGGCTATCTGATCGGCATCAATACCGCCATTTTCTCCAAGTCGGGCGGATCCCAGGGTATCGGCTT 770
3 -- 129
4 CCAATGGCTATCTGATCGGCATCAATACCGCCATTTTCTCCAAGTCGGGCGGATCCCAGGGTATCGGCTT 562
1 CGCGATTCCGGCCAAGCTTGCCCTGGAGGTGATGGAGGAAATCATCAAGCACGGTCAGGTAATTCGCGGC 840
2 CGCGATTCCGGCCAAGCTTGCCCTGGAGGTGATGGAGGAAATCATCAAGCACGGTCAGGTAATTCGCGGC 840
3 -- 129
4 CGCGATTCCGGCCAAGCTTGCCCTGGAGGTGATGGAGGAAATCATCAAGCACGGTCAGGTAATTCGCGGC 632
1 TGGCTCGGACTCGAGGTGCAACCACTGACCAAGGAGTTGGCCGAATCCTTCGGCCTGGAAGGCCGGCCAG 910
2 TGGCTCGGACTCGAGGTGCAACCACTGACCAAGGAGTTGGCCGAATCCTTCGGCCTGGAAGGCCGGCCAG 910
3 -- 129
4 TGGCTCGGACTCGAGGTGCAACCACTGACCAAGGAGTTGGCCGAATCCTTCGGCCTGGAAGGCCGGCCAG 702
1 GCATCGTCGTCGCCGGCATATACCGTGACGGCCCCGCACAACGGGCCGGTCTGCAGCCGGGCGACCTGAT 980
2 GCATCGTCGTCGCCGGCATATACCGTGACGGCCCCGCACAACGGGCCGGTCTGCAGCCGGGCGACCTG-- 978
3 -- 129
4 GCATCGTCGTCGCCGGCATATACCGTGACGGCCCCGCACAACGGGCCGGTCTGCAGCCGGGCGACCTGAT 772
1 CGTCAGTATCGATGGCCAGCCGGCCACCGATGGACGCCATGCCATGAATCAGGTCGCCCAGACTCGACCG 1050
2 -- 978
3 -- 129
4 CGTCAGTATCGATGGCCAGCCGGCCACCGATGGACGCCATGCCATGAATCAGGTCGCCCAGACTCGACCG 842

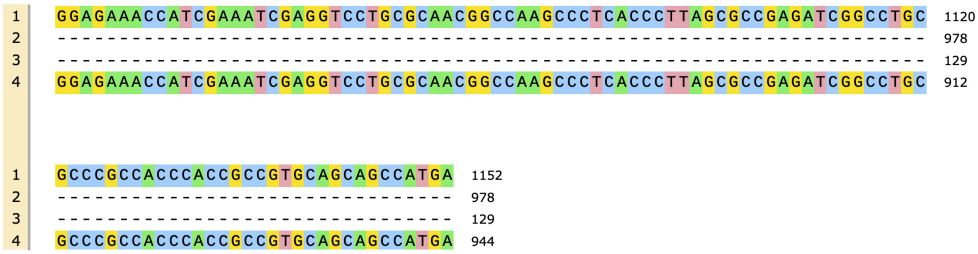
1 GGAGAAACCATCGAAATCGAGGTCCTGCGCAACGGCCAAGCCCTCACCCTTAGCGCCGAGATCGGCCTGC 1120
2 ---------- 978
3 ---------- 129
4 GGAGAAACCATCGAAATCGAGGTCCTGCGCAACGGCCAAGCCCTCACCCTTAGCGCCGAGATCGGCCTGC 912
1 GCCCGCCACCCACCGCCGTGCAGCAGCCATGA 1152
2 ---------- 978
3 ---------- 129
4 GCCCGCCACCCACCGCCGTGCAGCAGCCATGA 944

J Sequencing of pHMT14

The successful cloning of pHMT14 was confirmed by sequencing with the primers M13F, algLsjekkF, algXBF and 27IR, and aligned with the *algA-algG* fragment of pHMT14 using Benchling and SnapGene. The alignment is presented here, with any mismatches at each sequence end removed. The results show a complete overlap with the entire gene, with no mismatches.

1. *algA-algG* of pHMT14
2. M13F
3. algLsjekkF
4. algXB F
5. 27IR

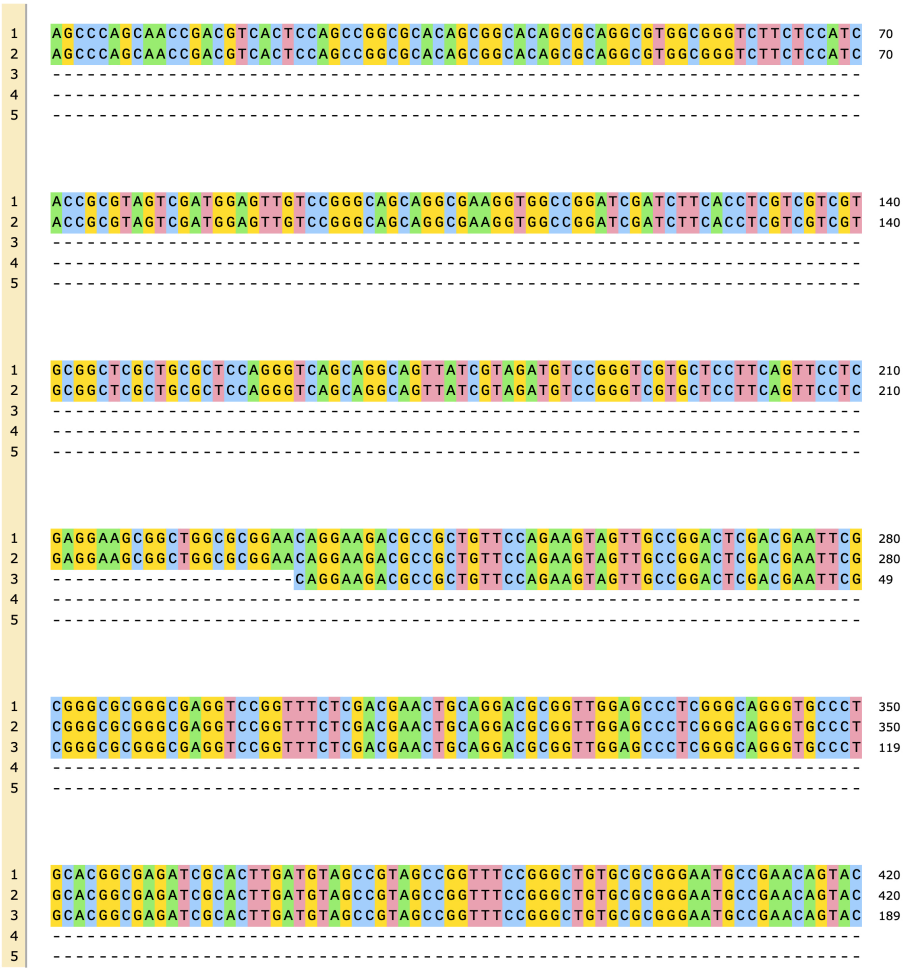

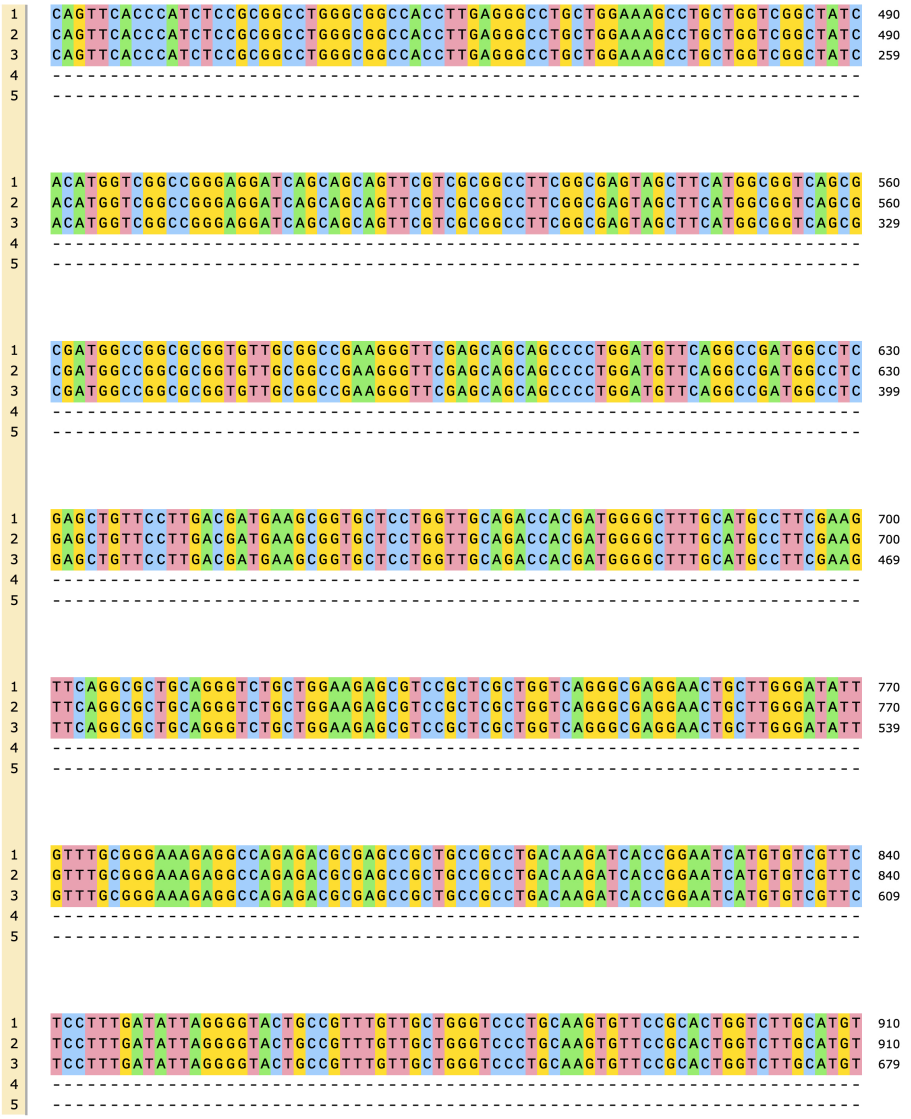
1 CAGTTCACCCATCTCCGCGGCCTGGGCGGCCACCTTGAGGGCCTGCTGGAAAGCCTGCTGGTCGGCTATC 490
2 CAGTTCACCCATCTCCGCGGCCTGGGCGGCCACCTTGAGGGCCTGCTGGAAAGCCTGCTGGTCGGCTATC 490
3 CAGTTCACCCATCTCCGCGGCCTGGGCGGCCACCTTGAGGGCCTGCTGGAAAGCCTGCTGGTCGGCTATC 259
4 ----------
5 ----------
1 ACATGGTCGGCCGGGAGGATCAGCAGCAGTTCGTCGCGGCCTTCGGCGAGTAGCTTCATGGCGGTCAGCG 560
2 ACATGGTCGGCCGGGAGGATCAGCAGCAGTTCGTCGCGGCCTTCGGCGAGTAGCTTCATGGCGGTCAGCG 560
3 ACATGGTCGGCCGGGAGGATCAGCAGCAGTTCGTCGCGGCCTTCGGCGAGTAGCTTCATGGCGGTCAGCG 329
4 ----------
5 ----------
1 CGATGGCCGGCGCGGTGTTGCGGCCGAAGGGTTCGAGCAGCAGCCCCTGGATGTTCAGGCCGATGGCCTC 630
2 CGATGGCCGGCGCGGTGTTGCGGCCGAAGGGTTCGAGCAGCAGCCCCTGGATGTTCAGGCCGATGGCCTC 630
3 CGATGGCCGGCGCGGTGTTGCGGCCGAAGGGTTCGAGCAGCAGCCCCTGGATGTTCAGGCCGATGGCCTC 399
4 ----------
5 ----------
1 GAGCTGTTCCTTGACGATGAAGCGGTGCTCCTGGTTGCAGACCACGATGGGGCTTTGCATGCCTTCGAAG 700
2 GAGCTGTTCCTTGACGATGAAGCGGTGCTCCTGGTTGCAGACCACGATGGGGCTTTGCATGCCTTCGAAG 700
3 GAGCTGTTCCTTGACGATGAAGCGGTGCTCCTGGTTGCAGACCACGATGGGGCTTTGCATGCCTTCGAAG 469
4 ----------
5 ----------
1 TTCAGGCGCTGCAGGGTCTGCTGGAAGAGCGTCCGCTCGCTGGTCAGGGCGAGGAACTGCTTGGGATATT 770
2 TTCAGGCGCTGCAGGGTCTGCTGGAAGAGCGTCCGCTCGCTGGTCAGGGCGAGGAACTGCTTGGGATATT 770
3 TTCAGGCGCTGCAGGGTCTGCTGGAAGAGCGTCCGCTCGCTGGTCAGGGCGAGGAACTGCTTGGGATATT 539
4 ----------
5 ----------
1 GTTTGCGGGAAAGAGGCCAGAGACGCGAGCCGCTGCCGCCTGACAAGATCACCGGAATCATGTGTCGTTC 840
2 GTTTGCGGGAAAGAGGCCAGAGACGCGAGCCGCTGCCGCCTGACAAGATCACCGGAATCATGTGTCGTTC 840
3 GTTTGCGGGAAAGAGGCCAGAGACGCGAGCCGCTGCCGCCTGACAAGATCACCGGAATCATGTGTCGTTC 609
4 ----------
5 ----------
1 TCCTTTGATATTAGGGGTACTGCCGTTTGTTGCTGGGTCCCTGCAAGTGTTCCGCACTGGTCTTGCATGT 910
2 TCCTTTGATATTAGGGGTACTGCCGTTTGTTGCTGGGTCCCTGCAAGTGTTCCGCACTGGTCTTGCATGT 910
3 TCCTTTGATATTAGGGGTACTGCCGTTTGTTGCTGGGTCCCTGCAAGTGTTCCGCACTGGTCTTGCATGT 679
4 ----------
5 ----------

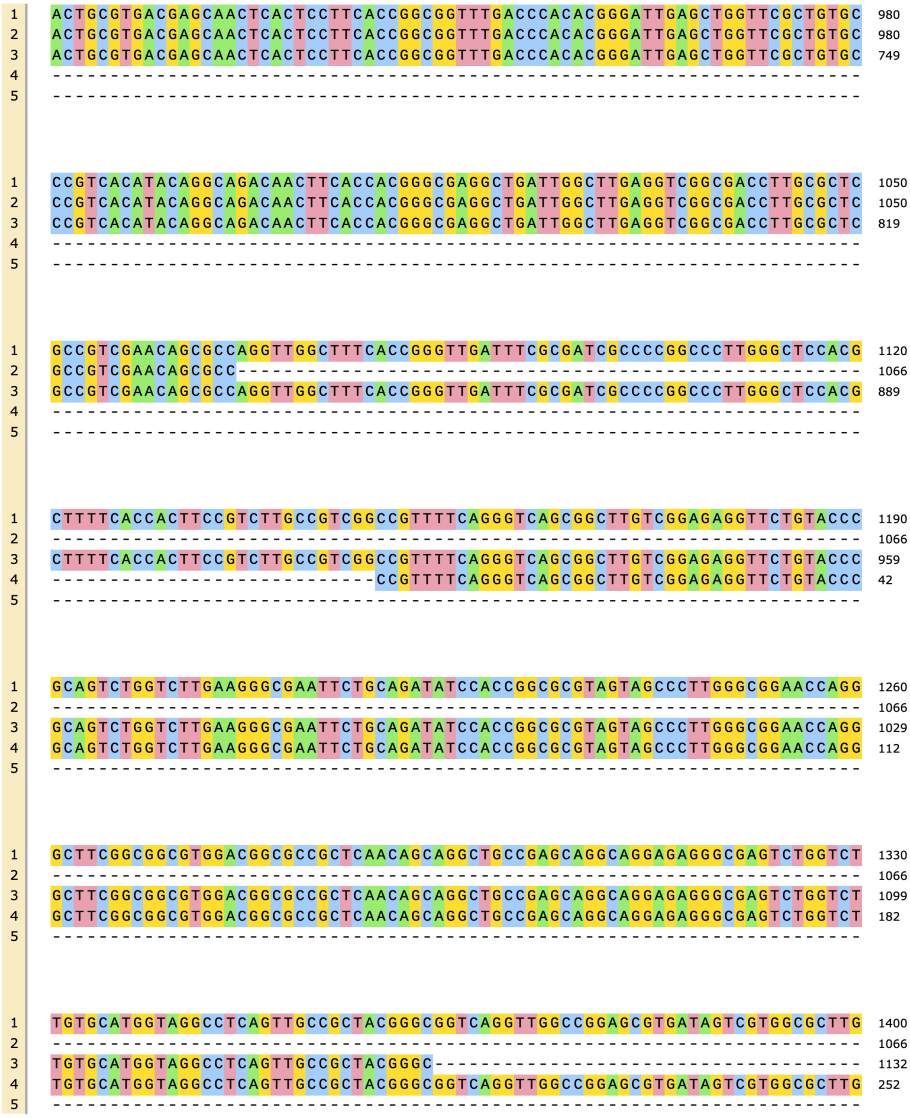
1 ACTGCGTGACGAGCAACTCACTCCTTCACCGGCGGTTTGACCCACACGGGATTGAGCTGGTTCGCTGTGC 980
2 ACTGCGTGACGAGCAACTCACTCCTTCACCGGCGGTTTGACCCACACGGGATTGAGCTGGTTCGCTGTGC 980
3 ACTGCGTGACGAGCAACTCACTCCTTCACCGGCGGTTTGACCCACACGGGATTGAGCTGGTTCGCTGTGC 749
4 ----------
5 ----------
1 CCGTCACATACAGGCAGACAACTTCACCACGGGCGAGGCTGATTGGCTTGAGGTCGGCGACCTTGCGCTC 1050
2 CCGTCACATACAGGCAGACAACTTCACCACGGGCGAGGCTGATTGGCTTGAGGTCGGCGACCTTGCGCTC 1050
3 CCGTCACATACAGGCAGACAACTTCACCACGGGCGAGGCTGATTGGCTTGAGGTCGGCGACCTTGCGCTC 819
4 ----------
5 ----------
1 GCCGTCGAACAGCGCCAGGTTGGCTTTCACCGGGTTGATTTCGCGATCGCCCCGGCCCTTGGGCTCCACG 1120
2 GCCGTCGAACAGCGCC---------- 1066
3 GCCGTCGAACAGCGCCAGGTTGGCTTTCACCGGGTTGATTTCGCGATCGCCCCGGCCCTTGGGCTCCACG 889
4 ----------
5 ----------
1 CTTTTCACCACTTCCGTCTTGCCGTCGGCCGTTTTCAGGGTCAGCGGCTTGTCGGAGAGGTTCTGTACCC 1190
2 ---------- 1066
3 CTTTTCACCACTTCCGTCTTGCCGTCGGCCGTTTTCAGGGTCAGCGGCTTGTCGGAGAGGTTCTGTACCC 959
4 ----------CCGTTTTCAGGGTCAGCGGCTTGTCGGAGAGGTTCTGTACCC 42
5 ----------
1 GCAGTCTGGTCTTGAAGGGCGAATTCTGCAGATATCCACCGGCGCGTAGTAGCCCTTGGGCGGAACCAGG 1260
2 ---------- 1066
3 GCAGTCTGGTCTTGAAGGGCGAATTCTGCAGATATCCACCGGCGCGTAGTAGCCCTTGGGCGGAACCAGG 1029
4 GCAGTCTGGTCTTGAAGGGCGAATTCTGCAGATATCCACCGGCGCGTAGTAGCCCTTGGGCGGAACCAGG 112
5 ----------
1 GCTTCGGCGGCGTGGACGGCGCCGCTCAACAGCAGGCTGCCGAGCAGGCAGGAGAGGGCGAGTCTGGTCT 1330
2 ---------- 1066
3 GCTTCGGCGGCGTGGACGGCGCCGCTCAACAGCAGGCTGCCGAGCAGGCAGGAGAGGGCGAGTCTGGTCT 1099
4 GCTTCGGCGGCGTGGACGGCGCCGCTCAACAGCAGGCTGCCGAGCAGGCAGGAGAGGGCGAGTCTGGTCT 182
5 ----------
1 TGTGCATGGTAGGCCTCAGTTGCCGCTACGGGCGGTCAGGTTGGCCGGAGCGTGATAGTCGTGGCGCTTG 1400
2 ---------- 1066
3 TGTGCATGGTAGGCCTCAGTTGCCGCTACGGGC---------- 1132
4 TGTGCATGGTAGGCCTCAGTTGCCGCTACGGGCGGTCAGGTTGGCCGGAGCGTGATAGTCGTGGCGCTTG 252
5 ----------

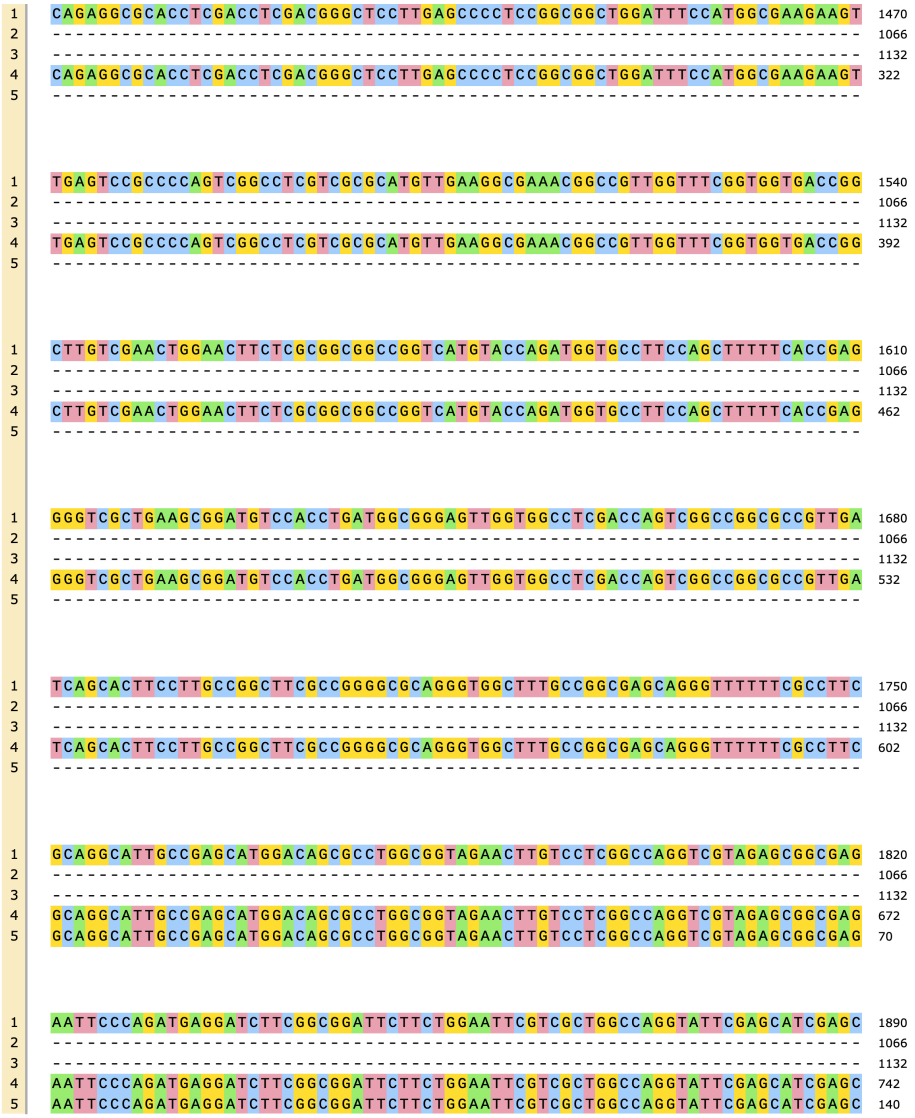
1 CAGAGGCGCACCTCGACCTCGACGGGCTCCTTGAGCCCCTCCGGCGGCTGGATTTCCATGGCGAAGAAGT 1470
2 ---------- 1066
3 ---------- 1132
4 CAGAGGCGCACCTCGACCTCGACGGGCTCCTTGAGCCCCTCCGGCGGCTGGATTTCCATGGCGAAGAAGT 322
5 ----------
1 TGAGTCCGCCCCAGTCGGCCTCGTCGCGCATGTTGAAGGCGAAACGGCCGTTGGTTTCGGTGGTGACCGG 1540
2 ---------- 1066
3 ---------- 1132
4 TGAGTCCGCCCCAGTCGGCCTCGTCGCGCATGTTGAAGGCGAAACGGCCGTTGGTTTCGGTGGTGACCGG 392
5 ----------
1 CTTGTCGAACTGGAACTTCTCGCGGCGGCCGGTCATGTACCAGATGGTGCCTTCCAGCTTTTTCACCGAG 1610
2 ---------- 1066
3 ---------- 1132
4 CTTGTCGAACTGGAACTTCTCGCGGCGGCCGGTCATGTACCAGATGGTGCCTTCCAGCTTTTTCACCGAG 462
5 ----------
1 GGGTCGCTGAAGCGGATGTCCACCTGATGGCGGGAGTTGGTGGCCTCGACCAGTCGGCCGGCGCCGTTGA 1680
2 ---------- 1066
3 ---------- 1132
4 GGGTCGCTGAAGCGGATGTCCACCTGATGGCGGGAGTTGGTGGCCTCGACCAGTCGGCCGGCGCCGTTGA 532
5 ----------
1 TCAGCACTTCCTTGCCGGCTTCGCCGGGGCGCAGGGTGGCTTTGCCGGCGAGCAGGGTTTTTTCGCCTTC 1750
2 ---------- 1066
3 ---------- 1132
4 TCAGCACTTCCTTGCCGGCTTCGCCGGGGCGCAGGGTGGCTTTGCCGGCGAGCAGGGTTTTTTCGCCTTC 602
5 ----------
1 GCAGGCATTGCCGAGCATGGACAGCGCCTGGCGGTAGAACTTGTCCTCGGCCAGGTCGTAGAGCGGCGAG 1820
2 ---------- 1066
3 ---------- 1132
4 GCAGGCATTGCCGAGCATGGACAGCGCCTGGCGGTAGAACTTGTCCTCGGCCAGGTCGTAGAGCGGCGAG 672
5 GCAGGCATTGCCGAGCATGGACAGCGCCTGGCGGTAGAACTTGTCCTCGGCCAGGTCGTAGAGCGGCGAG 70
1 AATTCCCAGATGAGGATCTTCGGCGGATTCTTCTGGAATTCGTCGCTGGCCAGGTATTCGAGCATCGAGC 1890
2 ---------- 1066
3 ---------- 1132
4 AATTCCCAGATGAGGATCTTCGGCGGATTCTTCTGGAATTCGTCGCTGGCCAGGTATTCGAGCATCGAGC 742
5 AATTCCCAGATGAGGATCTTCGGCGGATTCTTCTGGAATTCGTCGCTGGCCAGGTATTCGAGCATCGAGC 140

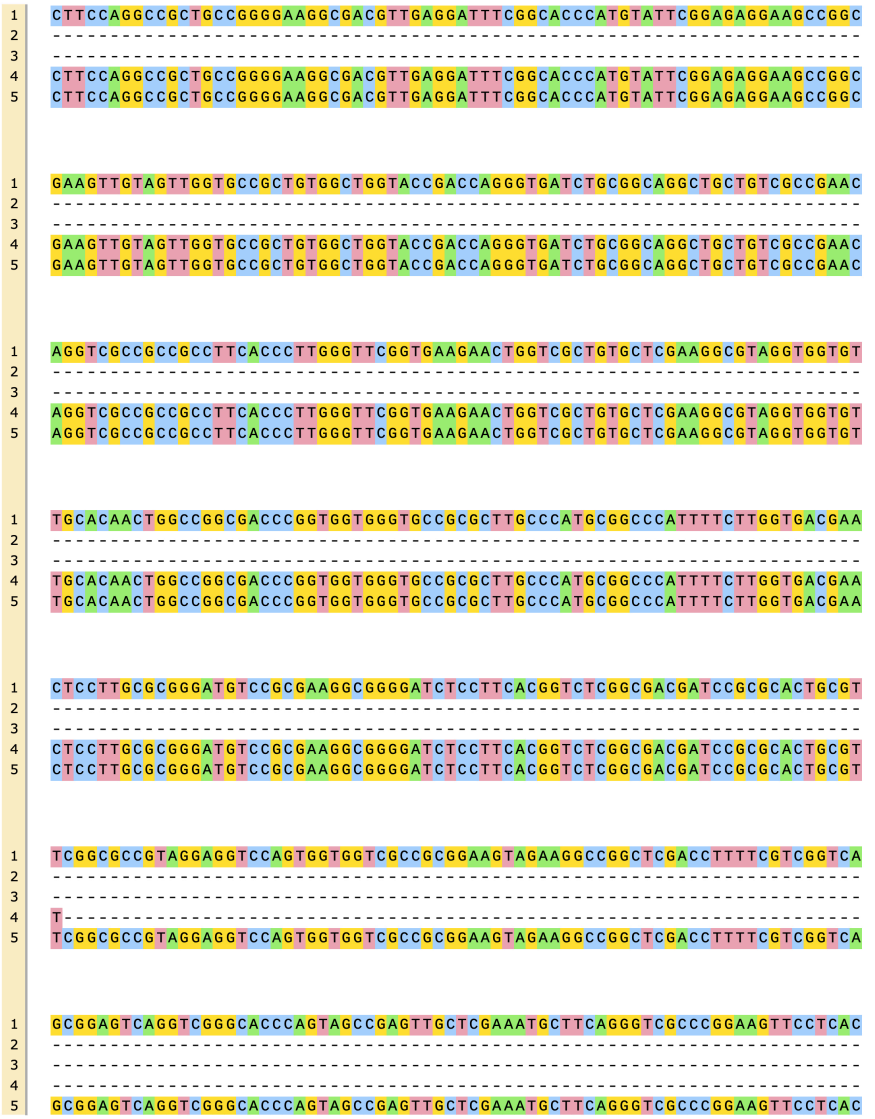
1 CTTCCAGGCCGCTGCCGGGGAAGGCGACGTTGAGGATTTCGGCACCCATGTATTCGGAGAGGAAGCCGGC 1960
2 ---------- 1066
3 ---------- 1132
4 CTTCCAGGCCGCTGCCGGGGAAGGCGACGTTGAGGATTTCGGCACCCATGTATTCGGAGAGGAAGCCGGC 812
5 CTTCCAGGCCGCTGCCGGGGAAGGCGACGTTGAGGATTTCGGCACCCATGTATTCGGAGAGGAAGCCGGC 210
1 GAAGTTGTAGTTGGTGCCGCTGTGGCTGGTACCGACCAGGGTGATCTGCGGCAGGCTGCTGTCGCCGAAC 2030
2 ---------- 1066
3 ---------- 1132
4 GAAGTTGTAGTTGGTGCCGCTGTGGCTGGTACCGACCAGGGTGATCTGCGGCAGGCTGCTGTCGCCGAAC 882
5 GAAGTTGTAGTTGGTGCCGCTGTGGCTGGTACCGACCAGGGTGATCTGCGGCAGGCTGCTGTCGCCGAAC 280
1 AGGTCGCCGCCGCCTTCACCCTTGGGTTCGGTGAAGAACTGGTCGCTGTGCTCGAAGGCGTAGGTGGTGT 2100
2 ---------- 1066
3 ---------- 1132
4 AGGTCGCCGCCGCCTTCACCCTTGGGTTCGGTGAAGAACTGGTCGCTGTGCTCGAAGGCGTAGGTGGTGT 952
5 AGGTCGCCGCCGCCTTCACCCTTGGGTTCGGTGAAGAACTGGTCGCTGTGCTCGAAGGCGTAGGTGGTGT 350
1 TGCACAACTGGCCGGCGACCCGGTGGTGGGTGCCGCGCTTGCCCATGCGGCCCATTTTCTTGGTGACGAA 2170
2 ---------- 1066
3 ---------- 1132
4 TGCACAACTGGCCGGCGACCCGGTGGTGGGTGCCGCGCTTGCCCATGCGGCCCATTTTCTTGGTGACGAA 1022
5 TGCACAACTGGCCGGCGACCCGGTGGTGGGTGCCGCGCTTGCCCATGCGGCCCATTTTCTTGGTGACGAA 420
1 CTCCTTGCGCGGGATGTCCGCGAAGGCGGGGATCTCCTTCACGGTCTCGGCGACGATCCGCGCACTGCGT 2240
2 ---------- 1066
3 ---------- 1132
4 CTCCTTGCGCGGGATGTCCGCGAAGGCGGGGATCTCCTTCACGGTCTCGGCGACGATCCGCGCACTGCGT 1092
5 CTCCTTGCGCGGGATGTCCGCGAAGGCGGGGATCTCCTTCACGGTCTCGGCGACGATCCGCGCACTGCGT 490
1 TCGGCGCCGTAGGAGGTCCAGTGGTGGTCGCCGCGGAAGTAGAAGGCCGGCTCGACCTTTTCGTCGGTCA 2310
2 ---------- 1066
3 ---------- 1132
4 T--------- 1093
5 TCGGCGCCGTAGGAGGTCCAGTGGTGGTCGCCGCGGAAGTAGAAGGCCGGCTCGACCTTTTCGTCGGTCA 560
1 GCGGAGTCAGGTCGGGCACCCAGTAGCCGAGTTGCTCGAAATGCTTCAGGGTCGCCCGGAAGTTCCTCAC 2380
2 ---------- 1066
3 ---------- 1132
4 ---------- 1093
5 GCGGAGTCAGGTCGGGCACCCAGTAGCCGAGTTGCTCGAAATGCTTCAGGGTCGCCCGGAAGTTCCTCAC 630

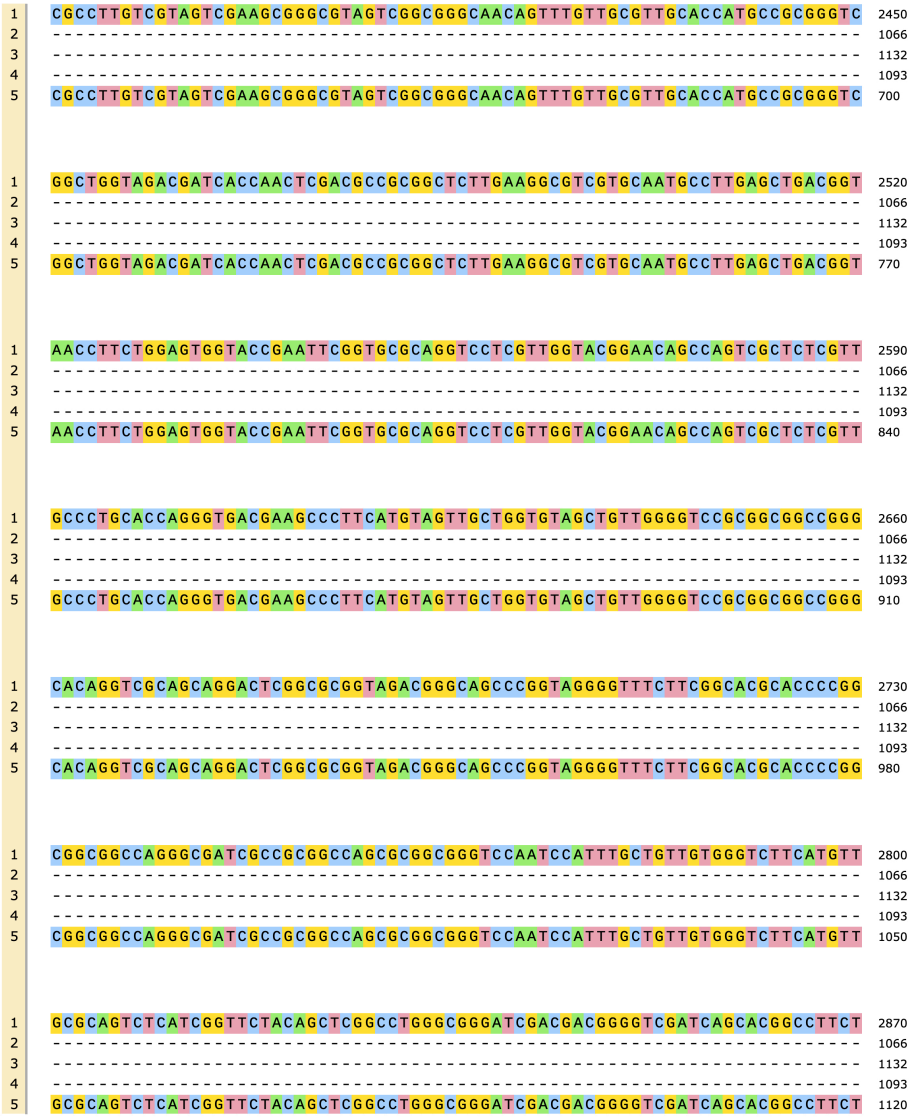
1 CGCCTTGTCGTAGTCGAAGCGGGCGTAGTCGGCGGGCAACAGTTTGTTGCGTTGCACCATGCCGCGGGTC 2450
2 ---------- 1066
3 ---------- 1132
4 ---------- 1093
5 CGCCTTGTCGTAGTCGAAGCGGGCGTAGTCGGCGGGCAACAGTTTGTTGCGTTGCACCATGCCGCGGGTC 700
1 GGCTGGTAGACGATCACCAACTCGACGCCGCGGCTCTTGAAGGCGTCGTGCAATGCCTTGAGCTGACGGT 2520
2 ---------- 1066
3 ---------- 1132
4 ---------- 1093
5 GGCTGGTAGACGATCACCAACTCGACGCCGCGGCTCTTGAAGGCGTCGTGCAATGCCTTGAGCTGACGGT 770
1 AACCTTCTGGAGTGGTACCGAATTCGGTGCGCAGGTCCTCGTTGGTACGGAACAGCCAGTCGCTCTCGTT 2590
2 ---------- 1066
3 ---------- 1132
4 ---------- 1093
5 AACCTTCTGGAGTGGTACCGAATTCGGTGCGCAGGTCCTCGTTGGTACGGAACAGCCAGTCGCTCTCGTT 840
1 GCCCTGCACCAGGGTGACGAAGCCCTTCATGTAGTTGCTGGTGTAGCTGTTGGGGTCCGCGGCGGCCGGG 2660
2 ---------- 1066
3 ---------- 1132
4 ---------- 1093
5 GCCCTGCACCAGGGTGACGAAGCCCTTCATGTAGTTGCTGGTGTAGCTGTTGGGGTCCGCGGCGGCCGGG 910
1 CACAGGTCGCAGCAGGACTCGGCGCGGTAGACGGGCAGCCCGGTAGGGGTTTCTTCGGCACGCACCCCGG 2730
2 ---------- 1066
3 ---------- 1132
4 ---------- 1093
5 CACAGGTCGCAGCAGGACTCGGCGCGGTAGACGGGCAGCCCGGTAGGGGTTTCTTCGGCACGCACCCCGG 980
1 CGGCGGCCAGGGCGATCGCCGCGGCCAGCGCGGCGGGTCCAATCCATTTGCTGTTGTGGGTCTTCATGTT 2800
2 ---------- 1066
3 ---------- 1132
4 ---------- 1093
5 CGGCGGCCAGGGCGATCGCCGCGGCCAGCGCGGCGGGTCCAATCCATTTGCTGTTGTGGGTCTTCATGTT 1050
1 GCGCAGTCTCATCGGTTCTACAGCTCGGCCTGGGCGGGATCGACGACGGGGTCGATCAGCACGGCCTTCT 2870
2 ---------- 1066
3 ---------- 1132
4 ---------- 1093
5 GCGCAGTCTCATCGGTTCTACAGCTCGGCCTGGGCGGGATCGACGACGGGGTCGATCAGCACGGCCTTCT 1120
1 GGCGGCGCACCAGCAGATCGAGGATCTCTTCTTGTTTGTCCTC 2913
2 ---------- 1066
3 ---------- 1132
4 ---------- 1093
5 GGCGGCGCACCAGCAGATCGAGGATCTCTTCTTGTTTGTCCTC 1163

K Alginate assay data for an *algF, mucA* double mutant

An alginate assay was performed to measure alginate production in an *A. vinelandii algF, mucA* double mutant and compare to the alginate production of wild type and an *algF* mutant. Data for standards, the standard curve and data for mutants are presented in table K.1, figure K.1 and table K.2, respectively.

Table K.1: A_{230} before and after addition of lyases for three parallels of known alginate concentration and the calculated increase in A_{230}.

Alginate concentration (g/l)		**A_{230} before lyases**	Corrected for blank	Corrected for dilution	**A_{230} after lyases**	Corrected for blank and lyases	Corrected for dilution	**Increase in A_{230}**	**Mean ± SD**
Blank	I	0.192							
	II	0.205							0.200
	III	0.203							
0.0	I				0.590				
	II				0.539				0.548
	III				0.514				
0.1	I	0.200	0.000 345	0.001 04	0.803	0.255	0.819	0.818	
	II	0.197	−0.003 36	−0.0101	0.784	0.237	0.761	0.771	0.768 ± 0.0517
	III	0.215	0.0153	0.0458	0.784	0.237	0.761	0.715	
0.2	I	0.202	0.001 65	0.004 95	0.971	0.423	1.36	1.36	
	II	0.198	−0.002 45	−0.007 36	0.962	0.415	1.33	1.34	1.33 ± 0.0245
	III	0.223	0.0234	0.0702	0.976	0.429	1.38	1.31	
0.3	I	0.229	0.0293	0.0878	1.30	0.757	2.43	2.34	
	II	0.241	0.0407	0.122	1.27	0.718	2.31	2.19	2.25 ± 0.0845
	III	0.245	0.0450	0.135	1.28	0.731	2.35	2.21	
0.4	I	0.245	0.0450	0.135	1.50	0.955	3.07	2.93	
	II	0.238	0.0383	0.115	1.47	0.923	2.97	2.85	2.90 ± 0.0422
	III	0.239	0.0392	0.118	1.49	0.942	3.03	2.91	
0.5	I	0.239	0.0386	0.116	1.74	1.19	3.82	3.70	
	II	0.238	0.0380	0.114	1.67	1.13	3.62	3.50	3.55 ± 0.137
	III	0.240	0.0397	0.119	1.65	1.11	3.55	3.44	

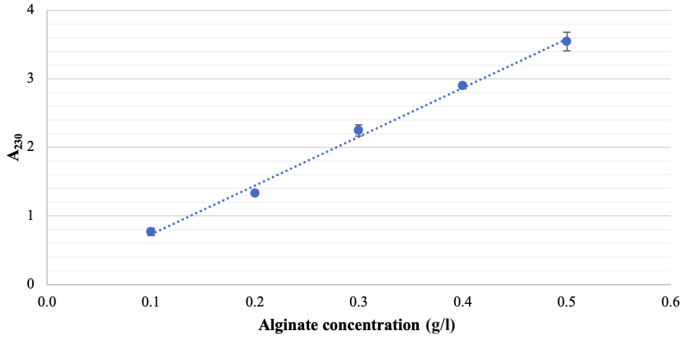

Figure K.1: The standard curve showing mean A_{230} values ± SD as a function of alginate concentration. A linear trendline produced the equation y = 7.1212x + 0.0225 and an R^2 of 0.9953

Table K.2: OD_{600} and A_{230} before and after addition of lyases for three parallels of *A. vinelandii* wild type and mutants. The calculated increase in A_{230} was used to determine alginate concentration (g/l) and alginate concentration (g/l) per OD_{600}. * means the measurement was omitted due to contamination.

			OD_{600}	**A_{230} before lyases**	Corrected for blank	Corrected for dilution	**A_{230} after lyases**	Corrected for blank and lyases	Corrected for dilution	**Increase in A_{230}**	Alginate concentration (g/l)	**Mean ± SD**	Alginate concentration (g/l) per OD_{600}	**Mean ± SD**
		I		1.25	1.05	13.1	2.01	1.46	19.4	6.37	0.892		0.150	
	24 h	II	5.93	1.25	1.05	13.0	1.98	1.44	19.1	6.09	0.852	0.898 ± 0.0486	0.144	0.151 ± 0.00819
Wild type		III		1.25	1.05	13.1	2.04	1.49	19.8	6.78	0.949		0.160	
I		I		1.25	1.05	13.0	2.41	1.86	24.7	11.8	1.65		0.183	
	48 h	II	9.00	1.22	1.02	12.7	2.37	1.82	24.2	11.5	1.62	1.66 ± 0.0565	0.179	0.185 ± 0.00628
		III		1.23	1.03	12.8	2.44	1.89	25.1	12.3	1.73		0.192	
		I		0.957	0.757	9.38	1.66	1.11	14.7	5.35	0.748		0.134	
	24 h	II	5.58	0.988	0.788	9.77	1.68	1.13	15.1	5.29	0.740	0.729 ± 0.0261	0.133	0.131 ± 0.00468
Wild type		III		0.950	0.750	9.30	1.62	1.08	14.3	5.00	0.699		0.125	
II		I		1.24	1.04	12.9	2.36	1.81	24.0	11.2	1.56		0.144	
	48 h	II	10.9	1.23	1.03	12.7	2.35	1.80	23.9	11.2	1.57	1.53 ± 0.0689	0.144	0.140 ± 0.00632
		III		1.23	1.03	12.7	2.28	1.74	23.0	10.3	1.45		0.133	
		I		0.975	0.775	9.61	1.57	1.02	13.5	3.91	0.546		0.102	
	24 h	II	5.36	0.932	0.732	9.08	1.51	0.960	12.8	3.67	0.512	0.490 ± 0.0694	0.0956	0.0915 ± 0.0129
Wild type		III		0.931	0.731	9.06	1.45	0.905	12.0	2.96	0.412		0.0770	
III		I		1.27	1.07	13.3	2.45	1.90	25.2	11.9	1.67		0.214	
	48 h	II	7.80	1.28	1.08	13.4	2.27	1.73	22.9	9.52	1.33	1.42 ± 0.216	0.171	0.182 ± 0.0277
		III		1.25	1.05	13.0	2.20	1.66	22.0	9.00	1.26		0.162	
		I		0.928	0.728	9.03	1.55	0.998	13.3	4.23	0.591		0.128	
	24 h	II	4.61	0.909	0.709	8.79	1.49	0.943	12.5	3.73	0.520	0.501 ± 0.101	0.113	0.109 ± 0.0219
algF		III		0.954	0.754	9.35	1.46	0.916	12.2	2.81	0.392		0.0849	
I		I		1.27	1.07	13.3	2.65	2.11	28.0	14.7	2.06		0.125	
	48 h	II	16.4	1.24	1.04	12.9	2.58	2.03	27.0	14.1	1.98	2.02 ± 0.0410	0.120	0.123 ± 0.00250
		III		1.25	1.05	13.0	2.61	2.06	27.4	14.4	2.02		0.123	
		I		0.941	0.741	9.19	1.66	1.12	14.8	5.63	0.788		0.139	
	24 h	II	5.66	1.03	0.834	10.3	1.70	1.15	15.3	4.91	0.686	0.724 ± 0.0558*	0.121	0.128 ± 0.00985*
algF		III		1.07	0.868	10.8	1.73	1.19	15.7	4.99	0.697		0.123	
II		I		0.238	0.0381	0.473	0.595	0.0474	0.630	0.157	0.0189		0.001 49	
	48 h	II	12.7	0.240	0.0395	0.490	0.552	0.004 37	0.0580	−0.432	−0.0638	-0.0187 ± 0.0419*	−0.005 02	-0.00147 ± 0.00330*
		III		0.235	0.0348	0.431	0.576	0.0282	0.374	−0.0569	−0.0111		−0.000 877	
		I		0.937	0.737	9.14	1.63	1.09	14.4	5.28	0.738		0.150	
	24 h	II	4.91	0.926	0.726	9.00	1.58	1.03	13.7	4.66	0.651	0.683 ± 0.0473	0.133	0.139 ± 0.00964
algF		III		0.923	0.723	8.96	1.58	1.03	13.7	4.73	0.662		0.135	
III		I		1.24	1.04	12.9	2.58	2.03	27.0	14.0	1.97		0.179	
	48 h	II	11.0	1.23	1.03	12.8	2.56	2.01	26.7	13.9	1.96	1.92 ± 0.0664	0.178	0.175 ± 0.00604
		III		1.22	1.02	12.7	2.49	1.95	25.8	13.2	1.85		0.168	

			OD_{600}	**A_{230} before lyases**	Corrected for blank	Corrected for dilution	**A_{230} after lyases**	Corrected for blank and lyases	Corrected for dilution	**Increase in A_{230}**	Alginate concentration (g/l)	**Mean ± SD**	Alginate concentration (g/l) per OD_{600}	**Mean ± SD**
		I		0.875	0.675	8.37	1.35	0.799	10.6	2.24	0.312		0.0429	
	24 h	II	7.28	0.881	0.681	8.44	1.23	0.687	9.12	0.681	0.0925	0.165 ± 0.127	0.0127	0.0227 + 0.0175
algF, mucA		III		0.884	0.684	8.48	1.24	0.689	9.15	0.667	0.0905		0.0124	
I		I		0.860	0.660	8.19	1.24	0.691	9.17	0.988	0.136		0.0105	
	48 h	II	12.9	0.859	0.659	8.17	1.23	0.679	9.01	0.844	0.115	0.290 ± 0.286	0.008 94	0.0225 + 0.0222
		III		0.864	0.664	8.23	1.50	0.954	12.7	4.44	0.620		0.0481	
		I		1.50	1.30	16.1	1.92	1.37	18.2	2.14	0.297		0.0516	
	24 h	II	5.75	1.45	1.25	15.5	1.84	1.29	17.2	1.67	0.232	0.259 ± 0.0341	0.0403	0.0450 + 0.00593
algF, mucA		III		1.46	1.26	15.6	1.86	1.31	17.4	1.78	0.247		0.0430	
II		I		1.07	0.869	10.8	1.42	0.876	11.6	0.853	0.117		0.0110	
	48 h	II	10.6	1.07	0.866	10.7	1.43	0.885	11.8	1.02	0.140	0.132 ± 0.0130	0.0132	0.0124 + 0.00122
		III		1.06	0.861	10.7	1.43	0.879	11.7	1.01	0.139		0.0131	
		I		0.964	0.763	9.46	1.33	0.782	10.4	0.918	0.126		0.0189	
	24 h	II	6.66	0.961	0.761	9.43	1.31	0.766	10.2	0.742	0.101	0.108 ± 0.0159	0.0152	0.0162 + 0.00238
algF, mucA		III		0.960	0.760	9.42	1.31	0.762	10.1	0.707	0.0962		0.0144	
III		I		0.948	0.748	9.28	1.31	0.758	10.1	0.794	0.108		0.0102	
	48 h	II	10.6	0.952	0.752	9.32	1.31	0.758	10.1	0.741	0.101	0.119 ± 0.0247	0.0095	0.0112 + 0.00233
		III		0.951	0.751	9.31	1.33	0.781	10.4	1.07	0.147		0.0139	

L Alginate assay data for *algB* and *algW* mutants

An alginate assay was performed to measure alginate production in *A. vinelandii algB* and *algW* mutants and compare to the alginate production of complemented strains. The standard curve used to calculate alginate concentration is presented in appendix K. Alginate assay data are presented in table L.1.

Table L.1: OD_{600} and A_{230} before and after addition of lyases for three parallels of *A. vinelandii* mutants and complemented mutants. The calculated increase in A_{230} was used to determine alginate concentration (g/l) and alginate concentration (g/l) per OD_{600}.

			OD_{600}	**A_{230} before lyases**	Corrected for blank	Corrected for dilution	**A_{230} after lyases**	Corrected for blank and lyases	Corrected for dilution	**Increase**	Alginate concentration (g/l)	**Mean ± SD**	Alginate concentration (g/l) per OD_{600}	**Mean ± SD**
		I		0.926	0.726	9.00	1.59	1.04	13.9	4.87	0.680		0.0900	
	24 h	II	7.56	0.942	0.742	9.19	1.57	1.02	13.6	4.41	0.616	0.622 ± 0.0551	0.0815	0.0823 ± 0.00729
algB		III		0.930	0.730	9.04	1.54	0.989	13.1	4.08	0.570		0.0754	
I		I		1.06	0.864	10.7	1.92	1.38	18.3	7.57	1.06		0.128	
	48 h	II	8.30	1.05	0.852	10.6	1.86	1.31	17.4	6.83	0.955	1.01 ± 0.0520	0.115	0.121 ± 0.00626
		III		1.07	0.874	10.8	1.90	1.36	18.0	7.17	1.00		0.121	
		I		0.914	0.714	8.85	1.54	0.995	13.2	4.36	0.609		0.0762	
	24 h	II	8.00	0.931	0.731	9.06	1.54	0.997	13.2	4.18	0.584	0.587 ± 0.0212	0.0730	0.0733 ± 0.00266
algB		III		0.912	0.712	8.83	1.52	0.971	12.9	4.06	0.567		0.0709	
II		I		0.910	0.710	8.80	1.67	1.12	14.9	6.07	0.849		0.0913	
	48 h	II	9.30	0.889	0.689	8.54	1.64	1.09	14.5	5.94	0.831	0.857 ± 0.0319	0.0893	0.0922 ± 0.00344
		III		0.892	0.692	8.57	1.67	1.13	15.0	6.38	0.893		0.0960	
		I		0.958	0.758	9.39	1.58	1.03	13.7	4.31	0.602		0.0739	
	24 h	II	8.15	0.942	0.742	9.20	1.60	1.06	14.0	4.81	0.673	0.630 ± 0.0376	0.0825	0.0773 ± 0.00461
algB		III		0.939	0.739	9.16	1.57	1.02	13.6	4.41	0.616		0.0755	
III		I		0.665	0.465	5.76	1.27	0.726	9.64	3.88	0.541		0.0589	
	48 h	II	9.20	0.662	0.462	5.73	0.773	0.225	2.99	−2.75	−0.389	0.209 ± 0.519	−0.0423	0.0228 ± 0.0564
		III		0.668	0.468	5.80	1.24	0.693	9.21	3.41	0.475		0.0517	
		I		0.781	0.581	7.21	1.14	0.593	7.87	0.666	0.0903		0.0106	
	24 h	II	8.50	0.791	0.591	7.33	1.14	0.596	7.91	0.580	0.0782	0.0906 ± 0.0214	0.009 20	0.0107 ± 0.00146
algW		III		0.784	0.584	7.23	1.15	0.602	7.99	0.757	0.103		0.0121	
I		I		0.671	0.471	5.84	0.994	0.447	5.93	0.0953	0.0102		0.000 866	
	48 h	II	11.8	0.660	0.460	5.71	0.992	0.445	5.90	0.199	0.0248	0.192 ± 0.302	0.002 10	0.0162 ± 0.0256
		III		0.656	0.456	5.65	1.26	0.717	9.52	3.87	0.540		0.0457	
		I		0.817	0.617	7.65	1.35	0.806	10.7	3.05	0.425		0.0478	
	24 h	II	8.90	0.830	0.630	7.81	1.21	0.658	8.74	0.929	0.127	0.225 ± 0.173	0.0143	0.0253 ± 0.0194
algW		III		0.819	0.619	7.67	1.19	0.646	8.58	0.906	0.124		0.0139	
II		I		0.549	0.349	4.32	0.872	0.324	4.31	−0.0123	−0.004 88		−0.000 452	
	48 h	II	10.8	0.556	0.356	4.41	0.886	0.339	4.50	0.0876	0.009 14	0.00873 ± 0.0134	0.000 846	0.000808 ± 0.00124
		III		0.550	0.350	4.33	0.888	0.340	4.51	0.179	0.0219		0.002 03	
		I		0.797	0.597	7.40	1.19	0.642	8.53	1.13	0.156		0.0208	
	24 h	II	7.50	0.763	0.562	6.97	1.13	0.578	7.67	0.695	0.0945	0.0923 ± 0.0646	0.0126	0.0123 ± 0.00861
algW		III		0.759	0.559	6.93	1.09	0.538	7.14	0.212	0.0267		0.003 55	
III		I		0.623	0.423	5.24	0.933	0.385	5.12	−0.120	−0.0200		−0.001 88	
	48 h	II	10.7	0.615	0.415	5.14	0.961	0.413	5.48	0.338	0.0443	0.0186 ± 0.0341	0.004 16	0.00175 ± 0.00320
		III		0.596	0.396	4.91	0.936	0.388	5.15	0.248	0.0316		0.002 97	

			OD_{600}	**A_{230} before lyases**	Corrected for blank	Corrected for dilution	**A_{230} after lyases**	Corrected for blank and lyases	Corrected for dilution	**Increase**	Alginate concentration (g/l)	**Mean ± SD**	Alginate concentration (g/l) per OD_{600}	**Mean ± SD**
		I		2.45	2.25	27.8	2.88	2.34	31.0	3.19	0.445		0.605	
algB	24 h	II	0.735	2.45	2.25	27.9	3.03	2.48	32.9	5.01	0.700	0.547 ± 0.135	0.953	0.744 ± 0.184
complemented		III		2.43	2.23	27.6	2.90	2.35	31.2	3.56	0.496		0.675	
with pHE539		I		1.93	1.73	21.5	2.33	1.78	23.7	2.21	0.308		0.350	
I	48 h	II	0.880	1.93	1.73	21.4	2.43	1.89	25.1	3.64	0.508	0.390 ± 0.105	0.577	0.443 ± 0.119
		III		1.94	1.74	21.5	2.36	1.81	24.1	2.54	0.353		0.401	
		I		2.44	2.24	27.8	2.87	2.32	30.9	3.08	0.429		0.604	
algB	24 h	II	0.710	2.45	2.25	27.9	2.91	2.36	31.4	3.45	0.481	0.479 ± 0.0492	0.677	0.675 ± 0.0693
complemented		III		2.41	2.21	27.4	2.90	2.35	31.2	3.78	0.528		0.743	
with pHE539		I		2.34	2.14	26.6	2.76	2.21	29.4	2.79	0.389		0.435	
II	48 h	II	0.895	2.30	2.10	26.1	2.72	2.17	28.9	2.78	0.387	0.422 ± 0.0581	0.433	0.471 ± 0.0649
		III		2.33	2.13	26.4	2.80	2.25	29.9	3.50	0.489		0.546	
		I		2.47	2.27	28.1	3.03	2.48	32.9	4.87	0.680		0.901	
algB	24 h	II	0.755	2.46	2.26	28.1	2.98	2.43	32.3	4.19	0.585	0.637 ± 0.0479	0.775	0.843 ± 0.0635
complemented		III		2.45	2.25	27.9	3.00	2.45	32.5	4.62	0.645		0.854	
with pHE539		I		2.60	2.40	29.8	3.14	2.59	34.4	4.67	0.653		0.622	
III	48 h	II	1.05	2.65	2.45	30.4	3.09	2.55	33.8	3.43	0.478	0.540 ± 0.0979	0.456	0.515 ± 0.0932
		III		2.67	2.47	30.6	3.12	2.57	34.1	3.51	0.490		0.466	
		I		2.45	2.25	27.9	3.04	2.50	33.1	5.19	0.726		0.869	
algB	24 h	II	0.835	2.46	2.26	28.0	3.04	2.49	33.0	5.06	0.707	0.717 ± 0.00926	0.847	0.859 ± 0.0111
complemented		III		2.46	2.26	28.1	3.05	2.50	33.2	5.14	0.719		0.861	
with pIB11		I		2.28	2.08	25.8	2.68	2.13	28.3	2.46	0.342		0.285	
I	48 h	II	1.20	2.26	2.06	25.5	2.69	2.15	28.5	2.98	0.416	0.385 ± 0.0385	0.347	0.321 ± 0.0321
		III		2.26	2.06	25.5	2.69	2.14	28.4	2.85	0.397		0.331	
		I		1.80	1.60	19.8	2.28	1.73	23.0	3.19	0.445		0.556	
algB	24 h	II	0.800	1.75	1.55	19.2	2.24	1.70	22.5	3.28	0.458	0.430 ± 0.0367	0.572	0.538 ± 0.0459
complemented		III		1.75	1.55	19.2	2.21	1.66	22.0	2.79	0.389		0.486	
with pIB11		I		2.35	2.15	26.6	2.75	2.20	29.2	2.57	0.358		0.312	
II	48 h	II	1.15	2.24	2.04	25.3	2.64	2.10	27.8	2.52	0.351	0.361 ± 0.0121	0.305	0.314 ± 0.0105
		III		2.29	2.09	25.9	2.70	2.15	28.6	2.69	0.375		0.326	
		I		1.82	1.62	20.1	2.30	1.75	23.3	3.22	0.449		0.565	
algB	24 h	II	0.795	1.80	1.60	19.9	2.24	1.69	22.4	2.55	0.355	0.405 ± 0.0474	0.446	0.510 ± 0.0596
complemented		III		1.82	1.62	20.1	2.28	1.73	23.0	2.96	0.412		0.518	
with pIB11		I		1.79	1.59	19.7	2.21	1.66	22.1	2.33	0.324		0.268	
III	48 h	II	1.21	1.76	1.56	19.3	2.14	1.59	21.2	1.86	0.258	0.294 ± 0.0333	0.213	0.243 ± 0.0275
		III		1.74	1.54	19.1	2.15	1.60	21.3	2.15	0.298		0.247	

			OD_{600}	**A_{230} before lyases**	Corrected for blank	Corrected for dilution	**A_{230} after lyases**	Corrected for blank and lyases	Corrected for dilution	**Increase**	Alginate concentration (g/l)	**Mean ± SD**	Alginate concentration (g/l) per OD_{600}	**Mean ± SD**
		I		1.67	1.47	18.3	2.25	1.70	22.5	4.26	0.595		0.862	
algW	24 h	II	0.690	1.74	1.54	19.1	2.25	1.70	22.6	3.50	0.488	0.487 ± 0.108	0.707	0.706 ± 0.157
complemented		III		1.73	1.53	19.0	2.18	1.64	21.7	2.72	0.378		0.548	
with pHE536		I		2.34	2.14	26.5	2.84	2.30	30.5	3.96	0.553		0.485	
I	48 h	II	1.14	2.30	2.10	26.1	2.74	2.19	29.1	2.97	0.414	0.449 ± 0.0916	0.363	0.394 ± 0.0804
		III		2.28	2.08	25.7	2.69	2.14	28.5	2.73	0.380		0.333	
		I		1.88	1.68	20.9	2.33	1.78	23.7	2.81	0.392		0.552	
algW	24 h	II	0.710	1.91	1.71	21.2	2.40	1.85	24.6	3.33	0.465	0.420 ± 0.0394	0.655	0.591 ± 0.0555
complemented		III		1.91	1.71	21.2	2.36	1.81	24.1	2.89	0.403		0.567	
with pHE536		I		2.37	2.17	26.9	3.07	2.52	33.5	6.56	0.918		0.791	
II	48 h	II	1.16	2.34	2.14	26.6	2.80	2.25	29.9	3.30	0.460	0.581 ± 0.295	0.397	0.501 ± 0.254
		III		2.33	2.13	26.4	2.73	2.18	29.0	2.63	0.366		0.316	
		I		1.10	0.900	11.2	1.46	0.916	12.2	0.996	0.137		0.171	
algW	24 h	II	0.800	1.10	0.900	11.2	1.48	0.935	12.4	1.25	0.173	0.157 ± 0.0183	0.216	0.196 ± 0.0229
complemented		III		1.09	0.892	11.1	1.47	0.920	12.2	1.17	0.160		0.201	
with pHE536		I		2.04	1.84	22.8	2.55	2.00	26.5	3.68	0.514		0.447	
III	48 h	II	1.15	2.02	1.82	22.6	2.41	1.86	24.8	2.19	0.304	0.379 ± 0.117	0.264	0.330 ± 0.102
		III		2.06	1.86	23.0	2.46	1.91	25.3	2.29	0.319		0.277	
		I		1.77	1.57	19.4	2.20	1.65	22.0	2.51	0.350		0.432	
algW	24 h	II	0.810	1.75	1.55	19.2	2.18	1.63	21.7	2.49	0.346	0.361 ± 0.0230	0.427	0.446 ± 0.0284
complemented		III		1.77	1.57	19.5	2.23	1.68	22.3	2.78	0.388		0.479	
with pIB11		I		2.40	2.20	27.3	2.90	2.35	31.2	3.88	0.542		0.456	
I	48 h	II	1.19	2.39	2.19	27.2	2.88	2.33	30.9	3.76	0.524	0.516 ± 0.0319	0.441	0.433 ± 0.0268
		III		2.33	2.13	26.4	2.80	2.25	29.8	3.44	0.480		0.404	
		I		1.68	1.48	18.4	2.15	1.60	21.3	2.93	0.408		0.527	
algW	24 h	II	0.775	1.74	1.54	19.1	2.20	1.65	21.9	2.89	0.402	0.377 ± 0.0484	0.519	0.487 ± 0.0625
complemented		III		1.64	1.44	17.9	2.07	1.52	20.2	2.31	0.322		0.415	
with pIB11		I		2.47	2.27	28.1	2.93	2.39	31.7	3.62	0.505		0.424	
II	48 h	II	1.19	2.49	2.29	28.4	2.90	2.35	31.2	2.89	0.402	0.420 ± 0.0773	0.338	0.353 ± 0.0650
		III		2.51	2.31	28.7	2.90	2.35	31.2	2.54	0.354		0.297	
		I		2.33	2.13	26.5	2.81	2.26	30.1	3.61	0.504		0.650	
algW	24 h	II	0.775	2.35	2.15	26.6	2.83	2.28	30.3	3.69	0.515	0.495 ± 0.0254	0.664	0.639 ± 0.0327
complemented		III		2.34	2.14	26.5	2.79	2.25	29.8	3.34	0.466		0.602	
with pIB11		I		2.53	2.33	28.9	2.95	2.40	31.9	2.95	0.411		0.309	
III	48 h	II	1.33	2.53	2.33	28.9	2.94	2.39	31.7	2.79	0.389	0.398 ± 0.0112	0.293	0.299 ± 0.00842
		III		2.47	2.27	28.1	2.88	2.33	31.0	2.83	0.395		0.297	

			OD_{600}	A_{230} before lyases	Corrected for blank	Corrected for dilution	A_{230} after lyases	Corrected for blank and lyases	Corrected for dilution	Increase	Alginate concentration (g/l)	Mean ± SD	Alginate concentration (g/l) per OD_{600}	Mean ± SD
		I		2.46	2.26	28.0	2.93	2.38	31.6	3.57	0.498		0.668	
Wild type	24 h	II	0.745	2.57	2.37	29.4	3.05	2.50	33.2	3.87	0.540	0.512 ± 0.0240	0.725	0.687 ± 0.0322
complemented		III		2.51	2.31	28.7	2.97	2.43	32.2	3.57	0.499		0.669	
with pHE539		I		2.75	2.55	31.6	3.19	2.64	35.1	3.51	0.490		0.542	
I	48 h	II	0.905	2.72	2.52	31.2	3.15	2.60	34.6	3.32	0.463	0.485 ± 0.0200	0.512	0.536 ± 0.0221
		III		2.72	2.52	31.2	3.17	2.62	34.8	3.60	0.502		0.555	
		I		2.07	1.87	23.2	2.52	1.97	26.1	2.89	0.402		0.563	
Wild type	24 h	II	0.715	2.05	1.85	23.0	2.49	1.94	25.7	2.77	0.386	0.403 ± 0.0177	0.539	0.564 ± 0.0247
complemented		III		2.07	1.87	23.1	2.52	1.97	26.1	3.02	0.421		0.589	
with pHE539		I		2.55	2.35	29.2	3.00	2.45	32.6	3.38	0.472		0.569	
II	48 h	II	0.830	2.59	2.39	29.7	3.04	2.49	33.1	3.44	0.480	0.541 ± 0.112	0.578	0.651 ± 0.135
		III		2.62	2.42	29.9	3.16	2.62	34.7	4.79	0.669		0.807	
		I		2.11	1.91	23.7	2.65	2.11	28.0	4.23	0.590		0.803	
Wild type	24 h	II	0.735	2.11	1.91	23.7	2.56	2.02	26.8	3.11	0.434	0.498 ± 0.0818	0.590	0.678 ± 0.111
complemented		III		2.14	1.94	24.0	2.61	2.06	27.4	3.37	0.470		0.640	
with pHE539		I		2.35	2.15	26.7	2.84	2.30	30.5	3.84	0.536		0.602	
III	48 h	II	0.890	2.38	2.18	27.0	2.83	2.28	30.3	3.31	0.461	0.465 ± 0.0685	0.518	0.523 ± 0.0770
		III		2.39	2.19	27.2	2.81	2.26	30.0	2.86	0.399		0.448	
		I		2.16	1.96	24.3	2.63	2.09	27.7	3.39	0.473		0.591	
Wild type	24 h	II	0.800	2.14	1.94	24.1	2.57	2.03	26.9	2.79	0.389	0.410 ± 0.0554	0.486	0.513 ± 0.0693
complemented		III		2.14	1.94	24.1	2.56	2.01	26.7	2.65	0.368		0.460	
with pHE536		I		2.16	1.96	24.2	2.58	2.03	26.9	2.71	0.377		0.401	
I	48 h	II	0.940	2.10	1.90	23.6	2.50	1.95	25.9	2.27	0.316	0.341 ± 0.0320	0.336	0.363 ± 0.0340
		III		2.16	1.96	24.3	2.56	2.01	26.7	2.38	0.331		0.352	
		I		1.95	1.75	21.7	2.36	1.81	24.1	2.37	0.330		0.393	
Wild type	24 h	II	0.840	1.97	1.77	21.9	2.39	1.85	24.5	2.61	0.363	0.359 ± 0.0274	0.432	0.427 ± 0.0326
complemented		III		1.97	1.77	22.0	2.41	1.86	24.7	2.76	0.384		0.457	
with pHE536		I		1.89	1.69	21.0	2.27	1.72	22.9	1.94	0.269		0.244	
II	48 h	II	1.10	1.93	1.73	21.5	2.30	1.76	23.3	1.83	0.254	0.244 ± 0.0301	0.231	0.222 ± 0.0274
		III		1.92	1.72	21.3	2.27	1.72	22.9	1.52	0.211		0.191	
		I		1.96	1.76	21.8	2.38	1.83	24.3	2.49	0.346		0.407	
Wild type	24 h	II	0.850	1.92	1.72	21.4	2.33	1.78	23.7	2.30	0.319	0.345 ± 0.0258	0.376	0.406 ± 0.0304
complemented		III		1.91	1.71	21.2	2.34	1.80	23.8	2.66	0.371		0.437	
with pHE536		I		2.29	2.09	25.9	2.66	2.11	28.1	2.19	0.304		0.325	
III	48 h	II	0.935	2.31	2.11	26.1	2.73	2.18	29.0	2.85	0.397	0.357 ± 0.0478	0.424	0.382 ± 0.0511
		III		2.27	2.07	25.6	2.68	2.13	28.3	2.66	0.370		0.396	

			OD_{600}	**A_{230} before lyases**	Corrected for blank	Corrected for dilution	**A_{230} after lyases**	Corrected for blank and lyases	Corrected for dilution	**Increase**	Alginate concentration (g/l)	**Mean ± SD**	Alginate concentration (g/l) per OD_{600}	**Mean ± SD**
Wild type complemented with pIB11	24 h	I	0.770	2.11	1.91	23.6	2.59	2.05	27.2	3.54	0.493	0.462 ± 0.0276	0.641	0.600 ± 0.0359
		II		2.11	1.91	23.6	2.56	2.02	26.8	3.16	0.441		0.573	
		III		2.19	1.99	24.7	2.65	2.10	27.9	3.24	0.452		0.587	
	48 h	I	0.955	2.51	2.31	28.6	3.05	2.51	33.3	4.71	0.658	0.556 ± 0.0896	0.689	0.582 ± 0.0938
		II		2.50	2.30	28.5	2.98	2.43	32.2	3.74	0.521		0.546	
		III		2.53	2.33	28.8	2.98	2.44	32.3	3.51	0.489		0.512	
Wild type complemented with pIB11 II	24 h	I	0.825	1.86	1.66	20.6	2.28	1.74	23.0	2.41	0.335	0.317 ± 0.0161	0.407	0.384 ± 0.0196
		II		1.82	1.62	20.1	2.23	1.68	22.3	2.24	0.311		0.378	
		III		1.84	1.64	20.4	2.25	1.70	22.6	2.19	0.305		0.369	
	48 h	I	1.05	2.29	2.09	25.9	2.72	2.17	28.8	2.89	0.403	0.418 ± 0.0157	0.384	0.398 ± 0.0150
		II		2.41	2.21	27.4	2.85	2.30	30.5	3.11	0.434		0.413	
		III		2.36	2.16	26.8	2.79	2.24	29.8	2.98	0.416		0.396	
Wild type complemented with pIB11 III	24 h	I	0.860	2.43	2.23	27.6	2.86	2.31	30.7	3.07	0.428	0.485 ± 0.0508	0.497	0.563 ± 0.0591
		II		2.49	2.29	28.4	2.97	2.43	32.2	3.76	0.525		0.611	
		III		2.41	2.21	27.5	2.89	2.34	31.0	3.59	0.501		0.582	
	48 h	I	0.995	2.68	2.48	30.7	3.17	2.63	34.9	4.13	0.577	0.536 ± 0.0393	0.577	0.536 ± 0.0393
		II		2.66	2.46	30.5	3.13	2.58	34.3	3.81	0.532		0.532	
		III		2.59	2.39	29.6	3.04	2.50	33.1	3.57	0.499		0.499	

M Alginate assay data for *algL* and *algLH199R* mutants

An alginate assay was performed to verify alginate production in *A. vinelandii* mutants with *algL* and *algLH199R* controlled by P*m*. Data for standards, the standard curve and data for mutants are presented in table M.1, figure M.1 and table M.2, respectively.

Table M.1: A_{230} before and after addition of lyases for three parallels of known alginate concentration and the calculated increase in A_{230}. * indicates that the measurement was omitted.

Alginate concentration (g/l)		**A_{230} before lyases**	Corrected for blank	Corrected for dilution	**A_{230} after lyases**	Corrected for blank and lyases	Corrected for dilution	**Increase in A_{230}**	**Mean ± SD**
Blank	I	0.220							
	II	0.224							0.224
	III	0.227							
0.0	I				0.497				
	II				0.507				0.502
	III				0.502				
0.1	I	0.220	−0.004 22	−0.0127	0.705	0.203	0.652	0.665	
	II	0.222	−0.002 19	−0.006 58	0.687	0.185	0.595	0.601	0.625 ± 0.0345
	III	0.219	−0.005 10	−0.0153	0.687	0.185	0.594	0.609	
0.2	I	0.225	0.001 61	0.004 82	0.934	0.432	1.39	1.38	
	II	0.228	0.004 02	0.0121	0.884	0.382	1.23	1.22	1.35 ± 0.124
	III	0.229	0.005 01	0.0150	0.960	0.458	1.47	1.46	
0.3	I	0.235	0.0115	0.0344	1.18	0.677	2.18	2.14	
	II	0.260	0.0367	0.110	1.14	0.635	2.04	1.93	1.97 ± 0.160
	III	0.254	0.0305	0.0915	1.10	0.597	1.92	1.83	
0.4	I	0.274	0.0505	0.152	1.33	0.827	2.66	2.51	
	II	0.253	0.0291	0.0874	1.28	0.777	2.50	2.41	2.50 ± 0.0859
	III	0.251	0.0271	0.0812	1.33	0.829	2.66	2.58	
0.5	I	0.259	0.0355	0.107	1.47	0.968	3.11	3.00	
	II	0.256	0.0327	0.0980	0.524	0.0220	0.0708	−0.0272*	3.47 ± 0.658
	III	0.273	0.0488	0.146	1.77	1.27	4.08	3.94	

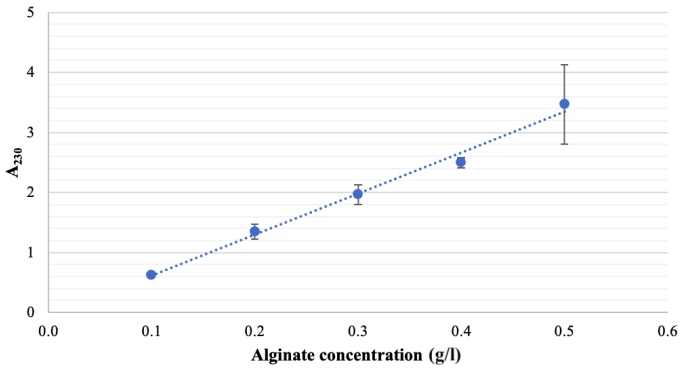

Figure M.1: The standard curve showing mean A_{230} values ± SD as a function of alginate concentration. A linear trendline produced the equation y = 6.8369x - 0.0688 and an R^2 of 0.9903

Table M.2: OD_{600} and A_{230} before and after addition of lyases for three parallels of *A. vinelandii* wild type and mutants. The calculated increase in A_{230} was used to determine alginate concentration (g/l) and alginate concentration (g/l) per OD_{600}.

		OD_{600}	**A_{230} before lyases**	Corrected for blank	Corrected for dilution	**A_{230} after lyases**	Corrected for blank and lyases	Corrected for dilution	**Increase in A_{230}**	Alginate concentration (g/l)	**Mean ± SD**	Alginate concentration (g/l) per OD_{600}	**Mean ± SD**
Wild type	I	1.01	0.355	0.131	1.62	0.673	0.171	2.27	0.651	0.105	0.225 ± 0.115	0.105	0.223 ± 0.114
	II		0.356	0.132	1.64	0.792	0.290	3.85	2.21	0.334		0.331	
	III		0.347	0.123	1.52	0.732	0.230	3.06	1.54	0.235		0.233	
algL* with P*m	I	0.730	0.262	0.0382	0.473	0.583	0.0814	1.08	0.607	0.0988	0.389 ± 0.274	0.135	0.731 ± 0.211
	II		0.269	0.0456	0.565	0.870	0.368	4.89	4.32	0.642		0.880	
	III		0.261	0.0374	0.464	0.750	0.249	3.30	2.84	0.425		0.582	
algLH199R* with P*m	I	0.646	0.268	0.0443	0.550	0.718	0.216	2.87	2.32	0.350	0.302 ± 0.0470	0.542	0.468 ± 0.0727
	II		0.265	0.0415	0.514	0.690	0.188	2.50	1.99	0.301		0.465	
	III		0.250	0.0259	0.320	0.653	0.151	2.00	1.68	0.256		0.396	

N Luciferase assay data for the promoters P*m*, P*lac* and P*const*

To measure promoter strength, a luciferase assay was performed on *A. vinelandii* mutants where P*m*, P*lac* and P*const* control expression of *luc*. The luciferase assay data are presented in table N.1

Table N.1: The luciferase assay data for the three promoters. Wild type was included as a blank. OD_{600}, RLU and RLU per OD_{600} for three parallels 24 and 48 hours after inoculation are presented. OD_{600} data for the P*m* promoter that was induced 8 hours after inoculation are also presented.

			OD_{600}	RLU	RLU (corrected for blank)	**RLU** (corrected for dilution)	**RLU per OD_{600}**
Wild type (blank)	24 h			107			
	48 h			96			
P*m* (induced)	8 h	I	0.108				
		II	0.092				
		III	0.108				
	24 h	I	0.390	490 528	490 421	10 898 244	27 944 217
		II	0.400	483 283	483 176	10 737 244	26 843 111
		III	0.370	371 302	371 195	8 248 778	22 293 994
	48 h	I	1.72	1 561 162	1 561 055	34 690 111	20 168 669
		II	1.19	537 795	537 688	11 948 622	10 040 859
		III	1.11	603 577	603 470	13 410 444	12 081 481
P*m* (uninduced)	24 h	I	0.400	3 183	3 076	68 356	170 889
		II	0.630	3 899	3 792	84 267	133 757
		III	0.500	3 147	3 040	67 556	135 111
	48 h	I	2.68	12 377	12 270	272 667	101 741
		II	2.67	8 084	7 977	177 267	66 392
		III	2.60	6 180	6 073	134 956	51 906
P*lac*	24 h	I	0.280	50 387	50 280	1 117 333	3 990 476
		II	0.330	65 926	65 819	1 462 644	4 432 256
		III	0.240	37 814	37 707	837 933	3 491 389
	48 h	I	2.10	233 894	233 787	5 195 267	2 473 937
		II	2.53	130 924	130 817	2 907 044	1 149 029
		III	0.800	51 918	51 811	1 151 356	1 439 194
P*const*	24 h	I	0.950	3 484 234	3 484 127	77 425 044	81 500 047
		II	0.840	2 309 411	2 309 304	51 317 867	61 092 698
		III	0.800	2 440 312	2 440 205	54 226 778	67 783 472
	48 h	I	3.22	1 696 593	1 696 486	37 699 689	11 707 978
		II	3.20	1 783 740	1 783 633	39 636 289	12 386 340
		III	3.33	2 625 943	2 625 836	58 351 911	17 523 096

Helga Munkeby Tingstad

NTNU
Kunnskap for en bedre verden